Vol. 116 No. 1, April 1, 1980 ISSN 0003-2670

ANALYTICA CHIMICA ACTA

International journal devoted to all branches of analytical chemistry

ELSEVIER SCIENTIFIC PUBLISHING COMPANY

ANALYTICA CHIMICA ACTA

International journal devoted to all branches of analytical chemistry
Revue internationale consacrée à tous les domaines de la chimie analytique
Internationale Zeitschrift für alle Gebiete der analytischen Chemie

PUBLICATION SCHEDULE FOR 1980 (incorporating the section on Computer Techniques and Optimization).

	J	F	M	A	M	J	J	A	S	O	N	D
Analytica Chimica Acta	113/1 113/2	114	115	116/1	116/2	117	118/1	118/2	119	120/1	120/2	121
Section on Computer Techniques and Optimization			122/1			122/2			122/3			122/4

Scope. *Analytica Chimica Acta* publishes original papers, short communications, and reviews dealing with every aspect of modern chemical analysis, both fundamental and applied. The section on *Computer Techniques and Optimization* is devoted to new developments in chemical analysis by the application of computer techniques and by interdisciplinary approaches, including statistics, systems theory and operation research. The section deals with the following topics: Computerized acquisition, processing and evaluation of data. Computerized methods for the interpretation of analytical data including chemometrics, cluster analysis, and pattern recognition. Storage and retrieval systems. Optimization procedures and their application. Automated analysis for industrial processes and quality control. Organizational problems.

Submission of Papers. Manuscripts (three copies) should be submitted as designated below for rapid and efficient handling:

Papers from the Americas to: Professor Harry L. Pardue, Department of Chemistry, Purdue University, West Lafayette, IN 47090, U.S.A.

Papers from all other countries to: Dr. A. M. G. Macdonald, Department of Chemistry, The University, P.O. Box 363, Birmingham B15 2TT, England.

For the section on *Computer Techniques and Optimization:* Dr. J. T. Clerc, Universität Bern, Pharmazeutisches Institut, Sahlistrasse 10, CH-3012 Bern, Switzerland.

American authors are recommended to send manuscripts and proofs by INTERNATIONAL AIRMAIL.

Information for Authors. Papers in English, French and German are published. There are no page charges. Manuscripts should conform in layout and style to the papers published in this Volume. Authors should consult Vol. 111, p. 343 for detailed information. Reprints of this information are available from the Editors or from: Elsevier Editorial Services Ltd., Mayfield House, 256 Banbury Road, Oxford OX2 7DE (Great Britain).

Reprints. Fifty reprints will be supplied free of charge. Additional reprints (minimum 100) can be ordered. An order form containing price quotations will be sent to the authors together with the proofs of their article.

Advertisements. Advertisement rates are available from the publisher.

Subscriptions. Subscriptions should be sent to: Elsevier Scientific Publishing Company, P.O. Box 211, 1000 AE Amsterdam, The Netherlands. The section on *Computer Techniques and Optimization* can be subscribed to separately.

Publication. *Analytica Chimica Acta* (including the section on *Computer Techniques and Optimization*) appears in 10 volumes in 1980. The subscription for 1980 (Vols. 113–122) is Dfl. 1390.00 plus Dfl. 160.00 (postage) (total approx. U.S. $795.00). The subscription for the *Computer Techniques and Optimization* section only (Vol. 122) is Dfl. 139.00 plus Dfl. 16.00 (postage) (total approx. U.S. $79.50). Journals are sent automatically by airmail to the U.S.A. and Canada at no extra cost and to Japan, Australia and New Zealand for a small additional postal charge. All earlier volumes (Vols. 1–112) except Vols. 23 and 28 are available at Dfl. 150.00 (U.S. $77.00), plus Dfl. 10.00 (U.S. $5.00) postage and handling, per volume.

Claims for issues not received should be made within three months of publication of the issue, otherwise they cannot be honoured free of charge.

Customers in the U.S.A. and Canada who wish to obtain additional bibliographic information on this and other Elsevier journals should contact Elsevier/North Holland Inc., Journal Information Center, 52 Vanderbilt Avenue, New York, NY 10017. Tel: (212) 867-9040.

ANALYTICA CHIMICA ACTA
VOL. 116 (1980)

ANALYTICA CHIMICA ACTA

International journal devoted to all branches of analytical chemistry

ELSEVIER SCIENTIFIC PUBLISHING COMPANY

Anal. Chim. Acta, Vol. 116 (1980)

Printed in The Netherlands.

Analytica Chimica Acta, 116 (1980) 1—6

DETERMINATION OF TRACE AMOUNTS OF SOME PHENYLAMIDE PESTICIDES BY RESONANCE RAMAN SPECTROMETRY

S. HIGUCHI, O. AIKO and S. TANAKA*

Department of Industrial Chemistry, Faculty of Engineering, The University of Tokyo, Hongo Bunkyo-ku, Tokyo (Japan)

(Received 16th October 1979)

SUMMARY

The resonance Raman spectrometric determination of 3-(4-chlorophenyl)-1,1-dimethylurea, 3-(3,4-dichlorophenyl)-1,1-dimethylurea, and α- and β-naphthylacetamides in water is described. These colorless samples exhibit no resonance Raman effect when an argon ion laser is used as excitation source, but when they are converted to azo dye derivatives (yields, 97 ± 1%), the resonance Raman spectra of the red products are analytically useful. Detection limits are $2—4 \times 10^{-8}$ M, and the analytical curves are linear up to 1×10^{-6} M. The analytical curve obtained by successive dilution of the most concentrated solution coincides with the curve for the products prepared separately at each concentration. The excellent selectivity of this method is demonstrated for structurally related samples and the possibility of their simultaneous determination is described.

Vibrational spectrometry shows excellent selectivity, because of the detailed spectra obtained by infrared and Raman techniques, but these methods provide very poor sensitivity. Resonance Raman spectrometry has recently become popular because both selectivity and high sensitivity are available [1—10]. With the resonance Raman effect the scattering intensities are often enhanced 10^5—10^6 times.

However, resonance Raman spectrometry has a disadvantage in trace analysis; its applicability is limited by the kinds of lasers readily available. With an argon ion laser, now common as an excitation source for Raman spectra, the samples must exhibit absorption bands in a wavelength range of about 450—550 nm in order to obtain sufficient intensity enhancement. Therefore, direct application of the method to the microanalysis of colorless compounds is impossible. An alternative approach in such cases is to transform the samples to colored derivatives by suitable chemical reactions. In a previous paper [10], resonance Raman spectrometry was used successfully for the determination of trace amounts of nitrite ion in waste and treated waters, the nitrite ion being converted to a colored azo dye. Recently, Van Haverbeke and Herman [9] reported the determination of three phenolic compounds by resonance Raman spectrometry, using a chemical reaction which transformed the samples to colored products.

In the present investigation, the resonance Raman spectrometric determination of some phenylamide pesticides is described. The report demonstrates that resonance Raman spectrometry may become a useful method of trace analysis in view of its high sensitivity, the shapes of the analytical curves, the influence of co-existent components, the additivity of intensities, and its excellent selectivity.

EXPERIMENTAL

A JASCO Model J-800 laser Raman spectrophotometer was used for the measurement of spectra. The excitation source was a Spectra-Physics Model 164 argon ion laser. The laser was operated at 488.0 nm with 200 mW of power at the samples. A HTV-R-464 photomultiplier was used as a detector. Depending on the noise levels of the spectra, the scans were repeated 4—16 times to improve the *S/N* ratios. The sample cell was rotated at 2500 rpm to avoid the effects of local heating of the sample solutions [8] and the possible decomposition of samples.

The samples examined were: α-naphthylacetamide, β-naphthylacetamide, 3-(4-chlorophenyl)-1,1-dimethylurea (Monuron) and 3-(3,4-dichlorophenyl)-1,1-dimethylurea (Diuron). Aqueous solutions of their colored products were measured.

RESULTS AND DISCUSSION

Chemical derivatization reactions

The first step of each derivatization reaction was the hydrolysis of the amide to the corresponding amine. The amines obtained were diazotized and coupled with 1-naphthol in order to transform them into the colored products (azo dyes):

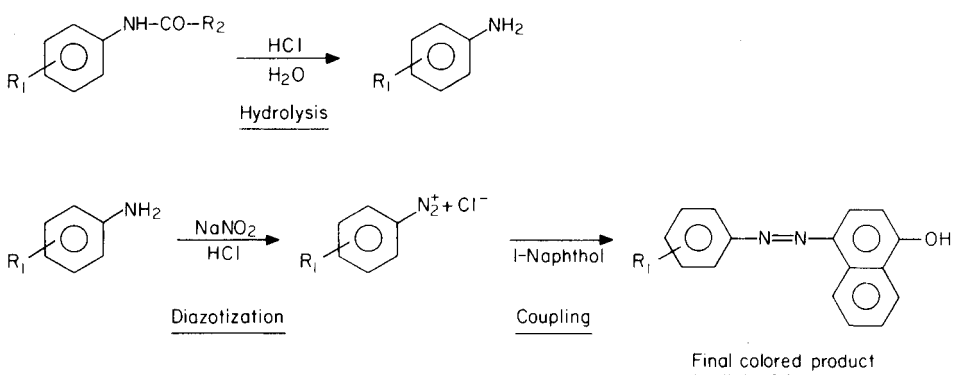

Preliminary studies showed that the method of El-Dib and Aly [11] for producing colored derivatives of phenylamides was unsatisfactory: hydrolysis of the amide was incomplete, and the sulfuric acid used generated a high-

intensity sulfate band in the final spectra. In the hydrolysis method finally adopted, the samples were boiled in water for a few hours, with 1 M hydrochloric acid as catalyst. Table 1 shows the product yields obtained: the amides were converted reproducibly and almost completely to the azo dyes after hydrolysis for 4 h.

Resonance Raman spectra of the colored products

All the colored product solutions exhibited absorption bands at about 500 nm with maximum molar absorptivities from 1.9×10^4 to 3.1×10^4 $l\ cm^{-1}\ mol^{-1}$. Thus, on excitation with the 488.0-nm laser line, the resonance Raman effect is obtained; as shown by the spectra in Fig. 1. It can be seen that even for closely related molecules identification is possible from these spectra.

Detection limits

The detection limits in resonance Raman spectrometry are limited by the background intensities from the sample solutions [12]. The main source of this background seems to be fluorescence. In the present study, the sample solutions were irradiated for up to an hour before the measurements to decrease the background intensities. Detection limits determined for selected intense bands are shown in Table 2. The detection limit is defined as the signal equivalent to twice the standard deviation of the base-line noise. The colorimetric detection limits determined by El-Dib and Aly [11] are also listed: these values were determined for an absorption cell path-length of 20 mm. It can be seen that the limits of detection obtained by resonance Raman spectrometry are considerably better than those by colorimetry, although better colorimetric detection limits might be obtained by using longer cells and solvents with lower background absorption.

Analytical curves

In resonance Raman spectrometry the relationship between intensity and concentration is determined by two competing factors. The increase of

TABLE 1

Yields obtained for the colored products of the samples

Sample	Yield (%) after hydrolysis for	
	3 h	4 h
Monuron	85.2	96.9
Diuron	85.2	95.9
α-Naphthylacetamide	94.6	97.3
β-Naphthylacetamide	85.2	97.3

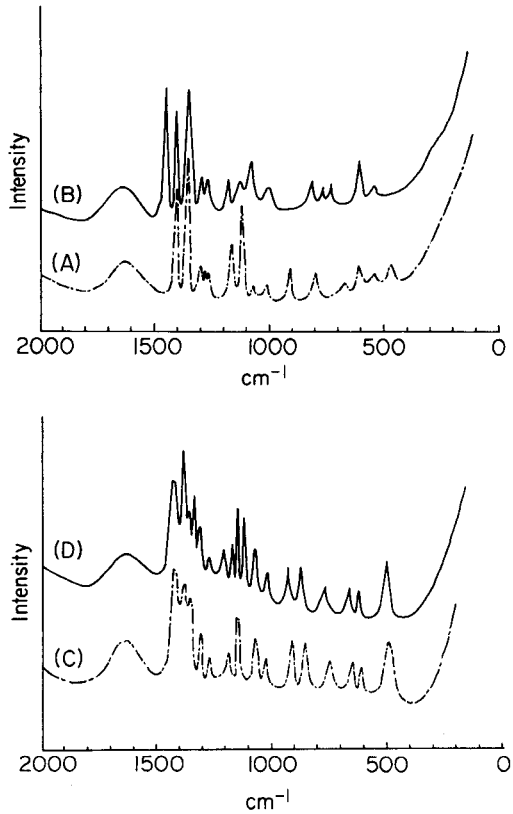

Fig. 1. Resonance Raman spectra of the colored products of monuron(A), diuron(B), α-naphthylacetamide (C) and β-naphthylacetamide(D).

Raman intensities with higher concentrations is partly offset by the increase of absorption effects. Figure 2 shows the resultant non-linear relationship between concentration and intensity for the derivative of α-naphthylacetamide. Only in the comparatively narrow range of concentrations up to 10^{-6} M was the plot linear. Excellent linear graphs were obtained for the range 2×10^{-8}—10^{-6} M. Similar results were obtained for the other samples.

Experiments were also carried out to verify that the analytical curves obtained by successive dilutions of the most concentrated product solutions coincided with those for the products prepared separately for each of the concentrations. Figure 3 shows an example of the results of such a study and confirms that the plots obtained by the two methods of sample preparation do not differ significantly. Thus, in constructing an analytical curve, it is permissible to prepare only one derivative solution and to make sample solutions of the required concentrations by dilution.

TABLE 2

Detection limits (mol l^{-1}) obtained in resonance Raman spectrometry and colorimetry

Sample	Band (cm^{-1})	Resonance Raman ($\times 10^8$)	Colorimetry ($\times 10^7$)
Monuron	1370	2	1
Diuron	1370	2	1
	1450	4	
α-Naphthylacetamide	1370	2	1
β-Naphthylacetamide	1370	2	1
	1120	4	

Selectivity and additivity of intensities

In resonance Raman spectrometry, the signal intensity of a component is generally affected by the co-existence of other components having absorption bands in the same wavelength range. This influence is due to the fact that both the exciting laser beam and the scattered light are absorbed by the co-existent component and thus weakened. However, if the concentrations of the co-existent components are very low, such effects may be negligible. As is seen in Fig. 1, a band at 1450 cm^{-1} is present only in the spectrum of diuron. Figure 4 shows that there is no appreciable influence on the intensity of this band when monuron is also present in the range 0—1 $\times 10^{-6}$ M, but that when the concentration of monuron is greater, the influence becomes apparent. The monuron concentrations which cause appreciable effects are in a range where the analytical curves are in any case non-linear so this result may not detract from the analytical usefulness of the method.

For the band at 1370 cm^{-1}, the products from both monuron and diuron contribute to the intensity. Figure 5 shows the analytical curves for monuron alone and in the presence of 1 $\times 10^{-6}$ M diuron. The additivity of the intensities is confirmed from the parallel nature of the two lines. Thus,

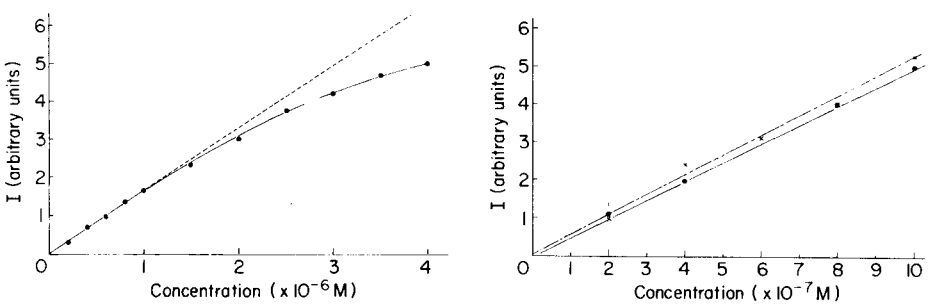

Fig. 2. Analytical curve for the 1370-cm^{-1} band of α-naphthylacetamide.

Fig. 3. Analytical curves for the 1370-cm^{-1} band of β-naphthylacetamide: (•) samples prepared by successive dilutions, $I = -0.03\ (\pm 0.07) + 0.50\ (\pm 0.02)C_m$; (×) separate reactions, $I = 0.05\ (\pm 0.13) + 0.52\ (\pm 0.03)C_m$.

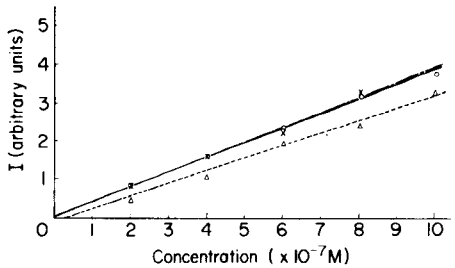

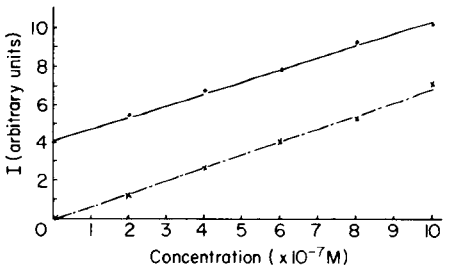

Fig. 4. Analytical curves for the 1450-cm^{-1} band of diuron in the presence of monuron: (•) for diuron only, I = 0.04 (±0.01) + 0.39 (±0.01)C_m; (×) for diuron + 1 × 10^{-6} M monuron, I = 0.00(±0.18) + 0.40(±0.04)C_m; (△) for diuron + 4 × 10^{-6} M monuron, I = —0.15(±0.10) + 0.34(±0.02)C_m.

Fig. 5. Analytical curves for the 1370-cm^{-1} band of monuron in the presence of diuron: (×) for monuron only, I = —0.15 + 0.70 (±0.04)C_m; (•) for monuron + 1 × 10^{-6} M diuron, I = 4.2 + 0.64 (±0.02)C_m.

simultaneous determination of the components of mixed solutions may be possible. Similar results were obtained for the other structurally related samples, α- and β-naphthylacetamide. In separate experiments it was further shown that up to 10^{-6} M monuron had no effect on the production of the colored derivative of diuron: the resultant analytical curves at 1450 cm^{-1} were coincident. These results indicate that the determination of the different components in mixed solutions will be possible.

The approach used for these colorless phenylamide pesticides, involving derivatization by hydrolysis and azo-dye formation, should have wider applicability. The results described demonstrate clearly the high sensitivity and excellent selectivity of the method, and suggest a new approach useful for the identification and the determination of phenylamide pesticides. Further applications of the method to a variety of samples are now under study.

This research was supported by a Grant-in-Aid of Scientific Research from the Ministry of Education, Science and Culture of Japan.

REFERENCES

1 Cheng-Wen Tsai and M. D. Morris, Anal. Chim. Acta, 76 (1975) 193.
2 M. S. Rahaman and M. D. Morris, Talanta, 23 (1976) 65.
3 M. D. Morris, Anal. Lett., 9 (1976) 469.
4 C. W. Brown and P. F. Lynch, J. Food Sci., 41 (1976) 1231.
5 L. C. Hoskins and V. Alexander, Anal. Chem., 49 (1977) 695.
6 L. Van Haverbeke, P. F. Lynch and C. W. Brown, Anal. Chem., 50 (1978) 315.
7 R. J. Thibeau, L. Van Haverbeke and C. W. Brown, Appl. Spectrosc., 32 (1978) 98.
8 S. Higuchi, J. Tanaka and S. Tanaka, J. Spectrosc. Soc. Jpn. (Bunko Kenkyu), 27 (1978) 353.
9 L. Van Haverbeke and M. A. Herman, Anal. Chem., 51 (1979) 932.
10 N. Furuya, A. Matsuyuki, S. Higuchi and S. Tanaka, Water Res., in press.
11 M. A. El-Dib and O. A. Aly, J. Assoc. Off. Anal. Chem., 55 (1972) 1276.
12 K. M. Cunningham, M. C. Goldberg and E. R. Weiner, Anal. Chem., 49 (1977) 70.

Analytica Chimica Acta, 116 (1980) 7—17

A VERSATILE SPECTROMETER FOR SECONDARY X-RAY FLUORESCENCE EXCITATION

LEIF HØJSLET CHRISTENSEN*, SVEND ERIK RASMUSSEN, NIELS PIND and KLAUS HENRIKSEN

Department of Chemistry, Aarhus University, Langelandsgade 140, DK-8000 Aarhus C (Denmark)

(Received 23rd October 1979)

SUMMARY

Inexpensive research equipment for secondary x-ray fluorescence excitation is described. The primary beam from a high-powered x-ray tube is collimated onto the targets, six of which may be easily and safely interchanged. A collimator system ensures that the detector receives radiation from well defined areas of the sample. The geometry minimizes radiation from Compton scattering, the twice-scattered continuum radiation from the x-ray tube, and the characteristic lines from the secondary target. The unit is designed for use with standard x-ray tubes and generators, and is part of an energy-dispersive spectrometer used for multielement analysis. The performance of the system with a variety of samples is described.

The improved resolution of solid-state detectors, e.g. Si(Li), greatly accelerated the development of energy-dispersive x-ray fluorescence spectrometers for multielement analysis. Around 1970 the first energy-dispersive spectrometers based on Si(Li) detectors became commercially available. In 1973 Porter [1] introduced the secondary fluorescence method, using standard spectrometer tubes for primary excitation. Goulding and Jaklevic [2] used the same method, but replaced the high-powered x-ray tubes with low-powered tubes. To obtain appropriate sensitivity they used a "tight" geometry. Energy-dispersive x-ray fluorescence spectrometers based on secondary fluorescence excitation, either with a high-powered or a low-powered x-ray tube configuration, are now becoming commercially available. Most of the commercial spectrometers have an integral mini-computer with extensive optional software packages for data reduction. Unfortunately, the hardware and software are very often integrated in such a way that a user change in the analytical scheme is difficult. In particular, the software routines cannot easily be modified to accommodate a special analytical problem.

The literature contains little information on research equipment for secondary fluorescence experiments [2—4].

In this paper, an energy-dispersive x-ray fluorescence spectrometer based on the secondary fluorescence excitation method is described. Except for the

irradiation chamber and the computer interface, which have been designed in this laboratory, standard commercially-available equipment is utilized. The spectrometer is interfaced to a time-shared computer. The necessary software for data acquisition and data reduction has been written in a high-level language, ALGOL, which facilitates modifications in the data reduction scheme.

To exploit the advantages of secondary x-ray fluorescence an irradiation chamber has been designed which allows easy changeover of fluorescence targets. The design makes use of standard sample holders and commercial spectrometer tubes and is easily built in a machine shop equipped with standard mills and lathes.

EXPERIMENTAL

Hardware

Figure 1 shows the hardware configuration of the spectrometer.

Detector and excitation system. The spectrometer includes a Princeton γ-Tech intrinsic Ge detector (PGT IG 55) with an active area of 50 mm^2 and a thickness of 5 mm. The crystal is mounted in a cryostat together with a FET preamplifier with pulsed optical feedback. The main amplifier (PGT 340) is used with a 6-μs shaping time constant and the base-line restorer in the High position. The main amplifier is connected to a Nuclear Data Gen II 100-mHz ADC. The digitized signals are stored in a 1K memory, which is a part of the interface. The HV supply for the x-ray tube is a highly stabilized PW 1140 generator (100 kV, 100 mA, max. 3 kW). The spectrometer x-ray tube used had a tungsten anode.

Irradiation chamber. Figure 2 shows an exploded view of the irradiation chamber. The top part shows the steel sample turret, which permits safe insertion and removal of samples in standard sample holders. The lower part of the drawing shows the irradiation chamber without the turret. The chamber is made of aluminium (99.5%) covered with a lead shield. The bottom part of the steel turret is similarly covered with a 10-mm layer of aluminium. The x-ray tube is labelled A; B is a microswitch which switches off the generator if the tube is removed. The tube compartment is separated by a wall from the other part of the unit. Not shown on the drawing is a

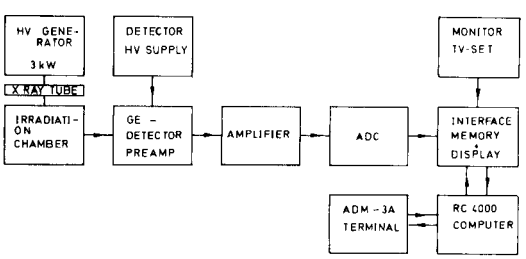

Fig. 1. Hardware configuration.

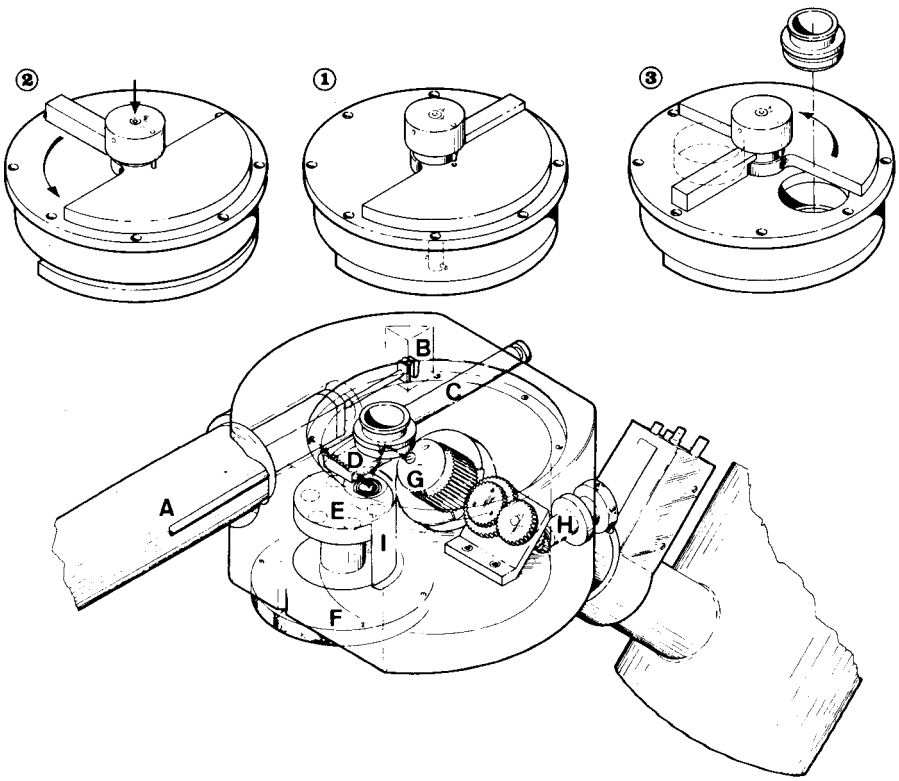

Fig. 2. Secondary x-ray fluorescence unit (see text for description).

tantalum shield, a pre-collimator, in front of the x-ray window which limits the solid angle through which x-rays are emitted. This shield reduces the background from high-energy radiation which might otherwise penetrate the wall. C is a tungsten rod carrying a tungsten collimator, D. The collimator hole is partly filled with 99.9999% Al tubes to reduce the intensity of fluorescent radiation. The collimated beam strikes a fluorescence target located in an aluminium cylindrical disc, E (diameter 80 mm, height 15 mm). The diameter of the target is 19 mm. The angle of incidence of the x-rays on the target is 20° and in order to utilize the whole target area the hole in the collimator is made elliptical. By turning a handwheel, F, six different targets can be positioned. The targets "click" into place by means of a standard ball and notch method, and the numbers 1 to 6 become visible when targets are correctly positioned. The disc can readily be replaced by another carrying six further targets with only a screwdriver. At present the following six targets are used: Ti, Se, Mo, Ag, Te and Sm.

The fluorescence radiation from the target emanates in a solid angle of 2π. The sample surface is parallel to the target surface. The distance between the two planes is 27 mm, and the centre of the sample is displaced 27 mm

from the centre of the target. Thus the angle between the line joining the two centres and the plane of the secondary target is 45°. The fluorescence radiation from the sample and the twice-scattered direct beam is directed onto the detector crystal through a collimator located in an aluminium cylinder, G (diameter 50 mm, length 50 mm). To reduce the intensity of scattered radiation entering the detector, the front part of the collimator is conical, so the solid angle subtended by the detector is limited. The surface of the collimator is covered by a 1-mm layer of tungsten and then a 1-mm layer of aluminium (99.9999%). Four holes, the collimators, pass through G. Three of the four holes are elliptical, to ensure that the detector "sees" nearly circular areas of the sample corresponding to masks of varying sizes. By using a numbered knob, H, the four different collimators can be positioned through a system of gears; again the correct positioning of the collimators is ensured mechanically.

In order to reduce the scattered radiation from the secondary target, a shield I (tungsten covered with aluminium foil) is placed between E and G.

The plane defined by the direct collimated beam and the line joining the centres of target and sample is perpendicular to the plane defined by the latter line and the collimator immediately before the detector crystal. The angle between the two latter lines is also 90°. This geometry was chosen, partly to minimize the spectral background caused by rescattering of the direct beam and partly to minimize the intensity of the Compton-scattered radiation. The differential Compton scattering cross-section is minimal for a 90° angle.

Aluminium was used as much as possible inside the unit because the intrinsic germanium detector was not supposed to be applicable to low-energy radiation such as that of Al-*K* radiation. A lead shield covering the outer part of the unit ensures radiation safety and Pb-*L* radiation excited by x-rays passing through the aluminium walls is strongly attenuated when re-entering through the walls.

The spectrometer can be evacuated in order to enhance the sensitivity for low-energy elements.

To minimize the noise level, the detector and its cryostat are isolated from any metal contact and the spectrometer is placed on vibration isolators.

Computer and interface. The spectrometer is interfaced to a medium-sized time-shared computer, an RC4000, with extensive standard software packages. The RC4000 is a general-purpose computer with an internal store of 48K 24-bit words. The computer is backed by two discs (2 and 8M words) and via a transmission system linked to a Cyber 173 computer placed in a central computer facility. ALGOL and FORTRAN compilers are available with the RC4000. Monitor programs including drivers for various instruments are programmed in assembler language.

The interface consists of a 1K 24-bit memory module (DRAM type, Texas Instruments TMS 4030), a 12-bit time register and a graphic display module

[5]. An ordinary TV set (192 × 256 points) is used as spectrum monitor. The spectrometer interacts with the RC4000 in the on-line mode and the communication between the two units goes through the low-speed data channel (I/O bus).

Software

EDXRF. The main program EDXRF is coded in ALGOL and performs the on-line control of the spectrometer, data acquisition, spectrum display and data transport, e.g. transport of a spectrum to a reserved area on the RC4000 disc. Further, the program performs the preliminary data reduction of a spectrum, i.e. the qualitative analysis and extraction of peak intensities. The program may also activate the RC4000 plotter or tape puncher systems if a hardcopy of a spectrum is necessary.

The strategy of the EDXRF program is outlined in Fig. 3. All the commands have a five-character code and this code (or a sequence of codes) is given as input to the program. A new command may easily be implemented by adding an appropriate subroutine to the existing list of subroutines. Table 1 shows some of the command codes and their functions.

The automatic search for peaks in an unknown spectrum is based on the second difference method [6]. An x-ray energy table is stored on the disc and the output from the program using PEAKF contains an identification of the peaks in the list, e.g. No. 2 Cu Kα, No. 3 Cu Kβ, etc. Although the energy calibration does not change much, this option is useful when an inexperienced person uses the spectrometer. The peak intensities are estimated by an iterative non-linear least-squares fitting of a Gaussian function plus a linear background to the observed profiles [6—8]. This is done auto-

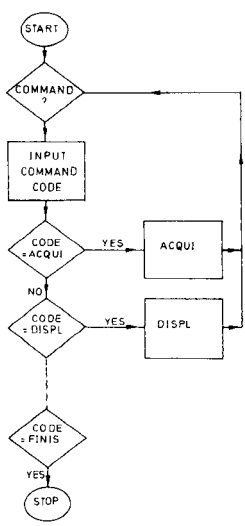

Fig. 3. Flow-chart for EDXRF.

TABLE 1

Some command codes in EDXRF

Command code	Function of code
ACQUI	Acquire a spectrum
BACKG	Acquire a background spectrum
SUBTR	Subtract spectra
DISPL	Display part of a spectrum. Scales automatically
SPSTO	Store a spectrum on a disc area
SPGET	Get a spectrum from the disc area
KALIB	Performs the energy calibration automatically
PEAKF	Performs an automatic qualitative analysis (peakfind)
PAREA	Extract elemental peak intensities using a non-linear least squares fitting technique
GTEST	Performs an automatic long or short term stability test of the x-ray generator
FINIS	Terminates the program

matically for the list of peaks found by PEAKF. A maximum of two peaks can be handled in one fit.

SAMPO. The FORTRAN program SAMPO [7] running on the Cyber 173 is used to extract element peak intensities, and is a more sophisticated non-linear least-squares fitting program. A maximum of five peaks can be handled in one fit. SAMPO is used for analyzing spectra with a high density of peaks where overlap problems may be severe, e.g. geological samples. Spectra stored on the RC4000 disc are automatically transferred to the Cyber 173.

MATRIX. This program is used to convert estimated intensities to weight fractions. For thin samples, e.g. samples prepared on Millipore filters, matrix effects can be neglected. For thick samples, e.g. pressed pellets, both absorption and enhancement effects are involved. The MATRIX program, which is based on the fundamental parameter approach [9], simplifies the calibration of the instrument and calculates the matrix effects from tabulated physical parameters. The same calibration and the same model are applied to a variety of samples, e.g. waste water, fly ash, rocks, etc. MATRIX is coded in ALGOL and runs as a batch job on the RC4000.

RESULTS AND DISCUSSION

The secondary excitation method

Several authors [1, 2, 10] have compared the signal-to-noise ratios of the direct excitation method and the secondary excitation method. In general, the secondary excitation method offers a lower background, and thereby better detection limits, than the direct excitation method. Further, various nearly monochromatic excitation energies are cheaply and easily available with this method. The monochromatic excitation radiation facilitates calculation of absorption and enhancement effects by means of the fundamental parameter approach.

Most energy-dispersive spectrometers use a lithium-drifted silicon detector, but the usefulness of an intrinsic germanium detector has been studied in the present work. For lower energies the full energy detection efficiency of the Si(Li) detector is better than that of the germanium detector, but for higher energies the efficiency of the former decreases because of complete absorption in the detector crystal. For the germanium detector, the *K*-shell absorption jump at 11.1 keV causes an abrupt decrease in the efficiency, but for energies beyond ca. 20 keV the germanium detector is advantageous. The escape peak problem [11, 12] encountered in both detectors is more severe for the germanium detector. To avoid this problem, and to enhance the excitation efficiency, the analysis of elements having a $K\alpha$ or $L\alpha$ line in the energy range 2—40 keV is divided into six groups, e.g. one group for each secondary target. For most practical purposes only two or three targets are used for a complete analysis.

The excitation and detection efficiency for element i ($K\alpha$ line) is given [2] by

$$K_i = \tau(1 - 1/J_{K,L})\omega_{K,L} f A \epsilon(1 - P) \qquad (1)$$

where τ is the photoelectric cross-section for a particular exciting energy, $J_{K,L}$ the absorption jump ratio, $\omega_{K,L}$ the fluorescence yield of the K shell and f is the fraction of radiation emitted as $K\alpha$ radiation. The values of each of these terms are reported in the literature [13—16]. The absorption factor for the air path, A, and the detector efficiency, $\epsilon(1 - P)$, can be calculated from mass absorption coefficients tabulated in the literature. The fraction of $K\alpha$ photons which escapes the detector, P ($P = 0$ for $E < 11.1$ keV), has been described [11].

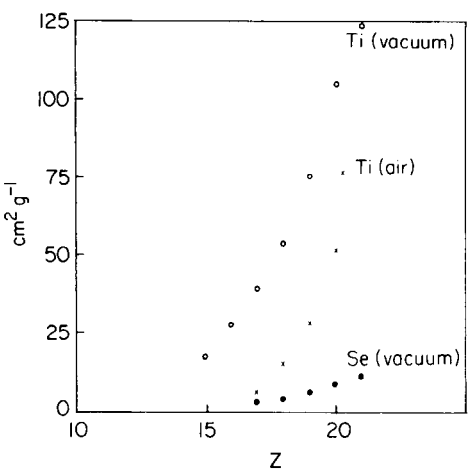

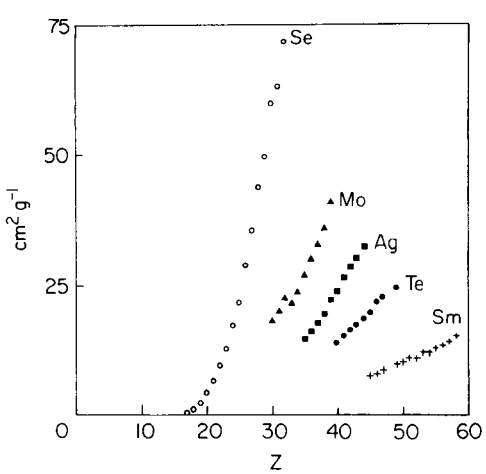

Fig. 4. Calculated $K\alpha$ excitation and detection efficiencies for the Ti and Se targets: (○) Ti (chamber evacuated); (×) Ti (air path); (●) Se (chamber evacuated).

Fig. 5. Calculated $K\alpha$ excitation and detection efficiencies for Se (○), Mo (▲), Ag (■), Te (●) and Sm (+).

Figure 4 shows the calculated $K\alpha$ excitation and detection efficiency for the titanium target with and without air. The sensitivities for lighter elements are clearly enhanced when the irradiation chamber is evacuated. Also shown in Fig. 4 are the sensitivities which can be obtained if the selenium target is used for the lighter elements. Figure 5 shows the calculated sensitivities for the Se, Mo, Ag, Te and Sm target.

Detection limits

Giauque et al. [17] have discussed several ways of calibrating energy-dispersive spectrometers for thin samples where absorption and enhancement effects can be neglected. The intensity, I_i, for element i can be expressed as $I_i = I_0 G K_i m_i$ where I_0 is the exciting radiation intensity, G a geometry factor and m_i (g cm^{-2}) the concentration of element i. The dimension of K_i is cm^2 g^{-1}. The sensitivity for element i, S_i (cps μg^{-1} cm^{-2}) is given by $I_i = S_i m_i$.

Relative K_i or S_i values can either be calculated using eqn. (1), or experimentally determined by using mixtures of elemental stock solutions. The absolute calibration for a given set of experimental conditions (kV, mA, target, etc.) is accomplished by using single-element thin-film standards prepared by vacuum vapor deposition of pure elements (Micromatter, Seattle).

The detection limit C(MDL) [18] is given by $C(\mathrm{MDL}) = 3.29\,(R_b/t)^{1/2}\,S^{-1}$, where R_b is the background count rate (cps) under the peak and t is the counting time.

Table 2 shows the experimentally determined sensitivities and detection limits obtained. The counting time was 100 s and R_b was determined by using a blank Millipore filter (5 mg cm^{-2}). The calculated and experimentally determined K_i values agreed within two standard deviations (c.v. $\approx$ 2—5%). In general the background was low and the detection limits obtained are similar to those quoted for commercial systems [19].

Effect of the detector collimator

In the present design, the sensitive region of the detector, e.g. the detector view, can be varied in four steps. This option is useful when small and irregularly shaped samples have to be analyzed. Some work in this laboratory involves the analysis of cross-sections of zone-melted rods of intermetallic compounds, e.g. Nb_4Ge, Nb_5Ge and Nb_3Ga, with the purpose of measuring the compositional changes within the specimens and if possible detecting impurities. The diameter of each section may vary from 2 to 20 mm; in the latter case masking of the sample is necessary. In order to minimize surface heterogeneity among the samples, samples are mounted in plastic and both ends of a section are machine-polished. If the detector view covered the whole sample surface, impurities would be imbedded in scattered background radiation caused by the plastic or the sample holder.

TABLE 2

Calculated detection limits for infinitely thin samples
(Background: Millipore, 5 mg cm^{-2}; counting time, 100 s.)

Operating conditions	Element	R_b (cps)	S (cps μg^{-1} cm^{-2})	C(MDL) (ng cm^{-2})
Se	Ti[a]	1.6	9.8	43
40 kV	V	1.7	8.9	48
40 mA	Cr	1.8	20.1	22
Coll. 3	Mn	2.1	19.7	24
	Fe	1.9	30.0	15
	Co	1.6	31.4	13
	Ni	3.6	38.4	16
	Cu[b]	6.6	46.8	18
	Zn	6.9	50.1	17
	Ga	7.9	55.2	17
Mo	As[a]	8	20.5	45
45 kV	Se	8	20.6	45
50 mA	Br[a]	10	25.8	40
Coll. 3	Rb	14	31.9	39
	Sr[b]	16	34.3	38
	Hg[b]	14	13.7	90
	Pb	8	12.5	74
Te	Ag[b]	64	12.1	216
45 kV	Cd	60	13.0	196
50 mA				
Coll. 3				

[a]The sensitivity has been calculated from eqn. (1). [b]Absolute standards.

The detector view was determined by moving a small piece of copper (2 × 2 mm) in two perpendicular directions on a sheet of graph paper placed at the bottom of the sample holder. Table 3 shows the measured detector view for the four collimators. Position 4 does not give a circular view for the reason mentioned above.

Table 3 also shows that a decrease in the solid angle (position 3 to 2) covered by the detector decreased the Compton-scattered radiation more than the elemental lines of interest: the intensity of the Compton- and Rayleigh-scattered Ag $K\alpha$ and $K\beta$ lines, $I_{\text{Ag Scatt}}$, is reduced by 47% and the elemental intensities by only 10%. Further, the signal-to-noise ratio is improved throughout the whole spectrum. The use of collimator position 1 results in a 78% reduction of $I_{\text{Ag Scatt}}$ and a 30% reduction in the elemental intensities.

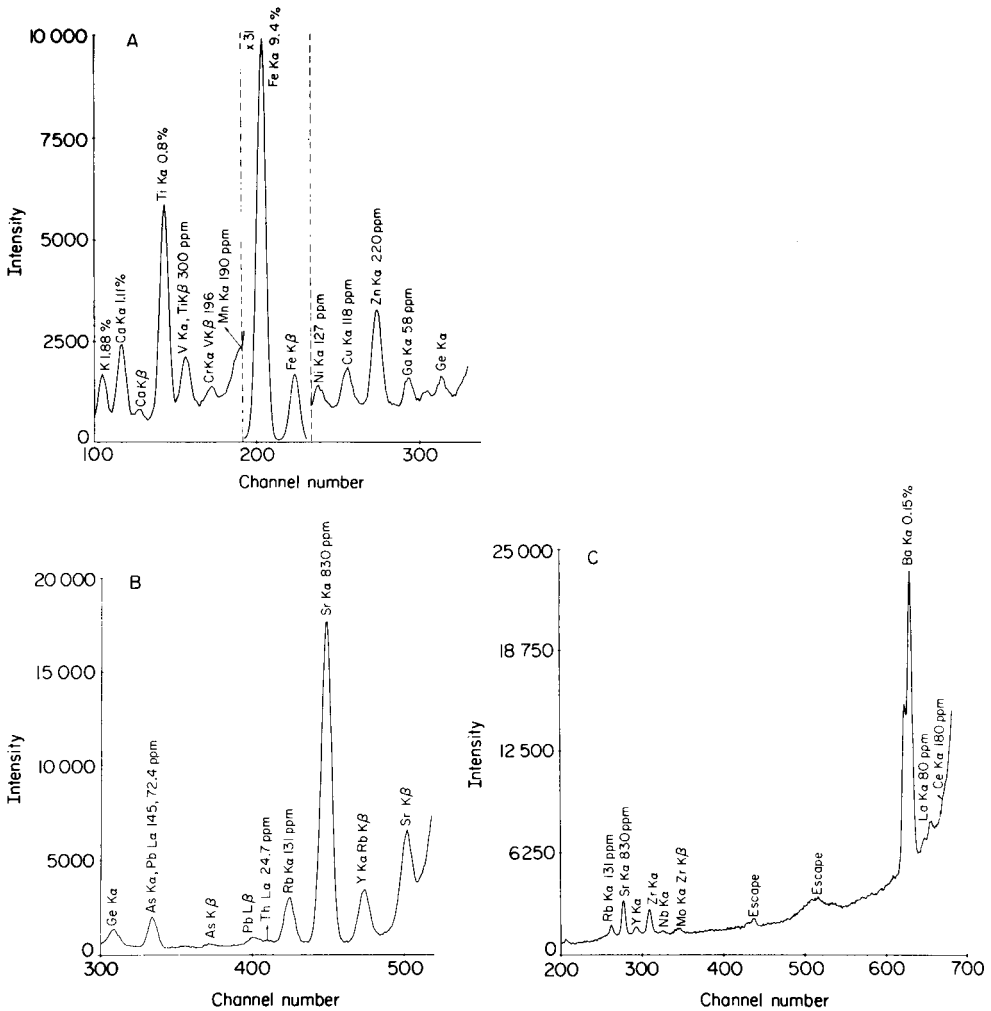

Fig. 6. Spectrum of NBS fly ash standard 1633 a with (A) Se target (40 kV, 6 mA, Coll. 3, 1000 s), (B) Mo target (45 kV, 4 mA, Coll. 3, 1000 s), and (C) Sm target (60 kV, 4 mA, Coll. 3, 1000 s).

Thick samples

For thick samples both absorption and enhancement effects are involved, but, in principle, the excitation and detection efficiencies (eqn. 1), should be the same for all sample types. Two calibration schemes are in use in such cases: one makes use of thin film standards, and the other of single element standards (1—2% aqueous solutions). Matrix effects are then calculated by using tabulated physical parameters.

Results obtained so far on NBS standards show some discrepancies from the NBS certified values. Figure 6 shows the spectra obtained for the NBS Coal Fly Ash standard 1633a with different targets. Nearly all elements

TABLE 3

Effect of the detector collimator
(Secondary target, Ag; sample, Nb_4 Ge.)

Collimator position	Detector view diameter (mm)	kV/mA	I_{Ge} (cps)	I_{Nb} (cps)	$I_{Ag\ Scatt}$ (cps)
4	14/18	—	—	—	—
3	12	40/4	469	4625	642
2	8	40/4	428	4181	339
1	1	40/25	328	3313	141

above 10 ppm in concentration can be identified, but severe overlap complicates quantification in several cases.

We are grateful to the Danish National Science Research Council for covering the cost of the germanium detector and for a research fellowship to L.H.C. and to Dr. L. Kryger who supplied the driver for the interface system. We thank Mr. P. Christensen, Mr. F. Homann and Mr. P. Kjærgaard for constructional work and Mr. H. J. Skov who designed the interface.

REFERENCES

1 D. E. Porter, X-Ray Spectrom., 2 (1973) 85.
2 F. S.. Goulding and J. M. Jaklevic, Annu. Rev. Nucl. Sci., 23 (1973) 45.
3 R. P. Larsen and J. L. Karttunen, Adv. X-Ray Anal., 17 (1974) 571.
4 R. Spatz and K. H. Lieser, X-Ray Spectrom., 8 (1979) 110.
5 H. K. Skov, L. Kryger and D. Jagner, Anal. Chem., 48 (1976) 933.
6 M. A. Mariscotti, Nucl. Instrum. Methods, 50 (1967) 309.
7 J. T. Routti and S. G. Prussin, Nucl. Instrum. Methods, 72 (1969) 125.
8 V. Barnes, IEEE Trans. Nucl. Sci., NS-15-3 (1968) 437.
9 C. J. Sparks, Jr., Adv. X-Ray Anal., 19 (1976) 19.
10 D. A. Gedcke, E. Elad and P. B. Denee, X-Ray Spectrom., 6 (1977) 21.
11 L. Højslet Christensen, X-Ray Spectrom., 8 (1979) 146.
12 M. P. Fioratti and S. R. Piermattei, Nucl. Instrum. Methods, 96 (1971) 605.
13 W. Bambynek, B. Craseman, R. W. Fink, H. U. Freund, H. Mark, C. D. Swift, R. E. Prince and P. Venugopala Rao, Rev. Mod. Phys., 44 (1972) 716.
14 H. U. Freund, X-Ray Spectrom., 4 (1975) 90.
15 W. H. McMaster, N. Kerv Del Grande, J. H. Mallet and J. H. Hubbell, Lawrence Livermore Lab. Rep. UCRN 50174 (1970).
16 J. S. Hansen, H. U. Freund and R. W. Fink, Nucl. Phys. A142 (1970) 604.
17 R. D. Giauque, R. B. Garrett and L. Y. Goda, in T. G. Dzubay (Ed.), X-Ray Fluorescence Analyses of Environmental Samples, Ann Arbor Science Publishers, Ann Arbor, 1977, p. 153.
18 J. M. Jaklevic and R. L. Walter, in T. G. Dzubay (Ed.), X-Ray Fluorescence Analyses of Environmental Samples, Ann Arbor Science Publishers, Ann Arbor, 1977, p. 63.
19 L. S. Birks and J. V. Gilfrich, Appl. Spectrosc., 32 (1978) 204.

Analytica Chimica Acta, 116 (1980) 19—24

QUALITATIVE EXAMINATION OF CHEMICALLY-MODIFIED SILICA SURFACES BY NEAR-INFRARED PHOTOACOUSTIC SPECTROSCOPY

C. H. LOCHMÜLLER* and D. R. WILDER

Paul M. Gross Chemical Laboratory, Duke University, Durham, N.C. 27706 (U.S.A.)

(Received 25th September 1979)

SUMMARY

Microparticulate silica gel, modified through the chemical bonding of hydrocarbonaceous moieties to the silica surface, was examined in the near infrared spectral region by using photoacoustic spectroscopy. A rapid and simple qualitative assessment of the success of modification procedures that introduce carbocyclic functions on silica gel was accomplished. The extent of coverage on alkyl-modified silica was evaluated by using a comparison of methyl and methylene overtone bands.

Photoacoustic spectroscopy (p.a.s.) has become established as a rapid and convenient method for obtaining optical absorption data from condensed state samples and is a particularly useful technique when applied to samples that are traditionally troublesome for conventional transmission spectroscopy, notably powders and suspensions [1—4]. The method has recently shown potential for the characterization of chemically-modified surfaces, as exemplified by the study of derivatized microparticulate silica [5—7]. Chemically-modified silicas find use in a variety of applications such as chemically-bonded stationary phases for chromatography, as catalysts, and as preconcentrating sorbents. For this reason the acquisition of molecular spectroscopic information from these unique surfaces is of considerable practical significance, both for the evaluation of interactions on the modified silica surface and as a means, along with conventional elemental analysis, for more definitively describing such surfaces. P.a.s. represents one of the few methods capable of easily and reliably furnishing this information.

This paper presents a further application of p.a.s. to the characterization of chemically-modified silica surfaces. It reports an extension of work on the description of such surfaces to the near infrared spectral region. The study utilizes the capability of a spectrometer employing a broad-band source and appropriate gratings to provide information over the entire near infrared, in addition to its more generally used capability in the ultraviolet and visible regions. This allows the examination of samples that possess no distinctive u.v.-visible chromophores. In particular, information from the near i.r. permits a qualitative evaluation of silicas that have been modified with hydrocarbonaceous functions and allows an assessment of the success of the

derivatization scheme in bonding such species to the silica surface. This is possible because an analysis of materials in the near i.r. most commonly furnishes information about the vibrational overtones and combination bands of a number of the familiar group frequencies of the fundamental i.r. region that are so useful in organic structural analysis. Distinctive bands in the near-i.r. p.a.s. absorption spectrum which arise from the C—H stretch overtones in hydrocarbonaceous samples may be used to discern qualitative features of the group producing the absorption, e.g., adjacent unsaturation. In this way, the nature of the monolayer of organic molecules on the modified silica surface may be probed by near-i.r. p.a.s.

While information from the near-i.r. region is somewhat less definitive than that obtained from the fundamental i.r. region [8], near-i.r. spectrophotometry has been previously used with success, particularly when applied to hydrocarbonaceous samples [9]. There can be several experimental advantages in utilizing the near i.r. The first of these stems from the fact that this region contains overtones or harmonics of molecular vibrational frequencies, and shifts in the absorption maxima, elicited by perturbations in the chemical environment of the group involved, will be amplified by a factor slightly less than the integer that is the order of the harmonic, i.e., $(\sim 2\nu_f + \sim 2\Delta\nu)$ vs. $(\nu_f + \Delta\nu)$. Theory predicts no serious concomitant broadening of the overtone absorption envelope (the rotational sublevels are not harmonics), so a net advantage in the ability to detect shifts and measure them more accurately should be realized. Another advantage arises from the observation that the molar absorptivity of certain molecular vibrational frequencies are so diminished in the near-i.r. that some potential broad-band interferences are virtually eliminated, e.g., the H-bonded O—H stretching overtone [10]. These facts, combined with the minimal sample preparation and manipulation required to obtain a p.a.s. spectrum, would seem to make near-i.r. p.a.s. an attractive method for the characterization of silicas whose surfaces have been altered through the addition of a layer of surface-bound organic molecules.

EXPERIMENTAL

Preparation of chemically-modified silicas

Approximately 1.5 g of a microparticulate silica gel, LiChrosorb SI-60 (EM Laboratories, Elmsford, N.Y.), with a mean particle size of 10 μm, were introduced into a reaction vessel containing 50 ml of dry toluene (distilled from calcium hydride and stored over sodium metal) in an atmosphere of dry nitrogen gas. An excess (8 mmol) of organomethyldichlorosilane reagent (Petrarch Systems, Levittown, Pa.) was added to the mixture followed by 2.5 ml of dry pyridine, and the reaction mixture was allowed to reflux under dry nitrogen for 24 h. The organic substituents on the silane reagents included cyclohexyl, 2-(3-cyclohexenyl)-ethyl, β-phenethyl, bicyclo[2.2.1.]hept-3-yl, bicyclo[2.2.1.]hept-5-en-3-yl, and n-heptyl moieties. After completion of the reaction, the silica was collected and washed with benzene, acetone,

methanol, methanol/water, and acetone. The washed silica was oven-dried at 110°C for 2 h. The resulting material was submitted for elemental carbon and hydrogen determinations (MHW Laboratories, Phoenix, AZ) and the results obtained agree satisfactorily with expected carbon coverages. The mean surface coverage of the samples examined in this report ranged from 1.1 to 1.3 organic molecules per nm^2 (100 $Å^2$).

Photoacoustic studies

All p.a.s. spectra were acquired with a Princeton Applied Research (Princeton, N.J.) model 6001 spectrometer. The instrument is capable of spectral data acquisition from 200 to 2600 nm but only the region between 1000 and 2000 nm was used in this study. A high-pressure xenon lamp is employed as the source and three gratings provide wavelength isolation over the scanning range of the spectrometer. The powdered samples were contained in cylindrical stainless steel sample cells with cavity volumes of 0.1 ml. The molar absorptivities of the C—H stretch overtones examined in the near-i.r. are low and consequently dilution of the samples with a photoacoustically transparent solid to prevent signal saturation was unnecessary.

RESULTS AND DISCUSSION

Photoacoustic spectra of three hydrocarbonaceous cyclic systems (cyclohexyl, cyclohexenyl, and phenyl) bonded to silica gel are shown in Fig. 1.

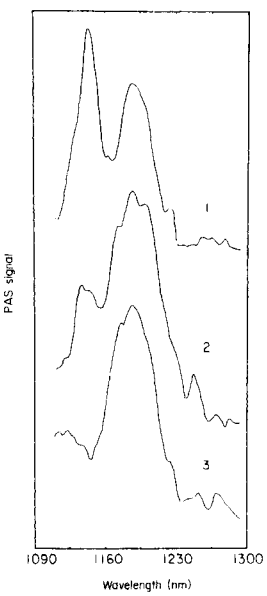

Fig. 1. P.a.s. spectra of silica gel modified through reaction with silane reagents which introduce phenyl (1), cyclohexenyl (2) and cyclohexyl (3) moieties on the silica surface.

The bands in the spectra arise from absorptions corresponding to the second overtone of the C—H stretch vibrational mode. Even though the molar absorptivity of this overtone is low, the detection system is sufficiently sensitive to yield well-resolved, relatively noise-free spectra. The second overtone was chosen for study in preference to the more strongly absorbing first overtone, because it is more completely separated from potential interferences, e.g., combination bands of C—H and O—H vibrational modes. It may be seen that the spectrum of the cyclohexyl-modified silica displays a relatively symmetric band that is a result of the similarity of the C—H stretches giving rise to the absorption. The prominent peak at 1186 nm results from the methylene carbons of the cyclohexyl ring and the small partially resolved feature at 1173 nm arises from the methyl group that comprised the adjacent moiety on the organomethyldichlorosilane. The cylcohexenyl system yields a spectrum with the characteristic methylene and methyl bands, as well as a band at 1140 nm which is indicative of the two *cis* hydrogens attached to sp^2 carbons in this system. This trend culminates in the spectrum of the phenyl system where the band at 1140 nm is seen to be the most prominent aspect. The band at 1186 nm occurs because the silane reagent employed to produce this and the cyclohexenyl-modified silica contained an ethyl linkage between the cyclic moiety and the silicon atom of the silane.

The spectra of the bonded cyclohexyl and phenyl systems were compared to near-i.r. p.a.s. spectra obtained for the corresponding neat liquids and good agreement was observed. In general, the liquid spectra were better resolved than the bonded system spectra and the absorption maxima in the liquid spectra were shifted slightly to shorter wavelengths. These results suggest that the bonded phase may manifest a blend of liquid- and solid-state behavior because of the loss in mobility that the bonded molecules suffer as a consequence of their immobilization on the silica surface. Poorer resolution in the bonded system spectra may then parallel the poorer resolution that is an inherent feature of solid-state vibrational spectroscopy. Additionally, the bonding of the organic moiety to the effectively infinite mass of the silica gel substrate produces molecular vibrations, for those C—H groups adjacent to the point of immobilization, that are slightly lower in frequency than the corresponding groups in the free molecule. Such an effect could account for the shift observed in the bonded system spectra.

Another example of the ability of p.a.s. to characterize qualitatively the surface of modified silicas is demonstrated in Fig. 2. These silicas had been modified with reagents which introduce bicycloheptyl and bicycloheptenyl functions on the surface. It may be seen that the spectrum for the bicycloheptyl system shows a band that is indicative of $-CH_2-$ groups, but this band is shifted somewhat from the methylene absorption in the cyclohexyl system. The bicycloheptenyl bonded system yields a spectrum that displays the methylene absorption observed above as well as a band (at 1140 nm) arising from hydrogens bonded to sp^2 carbons in the ring. To assess the ability of

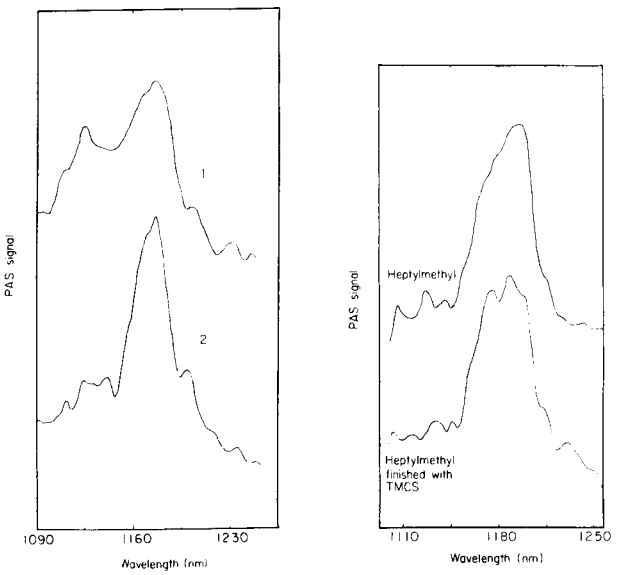

Fig. 2. Near-i.r. p.a.s. spectra of (1) bicycloheptenyl- and (2) bicycloheptyl-modified silica gel.

Fig. 3. Spectra of silica gel which has been reacted with n-heptylmethyl-dichlorosilane for 30 min (upper trace) and of the same silica after a finishing reaction with trimethylchlorosilane for 12 h (lower trace).

near-i.r. p.a.s. to discriminate between closely similar bonded moieties, a bicycloheptyl-modified silica in which the silyl group was substituted in the *endo* position on the ring (at the 2-position) was prepared for comparison with the *exo*-substituted bicycloheptyl system. Essentially identical spectra were produced for both bonded systems under the conditions employed in the comparison, i.e., data acquired at room temperature with 8-nm spectral resolution.

A further illustration of the qualitative utility of near-i.r. p.a.s. makes use of its ability to discriminate between methyl and methylene vibrational overtones. In this example, silicas that have been modified with an n-alkylmethyldichlorosilane and finished with a treatment of trimethylchlorosilane (TMCS) are employed to typify a currently important application of silica modification chemistry, that is, in the preparation of chemically-bonded reverse phases for use in liquid chromatography. Figure 3 presents spectra of an n-heptylmethyl modified silica gel (upper trace) and the same modified silica after a finishing reaction with TMCS (lower trace). It can be seen in the lower trace that those bands which signify methyl group absorptions (at 1174 nm) have grown at the expense of the methylene band at 1186 nm. This result suggests that the silica surface had been incompletely covered by the heptylmethyl function and that a significant number of residual surface silanol

groups had gone on to react with TMCS. It is a common practice in the preparation of chromatographic bonded reverse phases to finish the alkylated silica by a final reaction with a methylsilane to remove unreacted silanol groups which might complicate chromatographic retention, but it is usually found that the most satisfactory bonded reverse phases are those which undergo negligible further reaction with TMCS, implying a fully alkylated surface with no accessible silanol groups remaining. It appears that p.a.s. could offer a convenient means for monitoring the success of an optimization scheme applied to the preparation of bonded hydrocarbonaceous chromatographic stationary phases through its potential for the detection of methyl and methylene absorbances. The reaction time and conditions necessary for complete alkylation of the silica surface might be readily assessed through an examination of the spectrum of the modified material; a methyl band in the spectrum that does not increase after TMCS finishing would imply a complete reaction of the surface with the alkyl reagent.

An attempt to quantify coverage on the silicas was not undertaken in this study, but the near-i.r. has previously been shown to be an especially useful region for the assessment of relative ratios of methyl and methylene groups in hydrocarbon samples [11]. Although quantitative measurement with p.a.s. is more complex than with conventional absorption spectroscopic techniques [12, 13], it is hoped that relative measurements, employing well-characterized materials, will permit rapid and simple quantitative analysis of organically-modified silicas by p.a.s.

The authors gratefully acknowledge the assistance of Dr. Jon Howell in acquiring the photoacoustic records and of Helen H. Hangac for preparing several of the modified silica samples. This work was supported by a grant (to C. H. L.) from the National Science Foundation, CHE-781807.

REFERENCES

1 A. Rosencwaig, Opt. Comm., 7 (1973) 305.
2 A. Rosencwaig, Anal. Chem., 47 (1975) 592A.
3 M. J. Adams, B. C. Beadle, A. A. King and G. F. Kirkbright, Analyst, 101 (1976) 553.
4 E. M. Monahan, Jr. and A. W. Nolle, J. Appl. Phys., 48 (1977) 3519.
5 M. J. D. Low and G. A. Parodi, Spectrosc. Lett., 11 (1978) 581.
6 D. E. Leyden, M. L. Steele, B. B. Jablonski and R. B. Somoano, Anal. Chim. Acta, 100 (1978) 545.
7 C. H. Lochmüller, S. F. Marshall and D. R. Wilder, Anal. Chem., 52 (1980) 19.
8 J. B. Lambert, H. F. Shurvell, L. Verbit, R. G. Cooks and G. H. Stout, Organic Structural Analysis, 1976, MacMillan, New York, p. 156.
9 O. H. Wheeler, Chem. Rev., 59 (1959) 629.
10 W. A. P. Luck in F. Franks, Water — A Comprehensive Treatise, Vol. 2, Plenum Press, New York, 1973, p. 288.
11 A. Evans and R. R. Hibbard, Anal. Chem., 23 (1951) 1604.
12 A. Rosencwaig, J. Appl. Phys., 49 (1978) 2905.
13 J. C. Roark, R. A. Palmer and J. S. Hutchison, Chem. Phys. Lett., 60 (1978) 112.

Analytica Chimica Acta, 116 (1980) 25—32

MEASUREMENT OF ETCHING AFTER IRRADIATION WITH CHARGED PARTICLES BY USING THE MATRIX ACTIVATION

M. VALLADON, G. BLONDIAUX, A. GIOVAGNOLI, C. KOEMMERER and J. L. DEBRUN*

C.N.R.S., Service du Cyclotron 3A rue de la Ferollerie, 45045 Orleans Cedex (France)

(Received 17th September 1979)

SUMMARY

In the proposed method, activation of the sample matrix itself is used to measure the extent of etching after activation with charged particles. In a given energy region, a small variation of the incident beam energy, which corresponds to a small thickness of sample, will lead to a large variation of the activation yield. The method is applied to the determination of oxygen by the $^{16}O(^{3}_{1}H, n)^{18}F$ reaction, and of carbon by the $^{12}C(^{2}_{1}H, n)^{13}N$ reaction, in gallium arsenide and a titanium alloy. The results are in good agreement with those obtained by mechanical systems.

The possibility of eliminating surface contamination by etching after irradiation is one of the major advantages of activation analysis. Measurement of the etching is not very critical when neutron or photon activation is used, because in these cases the samples are quite uniformly activated; the etching process can be severe and need only be checked by weight loss measurements. In charged-particle activation, however, the etching is very critical because of the strong interaction of these ions with matter: as the charged particles penetrate the sample they rapidly lose their energy and the cross-sections of the reactions used for analysis vary very considerably. Consequently, the activation of the samples is uniform and is limited in depth. Furthermore, the lower the energy of the incident ions, the smaller their range in the sample and the larger the proportion of the activated sample eliminated by etching. Thus, the lower the energy, the bigger the analytical error for a given error of measurement of the amount of etching.

The measurement of this etching can be seriously in error, especially if weight loss measurements are used; and there are problems of radiation damage and/or of surface modification which can change the "normal" rate of etching. In order to improve the accuracy of low-energy charged-particle activation analysis, a mechanical system has been proposed to measure the etching only within the irradiated area [1]. This system requires much practice when the etching is of the order of only a few micrometres; also, the irradiated spot must be large compared to the tip of the measuring probe. Finally, the quality of the results depends on the surface roughness

after etching. The problem is the same when a surface-texture measuring instrument (e.g. Tallysurf or Tallystep) is used, after formation of a reference step on the sample surface. This paper describes a new method for the measurement of the amount of etching. It is based on activation of the matrix and does not require the use of any special apparatus. It measures the etching in the irradiated zone only and integrates any defects created during the etching.

Principle of the method

The method is based on the fact that when the energy of the incident particle is low, e.g. 2 MeV/nucleon, the thick target activation yields vary rapidly with energy. Precise etching measurements can then be achieved after irradiation, because a small change in energy (i.e., a small amount of etching) corresponds to a large variation in activity, which is easy to detect.

The first step is to construct the curve $Y = f(E)$ for the matrix to be analyzed, where Y is the normalized thick target yield:

$$Y = K \int_0^{E_i} \sigma(E)\mathrm{d}E/S(E, X)$$

Here, Y is the normalized thick target yield, and K is the normalizing factor. The latter is identical for all incident energies E_i, and includes the number of target atoms, the beam intensity, and corrections for decay and saturation. The cross-section of the reaction used is indicated by $\sigma(E)$, and $S(E, X)$ signifies the stopping power of the matrix X.

The curve $Y = f(E)$ can be constructed in any units as far as the Y values are concerned. After activation of the sample, the normalized thick target yield has to be measured after etching. The residual energy after etching, E_r, is then directly derived from the curve $Y = f(E)$ (see Fig. 1).

It is sometimes also possible to measure the thick target yield before etching; E_r can then be deduced from the experimental ratio $R = f(E_r)/f(E_i)$, by using the curve $f(E)/f(E_i)$ obtained from the curve $Y = f(E)$. This second procedure offers the advantage that relative yields are measured, instead of having to refer to the conditions used in construction of the thick target yield curve. Two measurements are necessary, however, whereas the first procedure requires only one.

When E_r is known, the value of the amount of etching (δx) can be obtained from the range—energy relationship $x = g(E)$ (see, for example, [2]). Thus $\delta x = g(E_i) - g(E_r)$, where δx is generally obtained in g cm^{-2}. The density of the sample is needed to calculate the amount of etching in units of length (e.g., μm). But the interesting point in utilizing activation of the matrix is that the value of δx need not be known. Only E_r is of interest since the various methods for quantification make use of the ratio of the ranges in the sample and in the standard at $E = E_r$ [3]; or the ratio of the stopping powers of the sample and of the standard at an energy derived from E_r [4—6]. The possibility of avoiding the use of the range—energy relationships is a definite advantage over all other existing methods of measuring the

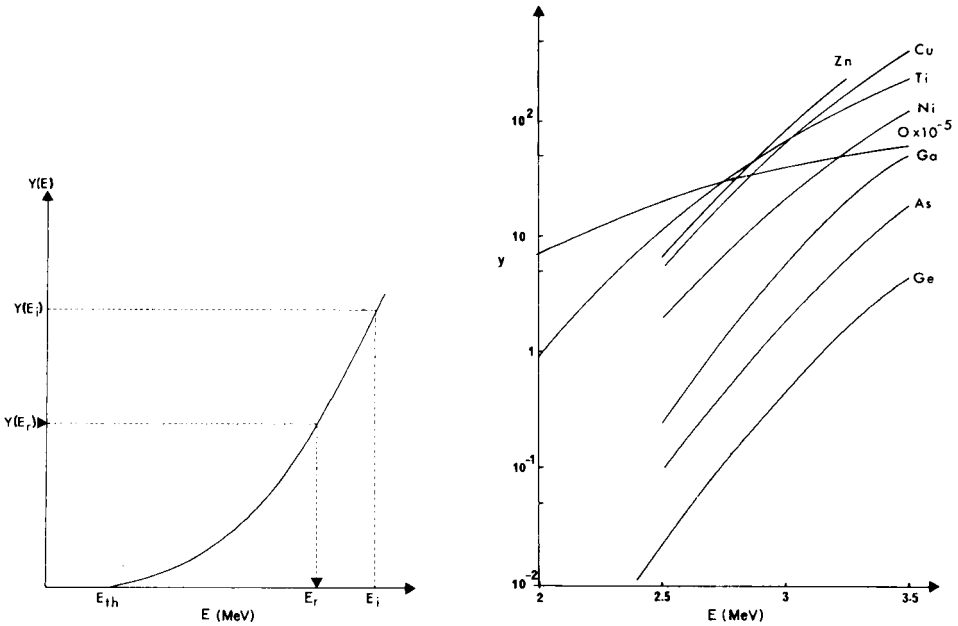

Fig. 1. Normalized thick target yield as a function of beam energy.

Fig. 2. Thick target yield (γ min^{-1} μC^{-1}) for various reactions with 1-min irradiation with 2—3.5-MeV tritons. The line corresponding to oxygen is for Al_2O_3; those for gallium and arsenic are for GaAs.

amount of etching, when the density of the sample is not well established. Also, when combined with the "double reaction method" [7], in which stopping power data or range data are unnecessary, the activation of the matrix has the possibility of being free from any systematic errors that may be introduced by these data. This is of special interest when heavy ions are used, because of the inaccuracy of the corresponding stopping power data at the present time. The technique was applied to the determination of oxygen in gallium arsenide and a titanium alloy by triton activation, and to the determination of carbon in gallium arsenide by deuteron activation.

LOW-ENERGY TRITON ACTIVATION ANALYSIS

Activation of various elements with low-energy tritons

The thick target yield curves were constructed between 2 and 3.5 MeV for the following reactions (Fig. 2): $^{16}O(^3_1H, n)^{18}F$, $^{48}Ti(^3_1H, \alpha)^{47}Sc$, $^{62}Ni(^3_1H, n)^{64}Cu$, $^{63}Cu(^3_1H, d)^{64}Cu$, $^{64}Zn(^3_1H, n)^{66}Ga$, $^{71}Ga(^3_1H, p)^{73}Ga$, $^{74}Ge(^3_1H, n)^{76}As$, $^{75}As(^3_1H, d)^{76}As$.

For matrices of medium atomic number (Ti, Ni, Cu, Zn, Ga, Ge, As), the thick target yield between 2.5 and 3.2 MeV can be fitted by approximation

either to an exponential function $Y = a \exp(bE)$ or to a power function $Y = aE^b$. In the case of the exponential function, the parameter b varies from 3 to 6. There is indeed a strong variation of Y with energy. If the yield of the $^{16}O(T, n)^{18}F$ reaction is compared with the yields of the other reactions listed above, it appears that the yields of the other reactions are much smaller, and that the yield of the reaction on oxygen is much less sensitive to energy variations. For oxygen, $b = 1.9$ for the exponential function. For these reasons, ca. 3-MeV triton activation is particularly well suited for the determination of oxygen in matrices of medium atomic number, and the activation of the matrix can be used to measure the energy after etching. Furthermore, the level of activity induced in these matrices is so small that non-destructive determination of oxygen down to ca. 10 ppb is feasible in germanium and gallium arsenide [1].

Application to the determination of oxygen in gallium arsenide and in a titanium-based alloy (TA6V)

For gallium arsenide and TA6V, the error on the final analytical result, Δx, is rectilinearly related to the error ΔE in E_r (the residual energy after etching). The calculations were based on residual energies of 2.7 MeV for gallium arsenide and 3.2 MeV for TA6V, because these are values often encountered in actual analyses. For ΔE in the range 0—2%, Δx increases from 0 to 6.5% for gallium arsenide, and from 0 to 4.7% for TA6V.

In the case of the mechanical system [1], the error is estimated to be 0.5 μm. Figure 3A, B shows the errors in ΔE and on Δx, introduced by this uncertainty of 0.5 μm, as a function of energy for the two matrices studied. When the activation of the matrix is used, the errors are due mainly to counting statistics; for GaAs and TA6V, the total error in the activation yield is usually less than 5%. Figure 3C, D indicates the variation of ΔE and Δx with E_r, for a total error of 5% in the activation yield. It is clear from Fig. 3 that the activation results are intrinsically more precise. The results obtained by the mechanical system and by matrix activation are shown in Tables 1 and 2. There is a good agreement, but if the activation method is chosen as the reference, it seems that the mechanical system tends to underestimate the etching for the smaller values and to overestimate it for the higher values.

LOW-ENERGY DEUTERON ACTIVATION ANALYSIS: DETERMINATION OF CARBON IN GALLIUM ARSENIDE

The reaction $^{12}C(^2_1H, n)^{13}N$ is very good for the determination of carbon. Figure 4 represents the specific γ-activities obtained by irradiation of carbon and gallium arsenide with 2.5—3-MeV deuterons. It is clear that carbon can be determined non-destructively at trace levels in this energy range [8]. As in the case of triton activation, the matrix activity can be used to measure the etching: between 2.5 and 3 MeV the ^{76}As activity from the $^{75}As(^2H, p)$

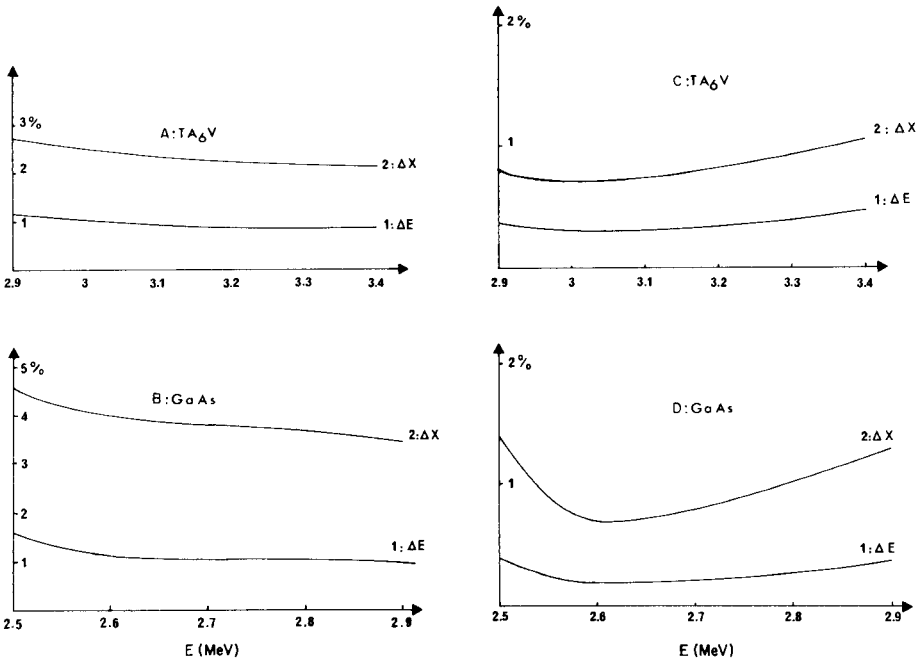

Fig. 3. Errors in E and x as a function of beam energy: (A, B) calculated for an estimated error of 0.5 μm in the mechanical system [1]; (C, D) calculated for a total error of 5% in the activation yield for the matrix activation method.

TABLE 1

Comparison of the results for gallium arsenide obtained for the energy after etching by the mechanical system and by activation of the matrix, after irradiation with 3-MeV tritons

Etching (μm)	Energy after etching, E_r (MeV)		Difference (%)	Etching	Energy after etching, E_r (MeV)		Difference (%)
	Mechanical system[a]	Activation system[b]			Mechanical system[a]	Activation system[b]	
3.5	2.794	2.766	+1	4.6	2.713	2.715	−0.07
4.1	2.758	2.698	+2.2	5.0	2.706	2.755	−1.8
4.2	2.752	2.749	+0.1	5.2	2.693	2.720	−1
4.3	2.748	2.698	+1.85	5.7	2.662	2.716	−2
4.4	2.742	2.738	+0.15	6.5	2.614	2.611	+0.1
4.5	2.736	2.718	+0.65				

[a]Measured with the mechanical system.
[b]Average from ^{76}As and ^{73}Ga.

^{76}As reaction increases by a factor of 7, and the same applies to the ^{72}Ga activity from the ^{71}Ga(^{2}H, p)^{72}Ga reaction. Table 3 compares results obtained with a Tallysurf with results obtained by activation of the matrix. There is good agreement between the two methods, and between the three different activation measurements.

TABLE 2

Comparison of the results for TA6V obtained for the energy after etching, by the mechanical system and the activation of the matrix after irradiation with 3.5 MeV tritons

Etching (μm)	Energy after etching, E_r (MeV)		Difference (%)	Etching (μm)	Energy after etching, E_r (MeV)		Diffe (%)
	Mechanical system[a]	Activation system[b]			Mechanical system[a]	Activation system[b]	
4.9	3.212	3.225	−0.4	5.5	3.174	3.20	−0.8
5.0	3.205	3.185	+0.63	5.5	3.174	3.207	−1.0
5.1	3.20	3.192	+0.25	5.5	3.174	3.215	−1.2
5.2	3.193	3.146	+1.5	5.7	3.162	3.168	−0.1
5.3	3.187	3.188	−0.03	6.2	3.132	3.125	+0.2
5.5	3.174	3.153	+0.67	6.3	3.126	3.165	−1.2
5.5	3.174	3.165	+0.28	6.5	3.113	3.084	+0.8
5.5	3.174	3.170	+0.13	6.7	3.102	3.12	−0.5

[a]Measured with the mechanical system.
[b]Calculated from the ^{47}Sc activity.

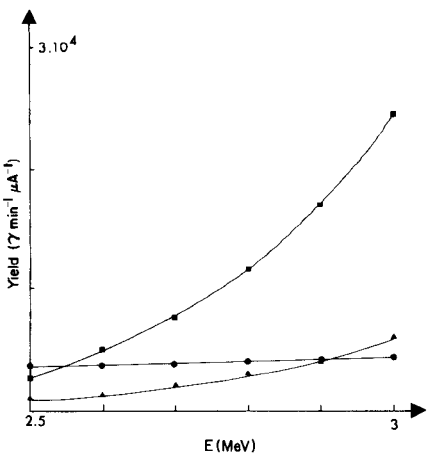

Fig. 4. Activation of gallium arsenide with 2.5—3-MeV deuterons: (■) ^{72}Ga; (▲) ^{76}As; (●) ^{13}N (× 10^{-6}).

DISCUSSION

The matrix activity cannot always be used to measure the amount of etching. To obtain good precision, one is limited to an energy region where the activation of the matrix increases exponentially (i.e. subcoulombic activation). It is also necessary to consider the effect of the nuclear reaction on the sought impurity: the activity from the impurity must be high enough, and there should be no interfering nuclear reactions. This last point may set an upper limit to the energy that can be used.

Other limitations of the method are imposed by nuclear reactions

TABLE 3

Comparison of the results for gallium arsenide obtained for the residual energy after etching (in MeV) by the mechanical system and the activation of the matrix after irradiation with 3-MeV deuterons

Mechanical system	Activation system			Difference (%)[a]
	from 560-keV ^{76}As	from 630-keV ^{72}Ga	from 835 keV ^{72}Ga	
2.990	2.985	2.960	2.970	+0.6
2.950	2.942	2.955	2.960	—0.08
2.850	2.820	2.840	2.835	+0.6
2.805	2.770	2.785	2.780	+1
2.780	2.763	2.760	2.780	+0.4
2.775	2.730	2.735	2.735	+1.5

[a]Difference between E_r values for the mechanical system and the mean of the activation values.

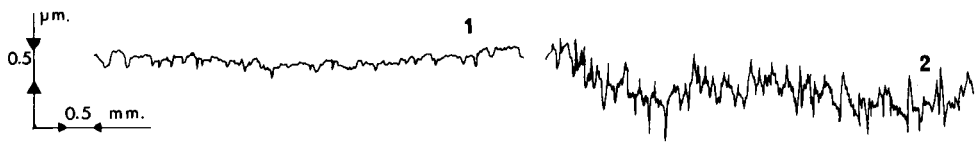

Fig. 5. Surface profiles before (1) and after (2) etching of the titanium alloy with $HF—H_3PO_4—H_2O$ (1 + 1 + 20).

yielding stable isotopes or radioisotopes with unfavourable characteristics (e.g. too short a half-life). However, when no suitable matrix activity is obtained with the particle used, it is sometimes possible to pre-activate with another particle; the use of range—energy relationships then becomes necessary. When the method can be fully used, it presents several advantages. No special equipment (Tallysurf, electronic comparator, etc.) is required. The sample density need not be known. When used with the double reaction method [7], no stopping data or ranges are needed; this is a definite advantage in the case of heavy ions, for which accurate data are scarce. The value obtained for E_r represents an average, taking into account any surface roughness. The last point is especially interesting because it is not always possible to obtain very flat surfaces after chemical etching. For instance, in the case of the titanium alloy, the surface roughness is of the order of 0.5 μm (Fig. 5). This introduces uncertainty into the mechanical measurement of the etching. However, the value obtained by the activation of the matrix is a good estimate of the average etching.

Considering the conditions of use of this method and its characteristics, it is probably advantageous to use it when the etching is limited (e.g. $\leqslant 5$ μm) and/or when the particles used for activation have a limited energy, say less than 2—3 MeV/nucleon for most particles.

We are grateful to the C.N.R.S. (Centre de recherches nucléaires de Strasbourg-Cronenbourg) for permission to use the Van de Graaff accelerators.

REFERENCES

1 M. Valladon and J. L. Debrun, J. Radioanal. Chem., 39 (1977) 385.
2 C. F. Williamson, J. P. Boujot and J. Picard, Rapport CEA-R 3042 (1966).
3 E. Ricci and R. L. Hahn, Anal. Chem., 37 (1965) 742; 39 (1967) 794.
4 M. A. Chaudhri, G. Burns, E. Reen, J. L. Rouse and B. M. Spicer, Proceedings of the International Conference on Modern Trends in Activation Analysis, München, 1976.
5 G. Deconninck, J. Radioanal. Chem., 12 (1972) 157.
6 K. Ishii, M. Valladon and J. L. Debrun, Nucl. Instrum. Methods, 150 (1978) 213.
7 K. Ishii, C. S. Sastri, M. Valladon, B. Borderie and J. L. Debrun, Nucl. Instrum. Methods, 153 (1978) 507.
8 M. Valladon, G. Blondiaux, C. Koemmerer, J. Hallais, G. Poiblaud, A. Huber and J. L. Debrun, J. Radioanal. Chem., in press.

Analytica Chimica Acta, 116 (1980) 33—39

AMPEROMETRIC FLOW-THROUGH WIRE DETECTOR: A PRACTICAL DESIGN WITH HIGH SENSITIVITY

JEAN A. LOWN**, ROSS KOILE*** and DENNIS C. JOHNSON*

Department of Chemistry, Iowa State University, Ames, Iowa 50011 (U.S.A.)

(Received 23rd October 1979)

SUMMARY

A flow-through detector is described which is easily constructed at low cost for application to flow-injection analysis, liquid chromatography and continuous stream analysis. The platinum wire indicating electrode is stretched through a narrow channel cut in a glass-filled teflon block, which also holds the reference and auxiliary electrodes. The response of the detector to ca. 10^{-5} M iodide and arsenic(III) solutions is compared with theoretical predictions for an annular flow cell under laminar fluid dynamics.

The investigation of new electrode geometries for application to hydrodynamic voltammetry, and the solution of the equation of mass transport for these geometries, has long been fashionable for academic electroanalytical research. While the achievement of higher analytical sensitivity and convenience would seem to be sufficient motivation for such research, the work is usually considered unfinished unless equations are presented which predict quantitatively the shapes of current—potential curves and permit quantitative measurement of heterogeneous rate constants. Indeed, from a cursory study of the modern literature on analytical voltammetry, one can hardly avoid the false conclusion that applications of voltammetry for quantitative analysis are possible only if the theoretical relationship between the limiting electrode current and bulk analyte concentration is fully described as a function of all experimental variables. In practice, however, amperometric applications of hydrodynamic voltammetry always rely on calibration with suitable standards. Even for an absolute detector such as the coulometric flow-through electrode (100% efficient), a standard sample is usually analyzed to verify coulometric operation under the appropriate experimental conditions in careful work [1].

The tubular electrode is one geometry which has become popular and the equation of mass transport under laminar fluid flow has been solved [2—4]. Tubular electrodes constructed from noble metals and carbon have found many applications as flow-through detectors [5]. Construction of usable tubular electrodes can, however, be a frustrating experience. The greatest source of difficulty comes from degradation of the interface between the

**Present address: Union Carbide Corp., Bound Brook, NJ, U.S.A.
***Present address: Dow Chemical Co., Midland, MI, U.S.A.

electrode and the inert material used to construct the cell. Leakage of the electrolyte solution into the interface can cause a large increase in the residual current, and diffusion of analyte into the trapped solution can lead to significant tailing in applications for flow-injection analysis or liquid chromatography. Also, irregularities in the dimensions of the inlet channel, resulting from construction error or aging of materials, can cause local turbulence. This turbulence tends to invalidate the mathematical derivations based on the assumption of laminar flow, and calibration of the detector response is essential [6]. These problems have been experienced for a variety of cell materials including teflon, Kel-F and epoxy.

The design and operation of a very inexpensive, easily constructed flow-through detector with a noble-metal wire electrode are described below. The detector has reasonable efficiency (15—30%) and has given trouble-free operation for three years. The equation of mass transport has not been solved exactly for this particular design but quantitative applications with calibration have been quite satisfactory.

EXPERIMENTAL

Detector design

Diagrams of the flow-through detector are shown in Fig. 1. The body of the detector was machined from a rod (1.0 in. × 1.5 in.) of 25% glass-filled teflon (GFT; Crown Plastic, Inc., St. Paul, Minnesota). The GFT is harder than teflon with machining properties similar to Kel-F, but costs much less than Kel-F. The indicating electrode (IE) was a 16-gauge platinum wire (0.130-cm diameter) inserted through a 0.060-in. i.d. (0.152 cm) tubular channel drilled through the GFT. The choice of wire diameter was a matter of convenience and the diameter of the channel was chosen to be only slightly larger than that of the wire so that maximum sensitivity could be obtained. Compression seals at each end of the indicating electrode were made from 1/8 in. FETFE, a pliable fluoroelastomer (Ace Glass, Inc., Vineland, New Jersey). FETFE is very inert to corrosive and strong acids, and no deterioration has been observed in the seals over the three-year period that the detector has been used. The FETFE seals were compressed with polypropylene tube-end fittings (Laboratory Data Control, Riviera Beach, Florida). The length of the exposed portion of the indicator electrode in the fluid channel was 2.1 cm and the dead volume was calculated to be 10.2 μl.

The 0.060-in. i.d. (0.152-cm) channel directing fluid from the indicator electrode compartment to the reference electrode compartment (RE) was drilled from the side of the GFT and the unused portion was plugged with a small piece of teflon which had been machined to the appropriate dimensions. The counter electrode was a short length of platinum wire inserted into the reference electrode compartment through a FETFE seal. The reference electrode was a miniature calomel reference electrode (No. 476017;

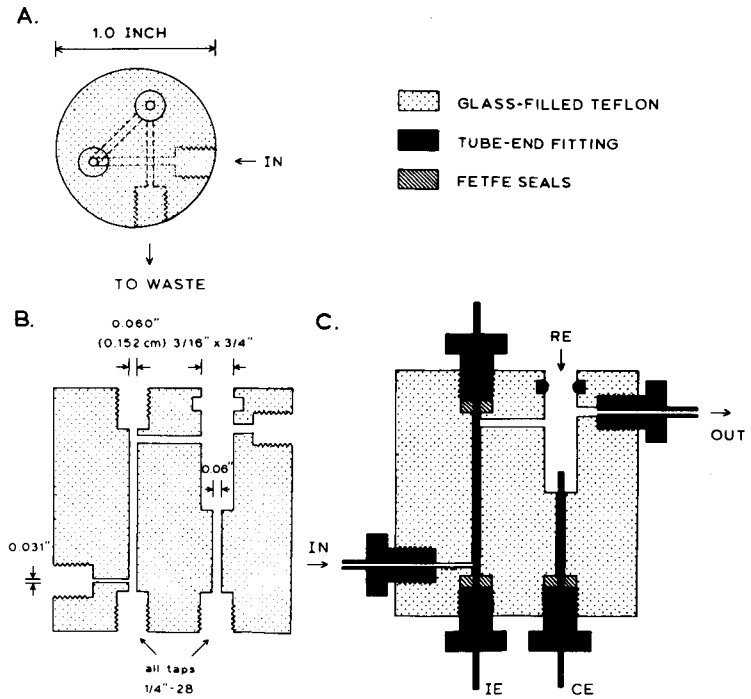

Fig. 1. Cross-sectional diagram of wire flow-through detector. (A) Top view of cell; (B) fold-out side projection of teflon body; (C) projection of assembled cell; (IE) indicator electrode; (CE) counter electrode; (RE) position of miniature saturated calomel reference electrode.

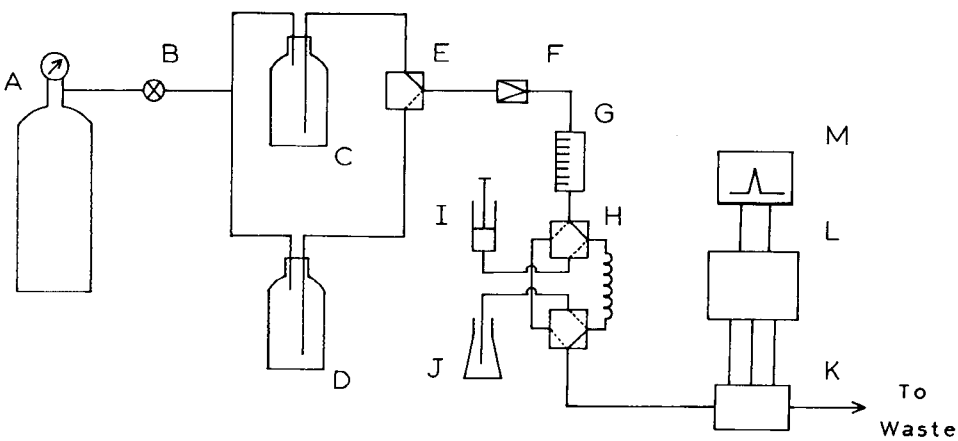

Fig. 2. Schematic diagram of flow analyzer. (A) Helium tank; (B) on/off valve; (C) reagent bottle 1; (D) reagent bottle 2; (E) selector valve; (F) needle valve; (G) flow meter; (H) sample injection valve; (I) syringe; (J) sample; (K) detector; (L) potentiostat; (M) recorder.

Corning Scientific Instruments, Medfield, Massachusetts) with a fiber junction. The tip of this electrode was inserted into the RE compartment below the level of the horizontal channels. A FETFE O-ring, placed about the tip of the reference electrode and positioned near the top of the RE compartment, provided a leak-free seal. Consequently, all fluid left the detector through the teflon tubing to a waste container.

Flow analyzer

The flow analyzer is outlined in Fig. 2. Compressed helium (<30 psi) applied to the head space of the reagent bottles caused the flow of solution. Fluid flow rates were monitored by a compact spherical-float flow meter (Gilmont Instruments, Inc., Great Neck, New Jersey). The flow meter was calibrated for the solutions used in this research. Uncertainty in the flow rates is approximately 5% at 2 ml min^{-1} and about 10% at 0.5 ml min^{-1}. All teflon tubing and tube-end fittings for interconnecting the components of the analyzer were from Laboratory Data Control.

For steady-state analysis, the selector valve (E) was set to pass a solution of the analyte in 1.0 M H_2SO_4 (Reagent 1) continuously through the detector. For flow-injection analysis, the selector valve was set to pass a solution containing only 1.0 M H_2SO_4 (Reagent 2). Samples were injected by a pneumatically activated valve (H) from Laboratory Data Control. The sample volume was 0.226 ml. Solutions of sodium iodide were deaerated and maintained under an atmosphere of helium to prevent oxidation by dissolved oxygen.

Potentiostatic control and measurement of detector current was provided by a Polarographic Analyzer (Princeton Applied Research, model 174A). Current—time data were monitored on a stripchart recorder (Heath-Schlumberger model SR-204). Peaks on the chart were integrated with a Kueffel-Esser compensating planimeter.

All chemicals were reagent grade and water was triply distilled with demineralization after the first distillation.

THEORY OF DETECTOR RESPONSE

The limiting current (I_l) response for flow-through electrodes is described by the general equation $I_l = nFAK_l v_f^{\alpha} C$. Here, n is the number of electrons in the reaction (eq mol^{-1}), F is the faraday constant (C eq^{-1}), A is electrode area (cm^2), v_f is the fluid flow rate (cm^3 s^{-1}), α is a fraction which is characteristic of electrode geometry and fluid dynamics, C is the concentration of analyte in the stream entering the detector (mol cm^{-3}) and K_l is the limiting, specific, mass transfer coefficient ($cm^{1-3\alpha}$ $s^{\alpha-1}$). The limiting detector current produced by the continuous flow of analyte, at a bulk concentration of C_b, has a steady-state value of I_{ss}. The electrolytic efficiency of the detector under steady-state conditions is

$$Eff = I_{ss}/I_{max} = nFAK_l v_f^{\alpha} C_b / nFV_f C_b = AK_l v_f^{\alpha-1} \quad (1)$$

When a small volume of sample, e.g., $V_s < 1$ ml with concentration C_b, is injected into a stream of electrolyte passing through the detector, the concentration of analyte will be lower than C_b at all points in the sample plug because of dispersion within the fluid stream. Hence, the peak current I_p will be less than I_{ss} when peak height is measured. Values of I_p may not be a reliable analytical measure of C_b, even with calibration, unless the factors controlling dispersion are maintained constant. For example, even small changes in the curvature of tubing which connects the sample injection valve to the detector cell can change I_p by several per cent [6]. The area of the detection peak, Q_p, can be a more reliable analytical measure of C_b. For small diameter tubing (< 1 mm) and moderately low flow rates (0.2—5 ml min^{-1}), Q_p is independent of the extent of sample dispersion:

$$Q_p = \int I_l dt = nFAK_l v_f^{\alpha} \int C dt = nFAK_l v_f^{\alpha-1} V_s C_b \quad (2)$$

The efficiency of the detector for flow-injection analysis is identical to that for steady-state analysis.

$$Eff = Q_p/Q_{max} = nFAK_l v_f^{\alpha-1} V_s C_b/nFV_s C_b = AK_l v_f^{\alpha-1} \quad (3)$$

The exact treatment of the problem of mass transport in the wire flow-through detector would be a formidable challenge because of the turbulence created by the abrupt change in the direction of the fluid flow at the entrance of the detector. Furthermore, no attempt was made in the assembly of the detector to maintain a uniform spacing between the surface of the wire and the wall of the tubular channel drilled into the GFT cell block. This electrode is, however, rather similar to the "annular" electrode treated theoretically by Ross and Wragg [7] and illustrated in Fig. 3. In their case, laminar flow was assumed for fluid in the annular space surrounding a cylindrical electrode. The predicted value of $AK_l v_f^{\alpha}$ is given by

$$AK_l v_f^{\alpha} = 3.22[\phi(a)]^{1/3} [\pi^{2/3} L^{2/3} r_l D^{2/3} v_f^{1/3}/d_e^{1/3}(r_2^2 - r_1^2)^{1/3}] \quad (4)$$

where D is the diffusion coefficient of the analyte (cm^2 s^{-1}). The remaining terms in eqn. (4) are defined as follows: $d_e = 2(r_2 - r_1)$, $a = r_1/r_2$, and

$$\phi(a) = \frac{1-a}{a}\left\{\left[0.5 - \frac{a^2}{(1-a^2)}\ln(1/a)\right]\Big/\left[\left(\frac{1+a^2}{1-a^2}\right)\ln(1/a) - 1\right]\right\} \quad (5)$$

If eqn. (4) is assumed to be applicable to the wire electrode described, AK_l

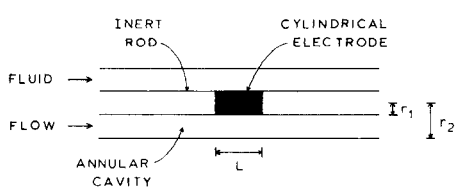

Fig. 3. Longitudinal cross-section of the "annular" electrode of Ross and Wragg [7].

is calculated to be $24.2D^{2/3}$ for r_1 = 0.0650 cm, r_2 = 0.0760 cm and L = 2.1 cm. Since the exponent, α, of v_f in eqn. (4) is 1/3, the slope of a plot of log *Eff* vs. log v_f is predicted to be −2/3.

RESULTS AND DISCUSSION

A typical recording of detection peaks for repeated injections of 6.81 × 10^{-5} M sodium iodide in 1.0 M H_2SO_4 is shown in Fig. 4. The average area for 4 peaks in the series was 201 μC with a relative standard deviation of 3%. The wire flow-through detector was used for flow-injection analysis and steady-state analysis of solutions containing either 6.81 × 10^{-5} M iodide or 1.64 × 10^{-5} M arsenic(III). The detector efficiency is plotted vs. flow rate on a log—log scale in Fig. 5. Also shown is the value of slope (α − 1) for each set of data. The experimental slopes are very nearly equal to the value of −0.667 predicted by Ross and Wragg for their annular electrode under laminar fluid flow [7]. The plot of log *Eff* vs. log v_f calculated from the function $AK_1v_f^{\alpha} = 24.2D^{2/3}v_f^{-2/3}$, using D = 1.99 × 10^{-5} cm^2 s^{-1} for iodide [8], is shown for comparison.

The precision of results obtained during continuous use of the detector is limited by the precision of the control and measurement of the flow rate. The large variation of efficiency between experiments resulted from disassembly of the detector for inspection. As specified earlier, no attempt was made to control the position of the wire within the indicator electrode channel. According to Ross and Wragg [7], the dimension of the spacing between the electrode and the channel wall is important in determining the numerical value of K_1. Once assembled, the position of the wire did not vary

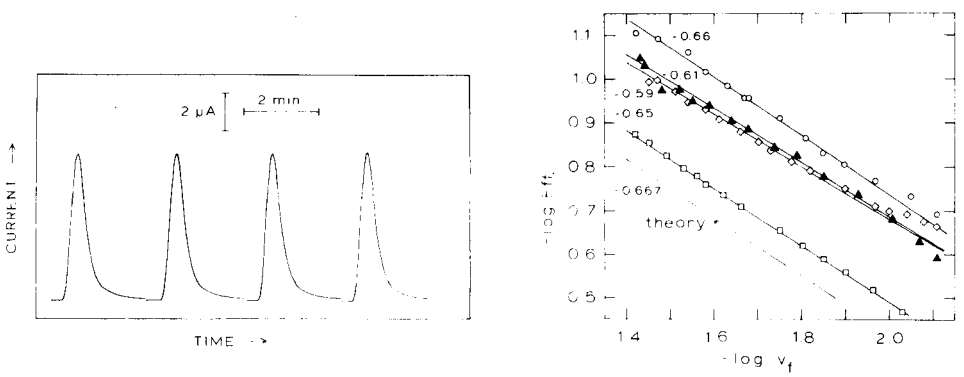

Fig. 4. Detection peaks for repeated injections of 6.81 × 10^{-5} M NaI in 1.0 M H_2SO_4, V_s = 0.226 ml, v_f = 0.99 ml min^{-1}, E = 0.80 V vs. SCE.

Fig. 5. Log—log plot of detector efficiency, *Eff*, vs. volume flow rate, v_f. Steady-state analysis: (◇) 6.81 × 10^{-5} M NaI, E = 0.80 V vs. SCE; (□) 1.64 × 10^{-5} M As(III), E = 1.0 V vs. SCE. Flow-injection analysis: (△) 6.81 × 10^{-5} M NaI, v_s = 0.226 ml, E = 0.80 V vs. SCE; (○) 1.64 × 10^{-5} M As(III), v_s = 0.226 ml, E = 1.0 V vs. SCE. (—) Theory [7]. Values of slopes given on the plots.

within the channel during normal use and K_1 was, therefore, constant.

The electrolytic efficiency of the wire detector was slightly less than predicted by eqns. (1) and (3) on the basis of eqn. (4). This results primarily from the fact that the boundary condition $C = C_b$ was assumed for the solution beyond the diffusion layer in the derivation of eqn. (4). The wire flow-through detector is similar to a flow-through thin-layer cell wherein the depletion of analyte is significant and the boundary condition given above is not applicable. Hence, the flux per unit area of electrode steadily decreases below the prediction of Ross and Wragg as the fluid passes along the indicating electrode.

The wire flow-through electrode, while not adhering strictly to the published theory for annular electrodes, has proven itself to be a very reliable detector. As with any detector applied to analysis of fluid streams, accurate analytical application requires careful control of the fluid flow rate and calibration with suitable standards.

The authors are grateful to Eldon Ness and George Steininger for construction of the detectors.

REFERENCES

1 D. C. Johnson and J. H. Larochelle, Talanta, 20 (1973) 959.
2 V. G. Levich, Physicochemical Hydrodynamics, Prentice-Hall, Englewood Cliffs, New Jersey, 1962, pp. 112—116.
3 W. J. Blaedel, C. L. Olson and L. R. Sharma, Anal. Chem., 35 (1963) 2100.
4 W. J. Blaedel and L. N. Klatt, Anal. Chem., 38 (1966) 879.
5 P. T. Kissinger, Anal. Chem., 49 (1977) 4.
6 P. L. Meschi and D. C. Johnson, to be published.
7 T. K. Ross and A. A. Wragg, Electrochim. Acta, 10 (1969) 1093.
8 A. L. Beilby and A. L. Crittenden, J. Phys. Chem., 64 (1960) 177.

Analytica Chimica Acta, 116 (1980) 41—51

ANODIC DETECTION OF ARSENIC(III) IN A FLOW-THROUGH PLATINUM ELECTRODE FOR FLOW-INJECTION ANALYSIS

JEAN A. LOWN** and DENNIS C. JOHNSON*

Department of Chemistry, Iowa State University, Ames, Iowa 50011 (U.S.A.)

(Received 1st November 1979)

SUMMARY

Arsenic(III) can be amperometrically detected by oxidation at a platinum or gold electrode in perchloric acid solutions. Platinum is the preferred material because halides interfere with the oxidation of arsenic(III) at gold electrodes. The limiting current for arsenic(III) at the platinum electrode is less than the value predicted for a mass transport-limited reaction. This decrease results either from slow linear diffusion of arsenic(III) through the oxide film, or from cylindrical diffusion to widely dispersed active sites on an inhomogeneous electrode surface. The anodic current for arsenic(III) is reproducible when the oxide film reaches a constant thickness. The detection limit for a platinum-wire flow-through detector is approximately 0.4 ppb arsenic(III). Arsenic(V) is determined after reduction to arsenic(III) by hydrazine sulfate. A cation-exchange column in the flow analyzer prevents interference from excess of hydrazine.

Previous work on the direct amperometric detection of arsenic(III) has tended to emphasize the use of mercury electrodes [1, 2]. Arsenic(V) is usually not reduced polarographically, but in the presence of 11.5 M hydrochloric acid [3] and certain complexing agents such as pyrogallol [4], a two-electron reduction is observed. Arsenic(III) is polarographically reduced to the element in acidic, neutral and alkaline media [5—7]. Detection below 10^{-4} M is difficult by conventional polarography [8, 9]. Lower detection limits have been obtained by using organic acids such as lactic [10], citric [11], ascorbic [12, 13], oxalic [14] or acetic [15] acid as the supporting electrolyte. Detection limits of about 10^{-7} M have been reported for pulse polarography [16—18] and differential pulse polarography [19—22]. Anodic stripping voltammetry (a.s.v.) has also been applied for determination of arsenic(III) at mercury electrodes [23—25].

Applications of solid electrodes for determination of arsenic(III) by a.s.v. have included gold [26—28], platinum [29, 30] and graphite [31, 32]. A detection limit of 4×10^{-9} M was reported for gold electrodes under optimum conditions [28]. Severe interference can occur in a.s.v. from the formation of interelemental species at the electrode surface.

The application of mercury or solid electrodes for the continuous

**Present address: Union Carbide Corporation, Bound Brook, New Jersey, U.S.A.

cathodic detection of arsenic(III) at trace levels in flowing streams is handicapped by the simultaneous reduction of dissolved oxygen. Continuous amperometric detection would be useful for flow-injection analysis and ion-exchange chromatography if the interference by oxygen could be eliminated. The plastic connectors and tubing used for construction of such analytical systems are, however, highly permeable to oxygen from the laboratory atmosphere, and this prevents the maintenance of a uniformly low level of oxygen in the carrier stream. The anodic detection of arsenic (III) which is free of interference from dissolved oxygen was therefore examined. Here voltammetric data leading to the choice of a platinum detector are reported. Analytical results are also presented for the determination of arsenic(V) after chemical reduction to arsenic(III).

EXPERIMENTAL

Chemicals and reagents

All chemicals were of analytical-reagent grade (J. T. Baker Chemical Co.) unless specified to the contrary. Perchloric acid was from G. F. Smith Chemical Co., Columbus, OH. All water was triply distilled with demineralization after the first distillation; the second distillation was from an alkaline permanganate solution. Primary standard stock solutions of arsenic (III) were prepared by dissolving arsenic trioxide in a minimal volume of 5 M sodium hydroxide, neutralizing the solution with perchloric acid and diluting with triply distilled water. A stock solution of arsenic(V) was prepared similarly from arsenic pentoxide. The solution of arsenic(V) was standardized by a coulometric titration as follows. An aliquot containing approximately 1 mmol of arsenic(V) was transferred to a 500-ml Erlenmeyer flask containing 10 ml of 2 M sulfuric acid and 1 g of potassium iodide; with gentle boiling, iodide quantitatively reduced As(V) to As(III), and the generated iodine was destroyed with a few drops of 1 M sodium thiosulfate. The solution was then saturated with sodium hydrogencarbonate to neutralize the acid and diluted to volume in a 100-ml volumetric flask. Coulometric analysis, with generation of iodine at constant current to the starch end-point, was applied to 10.00-ml aliquots in a buffered solution containing 0.1 M KH_2PO_4, 0.1 M K_2HPO_4 and 0.1 M KI.

A sample of Standard Reference Material 1571 (Orchard Leaves) from the National Bureau of Standards was analyzed for arsenic. The certificate value given for arsenic is 14 ± 2 $\mu g\ g^{-1}$, which was obtained by neutron activation.

Instrumentation

Voltammetric data were obtained at rotating disk electrodes (Pine Instrument Company, Grove City, PA). The areas of the gold and platinum electrodes were 0.435 cm^2 and 0.447 cm^2, respectively. These electrodes were polished to a mirror finish by a metallographic procedure in which

0.3-μm alumina was used in the final step (details are available from the authors on request). Voltammetric curves were obtained with a three-electrode potentiostat constructed from operational amplifiers. The reference electrode was a miniature Beckman saturated calomel electrode (SCE) filled with a saturated solution of sodium chloride. All potential values reported here are given with respect to that reference.

The flow-injection analyzer and flow-through detector were as described earlier [33]. The volume of the sample loop, V_s, was 0.226 ml. Potential control and current monitoring for the flow-through detector were provided by a Princeton Applied Research Polarographic Analyzer (Model 174A).

A small column (3 mm i.d. × 10 cm) of strong cation-exchange resin (AG 50W-X8; Bio-Rad Laboratories) was placed in the analyzer stream between the injection valve and the detector, when samples which had been reduced by hydrazine hydrogensulfate were analyzed. The hydrazonium ion was quantitatively adsorbed in the cation-exchange column and did not interfere with the anodic detection of arsenic(III). Carrier solutions for analysis of samples were 0.5 M or 1.0 M in perchloric acid. Adsorbed $N_2H_5^+$ was removed from the column by passing 4 M $HClO_4$ for approximately 5 min.

Reduction procedures

Hydrazine has been successfully used for the reduction of As(V) to As(III) in acidic solutions [16, 19, 34, 35]. Nitrogen is the product of oxidation of hydrazine.

Procedure A. A sample containing arsenic(V) was mixed in a 30-ml Kjeldahl flask with 0.2 g of hydrazine sulfate and 5 ml of concentrated sulfuric acid. The mixture was heated to the appearance of sulfur trioxide fumes, cooled, transferred to a 100-ml volumetric flask and diluted to volume with water.

Procedure B. Weighed samples of NBS SRM 1571 (Orchard Leaves) were mixed in 250-ml Erlenmeyer flasks with 15 ml each of concentrated nitric, sulfuric and perchloric (72%) acids. A reflux condenser was attached and the flask heated to boiling. Reddish fumes of nitrogen dioxide appeared first and were replaced by white fumes of $HClO_4 \cdot 2H_2O$. Heating was discontinued, the solution cooled, and 0.3 g of hydrazine sulfate was added with 100 ml of water. The mixture was heated until the volume was reduced by evaporation to about 50 ml. The solution was then cooled, transferred to a 100-ml volumetric flask and diluted to volume with water.

Procedure C. This was a modification of Procedure B in which perchloric acid was removed from the digestion mixture before the reduction. After the white fumes of $HClO_4 \cdot 2H_2O$ had appeared, the reflux column was removed and heating continued to volatilize all the perchloric acid from the solution. When the temperature exceeded 205°C, heating was stopped, the solution was cooled, and 0.3 g of hydrazine sulfate and 50 ml of water were added. The further treatment was as described for Procedure B.

RESULTS AND DISCUSSION

Voltammetry at a gold disk electrode

Current—potential curves (I—E) for arsenic(III) at a gold electrode in 1.0 M perchloric acid are shown in Fig. 1A in comparison to the residual curve obtained in 0.5 M $HClO_4$. The residual curve illustrates that gold oxide forms during the positive potential scan for $E > 1.1$ V. The anodic breakdown of the aqueous solvent with evolution of oxygen occurs rapidly for $E > 1.5$ V. The film of gold oxide, formed during the positive potential scan, is removed cathodically during the negative potential scan resulting in a sharp current peak at 0.9 V. Arsenic(III) is oxidized with $E_{1/2} = 0.8$ V, yielding a current plateau ($0.9 < E < 1.1$ V) with a limiting current value which is proportional to the bulk concentration of arsenic(III), C^b, and the square root of the velocity of electrode rotation, $\omega^{1/2}$, as expected for a mass transport-limited process [36]. The formation of gold oxide at $E > 1.1$ V seriously interferes with oxidation of arsenic(III) and virtually zero current is detected for arsenic(III) on the negative scan following reversal of the scan direction at 1.5 V. A sharp anodic peak for arsenic(III) is obtained during the negative scan in the narrow region between the value for

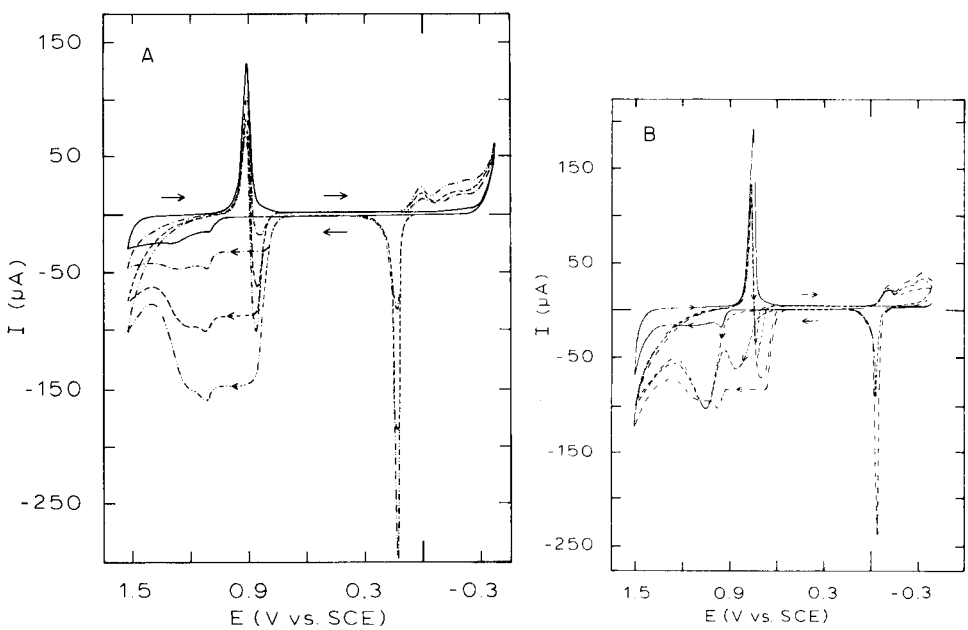

Fig. 1. Current—potential curves for arsenic(III) at a rotating gold-disk electrode: (A) as a function of concentration, and (B) as a function of added chloride. Supporting electrolyte, 0.5 M $HClO_4$; rotation speed, 3600 rev min^{-1}; scan rate, 1.0 V min^{-1}. Curves in (A):(——) 0.0 M As(III); (·--) 2.8 × 10^{-5} M As(III); (---) 8.6 × 10^{-5} M As(III); (····) 14.4 × 10^{-5} M As(III). Curves in (B): (——) 0.0 M As(III), 0.00 ppm NaCl; (····) 7.4 × 10^{-5} M As(III), 0.00 ppm NaCl; (---) 7.4 × 10^{-5} M As(III), 0.06 ppm NaCl; (·--) 7.4 × 10^{-5} M As(III), 0.12 ppm NaCl.

reduction of the oxide layer and the $E_{1/2}$ for the oxidation of arsenic(III). The cathodic and anodic processes for $E < 0.2$ V correspond to the deposition and stripping of elemental arsenic [26—28]. Reduction of dissolved oxygen is observed for an aerated solution at $E < 0.3$ V.

The oxidation of arsenic(III) at a gold electrode is severely inhibited by the presence of chloride ion in the solution (Fig. 1B). The anodic current at 0.9 V is significantly decreased in the presence of 0.06 ppm chloride and virtually no wave is obtained in the presence of 0.12 ppm chloride. The presence of bromide or iodide has a similar effect on the wave for arsenic (III). The adsorption of halide ions at metal electrodes is known to influence dramatically the electrode reactions of many metal ions; both electrocatalysis and inhibition have been reported [37—41]. Because trace amounts of halides can seriously interfere with the oxidation of arsenic(III) on gold electrodes, this electrode material was rejected for general applications. In real samples, the presence of impurities such as halides can be neither predicted nor easily controlled.

Voltammetry at a platinum disk electrode

Current—potential curves for oxidation of arsenic(III) at the platinum electrode in 1.0 M perchloric acid are shown in Fig. 2A. The residual curve illustrates that the formation of platinum oxide occurs during the positive potential scan for $E > 0.7$ V. The oxide is reduced during the negative scan producing the cathodic peak current at 0.4 V. The anodic wave for arsenic

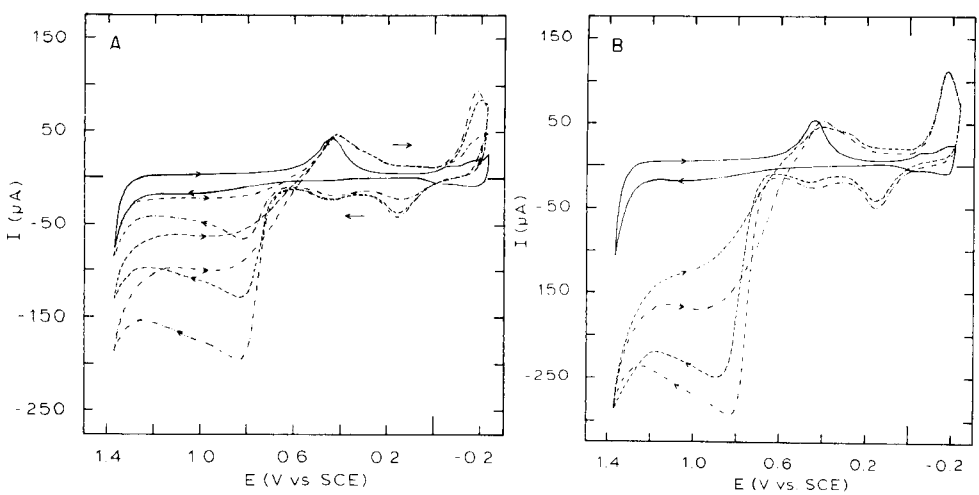

Fig. 2. Current—potential curves for arsenic(III) at a rotating platinum-disk electrode: (A) as a function of concentration, and (B) as a function of added chloride. Supporting electrolyte, 0.5 M $HClO_4$; rotation speed, 3600 rev min^{-1}; scan rate, 1.0 V min^{-1}. Curves in (A): (——) 0.0 M As(III); (---) 2.8 × 10^{-5} M As(III); (---) 8.6 × 10^{-5} M As(III); (·---) 14.4 × 10^{-5} M As(III). Curves in (B): (——) 0.0 M As(III), 0.00 ppm NaCl; (·---) 2.2 × 10^{-4} M As(III), 0.00 ppm NaCl; (---) 2.2 × 10^{-4} M As(III), 40 ppm NaCl.

(III) ($E_{1/2} \simeq 0.75$ V) is not resolved from the wave attributed to the formation of platinum oxide. The oxidation process for arsenic(III), however, is not as seriously inhibited by the presence of the platinum oxide as it was by the presence of gold oxide. The anodic current for arsenic(III), measured during the negative potential scan for $0.9 < E < 1.2$ V, is proportional to the concentration of arsenic(III) in the range $3—14 \times 10^{-5}$ M. The current is virtually zero in the absence of arsenic(III) on the negative scan. Electrode reactions for $E < 0.5$ V are probably associated with deposition and stripping of elemental arsenic, and are not linear functions of the concentration of arsenic(III) over the range of interest.

Current—potential curves obtained in the presence of chloride are shown in Fig. 2B. Chloride at the ppm level slightly suppresses the anodic current for arsenic(III) at a platinum electrode but does not have the severely deleterious effect observed at a gold electrode. The value of $E_{1/2}$ is not shifted significantly and the inhibitory effect appears to be unrelated to the kinetics of electron transfer.

Investigation of partial kinetic control

For the amperometric determination of arsenic(III) by flow-injection analysis, the electrode processes should be controlled strictly by the rate of mass transport rather than by changes in the state of the electrode

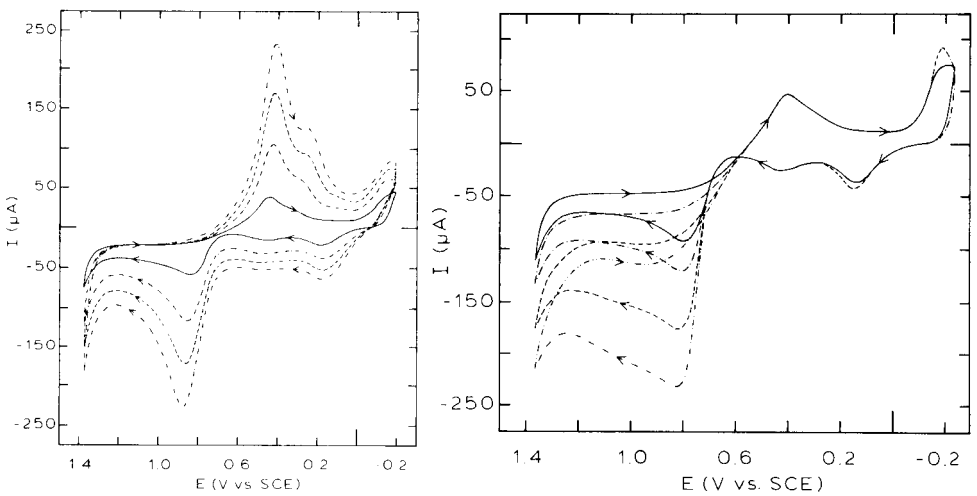

Fig. 3. Current—potential curves at a rotating platinum-disk electrode as a function of scan rate. Supporting electrolyte, 0.5 M $HClO_4$; rotation speed, 3600 rev min^{-1}; 4.0×10^{-5} M As(III). Curves: (—) 1.0 V min^{-1}; (- · -) 3.0 V min^{-1}; (- - -) 5.0 V min^{-1}; (- · · -) 7.0 V min^{-1}.

Fig. 4. Current—potential curves at a rotating platinum-disk electrode as a function of rotation speed. Supporting electrolyte, 0.5 M $HClO_4$; scan rate, 1.0 V min^{-1}; 1.42×10^{-5} M As(III). Curves: (—) 400 rev min^{-1}; (- · -) 900 rev min^{-1}; (- - -) 2500 rev min^{-1}; (- · · -) 4900 rev min^{-1}.

surface. Cyclic voltammetry was used to study the nature of the electrode reaction. Mass transport-controlled processes at rotating disk electrodes are characterized by limiting current values which have a linear dependence on C^b and $\omega^{1/2}$ [36] but a negligible dependence upon potential scan rate, θ. Faradaic processes controlled by potential-dependent changes in the surface state yield currents which are proportional to θ but independent of C^b and $\omega^{1/2}$. The I—E curves obtained as a function of θ and ω are shown in Figs. 3 and 4, respectively.

The anodic wave for $E > 0.8$ V obtained during the positive potential sweep results from the simultaneous oxidation of arsenic(III) and the potential-dependent formation of platinum oxide on the electrode surface. Hence, this composite wave is dependent on scan rate (Fig. 3). During the negative potential scan for $E > 0.8$ V, the growth of the oxide film virtually ceases, on the time scale of this experiment, and the remaining current for oxidation of arsenic(III) is independent of scan rate. All processes occurring for $E < 0.8$ V are strongly dependent on scan rate, i.e., not limited by the mass transport of arsenic(III) in the solution at the electrode surface. Based on data obtained by cyclic voltammetry, the anodic detection of arsenic(III) should be possible at a platinum electrode at 1.0 V. The equilibrium coverage of the electrode surface by oxide is expected to develop nearly instantaneously following the application of the electrode potential, and the subsequent electrode current should be a linear function of arsenic(III) concentration.

Whereas the plateau current for arsenic(III) at 1.0 V does increase with higher $\omega^{1/2}$ (Fig. 4), the dependence is not linear as expected for an electrode process limited solely by mass transport in the solution phase. A nonlinear I—$\omega^{1/2}$ plot is diagnostic evidence for partial kinetic control of the electrode reaction. The fact that the current in the region of 1.0 V on the negative potential scan is potential-independent is strong evidence that the kinetic step does not involve electron transfer. The kinetic current, I_k, for an electrode reaction under mixed control (mass transport and chemical kinetics) can be modeled [42] approximately by

$$I_k = nFADC^b/(\partial + D/k) \quad (1)$$

where ∂ is the thickness of the diffusion layer at the electrode surface, k is the rate constant for the chemical step and the remaining terms have their usual electrochemical significance. Recognizing that the mass transport-limited current, I_l, is given by $nFADC^b/\partial$ and the value of ∂ for a rotating disk electrode is given by $1.61\, D^{1/3}\, \omega^{-1/2} \nu^{1/6}$, eqn.(1) can be rearranged to

$$I_k/\omega^{1/2} = (I_l/\omega^{1/2}) - (I_k/1.61D^{-2/3}\, \nu^{1/6}k) \quad (2)$$

where ν is the kinematic viscosity of the solution. The plot of $I_k\omega^{-1/2}$ vs. I_k is predicted to be linear with a slope of $0.62D^{2/3}\, \nu^{-1/6}k^{-1}$ and an intercept of $0.62nFAD^{2/3}\nu^{-1/6}C^b$. Data from Fig. 4 were plotted accordingly and yielded a straight line with a slope of -49.2 $s^{1/2}$. For $D = 0.94 \times 10^{-5}$ cm^2

s^{-1}, which was obtained for 0.50 M boric acid electrolyte [43], and ν = 9.0 × 10^{-3} cm^2 s^{-1}, corresponding to the value for 1.0 M $HClO_4$, k is calculated to be 1.2 × 10^{-5} cm s^{-1}. The predicted value of the intercept, for C^b = 1.43 × 10^{-7} mol cm^{-3} and A = 0.447 cm^2, is 0.74 × 10^{-6} C $s^{-1/2}$, which is in fair agreement with the experimental value of 1.1 × 10^{-6} C $s^{-1/2}$.

At least two explanations are possible for the slow process occurring before electron transfer. First, the slow step may indeed correspond to the diffusion (tunneling) of the arsenic(III) through the oxide film to reach a position near the platinum surface for electron transfer. Second, the oxide film may be impermeable to arsenic(III) but may cover the electrode surface in a non-uniform manner leaving a small number of widely dispersed active sites. This situation would lead to cylindrical rather than linear diffusion within the hydrodynamic boundary layer. The case of cylindrical diffusion at a rotating disk electrode is described by an equation of the same form as eqn. (1) with k being related to the geometry of the non-uniform surface [44]. Actually, both of these mechanisms invoke a slow diffusion step which is not directly governed by the thickness of the hydrodynamic boundary layer at the rotating electrode.

Platinum-wire flow-through detector

As presented above, the anodic current for arsenic(III) at a platinum electrode is less than the theoretical mass transport-limited value because of the presence of the oxide film. Relative deviation from the theoretical value will be greatest for electrodes with high fluid velocity, i.e. small ∂ in eqn. (1). However, for constant fluid velocity and film thickness, the anodic signal is predicted to be a reproducible and linear function of the concentration of arsenic(III). The growth rate of the oxide film at platinum electrodes in acidic media, following a step-wise change of electrode potential to a value more positive than 0.6 V vs. SCE, decays in an exponential manner and the thickness of the film increases at a nearly imperceptible rate after a few minutes [45]. The anodic current for arsenic(III) at 1.0 V in the platinum flow-through detector was recorded for a continuous flow of 8.2 × 10^{-5} M arsenic(III) over a 7-h period. The results are summarized in Table 1. The theoretical mass transport-limited current, which would correspond to the

TABLE 1

Decay of anodic current for arsenic(III) in the platinum flow-through detector as a function of time
[C^b = 8.2 × 10^{-5} M As(III) in 0.5 M $HClO_4$; V_f = 1.30 ml min^{-1}; E = 1.0 V; $I(t = 0)$ = 54.3 (calculated).]

t(h)	0.5	1.0	2.0	3.0	5.0	7.0
I(μA)	39.0	38.8	38.6	38.3	37.7	37.1

Decay rate $(10^2 \Delta I/I)/\Delta t$ = 0.7% h^{-1}

detection of arsenic(III) in the absence of an oxide film, was calculated on the basis of the current for a solution of bromide. Bromide is oxidized to bromine at 1.0 V without interference from the oxide film [46]. The signal for arsenic(III) after 0.5 h was 72% of the theoretical value. The rate of decay of the signal after 0.5 h was about 0.7% h^{-1}. This decay is not a problem for flow-injection analysis because of the general practice of making frequent calibration with standard samples.

Representative detection peaks for arsenic(III) obtained with the flow-through detector are shown in Fig. 5. These peaks were obtained without the cation-exchange column present in the flow analyzer. With the column present, the peak width is greater because of additional dispersion of the sample plug.

Calibration

The calibration curve for detection of arsenic(III) by flow-injection analysis based on peak areas is linear over more than three decades (0.3 ng—0.8 μg in the 0.226-ml sample) corresponding to 1.3 ppb to 3.5 ppm. The detection limit, defined as the analytical signal equal to twice the uncertainty in the background, is approximately 0.1 ng which corresponds to 0.4 ppb. Deviation from linearity occurs at high concentrations because the product of the large electrode current and the uncompensated cell resistance produces a shift of the true electrode potential off the limiting current plateau. Rather than make adjustments of electrode potential for determination of high concentrations, it is better to dilute the sample.

Reduction of arsenic(V)

Twelve samples containing 1.100 mg of arsenic(V) were analyzed following reduction according to Procedure A. The recovery, based on flow-injection analysis, was 95.9 ± 0.1%. This was concluded to be satisfactory for determinations of arsenic(V) at this level.

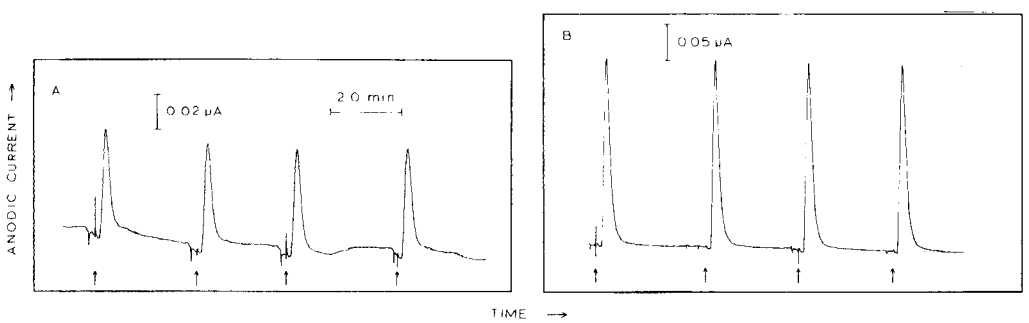

Fig. 5. Detection peaks for As(III) by flow-injection analysis with wire flow-through detector. Carrier stream, 0.1 M $HClO_4$; potential, 1.0 V vs. SCE; flow rate, 1.0 ml min^{-1}; sample volume, 0.226 ml. (A) 7.8 × 10^{-8} M As(III) (5.8 ppb); (B) 7.8 × 10^{-7} M As(III) (58 ppb). Arrow indicates point of injection.

Analysis of standard reference material

Dissolution of carbonaceous samples prior to elemental analysis is easily and safely performed in a boiling mixture of nitric, perchloric and sulfuric acids. Samples of NBS SRM 1571 (Orchard Leaves) were digested and reduced according to Procedure B, followed by flow-injection analysis. The cation-exchange column was present in the analyzer. An extraneous peak was observed following but not completely resolved from the arsenic(III) peak. By comparison of retention times obtained for standards, the extraneous peak was concluded to result from hydroxylamine. Thermodynamically, hydroxylamine is not predicted to be a stable product of the reaction between hydrazine and arsenic(V) in strongly acidic solutions. No evidence was observed for formation of hydroxylamine when inorganic samples of arsenic(V) were reduced in sulfuric acid alone (Procedure A).

Procedure B was modified to distil off the perchloric acid as the dihydrate prior to chemical reduction (Procedure C). No peak for hydroxylamine was observed for samples of NBS SRM 1571 (Orchard Leaves) which were digested and reduced according to Procedure C. The average of 10 results for analysis of the orchard leaves was $13.7 \pm 1.4\ \mu g\ g^{-1}$ which is in excellent agreement with the certificate value of $14 \pm 2\ \mu g\ g^{-1}$.

Great care is necessary in Procedure C to heat the mixture sufficiently to expel all perchloric acid. This ensures that any chloride which may be present will be expelled, following oxidation to chlorine or other volatile forms. If the reducing agent is added prior to elimination of chloride, volatile $AsCl_3$ will form which is lost at temperatures above 130°C.

REFERENCES

1 J. P. Arnold and R. M. Johnson, Talanta, 16 (1969) 1191.
2 A. P. Tomilov and N. E. Chomutov, in A. J. Bard (Ed.), Encyclopedia of Electrochemistry of the Elements, M. Dekker, New York, 1974, p. 21.
3 L. Meites, J. Am. Chem. Soc., 76 (1954) 5927.
4 S. M. White and A. J. Bard, Anal. Chem., 38 (1966) 61.
5 W. B. Swann, J. F. Hazel and W. M. McNabb, Anal. Chem., 32 (1960) 1064.
6 E. G. Vasilyeva, S. I. Zhdanov and T. A. Krjukova, Electrokhimiya, 4 (1968) 25.
7 M. V. Susic and M. G. Pjescic, J. Electroanal. Chem., 34 (1972) 535.
8 J. Suzuki, Jpn. Anal., 15 (1966) 548.
9 N. G. Elenkova and R. A. Tsoneva, Anal. Chim. Acta, 62 (1972) 435.
10 H. S. Mahanti, Fresenius Z. Anal. Chem., 274 (1975) 303.
11 N. G. Elenkova and R. A. Tsoneva, Zh. Anal. Khim., 28 (1973) 501; 29 (1974) 244, 1344.
12 M. V. Susic and M. G. Pjescic, Analyst, 91 (1966) 258.
13 N. G. Elenkova and R. A. Tsoneva, Russ. J. Inorg. Chem., 17 (1972) 356.
14 R. Geyer and M. Geissler, Fresenius Z. Anal. Chem., 201 (1964) 16.
15 P. Beran, J. Cihalik, J. Dolezal, V. Simon and J. Zyka, Chem. Listy, 47 (1953) 1315.
16 E. Temmerman and F. Verbeek, Anal. Chim. Acta, 43 (1968) 263.
17 E. Sudo and H. Okocki, Jpn. Anal., 18 (1969) 507.
18 W. Holak, J. Assoc. Off. Anal. Chem., 60 (1977) 1015.
19 K. Hagiwara and I. Murase, Jpn. Anal., 13 (1964) 788.

20 D. J. Myers, M. E. Heinbrook, J. Osteryoung and S. M. Morrison, Environ. Lett., 5 (1973) 53.
21 D. J. Myers and J. Osteryoung, Anal. Chem., 45 (1973) 267.
22 W. Holak, J. Assoc. Off. Anal. Chem., 59 (1976) 650.
23 T. Y. Belova, I. B. Berengard and B. Y. Kaplan, Zav. Lab., 41 (1975) 1314.
24 E. S. Pilkington and C. Weeks, Anal. Chem., 48 (1976) 1665.
25 V. F. Toropova, Y. N. Polyakov and L. N. Soboleva, Zh. Anal. Khim., 32 (1977) 985.
26 A. A. Kaplin, N. A. Veits and A. G. Stromberg, Zh. Anal. Khim., 28 (1973) 2192.
27 G. Forsberg, J. W. O'Laughlin and R. G. Megargle, Anal. Chem., 47 (1975) 1586.
28 P. H. Davis, G. R. Dulude, R. M. Griffin, W. R. Matson and E. W. Zink, Anal. Chem., 50 (1978) 137.
29 L. F. Trushina and A. A. Kaplin, Zh. Anal. Khim., 25 (1970) 1616.
30 T. Kuwabara, S. Suzuki and S. Araki, Bull. Chem. Soc. Jpn., 46 (1973) 1690.
31 T. A. Krapivkina, E. M. Roizenblat, V. V. Nosacheva, L. S. Zaretskii and V. S. Utenko, Zh. Anal. Khim., 29 (1974) 1818.
32 A. A. Kaplin, N. A. Veits, N. M. Mordvinova and G. G. Glukhov, Zh. Anal. Khim., 32 (1977) 687.
33 J. A. Lown, R. Koile and D. C. Johnson, Anal. Chim. Acta, 116 (1980) 33.
34 K. Hagiwara, Jpn. Anal., 19 (1970) 563.
35 W. Holak, J. Assoc. Off. Anal. Chem., 60 (1977) 478.
36 W. J. Albery and M. L. Hitchman, Ring-Disc Electrodes, Clarendon Press, Oxford, 1971.
37 F. Anson, J. Electrochem. Soc., 110 (1963) 436.
38 R. Parsons, J. Electroanal. Chem., 21 (1969) 35.
39 R. DeLevie, J. Electrochem. Soc., 118 (1971) 185C.
40 R. J. Davenport and D. C. Johnson, Anal. Chem., 45 (1973) 1755.
41 D. C. Johnson and E. W. Resnick, Anal. Chem., 49 (1977) 1918.
42 V. G. Levich, Physicochemical Hydrodynamics, Prentice-Hall, Englewood Cliffs, NJ, 1962, pp. 72—75.
43 D. C. Johnson and S. Bruckenstein, J. Am. Chem. Soc., 90 (1968) 6592.
44 R. Landsberg and R. Thiele, Electrochim. Acta, 11 (1966) 1243.
45 S. Gilman, The Anodic Film on Platinum Electrodes, in Electroanalytical Chemistry, Vol. 2, A. J. Bard (Ed.), M. Dekker, New York, 1967.
46 D. C. Johnson and S. Bruckenstein, J. Electrochem. Soc., 117 (1970) 460.

Analytica Chimica Acta, 116 (1980) 53—60

MODEL EXPERIMENTS FOR DETERMINATIONS OF ZINC—AMINO ACID COMPLEXES IN BIOLOGICAL FLUIDS BY POLAROGRAPHY

EDUARDO O. MARTINS and GILLIS JOHANSSON*

Department of Analytical Chemistry, University of Lund, P.O. Box 740, S-220 07 Lund (Sweden)

(Received 12th November 1979)

SUMMARY

The Ilkovič constant was determined for zinc and zinc—amino acid complexes by using differential pulse polarography in 0.1 M sodium chloride—sodium diethylbarbiturate buffer at pH 7.4. A single well-behaved wave was obtained, except for cysteine and cystine for which useful calibration curves could not be obtained. The non-equilibrium dialysis of the amino acid complexes was studied in a hollow-fiber dialyzer. It is concluded that the dialysis step could be used in a method intended to measure available zinc but that the polarographic method needs further modification.

Normal zinc concentration in human serum is about 1 mg l^{-1}, one third of which is strongly bound to globulin, mainly α-2-macroglobulin, and the remainder is loosely bound, principally to albumin. A smaller fraction, ca. 2% of the total, is complexed by amino acids. It is generally accepted that the non-protein-bound fraction of zinc may have an important role in the transport of this element. Amino acids, especially cysteine, histidine, glutamine, cystine and glycine, have been recognized as the principal ligands [1, 2]. Giroux and Henkin [2] concluded that amino acids compete effectively with albumin for binding of zinc, histidine and cysteine being the most successful. In physiological concentrations, addition of amino acids to predialyzed serum increased the ultrafiltrable ^{65}Zn several fold [1], histidine, glutamine, threonine, cystine and lysine showing the most marked effects.

Several pathological conditions provoke a redistribution of plasma zinc within body tissues [3]; in particular, it has been suggested that in the course of acute viral hepatitis, virtually all the detectable zinc exists in an ultrafiltrable state in low-molecular-weight complexes [4]. Also, amino acid-bound zinc may account for most of the urinary zinc in normal and pathological situations [5].

Determination of total zinc concentrations, e.g. by atomic absorption, does not provide information about the proportions present in the complexed and free forms. Present knowledge about available zinc has been obtained either by using complex-forming agents like dithizone or zincon followed by spectrophotometry, or by dialysis or ultrafiltration followed by various methods for analysis of the dialysate. Practically nothing has

been done to develop methods which can be used for routine determinations of available zinc in clinical samples. Even for research purposes the currently available methods are inadequate.

The prospects of finding methods for direct determination of available zinc in a serum sample without previous separation of proteins do not seem to be good at present. An ion-selective electrode was developed with this purpose in mind [6, 7] but neither sensitivity nor selectivity was sufficient for serum analysis. Direct use of voltammetric methods is out of the question as sulfhydryl and disulfide groups in the proteins adsorb on and react with mercury and other metals. The resulting waves are complicated and dependent on uncontrollable parameters, and it is generally impossible to use the method analytically.

This paper describes a study of a model system comprising a microdialyzer to prevent proteins from reaching the polarographic electrode. Continued work to develop a method for available zinc is in progress.

EXPERIMENTAL

Polarographic measurements were made with a PAR 174A polarograph equipped with a PAR drop timer. A pulse height of 50 mV, a drop time of 1 s and a scan rate of 2 mV s^{-1} were used throughout. A saturated calomel electrode was used as the reference and a platinum wire as the auxiliary electrode. Solutions were degassed with purified nitrogen which had been deoxygenated over copper turnings at 500°C and equilibrated with the supporting electrolyte. During the measurements, nitrogen was passed over the solution. The solutions were thermostatted at 25.0 ± 0.2°C.

The dialyzer was a flow-through hollow-filter microdialyzer (AB Gambro, P.O. Box 10015, S-220 10 Lund, Swedish patent 396819). When not in use it was soaked with glycerine to prevent bacterial growth and stored in a refrigerator. The microdialyzer was checked for copper contamination; the leakage of copper was found to be less than the detection limit, 10^{-7} M Cu^{2+}. The solutions were pumped with an Ismatec MP 13 GJ-4 multichannel peristaltic pump.

In the dialysis experiments, the synthetic sample was pumped through the outer tubing at a constant rate of 6.08 or 6.23 ml min^{-1}. It has previously been shown for glucose [8] that the flow rate in the outer tubing has no influence on the dialysis constant K if the flow is greater than 4.7 ml min^{-1}. The flow rate through the inner tubing, which was mounted coaxially inside the outer, was pumped in the opposite direction at the rates specified in the Results section. Steady state was attained within 5 min for the lowest inner-tubing flow, 0.09 ml min^{-1}.

Fractions of the inner-tube flow were collected and transferred to the polarographic cell for analysis.

The buffer used throughout was 0.10 M NaCl—1 mM sodium diethylbarbiturate adjusted to pH 7.4. All chemicals were of analytical-reagent

grade. The amino acids were obtained from Sigma. Solutions were prepared with water purified by a Millipore-Q system. Zinc contamination from reagents and laboratory ware could be kept below the detection limit, 10^{-7} M Zn^{2+}.

RESULTS AND DISCUSSION

Polarography of amino acid complexes

The reduction of zinc by polarographic techniques has been studied by several authors [9—11]. The reduction in buffer solutions occurs with different degrees of irreversibility. It is well known (see e.g. [12, 13]) that the zinc—amino acid complexes give two waves in unbuffered solutions. In this study a buffer containing sodium chloride and a barbiturate was selected because the waves of both zinc and the amino acid complexes behaved very well. In this particular buffer, the calibration graphs for both the metal and its complexes were strictly linear.

Table 1 summarizes the result of measurements with differential pulse polarography. Various metal and amino acid concentrations were tested. A mixture of seven amino acids taken in the proportion normally found in serum was also studied. In all cases a single wave was obtained and the peak potential was the same for the aquo ion as for all the complexes. The value of the Ilkovič constant, I_p/C, varied within ± 28% from the mean value of 1.56×10^{-5} M μA^{-1}. The reproducibility was very good. Several waves were produced by solutions containing both zinc and cysteine or/and cystine. The pattern of the polarograms was dependent on both the pH and the concentrations. There was one peak at −0.985 V as for the other zinc—amino acid complexes, but it was distorted and there was another peak in the cathodic direction which partly overlapped the first one. There were no linear calibration graphs within the serum concentration range. Even in a mixture, the presence of these two amino acids interfered.

The detection limit was 1×10^{-7} M Zn^{2+} if dissolved oxygen was thoroughly removed. Because of the cell construction, degassing for 80—90 min was necessary at this level.

Dialysis experiments

For linear dialysis, the concentration of the solute, C_e, in the dialysate should be

$$C_e = AD\,C_s/bf_i = KC_s \qquad (1)$$

where A is the membrane area, b its thickness, D the diffusion coefficient of the solute, f_i the inner-tubing flow rate and C_s the solute concentration in the sample. For a given experimental arrangement with constant flow rates, all parameters can be compounded to a new constant, K, and C_e should be a linear function of C_s. It has been shown by Gorton and Bhatti [8] that the Gambro hollow-fiber dialyzer was almost linear for the dialysis of

TABLE 1

Differential pulse polarography of zinc and zinc—amino acid (AA) solutions in 0.10 M NaCl—1 mM Na-diethylbarbiturate, pH 7.4

$[Zn^{2+}]_T$ (mM)	$[AA]_T$ (mM)	E_p (V vs. SCE)	I_p/C ($\times 10^{-5}$ M μA^{-1})
0.0050—0.024	—	—0.985	1.19
0.0010—0.024	GLY, 0.0010	—0.985	1.23
—	GLY, 0.0100	—0.985	1.24
—	GLY, 0.100	—0.985	1.25
—	GLY, 1.00	—0.987	1.31
—	GLY, 10.0	—0.987	1.29
—	ALA, 0.100	—0.985	1.43
—	ALA, 1.00	—0.985	1.43
0.0010—0.015	GLU, 0.910	—0.985	1.14
0.0010—0.050	GLU, 10.0	—0.985	1.12
0.0010—0.012	HIS, 0.131	—0.985	1.99
—	ARG, 0.0120	—0.985	1.79
—	ARG, 0.107	—0.985	1.82
0.00010—0.060	LYS, 0.150	—0.982	1.86
—	THR, 0.148	—0.985	1.82
0.00010—0.060	GLY, 0.300 GLU, 0.700 HIS, 0.120 LYS, 0.150 ALA, 0.350 ARG, 0.100 THR, 0.150	—0.987	1.77

glucose, resulting in a value of Kf_i = 0.0472 ml min^{-1}. The value of Kf_i is expected to be different for each solute, depending partly on different values of D but to a greater extent on differences in the interaction between the membrane and the solute molecules. This interaction is not explicitly included in eqn. (1), but for charged solute and charged membranes the effect may be very pronounced. In addition, there is a cut-off value for transport through the membrane which for the present dialyzers is somewhere above 1000 Daltons. It was shown by Gorton and Bhatti [8] that less than 0.01% (the detection limit) of serum albumin at physiological concentrations passes through the membrane.

Table 2 shows a test of dialyzer linearity for zinc—glycine complexes with glycine in excess, for two different dialyzers. Regression analysis showed that the slopes, b, are very close to zero indicating that the constant K in eqn. (1) is independent of C_s. Table 3 shows that Kf_i is the same for the two dialyzers. For substantially lower flow rates, the constant Kf_i decreases. The reason for this was not investigated but in experiments not tabulated it was shown that a small change in the outer-tubing flow rate had no effect whatsoever. It was also found that the dialysis was linear with concentration C_s at the lower flow rate.

TABLE 2

Dialysis of zinc from a solution 10 mM in glycine and 0.10 M in NaCl

Outer tubing	Inner tubing							
Flow rate	Flow rate 0.755 ml min^{-1}				Flow rate 0.964 ml min^{-1}			
6.083 ml min^{-1}	Dialyzer I		Dialyzer II		Dialyzer I		Dialyzer II	
$[Zn^{2+}]$ (mM)	[Zn—GLY] dialyzed (mM)	K(Zn—GLY)[a]	[Zn—GLY] dialyzed (mM)	K(Zn—GLY)[b]	[Zn—GLY] dialyzed (mM)	K(Zn—GLY)[c]	[Zn—GLY] dialyzed (mM)	K(Zn—GLY)[d]
0.040	0.00080	0.0199	0.0090	0.0219	0.00070	0.0175	0.00060	0.0162
0.200	0.00400	0.0198	0.00410	0.0206	0.00320	0.0158	0.00340	0.0170
0.400	0.00770	0.0193	0.00850	0.0212	0.00660	0.0164	0.00670	0.0167
1.00	0.0215	0.0215	0.0212	0.0212	0.0189	0.0189	0.0165	0.0165
2.00	0.0406	0.0203	0.0425	0.0212	0.0330	0.0165	0.0312	0.0156
3.00	0.0613	0.0204	0.0605	0.0202	0.0495	0.0165	0.0488	0.0163
4.00	0.0804	0.0210	0.0028	0.0207	0.0650	0.0164	0.0650	0.0162

[a] a = 0.0002 mM, b = 0.0202, r = 0.9998. (a = intercept; b = slope; r = correlation coefficient). [b] a = 0.0003 mM, b = 0.0205, r = 0.9997. [c] a = 0.0005 mM, b = 0.0164, r = 0.9993. [d] a = 0 mM, b = 0.0162, r = 0.9998.

TABLE 3

Dialysis parameters of two dialyzers for zinc—glycine solutions

Flow rate (ml min^{-1})		Dialyzer I		Dialyzer II	
Outer tubing	Inner tubing	K(Zn—GLY)	$K \times f_i$ (ml min^{-1})	K(Zn—GLY)	$K \times f_i$ (ml min^{-1})
6.08	0.755	0.0202	0.0152	0.0205	0.0155
6.08	0.964	0.0164	0.0158	0.0162	0.0156

Table 4 shows the values of K and Kf_i for zinc and for different zinc—amino acid complexes. Each value is the mean of five series; for each series, five different zinc concentrations were tested. It can be seen that these constants are higher for zinc ions than for the complexes. This is to be expected because the larger complexes should have smaller diffusion coefficients. The range of K for the complexes is 0.104—0.119 if the large outlying value for arginine is excluded. The standard deviation obtained for each value was 5—6%. The single outlying value for arginine was probably due to a change in the pump rate of a defective tubing. A somewhat better reproducibility should have been obtained if the dialyzer had been thermostatted.

A synthetic amino acid mixture with a composition near that of a normal serum gave a K value of 0.106. If the mixture is used as a calibration solution, a systematic error of at most 13% will result if a single amino acid dominates completely.

From the long-term stability of dialyzer I, shown in Table 5, it can be concluded that the device can be used, at least for synthetic solutions, with some confidence.

Prospects for application to serum analysis

The model experiments discussed above show that the dialysis of the various amino acid complexes occurs at almost the same rate. At most an error of 13% should result if a particular amino acid predominates when a mixture has been assumed. The free zinc is dialyzed more rapidly but this is of no practical importance as there is always an excess of amino acids in a real sample.

The polarographic data, however, showed a maximum deviation of —37% from a value obtained in the model mixture. This is of course unacceptable as a basis for an analytical method. Furthermore, cysteine and cystine interfere strongly and they are always present in a real sample. Even if differential pulse polarography is out of the question, other polarographic methods might be useful. Preliminary measurements by anodic stripping voltammetry from zinc—cysteine complexes have shown that the interferences can be overcome. Also the differences between the response factors of the various ligands are smaller than in differential pulse polarography.

TABLE 4

Results from dialysis experiments and dialysis parameters for dialyzer I. Zinc—amino acid (AA) solutions in 0.10 M NaCl, dialyzed against the buffer, at constant inner-tubing flow rate, 0.090 ml min^{-1}.

$[Zn^{2+}]_T$ (mM)	$[AA]_T$ (mM)	$K(Zn—AA)$	$K \times f_i$ (ml min^{-1})	$[Zn^{2+}]_T$ (mM)	$[AA]_T$ (mM)	$K(Zn—AA)$	$K \times f_i$ (ml min^{-1})
0.010—4.00	—	0.136	0.0122	0.010—0.60	GLY, 0.300	0.106	0.0095
0.010—0.60	GLY, 6.00	0.111	0.0100		GLU, 0.600		
0.010—1.00	GLY, 10.0	0.116	0.0104		HIS, 0.120		
0.010—1.00	GLY, 1.00	0.114	0.0103		LYS, 0.150		
0.010—0.60	ALA, 0.350	0.104	0.0094		ALA, 0.350		
	ALA, 1.00	0.119	0.0107		ARG, 0.100		
	GLU, 1.00	0.115	0.0103		THR, 0.150		
	GLU, 1.00	0.112	0.0100				
	GLU, 0.60	0.116	0.0104				
	ARG, 0.094	0.122	0.0110				
	ARG, 0.118	0.118	0.0106				
	HIS, 0.115	0.116	0.0104				
	THR, 0.148	0.104	0.0093				
	LYS, 0.15	0.106	0.0095				

TABLE 5

Dialysis parameters for dialyzer I. Zinc solutions, 0.02 mM in 0.10 M NaCl, dialyzed against the buffer at two different inner-tubing flow rates.

Inner tubing flow rate, f_i (ml min^{-1})	$K(Zn^{2+})$	$K \times f_i$ (ml min^{-1})
0.090	0.136	0.0122
0.964	0.0131	0.0126
0.090[a]	0.135	0.0122
0.964[a]	0.0128	0.0123

[a]After five months of experiments.

Polarographic methods have some attractive properties when compared, for example, to atomic absorption analysis of the dialysate. Only complexes with a reasonable rate of ligand exchange will be measured by polarographic method. It is known that there are some zinc complexes in the body with extremely slow exchange rates. If a measure of available zinc is required, a method which can differentiate between zinc bound to fast-exchanging and slow-exchanging ligands should be of considerable interest.

This work was supported by grants from the Swedish Natural Science Research Council. The authors thank Ulla Fiedler-Linnersund for valuable discussions.

REFERENCES

1 A. S. Prasad and D. Oberleas, J. Lab. Clin. Med., 76 (1970) 416.
2 E. L. Giroux and R. I. Henkin, Biochim. Biophys. Acta, 273 (1972) 64.
3 W. R. Beisel, Med. Clin. North Am., 60 (1976) 831.
4 R. I. Henkin and F. R. Smith, J. Med. Sci., 264 (1972) 401.
5 R. I. Henkin, H. R. Keiser and D. Bronzert, J. Clin. Invest., 51 (1972) 44a.
6 L. Gorton and U. Fiedler, Anal. Chim. Acta, 90 (1977) 233.
7 U. Fiedler-Linnersund and K. M. Bhatti, Anal. Chim. Acta, 111 (1979) 57.
8 L. Gorton and K. M. Bhatti, Anal. Chim. Acta, 105 (1979) 43.
9 Y. Ayabe, J. Electroanal. Chem., 55 (1974) 187.
10 J. H. Christie, E. P. Parry and R. A. Osteryoung, Electrochim. Acta, 11 (1966) 1525.
11 J. Koryta, Electrochim. Acta, 6 (1962) 67.
12 R. Sundaresan, S. C. Saraiya and A. K. Sundaram, Proc. Indian Acad. Sci., 66A (1967) 184.
13 R. Sundaresan, S. C. Saraiya, T. P. Radhakrishnan and A. K. Sundaram, Electrochim. Acta, 13 (1968) 443.

Analytica Chimica Acta, 116 (1980) 61—67

A POTENTIOMETRIC MICROBIAL SENSOR BASED ON IMMOBILIZED *ESCHERICHIA COLI* FOR GLUTAMIC ACID

MOTOHIKO HIKUMA, HARUO OBANA and TAKEO YASUDA

Central Research Laboratories, Ajinomoto Co. Inc., 1 Suzuki-cho, Kawasaki-ku, Kawasaki, 210 (Japan)

ISAO KARUBE* and SHUICHI SUZUKI

Research Laboratory of Resources Utilization, Tokyo Institute of Technology, Nagatsuta, Midori-ku, Yokohama 227 (Japan)

(Received 18th September 1979)

SUMMARY

The sensor consists of immobilized *E. coli* (which contains glutamate decarboxylase) and a carbon dioxide gas-sensor. Continuous introduction of sample solution into a flow system incorporating the sensor gives a potential which increases until a steady state is reached after 5 min. Measurements can also be made with only a 1- or 3-min introduction period with little loss of sensitivity. Calibration plots of mV measurements vs. logarithmic glutamic acid concentration are linear in the range 100—800 mg l^{-1}. The sensor is highly selective, stable and reproducible. It has been applied to the determination of glutamic acid in fermentation broths.

Large quantities of glutamic acid are produced by fermentation, so that rapid automatic measurements of glutamic acid in fermentation media are required. AutoAnalyzer-based enzymatic reactions [1] can be used, but the method has disadvantages such as consumption of expensive enzyme. Recently many techniques have been developed for immobilization of living micro-organisms [2]. These immobilized micro-organisms have been used in electrochemical sensors (microbial electrodes) for estimation of BOD [3, 4], antibiotics [5], vitamins [6], alcohol [7] and acetic acid [8], especially for application in fermentation processes. These sensors consisted of immobilized whole cells and electrochemical devices, such as an oxygen electrode, a fuel-cell electrode or a combined glass electrode. Rechnitz et al. have also reported electrodes consisting of living bacteria and an ammonia gas-sensing electrode for the determination of arginine [9] and aspartate [10].

Glutamate decarboxylase catalyzes the decarboxylation of glutamic acid, which produces carbon dioxide and amine [11], but the enzyme is expensive and unstable. However, certain micro-organisms contain glutamate decarboxylase. Consequently, it has been possible to construct a microbial sensor for glutamic acid by using immobilized micro-organisms having glutamate decarboxylase activity, in conjunction with a carbon dioxide gas-sensing electrode. A suitable sensor and its application to the determination of glutamic acid in a fermentation broth are reported in this paper.

EXPERIMENTAL

Materials

Casamino acid (Difco Laboratories), yeast extract (Takeda Yakuhin Kogyo) and glutamic acid (99.9%; Ajinomoto Co.) were required. Other reagents were commercially available laboratory-grade materials. Deionized water was used in all procedures. All solutions were deoxygenated by bubbling nitrogen through them before use.

Escherichia coli (ATCC 8739) was cultured under aerobic conditions at 30°C for 20 h in a 500-ml flask containing 50 ml of a medium composed of 1.0% glucose, 1.0% casamino acid, 0.5% K_2HPO_4, 0.2% monosodium glutamate and 0.2% yeast extract (all w/v). The cells were harvested by centrifuging at 6000 g and washed twice with 0.2% potassium chloride solutions. The cells were freeze-dried at −30°C and stored on ice.

Assembly of microbial electrode

A diagram of the microbial electrode is shown in Fig. 1. A gas-sensing electrode for carbon dioxide (Model E5036, Radiometer) was used, consisting of a silicone rubber membrane, a combined glass electrode and a sodium hydrogencarbonate and sodium chloride buffer solution. About 3 mg of the freeze-dried cells was mixed with one drop of water and coated on both sides of a nylon mesh (60-mesh, 7 mm diameter) which was placed on the surface of the silicone rubber membrane of the electrode and covered with a cellophane membrane (type C, Technicon) to entrap the micro-organisms between the two membranes. The cellophane membrane was fastened with a rubber ring.

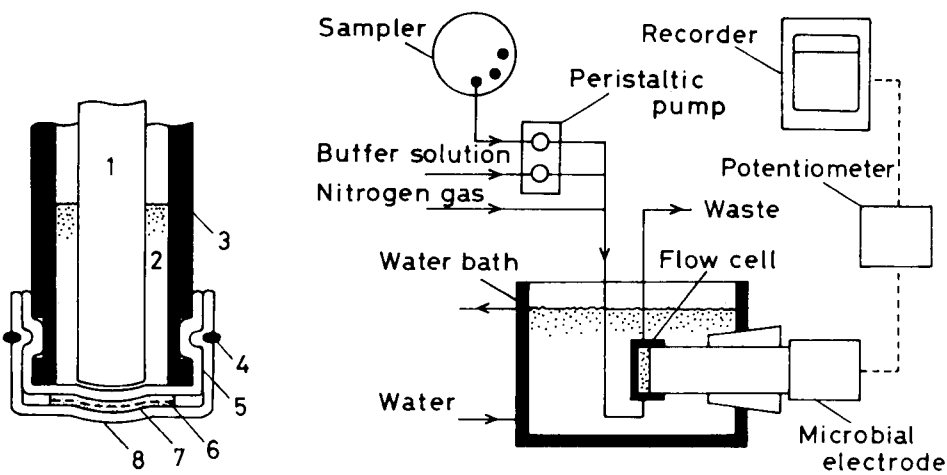

Fig. 1. Diagram of the microbial electrode for glutamic acid. (1) Combined glass electrode; (2) electrolyte; (3) insulator; (4) rubber ring; (5) silicone rubber membrane; (6) nylon net; (7) immobilized micro-organisms; (8) cellophane membrane.

Fig. 2. Schematic diagram of the sensor system.

Equipment

Figure 2 is a schematic diagram of the microbial sensor system. It includes a 0.5-ml flow cell, a peristaltic pump (Model I, Technicon), an automatic sampler (Model I, Technicon), a potentiometer (Model IM-20B, Toa Dempa Co.) and a recorder (Model LER-12A, Yokogawa Electric Works Co.).

Procedure

The temperature of the flow cell was maintained at 30 ± 0.2°C by the water bath. A buffer solution containing pyridine hydrochloride (8 g l^{-1}), KH_2PO_4 (5 g l^{-1}) and NaCl (5 g l^{-1}) was adjusted to pH 4.4 with hydrochloric acid. It was transferred to the flow cell at 3.9 ml min^{-1} with the peristaltic pump. When the potential of the glass electrode reached a constant value, a sample or standard was injected into the system at 1.0 ml min^{-1} for a 1-, 3- or 5-min period. In this paper, the concentrations of sample reported are those in the flow cell.

Alternative determination of glutamic acid. Glutamic acid in a culture broth was also determined by an AutoAnalyzer (Model I, Technicon) technique [1]. After removal of carbon dioxide, the sample was mixed with glutamate decarboxylase. The resulting carbon dioxide was measured colorimetrically after being absorbed in phenolphthalein solution.

RESULTS AND DISCUSSION

Electrode response

Preliminary experiments showed that the bacteria (*E. coli*) did not evolve carbon dioxide under anaerobic conditions, in the absence of glutamic acid. Therefore the normal respiration activity of the bacteria was depressed under anaerobic conditions, and any carbon dioxide produced by these bacteria under such conditions would result from the glutamate decarboxylase reaction. Nitrogen gas was passed through the flow cell at 500 ml min^{-1} in order to remove dissolved oxygen in buffer and sample solutions.

Figure 3 shows typical response curves of the sensor. The initial, constant potential (E) was obtained with the buffer solution only. When the sample solution containing glutamic acid was injected into the system, glutamic acid permeated through the cellophane membrane and was metabolized by the microorganisms to produce carbon dioxide:

$$HOOC{-}CH_2{-}CH_2{-}\underset{\displaystyle NH_2}{\underset{|}{CH}}{-}COOH \xrightarrow[\text{decarboxylase}]{\text{Glutamate}} HOOC{-}CH_2{-}CH_2{-}CH_2{-}NH_2 + CO$$

The enzyme reaction was carried out at pH 4.4, which was sufficiently below the pK_a value (6.34 at 25°C) of carbon dioxide to allow the carbon dioxide around the membranes to increase. As a result, the potential of the carbon dioxide gas-sensing electrode increased with time. When the sample was injected for 5 min or more, the potential became constant,

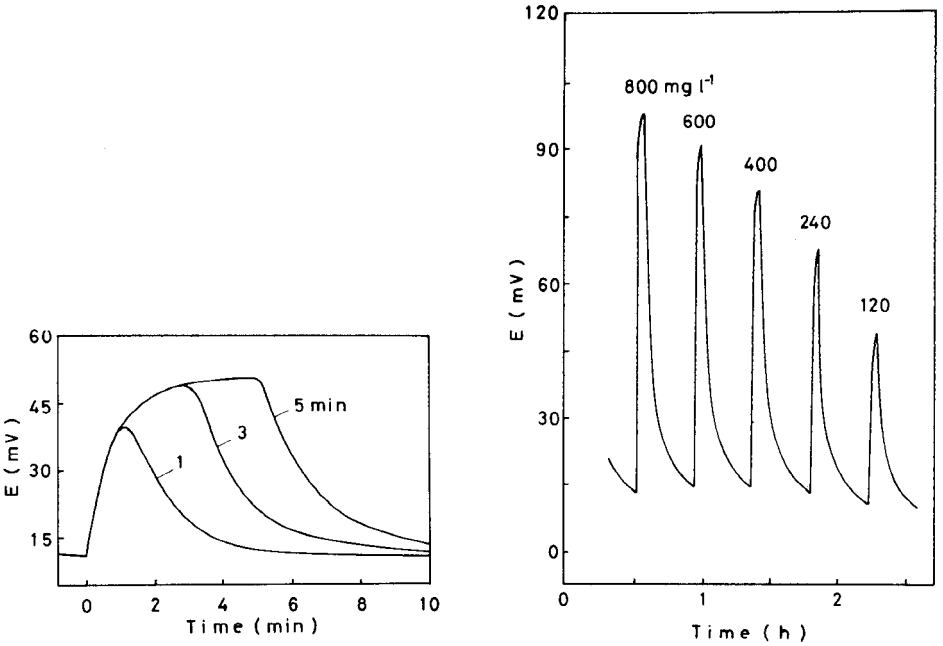

Fig. 3. Response curves of the microbial sensor when 1, 3, and 5 ml of pure aqueous sample solution containing glutamic acid (120 mg l^{-1}) were injected into the system. The determination was carried out under the recommended conditions.

Fig. 4. Responses given by the electrode for glutamic acid solutions of the concentrations stated. Sample solution (3 ml) was injected for 3 min. The determination was carried out under the recommended conditions.

indicating that the rates of formation of carbon dioxide by the enzymatic reaction and diffusion of carbon dioxide from the membrane to a sample solution were equal. This steady-state potential depended on the concentration of glutamic acid. When the pure buffer solution flow returned to the flow cell, the potential of the electrode returned to the initial value. The maximum potentials when sample was introduced for 1 and 3 min were 71 and 96%, respectively, of that obtained under steady-state conditions when the sample injection time was 5 min. Therefore, the assay can be done by using a 1—3 min injection period and measuring the maximum potential with little loss of sensitivity, and consequent increase in the sample throughput rate.

The influence of pH and temperature on the response of the electrode were examined. The response to glutamic acid solution (120 mg l^{-1}) decreased greatly below pH 4.0 or above pH 5.0. The maximum potential difference was obtained at pH 4.4, and this pH was used for all further work. An increase of the temperature shortened the response time, but the lifetime of the electrode was also shortened when used above 40°C. Consequently, the temperature for the determination of glutamic acid was set at 30°C.

Calibration

Figure 4 shows the response of the microbial sensor to various concentrations of glutamic acid. The plot of the maximum potential vs. the logarithm of the glutamic acid concentration was linear over the range shown in Fig. 4; the slope over this range was approximately Nernstian. When a glutamic acid solution (400 mg l^{-1}) was measured in replicate, the standard deviation was 1.2 mg l^{-1} (20 experiments).

Selectivity of the sensor

Table 1 shows the response of the sensor to various amino acids. The sensor responded to glutamic acid and glutamine and very slightly to some other amino acids. The response to glutamine can be decreased, if necessary, using acetone-treated *E. coli*. The selectivity of the microbial electrode was compared with that of the Warburg method using micro-organisms prepared by the same method. As shown in Table 1, the selectivity of the sensor was better than that of Warburg's method. This arises because of the long reaction time (1 h) used in the Warburg method, which permits decarboxylations of other amino acids to be catalyzed by the corresponding decarboxylases in the micro-organisms. The microbial sensor did not respond under the anaerobic conditions to organic substances such as glucose (7800 mg l^{-1}) and acetic acid (200 mg l^{-1}). The influence of inorganic ions on the response was negligible.

Application of the microbial sensor

The microbial electrode was applied to the determination of glutamic acid in fermentation broth. Known amounts of glutamic acid were added to a broth and the concentration of glutamic acid was determined. As shown in Table 2, satisfactory recovery data (99—103%) were obtained. The

TABLE 1

Selectivity of the microbial sensor and that of Warburg's method

Amino acid[a]	Relative sensitivity		Amino acid[a]	Relative sensitivity	
	Microbial sensor	Warburg method		Microbial sensor	Warburg method
Glutamic acid	100	100	Isoleucine	0	2.1
Glutamine	108 (11[b])	100	Leucine	0	2.9
Alanine	0.5	0	Lysine	0	1.6
Arginine	0.6	7.7	Methionine	0	11
Aspartic acid	1.0	0	Phenylalanine	0	2.6
Cystine	0.4	15	Proline, serine	0	0
Glycine	0.4	1.3	Tryptophan	0.4	24
Histidine	0	10	Tyrosine	1.1	45

[a]780 mg l^{-1}. [b]Microorganisms treated with acetone.

TABLE 2

Determination of glutamic acid added to a diluted fermentation broth

Glutamic acid (mg l^{-1})			Recovery (%)	Glutamic acid (mg l^{-1})			Recovery (%)
Added	Present	Found		Added	Present	Found	
0	180	180	—	200	380	383	102
100	280	283	103	300	480	481	100
150	330	333	102	400	580	574	99

TABLE 3

Determination of glutamic acid in fermentation broths with the microbial sensor and by the AutoAnalyzer procedure [1]

Broth	Glutamic acid (g l^{-1})		Broth	Glutamic acid (g l^{-1})	
	Sensor	AutoAnalyzer		Sensor	AutoAnalyzer
A	17.4	17.0	C	41.6	41.8
B	27.0	26.8	D	61.0	61.8

concentrations of glutamic acid in some fermentation broths were determined by the microbial sensor and by the AutoAnalyzer method. For the microbial sensor method, the broths were diluted (1 + 99) with deionized water before injection. Table 3 shows that the results were in good agreement. Therefore micro-organisms in the broth did not affect the proposed determination. Dissolved carbon dioxide in the culture broth at pH 4.4 was removed by passing nitrogen gas, and did not influence the determination.

Glutamic acid solutions (240—800 mg l^{-1}) and fermentation broths of glutamic acid were used to test the long-term stability of the sensor. The response of the electrode was constant for more than 3 weeks and 1500 assays. Thus the microbial sensor appears to be very attractive for the determination of glutamic acid.

The authors are grateful to Mr. T. Kiya, Dr. Y. Sakata, and Dr. K. Mitsugi, Central Research Laboratories, Ajinomoto Co., Inc., for their helpful advice and encouragement during this study and also to Mr. T. Shirakawa for his assistance.

REFERENCES

1 Monosodium Glutamate in Fermentor Solutions, Industrial Method No. 210–72A, Technicon Industrial Systems, New York, 1973.
2 I. Karube, T. Matsunaga, S. Tsuru and S. Suzuki, Biochim. Biophys. Acta, 444 (1976) 338.

3 I. Karube, T. Matsunaga, S. Mitsuda and S. Suzuki, Biotechnol. Bioeng., 19 (1977) 1535.
4 M. Hikuma, H. Suzuki, T. Yasuda, I. Karube and S. Suzuki, Eur. J. Appl. Microbiol., in press.
5 K. Matsumoto, H. Seijo, T. Watanabe, I. Karube and S. Suzuki, Anal. Chim. Acta, 105 (1979) 429.
6 T. Matsunaga, I. Karube and S. Suzuki, Anal. Chim. Acta, 99 (1978) 233.
7 M. Hikuma, T. Kubo, T. Yasuda, I. Karube and S. Suzuki, Biotechnol. Bioeng., 21 (1979) 1845.
8 M. Hikuma, T. Kubo, T. Yasuda, I. Karube and S. Suzuki, Anal. Chim. Acta, 109 (1979) 33.
9 G. A. Rechnitz, R. K. Kobos, S. J. Riechel and C. R. Gebauer, Anal. Chim. Acta, 94 (1977) 357.
10 R. K. Kobos and G. A. Rechnitz, Anal. Lett., 10 (1977) 751.
11 E. F. Gale, Advan. Enzymol., 6 (1946) 1.

Analytica Chimica Acta, 116 (1980) 69—76

POLAROGRAPHIC ANALYSIS FOR CORTICOSTEROIDS
Part 4. Determination of Corticosteroids in Multicomponent and Complex Pharmaceutical Preparations

H. S. DE BOER, P. H. LANSAAT and W. J. VAN OORT*

Department of Analytical Pharmacy, Faculty of Pharmacy, State University of Utrecht, Catharijnesingel 60, 3511 GH Utrecht (The Netherlands)

(Received 25th September 1979)

SUMMARY

Differential pulse polarographic methods for determination of corticosteroids in multicomponent and complex pharmaceutical preparations are described. The influence of other reducible common components of such preparations and excipients on the height of the reduction peaks of corticosteroids and the accuracy of the results was investigated, as well as the interference of excipients by adsorption processes at the electrode or at solid particles of the preparations. In the procedures developed, variations in composition of the supporting electrolyte according to the lipophilicity of the preparation, and the use of standard additions, produce results quickly and reliably. Standard deviations vary from 0.8 to 2.8%.

Earlier parts of this series dealt with polarographic analysis for corticosteroids in single-component pharmaceutical preparations [1, 2]. The main advantages of the described methods are the sensitivity and the speed of the determination. These characteristics are achieved by the application of differential pulse polarography (d.p.p.) and standard addition methods, combined with a simple clean-up procedure. Corticosteroids are frequently combined with antibiotics, analgesics and local anesthetics. Some of these compounds are electro-active, as are some excipients of lipophilic preparations. Furthermore, some of the excipients of lipophilic and hydrophilic preparations may interfere because of their adsorptive properties.

The aim of this work was to investigate the application of the clean-up procedure to the polarographic analysis of multicomponent preparations and preparations with complex mixtures of excipients.

EXPERIMENTAL

Apparatus

Three polarographs were used: a PAR model 174 polarograph and a Bruker E310 modular electrochemical system, both of which were equipped with a drop timer and a Houston model 2200-3-3 x-y recorder, and a Metrohm Polarecord E506 equipped with a polarographic stand E505. A

water-jacketed 10-ml polarographic cell (Metrohm EA 880-T-5) was employed with a dropping mercury electrode, a Metrohm EA 436 Ag/AgCl reference electrode and platinum wire auxiliary electrode. The cell was maintained at 20 ± 0.2°C. The "salt bridge" of the reference electrode was filled with the supporting electrolyte. Standard additions were made by a piston microburette (Metrohm E457-0.6) and a 100-μl or 50-μl micropipette (Oxford P7000).

Chemicals

The steroid preparations used are listed together with their sources in Table 1. The solvents and materials for the supporting electrolytes were: methanol (zur Analyse), dimethylformamide (DMF; Uvasol), tetramethylammonium hydroxide (Me_4NOH; 10% zur Polarographie), acetic acid (99% reinst), phosphoric acid (99% reinst) (all from Merck); toluene and boric acid (reagent grade; Baker). Toluene was distilled twice before use. All other reagents were used without further purification.

Procedure

Because of the variety of dosage forms of corticosteroids, three solvents were used with different lipophilic properties: a mixture of Britton–Robinson buffer in methanol (50% v/v) at pH 10, 0.03 M Me_4NOH in methanol and 0.02 M Me_4NOH in a mixture of DMF (87% v/v) and water. A d.p.p. curve of 10 ml of the supporting electrolyte (solvent) was recorded after deaeration with oxygen-free nitrogen [3] for 15 min. Then, a suitable amount of the sample was added, to obtain a concentration between 10^{-3} and 10^{-5} M steroid in the polarographic cell. After further deaeration for 1 min, the polarogram was recorded. A small volume of the standard solution containing about the same amount of steroid was then added and the polarogram was recorded again. Deaeration for 1 min was sufficient. Dilution by addition of the standard should not exceed 1%. Standard solutions of the steroids were prepared in methanol or DMF depending on the supporting electrolyte used.

The normal scan parameters were: drop time 2 s, scan rate 2 mV s^{-1}, modulation amplitude 100 mV.

RESULTS

Ointments

A suitable amount of ointment was dissolved completely in 5.00 ml of toluene. An aliquot was added to the supporting electrolyte, consisting of 0.02 M tetramethylammonium hydroxide in a mixture of DMF (87% v/v) and water. The fatty constituents did not dissolve in the electrolyte solution, whereas the active compound was extracted into the aqueous DMF. This layer was analyzed by d.p.p.; the results are listed in Table 1. Gentamycin, neomycin and bacitracin in preparation Nos. 1, 2, 4 and 5 are not reducible

TABLE 1

Compositions and analytical results for some multicomponent preparations[a]

No.	Name	Source	Active constituents	Content (mg g^{-1})	Found (mg g^{-1})	R.s.d. (%)
Ointments						
1	Celestoderm-V with garamycin	Schering	Bethamethasone[b] (as 17-valerate)	1	0.98	2.7
			Gentamycin	1		
2	Celestoderm-V with neomycin	Schering	Bethamethasone[b] (as 17-valerate)	1	0.96	2.8
			Neomycin	5		
3	Dexatopic	Organon	Dexamethasone[c]	0.4	0.412	2.7
			Nandrolone decanoate	0.4		
			Chlorhexidine-HCl	10		
4	Corneo	Centrapharm	Prednisolone[c]	2	2.00	2.1
			Neomycin (as sulphate)	5		
			Bacitracin	200		
Cream						
5	Hydrocortisone with neomycin	—[d]	Hydrocortisone acetate[c]	10.0	10.3	1.7
			Neomycin	5		
Alcoholic solutions						
6	Composed triamcinolone acetonide solution	—[d]	Triamcinolone acetonide[c]	1.01[e]	1.01[e]	0.8
			Salicylic acid	20[e]		
			Benzalkonium chloride	0.1[e]		
7	Kenalog Tincture	Squibb	Triamcinolone acetonide[c]	2[e]	1.91[e]	1.3
			Salicylic acid	20[e]		
			Benzalkonium chloride	0.5[e]		
Tablets						
8	Delta-butazolidine	Geigy	Prednisone[c]	1.25[f]	1.26[f]	2.0
			Phenylbutazone	50[f]		
9	Rheulysin	Organon	Prednisone[c]	0.5[f]	0.3[f]	
			Acetylsalicylic acid	300[f]		
Suppositories						
10	Proctosedyl	Roussel	Hydrocortisone[c]	5[g]	5.24[g]	1.3
			Cinchocaine-HCl	5[g]	4.96[g]	1.4
			Framycetin sulphate	10[g]		
11	Tri-Anal	Will Pharma	Triamcinolone acetonide[c]	0.5[g]	0.50[g]	1.5
			Lidocaine-HCl	50[g]		
12	Triamcinolone acetonide	—[d]	Triamcinolone acetonide[c]	0.5[g]	0.50[g]	1.9
			Lidocaine-HCl[c]	50[g]		
Enema						
13	Predniment enema	Pharmachemie	Prednisone[c]	25[e]	28.5[e]	1.7
14	Prednisone enema	—[d]	Prednisone[c]	100[e]	102[e]	1.6

[a]Relative standard deviations of 5 separate determinations with individual sampling. [b]Obtained in pure form from Glaxo. [c]Obtained in pure form from Nogepha. [d]Made in the laboratory. [e]Content in mg ml^{-1}. [f]Content in mg/tablet. [g]Content in mg/suppository.

in the potential range studied and do not interfere. Nandrolone decanoate in preparation No. 3 is a Δ^4-3-ketosteroid. The half-wave potentials of the enones lie about 200 mV more negative than those of dienones. Synthetic mixtures of equimolar amounts of a dienone and an enone showed a small increase in current immediately before and after the d.p.p. peak of the

dienone. This affected the measurement of the peak of the dienone and resulted in a systematic error of +3% of the amount of the dienone. No better results were obtained with normal pulse polarography, in spite of the additivity of the individual waves. The amount of the enone cannot be determined by d.p.p. because of the overlap of the reduction peak of the enone with the more negative peak of the dienone (Fig. 1). Chlorhexidine in preparation No. 3 is also reducible, but the reduction occurs at potentials 250 mV more negative than those for dexamethasone (Fig. 1). Furthermore, the interference of chlorhexidine is diminished by its limited solubility in toluene. Thus none of the other components interferes in the determination of dexamethasone in preparation No. 3.

Some excipients of ointments cause an increase in the base-line, resulting in high results for the corticosteroids. The effects of several common excipients are listed in Table 2. These results make it possible to predict which preparations other than those listed in Table 1 can be successfully analyzed by pulse polarography. For example, the Locacorten ointment (Ciba) contains white beeswax and the results can be expected to have limited

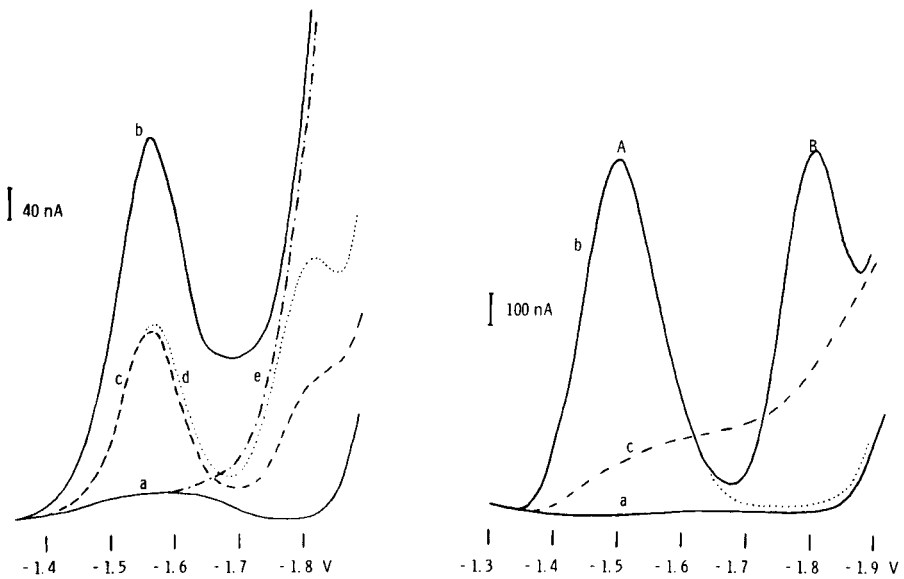

Fig. 1. Differential pulse polarogram of Dexatopic ointment with 0.02 M Me_4NOH in a mixture of DMF (87% v/v) and water. (a) Blank solution; (b) blank solution + sample addition; (c) blank solution + dexamethasone; (d) blank solution + dexamethasone + equimolar amount of an enone; (e) blank solution + chlorhexidine-HCl.

Fig. 2. Differential pulse polarogram of Proctosedyl suppositories with 0.02 M Me_4NOH in a mixture of DMF (87% v/v) and water. (a) Blank solution; (b) blank solution + sample addition, in which peak A is the reduction peak of cinchocaine-HCl and peak B of hydrocortisone and base-line increase by cinchocaine-HCl (dotted line); (c) blank solution + framycetin.

TABLE 2

Effects of lipophilic excipients on the determination of corticosteroids (0.1% corticosteroid)

Compound	Normal content (%) (when present)	Positive systematic error (%)		
		<1	1—5	>5
Arachis oil	50	X		
Cetiol V	20	X		
Cetomacrogol	15	X		
Lanette wax	15	X		
Liquid paraffin	10		X	
Methylhydroxybenzoate	0.2	X		
Monolein	6			X
Polyethylene glycol 400	60		X	
Polyethylene glycol 4000	40		X	
Polysorbate 80	8			X
Propylene glycol	10	X		
Propylhydroxybenzoate	0.2	X		
Sorbic acid	0.2		X	
Sorbitol	4	X		
Span 80	8			X
Spermaceti	10			X
Stearic acid	15			X
Triethanolamine	2	X		
White beeswax	5			X
White soft paraffin	90	X		
Witepsol	100	X		
Wool fat	10		X	
Yellow soft paraffin	90	X		

accuracy, whereas Tumeson ointment (Hoechst) contains wool fat and liquid paraffin, which should have a smaller effect on the accuracy of the results. An extended (mostly chromatographic) clean-up procedure is needed for preparations where large positive errors are expected [4—6].

Creams, alcoholic solutions and tablets

The analyzed cream (preparation No. 5, Table 1) is based on an oil-in-water emulsion in which the steroid ester and neomycin are dispersed; the composition is given in Table 3. The cream (250 mg) was dispersed in 5.00 ml of methanol, and the hydrocortisone dissolved in the methanolic solution; a 1.00-ml aliquot of this solution was transferred to 0.03 M tetramethylammonium hydroxide in methanol and analyzed as described before [1]. A small increase in the base-line was observed, resulting in a positive systematic error of about +3%.

With regard to the alcoholic solutions, neither salicylic acid nor benzalkonium chloride are reducible in the potential range studied and thus do not interfere in the determination of triamcinoline acetonide. An aliquot of the sample (containing 70% ethanol) of preparation Nos. 6 and 7 (Table 1) was

TABLE 3

Complete composition of some complex preparations

Name	Constituent	Content	
Hydrocortisone cream	Hydrocortisone	10	mg g^{-1}
	Neomycin	5	mg g^{-1}
	Cetomacrogol	75	g
	Cetiol V	100	g
	Sorbitol (aq. 70% v/v)	20	g
	Sorbic acid	1	g
	Water ad	500	g
Predniment enema	Prednisone	25	mg
	Sorbitol	5.5	g
	Polysorbate 80		
	Methyloxybenzoate		
	Propyloxybenzoate		
	Sodium carragenate		
	Water ad	100	ml
Prednisone enema	Prednisone	100	mg
	Na_3PO_4	20.5	mg
	Na_2HPO_4	30.0	mg
	NaCl	850	mg
	Methylhydroxybenzoate	150	mg
	Polividon	2.5	g
	Water ad	100	ml
Rheulysin tablets	Prednisone	0.5	mg/tablet
	Acetylsalicylic acid	300	mg/tablet
	$Al(OH)_3$	30	mg/tablet
	Magnesium trisilicate	50	mg/tablet
Triamcinolone acetonide suppositories	Triamcinolone acetonide	0.5	mg/supp.
	Lidocaine HCl	50	mg/supp.
	Witepsol ad	2	g

added to 0.03 M tetramethylammonium hydroxide in methanol and determined as described before [1]. The results agree with the claimed content.

The coated tablets of Delta-butazolidin (preparation No. 8, Table 1) had to be crushed mechanically before dispersion and dissolution in methanol. An aliquot was analyzed in 0.03 M tetramethylammonium hydroxide in methanol as described earlier [2]. Phenylbutazone is not reducible and therefore does not interfere [7]. Rheulysin tablets (preparation No. 9, Table 1) gave low results for prednisone. Neither the excipients nor the salicylic acid are reducible in the voltage range studied and therefore cannot affect the results; adsorption on aluminium hydroxide (Table 3) seems to be a plausible explanation for the low results found. In this particular case, a modification of the extraction procedure is needed.

Suppositories

Because of limited solubility of the hydrocortisone present in the suppository, a relatively high volume (100 ml) of toluene was needed for dissolution of the Proctosedyl suppositories (preparation No. 10, Table 1). Framycetin is itself not electro-active, but gives rise to excessively high results for hydrocortisone by d.p.p., probably because of adsorption processes. When the suppository is treated with 100 ml of toluene containing 1 ml of water, the framycetin dissolves in the aqueous layer and does not interfere in the analysis of the toluene phase. Such analyses were completed by using standard addition in 0.02 M tetramethylammonium hydroxide in DMF (87% v/v) and water. Cinchocaine-HCl is reduced at the DME at potentials 200 mV more positive than those for the hydrocortisone reduction and causes slightly high (about 3%) results for hydrocortisone by d.p.p. (Fig. 2). As can be expected, normal pulse polarography gave very little improvement. Tri-Anal suppositories (preparation No. 11) were analyzed by the procedure developed for ointments. The presence of lidocaine-HCl did not interfere (Table 3). High results were caused by relatively large amounts of Witepsol when the amount of steroid was low (0.25%). When laboratory-made suppositories of the same composition were analyzed, the systematic error could be diminished by adding some Witepsol to the electrolyte solution (Fig. 3). The results obtained by this procedure are listed in Table 1.

Enemas

When an aliquot of the sample was transferred in a methanolic solution containing 0.03 M tetramethylammonium hydroxide, high results were found for prednisone in Predniment enema (preparation No. 13), because of the polysorbate 80 present. Analysis of the prednisone enema (preparation

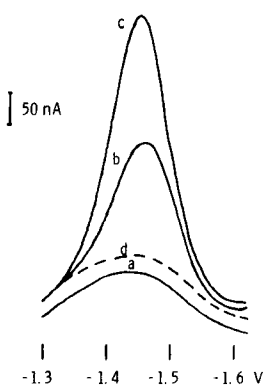

Fig. 3. Differential pulse polarogram of Tri-Anal suppositories with 0.02 M Me_4NOH in a mixture of DMF (87% v/v) and water. (a) Blank solution; (b) blank solution + sample addition; (c) blank solution + sample addition + standard addition; (d) blank solution + Witepsol.

No. 14) in 0.03 M tetramethylammonium hydroxide in methanol yielded a 102% recovery (Tables 1 and 3).

DISCUSSION

Most corticosteroids studied can be determined by differential or normal pulse polarography in the presence of other non-reducible active compounds (Table 1). Sometimes polarographic analyses are possible even in the presence of reducible species, when the waves are well separated, but in some cases interferences cannot be prevented by using the simple treatment proposed in this paper, because of similar reduction potentials and/or similar lipophilic properties. Compounds like iodochlorohydroxyquinoline present in Celestoform-V ointment (Schering), chloramphenicol in Bacicoline eye drops (Bournonville) or dextrochloropheniramine maleate in Polaronil tablets (Schering) interfere in steroid determinations. An analysis of these preparations involves a special sample pre-treatment. Some of the constituents of lipophilic preparations lead to high results, because of adsorption processes or reduction. The systematic error introduced is negligibly small in most cases. As the effects of likely excipients on this analytical procedure are known (Table 2), it is possible to predict situations involving limited accuracy. Tablet excipients, such as lactose, starch, gelatin, talc, magnesium stearate and trisilicate, sodium carboxymethylcellulose, calcium phosphate, acacia, hydroxypropylmethylcellulose, aerosil and aluminium hydroxide usually do not cause an increase in the base-line. At high contents, some of them (like aerosil and aluminium hydroxide) can interfere because of adsorption processes, either at the electrode or by a decrease in the bulk concentration. In the majority of cases, however, the method is reliable, sufficiently accurate and fast.

The authors thank Prof. Dr. P. Zuman (Potsdam, N.Y.) for his critical reading of the manuscript and his enthusiastic cooperation.

REFERENCES

1 H. S. de Boer, P. H. Lansaat and W. J. van Oort, Anal. Chim. Acta, 108 (1979) 389.
2 H. S. de Boer, P. H. Lansaat, K. R. Kooistra and W. J. van Oort, Anal. Chim. Acta, 111 (1979) 275.
3 L. Meites, Polarographic Techniques, Interscience, New York, 2nd edn., 1964, p. 87.
4 M. Amin and U. Jakobs, J. Chromatogr., 131 (1977) 391.
5 H. Hoffmann and J. Volke, in H. W. Nürnberg (Ed.), Advances in Analytical Chemistry and Instrumentation, Vol. 10, J. Wiley, New York, 1974, p. 306.
6 E. Jacobsen and H. Lindseth, Anal. Chim. Acta, 86 (1976) 123.
7 A. G. Fogg and Y. Z. Ahmed, Anal. Chim. Acta, 94 (1977) 453.

Analytica Chimica Acta, 116 (1980) 77—85

THE CONDITIONAL CONSTANT AS ERROR VARIABLE IN THE EVALUATION OF STABILITY CONSTANTS FROM COMBINED pH AND pM MEASUREMENTS

EBBE R. STILL*

Department of Chemistry, Åbo Akademi, SF-20500 Åbo 50 (Finland)

(Received 4th October 1979)

SUMMARY

Combined pH and pM measurements are useful in studies of chelate complexes. A plot of a conditional constant as a function of pH will indicate the species present in the solution and will give good estimates of the unknown stability constants. The values of the constants can be refined by non-linear regression analysis with the conditional constant as error variable. The approach enables programmable pocket calculators to be used in the optimization process.

The determination of stability constants comprises two steps: experimental measurements to obtain the necessary data, and mathematical treatment of these data to indicate which complexes are present, and to determine the value of the corresponding stability constant. In a system containing the three components (all charges omitted) M (metal ion), L (ligand) and H (or OH), and the complexes formed, the equilibrium constants can be determined in many different ways [1]. The problem is simple if it is possible to determine the concentrations of all the components present, but experimental difficulties usually prevent this solution. Precise pH measurements are usually possible, whereas determinations of pM and pL cause considerably more trouble. For pM measurements several kinds of electrodes are available, such as amalgam electrodes and ion-selective electrodes. Current demands are for simplicity both in the experimental procedure and in the method of calculation.

Combined pH and pM measurements have frequently been used for equilibrium studies. This technique is well suited to the study of chelate complexes [2] where the stoichiometry of the complex(es) formed is usually simple. The situation can be visualized by plotting the conditional constant for the formation reaction as a function of pH. Such plots indicate the protonated and deprotonated chelates present in solution and give good estimates of the unknown constants.

*On leave at Inorganic Chemistry Laboratory, University of Oxford, Oxford, U.K.

In the refinement procedure, different types of problems will arise: purely mathematical ones such as the choice of weighting procedure or error variable, purely chemical considerations such as the search for systematic errors in the experimental data, and computational problems. The general search programs that are available for the calculation of stability constants, require not only high-speed computers with a sufficiently large computer storage but also some specialization in the use of these programs. The development of cheap programmable pocket calculators means that the possibilities of solving complex calculation problems have increased dramatically [3]. Limited memory capacity, however, makes it necessary to run smaller tailor-made programs based on compact algorithms.

The aim of the present paper is to show that the conditional constant can serve in a compact algorithm for the evaluation of stability constants of chelate complexes. The theory is based on combined pH and pM (or pH and pL) measurements and the emphasis is on the formation of acidic and basic ternary complexes.

Stability constants can be determined from combined pH and pM measurements in different ways. Potentiostatic titration at a constant level of free hydrogen or metal ion concentration is useful. The pH-stat approach has been successfully applied to complicated metal—protein complexes [4], where the protonation constants of the ligand are often unknown. Another possibility is the stoichiometric approach. Given a known stoichiometry of the titration reaction, the composition of acidic and basic ternary complexes can be determined conveniently by varying the pH of a solution with a fixed ratio between the total concentrations of metal ion and ligand [3], if the protonation constants of the ligand are known.

This paper is concerned with the latter approach. The theory will be presented for 1:1 chelates affected by various side-reactions, but an analogous theory can easily be derived for, e.g., 2:1 or 1:2 chelates. The theory in this form is directed towards chelate formation rather than stepwise complex formation. Search techniques for the evaluation of the constants are also discussed.

THEORY

The cation M and the anion L (all charges are omitted) are assumed to react in a 1:1 ratio forming a number of acidic and basic chelates. In analogy to neutralization reactions, where pH measurements of a well buffered solution should be used for the calculation of the stability constant, it is necessary to use a pM-buffered solution for the pM measurements. The pM value of the solution will be governed by the conditional constant [2]

$$K^{M_iL'_j}_{(M_iL'_j)'} = [(ML)']/[M]\ [L'] = K^{M_iL_j}_{ML}\,\alpha_{ML(H,OH)}/\alpha_{LH} \qquad (1)$$

where

$$[(ML)'] = \sum_{i=-r}^{s} [MH_iL] = [M(OH)_rL] + \cdots + [MOHL] + [ML] + [MHL] + \cdots + [MH_sL] \quad (2)$$

$$[L'] = \sum_{i=0}^{t} H_iL = [L] + [HL] + [H_2L] + \cdots + [H_tL] \quad (3)$$

$\alpha_{L(H)}$ and $\alpha_{ML(H,OH)}$ denote distribution or side-reaction coefficients and have their usual definitions [5]

$$\alpha_{L(H)} = [L']/[L] = 1 + [H]\, K^{H}_{HL} + [H]^2\, K^{2H}_{H_2L} + \cdots \quad (4)$$

$$\alpha_{ML(H,OH)} = [(ML)']/[ML] \quad (5)$$

The mass-balance expressions will give

$$C_M = [M'] + [(ML)']; \; [(ML)'] = C_M - [M'] \quad (6)$$

$$C_L = [L'] + [(ML)']; \; [L'] = C_L - C_M + [M'] \quad (7)$$

C denotes total concentration and $[M']$ is the concentration of uncomplexed metal ion. If $[M']$ differs from $[M]$, it is mostly a question of metal hydrolysis. Substitution of eqns. (6) and (7) into eqn. (1) yields.

$$\log K_{ML} + \log \alpha_{ML(H,OH)} = pM + \log \alpha_{L(H)} + \log \{(C_M - [M'])/(C_L - C_M + [M'])\} \quad (8)$$

The l.h.s. of eqn. (8) contains the unknown constants of the chelates, whereas all the terms on the r.h.s. are calculable. The pM value of the solution can be measured at different pH values and $\log \alpha_{L(H)}$ can be calculated from the known protonation constants of the ligand. A plot of $\log K_{ML} + \log \alpha_{ML(H,OH)} = \log K^{M,L}_{(ML)'}$ as a function of pH will show the chelates formed in solution. If the plot is simply a horizontal line, this proves that the complex ML is formed, whereas a rise of the plot on either side of the horizontal part shows that acidic as well as basic chelates exist in solution. The curvature of the plot gives the number of protons taking part in the protonation and deprotonation reactions of the chelate ML. There is a strong resemblance between the logarithmic diagrams [5] and the plot outlined above.

The ratio C_M:C_L can be varied, but the plot of $\log K^{M,L}_{(ML)'}$ vs. pH will not alter unless some other reaction occurs in the solution (or significant systematic errors are present). In analogy with Bjerrum's half-$\bar{n}$ method [2], simplification can be achieved by preparing the solution with a C_M:C_L ratio of 0.5:1. If this condition if fulfilled, then

$$(C_M - [M'])/(C_L - C_M + [M']) = (C_M - [M'])/(C_M + [M']) \quad (9)$$

For strong complex formation, the concentration of uncomplexed metal ion can be neglected and eqn. (8) will take the simple form

$$\log K_{ML} + \log \alpha_{ML(H,OH)} = pM_{0.5} + \log \alpha_{L(H)} \quad (10)$$

(With known constants of the chelates, eqns. (8) and (10) can be used for the calculation of pM buffers; the buffer capacity of a solution attains its maximum value at a C_M:C_L ratio of 0.5:1.)

APPLICATION TO THE COPPER(II)—PHOSPHORYLSERYLGLYCINE SYSTEM

Österberg has reported very thorough investigations on copper complexes with ligands of biological interest [4, 6]. A copper amalgam electrode was used to determine the equilibrium concentration of free copper ion. The constants of the chelates were obtained by graphical methods (normalized curves) [2] and the values were refined by non-linear regression analysis (LETAGROP) [1]. It was of interest to apply the theory developed here to one of the systems investigated by Österberg. The example chosen is the copper(II)—*o*-phosphorylserylglycine system [6]; Österberg reported the results of series of measurements with varying C_{Cu}:C_L ratios so that the experimental space was extensively investigated. Here the series where C_{Cu} = 0.388 mmol l^{-1} and C_L = 0.767 mol l^{-1} is utilized. The ratio C_{Cu}:C_L is almost 1:2 and the influence of biligand chelates on the constants of the 1:1 complexes should be negligible [3]. Equation (8) was used to calculate the conditional constant. A plot of log $K'^{Cu,L}_{(CuL)}$ as a function of pH is given in Fig. 1.

From eqns. (2) and (8), the relationship between $K'^{M,L}_{(ML)}$ and the stability constants is

$$K'^{M,L}_{(ML)} = K_{ML}\{1 + [H]\,K^{H}_{MHL} + [H]^2\,K^{2H}_{MH_2L} + (1/[H])\,K^{-H}_{MOHL}\} \qquad (11)$$

It is obvious that the log $K'^{M,L}_{(ML)}$ vs. pH plot is built up of straight lines with slopes 0, −1, −2, and +1, indicating the formation of ML, MHL, MH_2L, and MOHL in solution. A possibility for evaluating the constants is to draw the tangents to the curve representing log $K'^{M,L}_{(ML)}$ with slopes of 0, −1, −2, and +1 [3]. The straight lines obtained are indicated in Fig. 1. The ordinate of the horizontal line and the intersection point between the lines gives a first

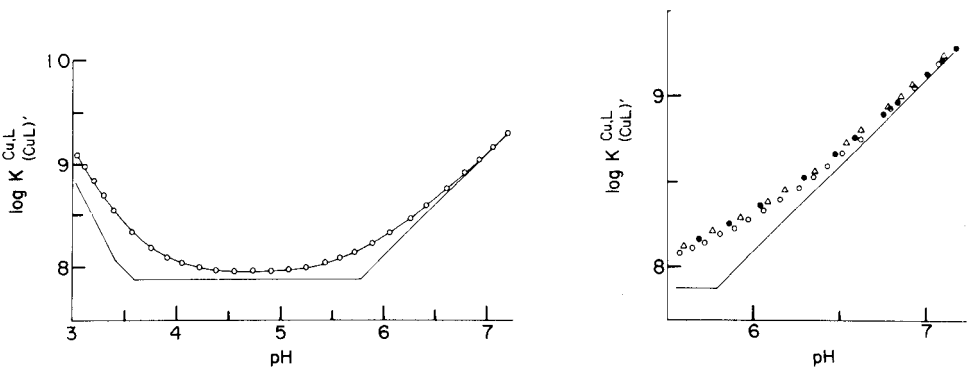

Fig. 1. log $K'^{Cu,L}_{(CuL)}$ of *o*-phosphorylserylglycine calculated from the pCu—pH data of Österberg [6] as a function of pH. C_{Cu} = 0.388 mmol l^{-1}; C_L = 0.767 mmol l^{-1}.

Fig. 2. log $K'^{Cu,L}_{(CuL)}$ as a function of pH calculated for increasing concentrations of the ligand. C_{Cu} = 0.388 mmol l^{-1}; C_L = 0.767 mmol l^{-1} (○), 1.906 mmol l^{-1} (△) and 2.368 mmol l^{-1} (●).

approximation of the constants: log ${}^1K_{ML}$, log ${}^1K^{H}_{MHL}$, log ${}^1K^{H}_{MH_2L}$, and log ${}^1K^{-H}_{MOHL}$. The values of the constants obtained by this graphical method are given in Table 1. These values can then be refined by numerical methods (see below).

Österberg also reported [6] constants for biligand complexes, although he added that the analytical errors could be too large to allow any definitive conclusions regarding the presence of such complexes. The large quantity of data available in Österberg's report was used to determine whether or not the constants obtained for the 1:1 chelates followed the trend that can be predicted when the existence of 1:2 chelates is neglected. As can be seen from Fig. 2, the conditional constant increases with C_L when the concentration of ligand is increased from 0.767 mmol l^{-1} to 2.368 mmol l^{-1}. If the other series of measurements in Österberg's paper is treated similarly, the increase in the conditional constant is found to depend not on the C_{Cu}:C_L ratio, but almost solely on the value of C_L alone. This suggests that there are analytical errors in the standardization of the ligand.

The analytical errors will be most serious close to the equivalence point. Figure 3 shows the plot obtained for C_{Cu} = 0.7025 mmol l^{-1}. In the series with a small excess of ligand (C_L = 0.763 mmol l^{-1}), the plot does not follow the predicted behaviour in the alkaline region. Conversely, the data in Fig. 3 can be used to standardize the ligand solution. The results obtained for a C_{Cu}:C_L ratio close to 1 are particularly suitable for this purpose. The situation is equivalent to a potentiometric titration where the data close to the equivalence point are the most meaningful analytically. The data in Fig. 3 can be used as a point-wise potentiometric titration for construction of a Gran plot [7]. The concentration of the ligand can also be calculated by solving eqn. (8) for C_L. Both these methods indicated that the reported C_L values may be too high by 2—3%.

The presence of analytical errors can also be demonstrated by a graph where the error in the proton number is plotted as a function of the proton number (Table 1 in ref. [6]). The graph is shown in Fig. 4; the positive

TABLE 1

Comparison of the constants obtained[a]

	Österberg [6]	Graphical method	Numerical method
log K_{CuL}	7.885 ± 0.007	7.88	7.887
log K^{-H}_{CuOHL}	—5.79 ± 0.01	—5.78	—5.810
log K^{H}_{CuHL}	3.70 ± 0.05	3.60	3.59
log $K^{H}_{CuH_2L}$	—	3.40	3.46

[a]The values reported by Österberg are based on all the titrations given in ref. [6], whereas the values given in the last 2 columns are based on the titration plotted in Fig. 1 [6].

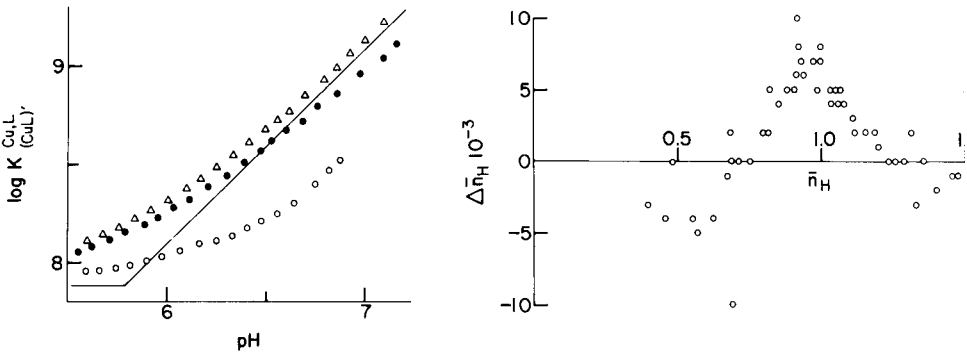

Fig. 3. log $K^{Cu,L}_{(CuL)'}$ as a function of pH calculated for increasing concentrations of the ligand. C_{Cu} = 0.7025 mmol l^{-1}. C_L = 0.767 mmol l^{-1} (○), 1.001 mmol l^{-1} (●) and 1.906 mmol l^{-1} (△).

Fig. 4. The error in the proton number plotted as a function of the proton number.

sign of the error in the region around the first equivalent point is notable.

The application described above shows that the proposed method can be used for determining stability constants of chelate complexes in a system containing a large number of protonated and unprotonated complexes. Analytical errors in the standardization of the solutions can, however, show up as extra species; this stresses the importance of interpreting residuals obtained in the calculations on chemical rather than mathematical grounds.

NUMERICAL METHODS

The values of the constants obtained by graphical methods can be improved by algebraic calculations [8]. The problem of determining the best fit of constants to the experimental data can be based on the classical regression or least-squares (L_2) technique, $E(y) = \frac{1}{2}\Sigma_{i=1}^{n} w_i (y_i - f_i)^2$, or on the weighted absolute (L_1) method, $E(y) = \Sigma_{i=1}^{n} w_i |y_i - f_i|$, where the w_i values are given positive weights associated with each data point, and y_i is the measured value of the error variable f (the vector k represents the parameters of interest): $f_i = f(x_i, \mathbf{k})$ and $\mathbf{k} = (k_1, k_2, \ldots, k_N)$. A further possibility is to allow symmetric generalizations of these equations [9]. For example, the systems illustrated in Figs. 2 and 3 show that the influence of an analytical error on log $K^{M,L}_{(ML)'}$ depends on the C_M:C_L ratio and on the value of the conditional constant. In the asymmetric generalization, the error of the residual is split into positive and negative parts: $y_i - f_i = u_i^+ - u_i^-$, where neither u_i^+ nor u_i^- can be negative. The asymmetric least-squares optimization problem then becomes:

$$\text{Min } E = \tfrac{1}{2}\sum_{i=1}^{n} [w_i^+ (u_i^+)^2 + w_i^- (u_i^-)^2] \qquad (12)$$

where the quadratic weights, w_i, have been generalized to asymmetric quadratic weights w_i^+ and w_i^-. A corresponding expression can be written for the weighted absolute method.

The necessary condition for a minimum in the least-squares equation is $\partial E(y)/\partial k_r = 0$ for $r = 1, 2, \ldots, N$. This expression represents the system of normal equations. If $f(x, k)$ is a linear function in k, the system of normal equations is linear and the constants can be obtained directly by linear algebra. The conditional constant $K^{M_iL}_{(ML)'}$ in eqn. (11) is a linear function of the unknown constants, and it is tempting to use $K^{M_iL}_{(ML)'}$ as error variable. The experimentally recorded quantities are, however, logarithmic, and the accuracy obtained is set by the accuracy in the measured pH and pM values. Thus a rigorous weighting procedure is needed as the standard deviation in [H] and [M] will vary from point to point by several orders of magnitude. It is possible to correct for such errors by introducing weighting factors calculated from error propagation theory [10, 11].

The calculation of weights tends to become a rather lengthy arithmetic operation and most optimization programs for use in solution chemistry try to avoid the weighting problem by choosing the error variable in such a form that weighting is not essential [12].

In the theory outlined, $\log K^{M_iL}_{(ML)'}$ can be used as error variable. Error propagation analysis shows that all the data points can be assumed to have approximately equal weights, although in the acidic region there is an increasing uncertainty in the data points. In the optimization program the simplification $w_i = 1$ is made, but the error variable is then no longer a linear function in the parameters to be refined. Non-linear regression procedures require iterative schemes and often some approximation method will be chosen.

The graphical plot provides an estimated set of values of the constants, i.e. the initial guess. The problem then reduces to that of determining the improvements of the estimated values. The example discussed above contains few unknowns, so that the numerical refinement of the constants can be done by any non-linear estimation program [13]. The regression analysis can be done conveniently by the Gaussian method, as good estimates of the constants are available. The approximation implies a first-order Taylor expansion of the function $f(x, k)$ around the initial guess. This means that in the Gaussian method the non-linear model is approximated by one that is linear, and each iteration can be regarded as the solution of a multiple regression problem.

A standard Gaussian program was written for the example discussed. The improvements in the constants were made in their logarithmic values, so that the iteration for, e.g., K_{ML} is [14]:

$$\log^{s+1} K_{ML} = \log {}^{s}K_{ML} + \Delta \log K_{ML} \qquad (13)$$

where s is the number of iterations. The procedure is repeated until a previously selected convergence condition is fulfilled.

A direct search method is needed for the parameter evaluation based on the L_1 criterion. In such methods the parameters are varied directly without explicit evaluation of derivatives, analytical or numerical. The use of direct

search methods is also attractive for implementation on mini and microcomputers, as a very modest amount of storage is required. The Powell 64 method [15] has been used successfully in many data-fitting problems [8], but is rather sophisticated and not easily adaptable to programmable pocket calculators. For the present purpose, simpler methods should be adequate and the choice of the Simplex method of Nelder and Mead [8] seemed appropriate. The program allows the Simplex to vary in size and shape in order to adjust for the local behaviour of the error variable.

The limited memory and the rather slow speed of programmable pocket calculators sets constraints on the algorithm used in the optimization procedure. Implicit functions, such as e.m.f. potentials, should be avoided as the error variable, as the calculations will require iterative methods such as the Newton—Raphson approximation to be introduced for allocating roots of higher-order equations. The volume of added titrant could be selected as the error variable, as this approach often leads to linear equations [3]. This paper deals with combined pH and pM measurements, and log $K^{M,L}_{(ML)'}$ is the obvious choice as error variable as far as chelate formation reactions are concerned.

The Gaussian method was restricted to the L_2 criterion, whereas the Simplex method was used both for the L_2 and L_1 criteria. The numerical calculations were done on a Honeywell H 316 digital computer. Identical results (within 0.001 log K units) were obtained in each case (Table 1). The direct search method showed poorer convergence properties than the Gaussian method.

The Simplex method was used in connection with a programmable pocket calculator with sufficient data storage. The refinement procedure was done manually. The use of the L_1 criterion reduced the calculating time slightly.

The predominant complex method [16] is very suitable for programmable pocket calculators. The method uses the predominating species of different regions to refine the corresponding constants. The graphical plot provides initial approximations to all constants and gives the predominant species in the different pH regions. Expression (8) can be used for successive refinement of the constants by using the appropriate pH region of the data.

A similar system, where the optimization was carried out by using log $K^{M,L}_{(ML)'}$ as error variable, is the copper (II)—nitrilo-triacetic acid—hydroxide system [17].

The author is greatly indebted to Prof. Francis J. C. Rossotti for his positive interest and his pertinent remarks on the manuscript.

REFERENCES

1 F. J. C. Rossotti and H. Rossotti, The Determination of Stability Constants, McGraw-Hill, New York, 1961.
2 A. Ringbom and L. Harju, Anal. Chim. Acta, 59 (1972) 33, 49.
3 E. Still and R. Sara, J. Chem. Educ., 54 (1977) 348.

4 R. Österberg, in H. Sigel (Ed.), Metal Ions in Biological Systems, Vol. 3 Chap. 2, Dekker, New York, 1974.
5 L. G. Sillén, in I. M. Kolthoff and P. J. Elving (Eds.), Treatise in Analytical Chemistry, Part I, Vol. 1, Chap. 8, Interscience, New York, 1959.
6 R. Österberg, Ark. Kemi, 25 (1966) 177.
7 G. Gran, Analyst, 77 (1952) 661.
8 P. Gans, Coord. Chem. Rev., 19 (1976) 99, and references therein.
9 R. J. Duffin and L. A. Kartovitz, SIAM (Soc. Ind. Appl. Math.) J. Appl. Math., 16 (1968) 662.
10 W. E. Deming, Statistical Adjustment of Data, Wiley, London, 1946.
11 G. L. Cumming, J. S. Rollett, F. J. C. Rossotti, and R. J. Whewell, J. Chem. Soc., Dalton Trans., (1972) 2652.
12 F. J. C. Rossotti, H. S. Rossotti, and R. J. Whewell, J. Inorg. Nucl. Chem., 33 (1971) 2051.
13 Y. Bard, Nonlinear Parameter Estimation, Academic Press, New York, 1974.
14 F. Karlsson and R. Vestin, Chem. Scr., 2 (1972) 207.
15 M. J. D. Powell, Comput. J., 7 (1964/65) 155 and 303.
16 D. I. McMaster and W. B. Schaap, Indiana Acad. Sci., 67 (1958) 111.
17 E. Still, Anal. Chim. Acta, 107 (1979) 1.

Analytica Chimica Acta, 116 (1980) 87—92

COMPARATIVE STUDY ON THE PRECISION OF POTENTIOMETRIC TECHNIQUES APPLIED WITH ION-SELECTIVE ELECTRODES
Part 3. Potentiometric Titrations

G. HORVAI and E. PUNGOR*

Institute for General and Analytical Chemistry, Technical University, Budapest (Hungary)

(Received 18th July 1979)

SUMMARY

Mathematical descriptions of potentiometric titration curves are considered. Methods for calculations of titration errors are discussed with particular reference to single-point and Gran methods of titration.

In potentiometric analysis, errors in the potential measurement cause well defined errors in the sample concentration calculated. Such errors were discussed for the direct potentiometric techniques which are most frequently applied in Parts 1 and 2 of this series [1, 2]. In the present paper, an important group of potentiometric titration techniques is discussed from the same point of view. The underlying theory makes it possible to develop some novel ideas concerning potentiometric titrations, which allow their scope to be broadened.

Potentiometric titrations can be evaluated either by graphical or by numerical, i.e. digital, methods. Digital methods have recently been reviewed by Ebel et al. [3, 4], who have distinguished approximation and mathematical methods. Approximation methods are used to locate the inflection point of the titration curve, which is not necessarily the equivalence point. The particular type of chemical reaction is not important with these methods; usually only a few points in the vicinity of the end-point are considered. In contrast, the so-called mathematical methods are used to locate the equivalence point on the basis of a mathematical description of the titration curve. Examples of approximation methods are the Keller—Richter modification [5] of the method of Hahn et al. [6] and Fortuin [7] and the method of Kohn and Zitko [8, 9]. Gran methods [10] and the method of Waldmeier and Rellstab [11] are examples of mathematical methods. The following discussion is restricted to mathematical methods.

MATHEMATICAL DESCRIPTION OF THE TITRATION CURVE

The mathematical description of a potentiometric titration curve requires two steps: (a) the concentration of the species sensed by the electrode must

be related to the titrant volume consumed, and (b) the potential of the electrode must be expressed as a function of the concentration of the measured species. The solution of problem (a) depends on the type of chemical reaction employed. A generalized solution may be written as

$$c_i = c_i(V_i\,;\, c_x\,;\, V_x, c_r; \text{different constants}) \qquad (1)$$

where c_i is the concentration of the sensed species after addition of the ith increment of titrant; V_i is the sum of the first i volume increments of titrant or, in the case of coulometric titrations, the amount of titrant generated in the first i titration steps; c_x is the analyte concentration before the titration is started; V_x is the volume of the sample solution before titration; and c_r is the reagent concentration. Among the constants are the concentrations of background components, masking agents, etc., which do not change appreciably from sample to sample, and equilibrium constants characterizing the equilibria prevailing in the solution under titration. Semicolons are used in expression (1) to separate the different types of quantities: V_i is the independent variable which will be assumed here to be accurately known; c_x is an unknown constant; V_x and c_r are accurately known constants; the quantities termed "different constants" may be accurately or approximately known. The quantity c_x can be replaced by V_{eq}, the volume of titrant equivalent to the analyte.

The solution of problem (b) is based on the equation $E_i = E' + S \log a_i$ if an ideally selective electrode is used; here E_i is the potential measured after addition of the ith increment of titrant, E' and S are constants, and a_i is the activity of the measured species. The potential of the electrode can be very easily related to the concentration of the measured species, if the activity coefficient, f_i, is practically constant throughout the titration:

$$E_i = E' + S \log f_i\, c_i = E' + S \log f_i + S \log c_i = E'' + S \log c_i$$

where E'' is again a constant.

The generalized equation of the potentiometric titration curve is obtained by substituting c_i from expression (1) into the above form of the Nernst equation:

$$E_i = E'' + S \log c_i\,(V_i; c_x; V_x, c_r; \text{different constants}) \qquad (2)$$

GENERALIZATION OF THE TITRATION CONCEPT

During the titration, corresponding pairs of values (E_i, V_i) are produced. Mathematical methods of evaluation use these pairs to calculate c_x or V_{eq} from expression (2). If some of the other quantities in expression (2) are also unknown, e.g. E', S or an equilibrium constant, these can be calculated if a sufficient number of pairs (E_i, V_i) is taken, and if the quantities to be calculated independently influence the potential. It is also possible to take more potential readings than are strictly necessary to calculate the unknown

quantities, in which case regression methods can be applied. It should be stressed that the theoretical possibility of calculating several constants from the same titration curve does not necessarily mean that it is practical, because the errors in the determination of the constants may be extremely high. This problem is very similar to that discussed in connection with multiple standard addition [2].

Expression (2) provides different outlooks on potentiometric titrations. It is easily seen that if all the constants except for c_x are known before the titration, then a single potential reading is enough to calculate c_x. Such a "titration" may be called single-point titration [12]; the electrode must be calibrated before these titrations. Two-point titrations may be used if, besides c_x, there is another unknown constant, e.g. E'' [12]. Known subtraction is also a two-point titration method in this sense. In the same way, it is possible to speak of three-point, etc. titrations with the restriction made above that the number of unknown constants cannot be made too high without significant loss in precision. When more titration points than the number of unknown constants are used, regression methods have to be applied. An example of this is the familiar Gran titration: in the simplest case, about ten titration points are used to calculate two unknowns, c_x and E'', by regression, although E'' is seldom expressed explicitly. To avoid confusion, the number of titration points used for the evaluation, their location and the number of unknown parameters, should always be specified.

The foregoing discussion proves that the conventional classification of potentiometric methods into direct potentiometry and potentiometric titrations has lost its classifying quality. Methods such as known subtraction can also be regarded as titrations, whereas titration methods such as Gran titrations can be regarded as multiple subtraction or addition. A widely applicable definition would perhaps include as titrations all those potentiometric methods which are based on reaction of the analyte with some reagent, while in direct potentiometric techniques no such reagent is used.

CALCULATION OF THE TITRATION ERROR

In order to calculate the titration error, the actual form of expression (1) must be known. The further discussion will concentrate only on the commonest form of this expression:

$$c_i = c_r(V_i - V_{eq})/(V_x + V_i) \text{ for } V_i > V_{eq} \tag{3}$$

where V_{eq} is used rather than c_x. This equation can be used if the excess of titrant is sensed by the electrode and the titration reaction can be regarded as complete at all points after the equivalence point. The concentrations are expressed in equivalents. Expression (2) becomes

$$E_i = E'' + S \log[c_r(V_i - V_{eq})/(V_x + V_i)] \tag{4}$$

where $i = 1,2, \ldots n$ if n titration points are used. V_{eq} and, if needed, E'' and/or S can be calculated by taking enough, or an excessive number of, titration points. The error in V_{eq} can also be calculated in each case, based on the methods developed earlier [1, 2, 13], by reducing the problem to the calculation of the error in different direct potentiometric techniques.

To this end, the error in V_{eq} will be expressed as a function of the error in c_1, i.e. the concentration of excess reagent in the first titration point after the equivalence point. Equation (3) must also hold for this point, according to the assumptions made, thus

$$c_1 = c_r(V_1 - V_{eq})/(V_x + V_1) \tag{5}$$

From eqn. (5) and the law of error propagation $c_r\, \sigma(V_{eq}) = (V_x + V_1)\, \sigma(c_1)$, where σ denotes standard deviations. By using eqn. (5) again this can be transformed to $\sigma(V_{eq}) = (V_1 - V_{eq})\sigma(c_1)/c_1$. Dividing by V_{eq} then gives

$$\sigma(V_{eq})/V_{eq} = (V_1 - V_{eq})/V_{eq}\, \sigma(c_1)/c_1 \tag{6}$$

This simple relation between the relative standard deviations of V_{eq} and c_1 shows that their ratio depends only on the degree of titration. If the first such titration point after the equivalence point for which the assumptions are valid is near the equivalence point, then the relative titration error will be much smaller than the relative error in the determination of c_1. It remains to show that $\sigma(c_1)/c_1$ can be calculated in a known manner. A few examples are therefore given.

Example 1: Single-point titration. An excess of reagent is added to the sample and the resulting excess is determined by the calibration method. $\sigma(c_1)/c_1$ can then be calculated as described earlier [1].

Example 2: Two-point titration. An excess of reagent is added to the sample and the potential is measured; this is followed by a further reagent addition and potential measurement. E'' is unknown; c_1 is calculated in exactly the same way as in conventional standard addition, hence the relation for $\sigma(c_1)/c_1$ is that given earlier [1] for standard addition.

Example 3: Gran titration. Several increments of reagent are added to the sample, the first of which is already in excess of the analyte. The potential is measured after each addition. The value of c_1 can be calculated in the same way as in multiple standard addition, hence its error is also calculated in the same way [13].

From these three examples, an important further conclusion may be drawn. According to the earlier discussion of direct potentiometric techniques [1, 2], in all three methods referred to above (i.e. calibration method, standard addition and multiple standard addition by the Gran method), it is possible to keep $\sigma(c_x)/c_x$ in the order of $\sigma(E)/S^*$ by appropriate choice of the concentration and volume of the increments and, within certain limits,

to keep it independent of c_x. According to eqn. (6), this means that the relative titration error will depend primarily on the degree of titration at the first titration point after the equivalence point. If, for example, the degree of titration is 110% at this point, i.e. $(V_1 - V_{eq})/V_{eq} = 0.1$, then the relative titration error will be ten times smaller than the relative error of the respective direct determination. A conclusion similar to this has been reached by Ingman and Still [14] but on a somewhat different basis.

It may appear that the relative titration error can be decreased deliberately by making $(V_1 - V_{eq})/V_{eq}$ very small. This is, however, not true: on the one hand, the assumptions made may become invalid near the equivalence point, and on the other hand, since V_{eq} is unknown, V_1 cannot be chosen equal or almost equal to V_{eq}. It should also be stressed again that the derivations were not based on the general expression (1) but only on the simplified eqn. (3).

A final comment can be made on the error of Gran titrations. If the error in the measured potential is constant throughout the titration, the error in the Gran function will not be constant, so that weighted linear regression should be used, just as in the case of Gran-type multiple standard addition. The usual graphical evaluation of Gran titrations is therefore also incorrect in the statistical sense. This may be an important point in judging the precision of Gran titrations from literature data.

DISCUSSION

The above considerations make it possible to compare the relative merits of a few recently suggested titration methods. Ivaska [15] realized that if all the other constants are known, c_x can be calculated from a single titration point and the result will be quite reliable if a glass electrode of good quality is used. Horvai et al. [12] improved this method by choosing the mentioned titration point near the equivalence point, thus increasing the attainable precision. They also pointed out, that two titration points near the equivalence point can be used to obtain good results when two constants, c_x and E', are unknown. Yamaguchi and Kusuyama [16] devised a high speed potentiometric titrator using only four titration points for the precise calculation of c_x. Johansson and Backén [17], Aström [18, 19] and Damokos and Havas [20] used mixtures of weak acids or bases for the titration of strong bases and acids, respectively. By suitable choice of the components of this mixture and their concentrations, they ensured that for any amount of analyte — between certain limits, of course — the near-equivalence-point situation prevailed, thus rendering the determination from a single titration point uniformly precise over a large concentration range of analyte. This is paid for, however, by the use of more complex solutions and a sophisticated theoretical background. Some authors [11, 21] have calculated several unknown parameters from a single titration; the number of titration points used in the calculation was normally higher than the number of unknown

parameters. General considerations concerning the precision of such calculations are beyond the scope of this article.

REFERENCES

1 G. Horvai and E. Pungor, Anal. Chim. Acta, 113 (1980) 287.
2 G. Horvai and E. Pungor, Anal. Chim. Acta, 113 (1980) 295.
3 S. Ebel and A. Seuring, Angew. Chem., 89 (1977) 129.
4 S. Ebel and W. Parzefall, Experimentelle Einführung in die Potentiometrie, Verlag Chemie, Weinheim, 1975.
5 H. J. Keller and W. Richter, Metrohm Bull., 2 (1971) 173.
6 F. L. Hahn, M. Frommer and R. Schulze, Z. Phys. Chem., 133 (1928) 390.
7 J. M. H. Fortuin, Anal. Chim. Acta, 24 (1961) 175.
8 R. Kohn and V. Zitko, Chem. Zvesti, 12 (1958) 261.
9 D. C. Cörmös and I. Marusciac, Stud. Univ. Babes-Bolyai, Ser. Chem., 16 (1971) 27.
10 G. Gran, Analyst, 77 (1952) 661.
11 K. Waldmeier and W. Rellstab, Fresenius Z. Anal. Chem., 264 (1973) 337.
12 G. Horvai, K. Tóth and E. Pungor, Anal. Chim. Acta, 107 (1979) 101.
13 J. Buffle, N. Parthasarathy and D. Monnier, Anal. Chim. Acta, 59 (1972) 427.
14 F. Ingman and E. Still, in E. Wänninen (Ed.), Analytical Chemistry, Pergamon, Oxford, 1977, pp. 183—188.
15 A. Ivaska, Talanta, 21 (1974) 377, 387.
16 S. Yamaguchi and T. Kusuyama, Fresenius Z. Anal. Chem., 295 (1979) 256.
17 G. Johansson and W. Backén, Anal. Chim. Acta, 69 (1974) 415.
18 O. Aström, Anal. Chim. Acta, 88 (1977) 17.
19 O. Aström, Anal. Chim. Acta, 97 (1978) 259.
20 T. Damokos and J. Havas, Hung. Sci. Instrum., 36 (1976) 7.
21 G. Arena, E. Rizzarelli, S. Sammartano and C. Rigano, Talanta, 26 (1979) 1.

Analytica Chimica Acta, 116 (1980) 93—103

MOLECULAR EMISSION CAVITY ANALYSIS
Part 16. Determination of Boron, Selenium and other Elements by using a Flame Generated within the Cavity

S. L. BOGDANSKI, E. HENDEN and ALAN TOWNSHEND*

Chemistry Department, Birmingham University, P.O. Box 363, Birmingham B15 2TT (Gt. Britain)

(Received 20th November 1979)

SUMMARY

Various designs of cavity within which hydrogen—oxygen flames are generated were investigated. After extraction with 2-ethylhexane-1,3-diol, boron (10—400 ng) can be determined in 10 μl of extract, based on BO_2 emission. Arsenic, antimony and tin, after conversion to hydrides, can be determined with similar sensitivity to previous m.e.c.a. procedures. The sensitivity for selenium was poor.

The basic cavity for molecular emission cavity analysis (m.e.c.a.) [1] is simply an aperture at the end of a rod into which a sample is deposited. The cavity is introduced into a hydrogen-based flame and the resulting emissions from within the cavity are measured by a suitably aligned detector. When this cavity is used, oxide emissions, such as that from BO_2, occur only in the flame above the cavity [2], because of the low temperature and low oxygen concentration within the cavity. However, such emissions may be confined to the cavity by introducing oxygen into the cavity through a small tube; this is termed an oxy-cavity [2].

The oxy-cavity has found a number of applications. Boron was extracted as its 2-ethylhexane-1,3-diol chelate into methyl isobutyl ketone and 5—80 ng of boron in the extract was determined by injection into the oxy-cavity [2]. Alternatively, 2—30 μg of boron was determined by conversion to methyl borate which was swept into the oxy-cavity by a stream of nitrogen [2, 3]. In both methods, the BO_2 emission intensity at 518 nm was measured. Belcher et al. [4] reduced arsenic(III) and antimony(III) with sodium tetrahydroborate to arsine and stibine which were also carried into the oxy-cavity by nitrogen. Broad oxide-based emission spectra were obtained covering the range 330—550 nm, with the most intense peaks at 400 nm for arsenic and 355 nm for antimony; 0.5—5 μg of arsenic and about twice as much antimony could be determined. The simultaneous determination of arsenic, antimony and tin, after separation of their hydrides by g.l.c., was achieved in this way by making measurements at 400 nm where there is appreciable spectral overlap between the emissions of the three oxides

[5]. The limits of detection were 0.2 μg of arsenic and 1 μg of antimony. Most interferences were eliminated by preparing the solutions in 0.01 M EDTA [6].

Phosphorus gives a whitish emission, probably the phosphorus continuum [7], in the oxy-cavity, and benzene and acetone give measurable CH emissions at 431.5 nm [8]. Sulphur emission is negligible and therefore the selectivity of the oxy-cavity for phosphorus (and carbon, but with poor sensitivity) is greater than that of other m.e.c.a. cavities and conventional flame photometric detectors. Silicon [3] and nitrogen compounds [9, 10] have also been determined on the basis of oxide-based emissions in the oxy-cavity, including their determination in g.l.c. effluents [8].

As the oxide-based emissions are obtained only when oxygen is supplied to a cavity which is placed in a hydrogen—nitrogen diffusion flame, it should also be possible to obtain the same emissions if the entire flame was generated within the cavity. The apparatus used in conjunction with this cavity would be smaller and cheaper as no burner—gas mixing assembly is required. Also, the running costs would be much less as it would require smaller gas flow rates. The design, scope and some applications of such cavities, therefore, were investigated.

EXPERIMENTAL

Instrumentation

A Unicam SP 900 flame spectrophotometer modified to accommodate an Allen screw cavity [11] was used initially to measure the emissions of cadmium, copper, phosphorus, selenium and boron. The preliminary emission studies of sulphur, tellurium and silicon, and the more detailed studies of boron and selenium, were made with an EEL 240 flame spectrophotometer modified in a similar way [1], with slit 12 (0.91 mm ≡ 3 nm). The output of each spectrophotometer was measured on a Servoscribe IS chart recorder (response time 0.5 s, f.s.d.).

Volatilization system

The g.l.c. column of the volatilization system described earlier [5] was replaced by a teflon tube (2 mm i.d., 70 cm long) which was placed in a Dewar flask containing liquid nitrogen (the cold trap). The tube was connected to the stainless steel tube from one of the rear openings of the cavity. For the determination of selenium, a PVC drying tube (7 mm i.d., 10 cm long), packed with cotton wool, was inserted before the cold trap just after the top stopper of the reaction vessel, and changed after every 4 or 5 experiments. For the determination of the other elements, the drying tube was packed with Drierite. For the determination of carbonate, the reaction vessel was replaced by a smaller one (6 cm long, 1.5 c.m. i.d.) and the cold trap was removed.

Flame-containing cavities and their properties

Several cavities were designed with the intention of obtaining a stable flame totally contained within the cavity. Stainless steel, duralumin and nickel were used as materials for cavities with different designs, so that cavities with different heat-up rates could be obtained. No attempt was made to optimise the cavity sizes.

The first cavity used was made by redrilling the hexagonal aperture of a stainless steel Allen screw to give a circular hole, 5 mm diameter and 3 mm deep. Two stainless steel tubes (0.8 mm i.d.) were connected via two drilled holes to the rear of the cavity, positioned diametrically opposite each other. When oxygen and hydrogen were introduced separately through the side tubes and the gas mixture was ignited, an unstable flame, flashing out of the cavity and resulting in a large variable flame background, was obtained. A stable flame vortex was obtained by introducing the gas tubes tangentially to the cavity wall, but the flame could be kept within the cavity only when a very high oxygen-to-hydrogen ratio with a total flow rate of less than 200 ml min^{-1} was used. The emissions obtained by injecting aqueous boric acid solutions into the cavity were not reproducible because some solution splashed out of the small cavity, so this design of cavity was not investigated further.

In order to develop cavities in which a greater variety of oxygen-to-hydrogen ratios and total flow rates could be used whilst retaining the flame inside the cavity, three water-cooled cavities (0.25 in. diameter, 0.5 in. deep) were constructed by drilling cylindrical stainless steel, nickel and duralumin rods (Fig. 1). A fourth, similar cavity (3/16 in. diameter and 3/8 in. deep) was constructed from duralumin. Two stainless steel tubes (1/16 in. i.d.) were connected (by welding to the outside wall) to the rear of each cavity in opposite directions as tangents to the cavity wall. The rod was also drilled from the other end to within a few mm of the cavity and two copper tubes were connected to the drilling hole for cooling water inlet and outlet (Fig. 1). The tips of the gas entry tubes were ground smooth with the inside wall of the cavity to avoid protruding tubes incandescing in the flame. Because of higher thermal conductivity, duralumin cavities were cooler than nickel and stainless steel cavities, but, because of the low melting point of duralumin

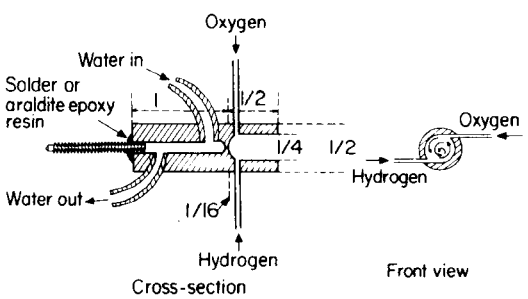

Fig. 1. Cavity cooled with water from the rear only. All dimensions in inches.

(ca. 650°C), at high gas flow rates the inner wall of the duralumin cavity melted and at low gas flow rates the water formed by the flame condensed within the cavity causing excessive background noise. With the smaller duralumin cavity, however, it was possible to adjust the gas and cooling water flow rates to obtain reasonable working conditions. The nickel cavity was cooler than the steel cavity and did not incandesce even when very high oxygen and hydrogen flow rates were used. The stainless steel cavity was used for those studies involving direct injection of aqueous solutions into the cavity and for the determination of boron.

In the water-cooled cavities described above, the temperature was least at the closed end of the cavity near the cooling system and gradually became hotter as the open end was approached. A more completely cooled cavity (Fig. 2) was constructed in order to obtain a cool cavity with a more uniform temperature distribution. It was made from stainless steel as above, except that the water-cooling section surrounded the cavity and three stainless steel gas tubes were introduced tangentially into the cavity. The cavity had a diameter of 0.25 in. When the depth was 0.5 in., water condensation in the cavity was observed, but not when the depth was only 3/8 in. Oxygen and hydrogen were introduced into the cavity through the two opposite gas inlet tubes and nitrogen (carrier gas) through the one between them. This cavity was used for all determinations with the volatilization system, and for the experiments with selenium powder.

As an alternative to these cavities, a tube device was also constructed (Fig. 3) by drilling a hole (0.25 in. diameter) through the length of a stainless steel rod (1 in. diameter, 1.75 in. long) and introducing two gas tubes tangentially to the tube surface. A third hole (1/16 in. diameter) was also drilled obliquely into the tube through which samples could be injected. The device allowed over 1.5 l min^{-1} of oxygen or hydrogen to be used while retaining the flame vortex within the tube. Green, red and yellow emissions were obtained by injecting boric acid, lithium hydroxide and sodium chloride

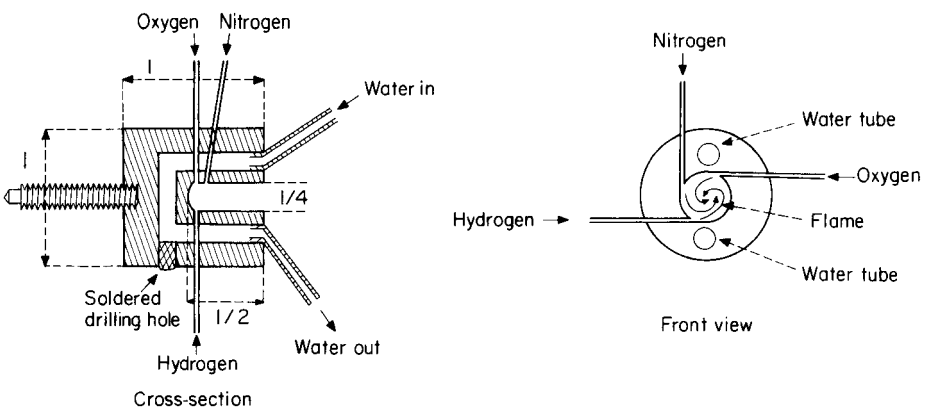

Fig. 2. Cavity cooled with water from side and rear. All dimensions in inches.

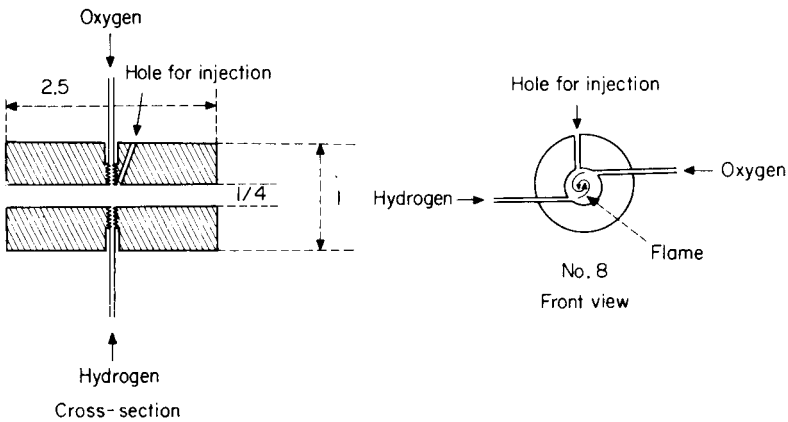

Fig. 3. Stainless steel tube device. All dimensions in inches.

solutions, respectively, either before or after igniting the flame. Sodium and lithium showed a memory effect, however, and the tube device did not appear to have any advantage over normal m.e.c.a. cavities when the injection technique was used. It was not investigated further at this stage.

Determination of boron

Solutions containing 0—500 μg of boron in 20 ml of aqueous solution were prepared in 250-ml separating funnels, and 5 ml of 6 M hydrochloric acid was added to each. The boron was extracted twice with 5 ml of a 10% (v/v) solution of 2-ethylhexane-1,3-diol into methyl isobutyl ketone and the extracts were combined in a 10-ml volumetric flask. When necessary, a few drops of the ketone were added to make up to volume.

The oxygen—hydrogen flame (optimal flows 340 and 400 ml min^{-1}, respectively) was burned for 30 s, then turned off, and the cavity allowed to cool for 60 s. Into the cavity, 5 μl or 10 μl of the extract was injected, and the hydrogen only was turned on and ignited. After 20 s, the oxygen was turned on and the emission intensity recorded as a function of time.

Determination of selenium

The volatilization apparatus was used to generate hydrogen selenide and transfer it to the cavity. A 1-ml portion of selenium(IV) solution (0—20 μg ml^{-1}), 2—5 M in hydrochloric acid, was added to the reaction vessel and the syringe containing 1 ml of 4% (w/v) sodium tetrahydroborate in 0.01 M sodium hydroxide was connected to the side-arm of the reaction vessel. The system was deaerated with nitrogen for 30 s, and then the trap was immersed in liquid nitrogen for 15 s before the tetrahydroborate solution was injected. The flame (200 ml O_2 min^{-1}, 260 ml H_2 min^{-1}) was ignited in the cavity after the first initial reaction had subsided. The hydrogen

selenide was condensed from the carrier gas stream (170 ml min^{-1}) for 1 min. The trap was then immersed in a water bath at 90—95°C and the emission from the cavity was measured at 413 nm as a function of time.

Measurement of other emissions

Arsenic, antimony, tin, tellurium and bismuth. Arsenic(III), antimony(III) and tin(II) solutions made 0.6 M in hydrochloric acid, and tellurium(IV) and bismuth(III) solutions in 2 M hydrochloric acid, were injected, as 1-ml aliquots, into the reaction vessel of the volatilization system containing about 30 mg of sodium tetrahydroborate powder. The generated hydrides were collected for 2 min in the cold trap and then swept to the flame in the cavity, as before. The emissions were recorded at the band heads or atomic lines of the expected emissions, as previously measured by m.e.c.a., viz. As (400 nm) [4], Sb (355 nm) [4], Sn (408 nm) [10], Te (390 or 500 nm) [12] and Bi (472 nm, atom line). Gas flows of 210 ml H_2 min^{-1}, 325 ml O_2 min^{-1} and 50 ml N_2 min^{-1} (carrier gas) were supplied to the flame.

Carbon compounds. Methyl isobutyl ketone (2 ml) was placed in the reaction vessel of the volatilization system, and purged continuously with nitrogen. Carbonate was determined as follows: after the system had been purged with nitrogen, 1 ml of carbonate solution (1000 μg ml^{-1}; K_2CO_3) was injected into the reaction vessel containing 1 ml of 5 M hydrochloric acid at 50°C. The carbon dioxide generated was swept directly to the cavity. The gas flows were as described for arsenic. Under such conditions, 1 ml of carbonate solution, measured at 431.5 nm, gave a peak area of 1.7 cm^2.

RESULTS

Emissions from injected aqueous solutions

Preliminary experiments were carried out to see what emissions could be obtained from various compounds, by using the water-cooled 0.25 × 0.5-in. stainless steel cavity. Air—hydrogen flames gave a very low flame background and oxygen—hydrogen flames a high but steady flame background; as the emissions in the latter flame were much more intense, it was used in the following preliminary studies.

A 10-μl aliquot of the solution to be studied was injected into the cavity and the emission was measured after igniting the flame. Blank emissions were also measured in the same way. Each emission was measured with various flame compositions. Table 1 shows the emissions obtained, and the flame compositions which gave the most intense emissions. Phosphorus gave a weak green HPO emission at low cavity temperatures and a stronger white emission, the phosphorus continuum, at a higher oxygen-to-hydrogen ratio and higher cavity temperatures. The emissions from boron and selenium were intense, and were selected for more detailed study.

TABLE 1

Emissions obtained by injecting aqueous solutions of various elements

Compound	Amount (μg)	Wavelength (nm)	Hydrogen (ml min^{-1})	Oxygen (ml min^{-1})	Colour of flame
$CuCl_2$	10 μg Cu	Green glass filter[a]	310	330	Green
H_3PO_4	10 μg P		310	280	Green
			500	650	White
$Cd(NO_3)_2$	5 μg Cd	326	870	650	
H_2SO_4	10 μg S	384	Various	Various	No colour change
SeO_2	100 μg Se	411	500	520	Blue
H_2TeO_4	1 mg Te	390	>700	>700	Blue
		500			
H_3BO_3	5 μg B	Green glass filter[a]	600	500	Green
Sodium silicate	1 mg Si	251.6	Various	Various	Yellow Na only

[a]519—548 nm.

Determination of boron after solvent extraction

A green boron emission was obtained by injecting aqueous boric acid solution into the cavity. The spectrum of the emission was scanned by generating methyl borate in a volatilization system and carrying it into the cavity by a small nitrogen flow. The spectrum was identical to the BO_2 emission obtained with a m.e.c.a. oxy-cavity [2]. Direct injection of boric acid solution into the water-cooled 0.25 × 0.5-in. steel cavity gave a linear calibration graph for 0.1—5 μg of boron, with a detection limit (2σ) of ca. 0.02 μg of boron.

Since sodium borate gave a less intense emission than boric acid, it was necessary to convert all borates into one form and also to avoid other possible interferences. For this purpose, borate was extracted as its chelate with 2-ethylhexane-1,3-diol into methyl isobutyl ketone [13]. The extraction efficiency from 1—6 M hydrochloric acid has been reported to be 100%; of the ions studied, only fluoride interfered [2]. The blank extract gave an immediate blue emission from the solvent (CH, C_2, etc.). A boron-containing extract also gave the blue emission which overlapped with the slightly later green BO_2 emission. As the solvent emission was intense at the major BO_2 band heads (493, 518 and 547 nm), it was necessary to separate the solvent and boron emissions. Attempts to resolve the emissions temporally by changing the flame composition and thus the cavity heating rate were unsuccessful, but it was found that the solvent could be selectively removed by first turning on the hydrogen flow only and igniting it. Introduction of oxygen then produced the BO_2 emission without interference from the solvent.

Changing the gas flow rates affected the flame volume and shape as well as the temperature. In the 0.25 × 0.5-in. steel cavity, as the oxygen flow rate and proportion increased the flame size diminished, finally forming a very small flame burning directly in front of the tube introducing hydrogen into the cavity, As the oxygen flow rate and proportion decreased, the flame started to burn at the oxygen inlet tube side of the cavity, then became larger with further decrease of the oxygen flow rate, and finally formed a flame coming out of the cavity. At a certain proportion of oxygen, the flame was round and burned in the centre of the cavity. This proportion approximately corresponded to that which gives maximum BO_2 emission intensity.

With hydrogen at 310 and 400 ml min^{-1}, and oxygen as 46% (v/v) of the total flow, maximum net BO_2 emission was obtained while the flame was entirely inside the cavity; with the hydrogen flow of 520 ml min^{-1} and oxygen as 42% (v/v) of the total gas flow, maximum net BO_2 emission was given by a flame partly out of the cavity. Thus oxygen and hydrogen flow rates of 340 and 400 ml min^{-1}, respectively, were used in the study of boron. Introduction of nitrogen with the oxygen decreased the BO_2 and background emission intensities; the greatest boron-to-background ratio, however, was obtained in the absence of nitrogen.

Under the established optimal conditions, a linear calibration graph was obtained by injecting 10 μl of the extract containing 0—400 ng of boron and measuring the peak emission intensities. The emission—time responses are shown in Fig. 4. Under these conditions, the flame background level was

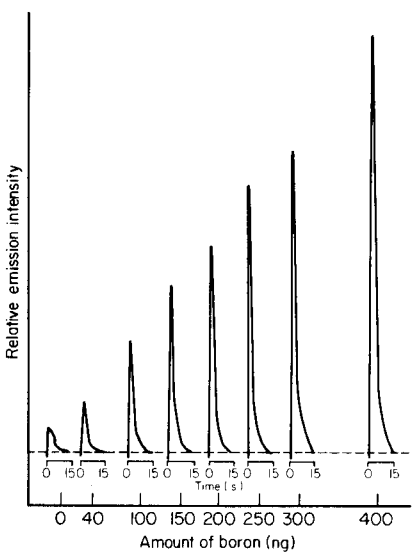

Fig. 4. Emission—time responses for various amounts of boron in the 10-μl extract injected into the cavity. The times (in s) relate to the time after ignition of the oxygen—hydrogen flame.

equivalent to the response from 130 ng of boron with a noise level of 1 ng of boron. The blank was equivalent to 16 ng of boron with a standard deviation (5 results) of 0.8 ng. The coefficients of variation for the determination of 10, 60, 120 (6 experiments) and 400 ng (11 experiments) of boron in 10 μl of extract were 9.2, 3.7, 2.2 and 2.1%, respectively. The limit of detection (2σ) was 1.6 ng of boron. These values are very similar to those obtained by conventional m.e.c.a. [2], but the linear range is at least five times greater when the present technique is used.

Determination of selenium after hydride generation

Selenium compounds gave a blue emission in the cavities described. The spectrum of the emission (Fig. 5) was scanned by placing a few mg of selenium powder in the cavity before igniting the flame. A very broad continuum spectrum from 330 to 550 nm was obtained with the most intense peak at 413 nm. In order to enhance the sensitivity and selectivity, selenium(IV) was determined after conversion to hydrogen selenide by reaction with sodium tetrahydroborate solution using the procedure previously described for conventional m.e.c.a. [14]. The hydrogen selenide was swept to the cavity by nitrogen. As previously, a cold trap was employed to separate hydrogen selenide from hydrogen generated by the reaction, so as to avoid the effect of the hydrogen on the flame background while the selenium emission was measured. The effect of oxygen flow was not very large over the range 130—290 ml min^{-1}, but higher oxygen flows greatly decreased the emission intensity. Changes in hydrogen and nitrogen flow rates in the ranges 260—330, and 150—225 ml min^{-1}, respectively, had little effect. Therefore the flow rates selected for the determination of selenium were 200 ml O_2 min^{-1}, 260 ml H_2 min^{-1} and 170 ml N_2 min^{-1}. The acidity of the selenium solution was not critical between 2 and 5 M hydrochloric acid. When sodium tetrahydroborate powder was used instead of a solution, an intense green emission was obtained, which was attributed to the formation of boranes, probably mainly diborane. The green emissions were very weak when tetrahydroborate solutions (up to 5%) and hydrochloric acid (up to 5 M) were used. Under the recommended conditions the blank reading was equivalent to 0.6 μg of selenium, and the flame background was equivalent to 6 μg of selenium, with a noise level of 0.15 μg.

The selenium emissions reached their maximum intensity 2.5 s after immersion of the cold trap in hot water. The emission—time responses obtained for various amounts of selenium are shown in Fig. 6. The calibration graph obtained from these results was slightly sigmoidal. The linear log—log calibration plot had a slope of 1.4, which is less than the expected slope of 2.0 for a second-order rate dependence for excited Se_2 formation (as has been found for S_2 emissions [14]), and compares with log—log slopes of 0.82 and 1.6 obtained in other m.e.c.a. investigations of selenium [15, 16]. Such widely divergent values probably indicate the important effect of flame conditions on the rate of formation of the emitting species. The

coefficient of variation for one determination of 7 μg of selenium (7 determinations) was 5.5%. The limit of detection (2σ) was 0.3 μg of selenium. The sensitivity and detection limit obtained are much inferior to that obtained by using a conventional m.e.c.a. cavity and a vapour-generation system [15].

Preliminary studies of some other elements by using vaporization systems

The hydrides of 10 μg of arsenic, antimony, tin, bismuth and tellurium were generated and transported to the completely water-cooled cavity, and introduced into an oxygen—hydrogen flame. No emissions were generated by bismuth or tellurium, probably because the cavity was too cold, but the other hydrides all gave blue emissions. The intensities, measured at the wavelengths of maximum intensity, were as follows: arsenic, 31 mV (400 nm); antimony, 30 mV (355 nm); and tin, 14 mV (408 nm). These intensities were very similar to those obtained in a conventional m.e.c.a. oxy-cavity [5].

Vapours of organic compounds gave a blue emission in the cavities. Methyl isobutyl ketone, for example, gave an emission in which the CH band (431.5 nm) was very prominent. Carbonate could be determined by conversion to carbon dioxide and measurement of the CH emission. However, the 2σ limit of detection (100 μg of carbonate) and sensitivity were poor.

Conclusions

It has been possible to design cavities for m.e.c.a. which totally enclose the flame. Such cavities eliminate the need for the burner system used in previous m.e.c.a. studies, and, because of the relatively small flows of gases

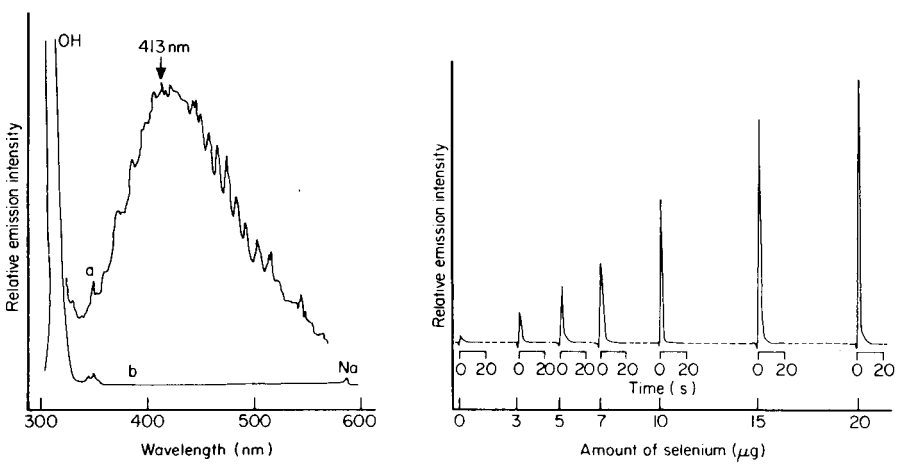

Fig. 5. Spectra of (a) selenium emission from selenium powder; (b) flame background: slit = 0.31 mm (= 1 nm).

Fig. 6. Emission—time responses for various amounts of selenium. The times (in s) relate to the time after immersion of the cold trap in hot water.

used, they are more economic in terms of gas consumption. A number of elements could be determined in such systems, with similar sensitivity to previous m.e.c.a. systems. These included many of the elements which can be determined in an oxy-cavity (boron, arsenic, antimony and tin), and phosphorus. Sensitivity for selenium and tellurium, however, was much poorer than obtained previously. Undoubtedly, the system could also be adapted to measure sulphur sensitively, and could be used as a g.l.c. detector for most of the elements investigated [8].

E. Henden thanks the Turkish Ministry of Education for providing a scholarship.

REFERENCES

1 R. Belcher, S. L. Bogdanski and A. Townshend, Anal. Chim. Acta, 67 (1973) 1.
2 R. Belcher, S. A. Ghonaim and A. Townshend, Anal. Chim. Acta, 71 (1974) 255.
3 M. Burguera, Ph.D. Thesis, Birmingham University, 1979.
4 R. Belcher, S. L. Bogdanski, S. A. Ghonaim and A. Townshend, Anal. Chim. Acta, 72 (1974) 183.
5 R. Belcher, S. L. Bogdanski, E. Henden and A. Townshend, Anal. Chim. Acta, 92 (1977) 53.
6 R. Belcher, S. L. Bogdanski, E. Henden and A. Townshend, Analyst, 100 (1975) 522.
7 R. W. P. Pearse and A. G. Gaydon, The Identification of Molecular Spectra, 4th edn., Chapman and Hall, London, 1976.
8 R. Belcher, S. L. Bogdanski, M. Burguera, E. Henden and A. Townshend, Anal. Chim. Acta, 100 (1978) 515.
9 R. Belcher, S. L. Bogdanski, A. Calokerinos and A. Townshend, Analyst, 102 (1977) 220.
10 I. Z. Al-Zamil, Ph.D. Thesis, Birmingham University, 1978.
11 R. Belcher, K. P. Ranjitkar and A. Townshend, Analyst, 100 (1975) 415.
12 R. Belcher, T. Kouimtzis and A. Townshend, Anal. Chim. Acta, 68 (1974) 297.
13 E. J. Agazzi, Anal. Chem., 39 (1967) 233.
14 D. G. Greer and T. J. Bydalek, Environ. Sci. Technol., 7 (1973) 153.
15 R. Belcher, S. L. Bogdanski, E. Henden and A. Townshend, Anal. Chim. Acta, 113 (1980) 13.
16 A. Iranpoor, unpublished results.

Analytica Chimica Acta, 116 (1980) 105—110

ATOMIC ABSORPTION SPECTROMETRIC DETERMINATION OF THE TOTAL CONTENT AND DISTRIBUTION OF CHROMIUM IN BLOOD SERUM

E. GRAF-HARSÁNYI** and F. J. LANGMYHR*
Department of Chemistry, University of Oslo, Oslo 3 (Norway)
(Received 22nd October 1979)

SUMMARY

Various atomic absorption spectrometric methods, including the solid sampling technique, were used to determine the total content of chromium in a lyophilized reference sample of animal serum. The concentration in the solid sample was found to be 61 ppb. The distribution of the element among the serum proteins was studied by gel filtration and atomic absorption spectroscopy. Chromium was found to be concentrated in the high and low molecular weight protein fractions.

The increasing interest in the effects of trace elements has initiated very many studies of their concentration and distribution in biological materials, with the purposes of establishing the normal values, and detecting illnesses, occupational diseases and toxic effects.

Chromium is an essential trace metal which is found in widely differing concentrations in the human and animal body. Data on the total content, distribution and metabolism of the element in the human body have been reported by Merz [1]. Earlier mean values for human serum chromium vary over wide ranges, from 0.16 to 150 ppb. As pointed out by some authors [2], the risk of introducing contaminations makes it probable that the more recent lower values have greater validity than earlier data. Thus in a recent critical compilation [3] of the elemental composition of human tissues and body fluids, the values given for chromium in serum are in the range 5—22 ppb.

The conventional methods for trace metal analysis have been applied to the determination of chromium in biological materials; several of these procedures are plagued by tedious and time-consuming decomposition, separation and concentration steps, and it is a prerequisite for the use of most of the methods that the sample be present in the liquid state. In a recent paper [4], the penetration of chromium into human skin was studied by the solid sampling technique of atomic absorption spectrometry

**On leave from Technical University Budapest, Institute for General and Analytical Chemistry, Gellert tér. 4, Budapest, Hungary.

(a.a.s.), the sections of the skin being inserted directly into a graphite furnace.

To the authors' best knowledge, studies of the distribution of chromium among the serum proteins have not been carried out. This paper presents various a.a.s. methods, including the solid sampling technique, for the determination of the total content of chromium in serum, and a study of the distribution of the element among the serum proteins.

EXPERIMENTAL

Apparatus

The measurements were made with a Perkin-Elmer (P-E) 400 S atomic absorption spectrophotometer with lamps for background correction, and a Pye—Unicam SP-9-01 atomizer equipped with pyrolytically coated graphite tubes of the profile type. Some measurements were also made with a P-E model 5000 instrument equipped with an HGA-500 graphite furnace and an AS-50 auto sampler for liquids.

Powdered solid samples were transferred to the furnace by means of a specially made injector made of silver; the end of the injector could be inserted in the injection port of the graphite tubes. Liquid samples were pipetted with plastic-tipped micropipettes. Weighings were made with a semimicro balance.

Lyophilized samples were wet-ashed in platinum dishes and polytetrafluoroethylene-lined aluminium bombs.

A TracerLab LTA-505 low-temperature plasma asher was used to decompose portions of the solid sample.

The proteins were separated on a LKB 2137 chromatography column. The fractions were collected with a Shandon-Jeffs gravimetric fraction cutter.

A Beckman DB spectrophotometer and 2-mm silica cells were used to record the absorption of the protein fractions at 280 nm.

Reagents and standard solutions

A primary 1000 ppm chromium standard solution was prepared by dissolving 1 g of metal (purity 99.97%) in 50 ml of (1 + 9) sulfuric acid and diluting the solution to 1 l with deionized water. Secondary standard solutions were prepared daily; they were 2.0% (v/v) in nitric acid.

The concentrated acids were of Suprapur quality (Merck). The chemicals were of reagent-grade quality.

The chromatography column was filled with LKB Ultrogel ACA 44. For the identification of peaks, the proteins used were albumin and gammaglobulin, molecular weight 66000 and 160000, respectively. A 0.05 M phosphate buffer (pH 7.0), 0.171 M in sodium chloride, and 0.02% in sodium azide (to prevent bacterial growth on the gel) was employed for elution.

The furnace was purged with argon of purity 99.9% (by volume).

Samples and sample preparation

The samples analyzed in the present study were portions of a stable lyophilized animal serum (Seronorm, produced and distributed by Nyegaard & Co., A/S, Oslo). During processing the serum is mainly in contact with plastic materials and glass; the only equipment made of stainless steel is a stirrer and the filling pump. By the lyophilization process, 10.040 g of serum give 0.7—0.9 g of solid material; chromium is thus concentrated 11—14 times. Seronorm is certified for more than 35 serum substances; however, among the trace metals recommended values are given only for copper and zinc. Before analysis, the content of the bottle was homogenized (in the bottle) by mixing with a plastic rod.

The solid samples were stored at about +4°C.

Decomposition

Solutions of Seronorm were prepared by four different methods as follows. Method (a) 0.1500 g was dissolved in 1.00 ml of water. Method (b) 0.2000 g was transferred to the bomb, 1.00 ml of concentrated nitric acid was added, and the bomb was closed and heated for 3 h at 150 ± 10°C. Method (c) 0.4000 g was transferred to a platinum dish, 4.00 ml of concentrated nitric acid were added, and the covered dish was heated on the hot plate until a clear solution was obtained, before final dilution to 5 ml. Method (d) 0.5239 g was plasma-ashed by heating for 3 h at about 130°C (oxygen flow 0.2 l min^{-1}, pressure 0.3 torr) and the residue was dissolved in 2.00 ml of 2.0% (v/v) nitric acid. Blank solutions were prepared for each method.

Preliminary studies

In addition to the organic components, serum contains large amounts of salts, sodium chloride predominating. The matrix may interfere in various ways with the determination of chromium; the analyte may be lost as a halide during the pyrolysis and atomization steps, and molecules and solid particles may absorb during atomization. (The absorption by gaseous sodium chloride molecules at the wavelength of the chromium line (357.9 nm) can be expected to be negligible.)

It was decided to base the analysis on matrix modification by adding (to the solid or liquid sample deposited in the graphite tube) a solution of nitric acid, or sulfuric acid, or ammonium nitrate. On subsequent heating chloride (and presumably other halides) is removed by evaporation. The effect of these three matrix-modifying agents was studied by pipetting into the graphite tube 5 µl of 0.04 ppm chromium solution, 5 µl of 3.0% (w/v) sodium chloride, and 5 µl of a 2.0% (v/v) solution of nitric acid, sulfuric acid or ammonium nitrate; for comparison, solutions of chromium alone and of chromium and sodium chloride were also measured.

The interference study, which was made with the P-E 400 S spectrophotometer and the Pye-Unicam atomizer, demonstrated that the background

corrector is incapable of compensating for the sodium chloride present in the serum, and that sulfate also gave high results. However, nitric acid and ammonium nitrate both removed the interference from sodium chloride and permitted the use of pyrolysis temperatures up to 1250°C. A procedure comprising the addition of nitric acid to solid or liquid samples and a drying step at about 120°C to remove a large part of the chlorides, a first pyrolysis step at 550°C to get rid of the organic matrix, and a second pyrolysis step at 1250°C to remove the remaining salts (except the phosphates), was chosen to secure interference-free measurements. The feasibility of this approach was tested by recording the signals from solid serum samples at the 357.9-nm chromium line with and without the background corrector, and at the adjacent 352-nm neon line (without the use of the corrector lamp).

Procedures

Before the start of the measurements, the hollow-cathode and background corrector lamps were heated for 15 min. The instrumental parameters are listed in Table 1. All analyses were based on measuring peak heights. Both instruments were used to establish the total content of chromium by atomizing liquid samples. The P-E 400 S instrument was employed in the direct analysis of the solid samples, while the P-E 5000 instrument was used in the analysis of the protein fractions.

Determination of the total content of chromium in solid samples. Portions (0.5—1.5 mg) of Seronorm were transferred to the furnace by means of the silver injector and the injector was reweighed; 5 μl of 2.0% (v/v) nitric acid, or 5 μl of a suitable chromium standard solution (2.0% in nitric acid) were added and the analysis was completed according to the program given in Table 1. After three atomizations the residue was removed from the tube by brushing. The analytical results reported below were obtained from a standard additions curve plotted from 10 additions of chromium.

TABLE 1

Instrumental parameters
(In both cases, measurements were made at 357.9 nm with a chromium hollow-cathode lamp, a spectral bandwidth of 0.7 nm, tungsten lamp background correction, and 5× scale expansion.)

Instrument	P-E 400 S	P-E 5000
Lamp current (mA)	17	25
Argon flow (ml min^{-1})	50	5 (internal)
Graphite tube	Profile	Standard
Drying	30 s at 120°C	30 s at 120°C, ramp time 10 s
Pyrolysis	30 s at 550°C	5 s at 200°C, ramp time 5 s
	40 s at 1250°C	20 s at 1200°C, ramp time 20 s
Atomization	5 s at 2500°C	10 s at 2300°C, ramp time 0 s
Cleaning step	3 s at 2700°C	2 s at 2700°C, ramp time 2 s

Determination of the total content of chromium in liquid samples. From each of the four liquid samples, a series of 10-μl portions were pipetted into the graphite tube of the P-E 400 S instrument, to one of the portions of each series 5 μl of water were added [to the portion of the sample dissolved by method (a) (see above) 5 μl of 2.0% nitric acid were added], to the remaining portions 5 μl of a suitable chromium standard solution (2.0% in nitric acid) was added, and the measurements were made under the conditions listed in Table 1.

The calibration and standard addition curves were plotted and the precision of the results calculated by regression analysis.

Separation of the proteins and determination of chromium in the fractions. The chromatography column was assembled, packed and run in as specified by the manufacturer. Portions (0.2 g) of Seronorm were dissolved in 1.00 ml of buffer, and the solution was transferred to the column and eluted at ambient temperature at a flow rate of 10 ml h^{-1}. The total number of fractions was 20; the volume of each fraction was 2.0 ml.

The amount of chromium in the sample subjected to gel filtration was about 12 ng, so that the amounts in the fractions will be near the lower limit of determination. In order to increase the content in the fractions, further separations were done with 0.5-g Seronorm samples to which 500 ng of chromium had been added in the form of a solution of a chromium(III) salt; after addition of 1.00 ml of buffer solution, the solution was heated at 40°C for 2 h, which, according to the literature [5], will cause the added chromium to react with some of the proteins. After gel filtration the chromium content in the fractions was determined as described above.

TABLE 2

Analytical results (in ppb) for chromium in a sample of lyophilized animal serum (Seronorm, batch no. 149i)

Method	Chromium found (ppb)	R.s.d.[a] (%)
1. Addition of Cr standard solutions to weighed portions of solid sample	59	22
2. Decomposition by method (a) [b], measurements against Cr standard solutions	61	10
3. Decomposition by method (a), standard additions	57	9
4. Decomposition by method (b), measurements against Cr standard solutions	60	10
5. Decomposition by method (b), standard additions	65	9
6. Decomposition by method (c), measurements against Cr standard solutions	63	20
7. Decomposition by method (c), standard additions	71	20
8. Decomposition by method (d), measurements against Cr standard solutions	66	—[c]

[a] From 8—10 determinations. [b] See Decomposition. [c] Insufficient data.

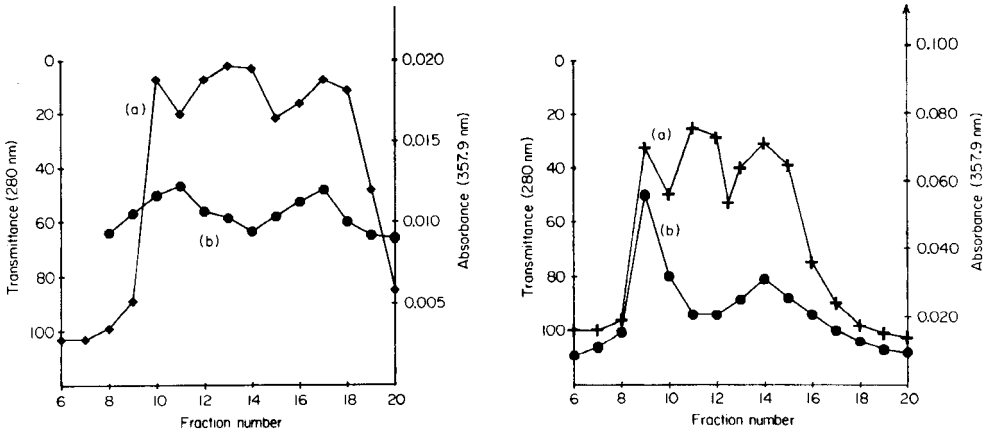

Fig. 1. The distribution of chromium among the proteins of a sample of lyophilized animal serum. Curve (a) transmittance at 280 nm of the fractions from the gel filtration column; curve (b) absorbance of the fractions at the 357.9-nm chromium line.

Fig. 2. The distribution of chromium with added analyte among the proteins of a sample of lyophilized animal serum. Curve (a) transmittance at 280 nm of the fractions from the gel filtration column; curve (b) absorbance of the fractions at the 357.9-nm chromium line.

RESULTS AND DISCUSSION

The analytical results for the total content of chromium in the solid sample of lyophilized animal serum (Seronorm, batch No. 149i) obtained by the various methods employed, are listed in Table 2. All the results were in the range 57—71 ppb, the weighted mean value was 61 ppb. The methods employed had relative standard deviations in the range 9—22%.

The distribution of chromium in serum without and with added analyte, and the absorbance of the protein fractions as measured at 280 nm by conventional spectrophotometry are shown in Figs. 1 and 2, respectively. These figures indicate the presence of two chromium-containing species, one of which is found in the high-molecular weight range (in the macroglobulin group), and the other among proteins of low molecular weight, such as albumin and transferrin. The present study confirms the observation reported in the early literature [6] that the chromium is largely bound to the transferrin component.

REFERENCES

1 W. Merz, Physiol. Rev., 49 (1969) 163.
2 E. J. Underwood, Trace Elements in Human and Animal Nutrition, Academic Press, New York, 1971.
3 G. V. Iyengar, W. E. Kollmer and H. J. M. Bowen, The Elemental Composition of Human Tissues and Body Fluids, Verlag Chemie, Weinheim, 1978.
4 S. Lidén and E. Lundberg, J. Invest. Dermatol., 72 (1979) 42.
5 H. Sakurai, T. Tachikawa and S. Shimomura, Anal. Lett., B11 (1978) 879.
6 L. L. Hopkins and K. Schwarz, Biochim. Biophys. Acta, 90 (1964) 484.

Analytica Chimica Acta, 116 (1980) 111—117

DETERMINATION OF TOTAL PARTICULATE MERCURY IN AIR WITH THE COLEMAN MERCURY ANALYZER SYSTEM

R. DUMAREY, R. HEINDRYCKX and R. DAMS*

Institute for Nuclear Sciences, Rijksuniversiteit Gent, Proeftuinstraat 86, B-9000 Gent (Belgium)

(Received 18th September 1979)

SUMMARY

A simple and rapid cold-vapour atomic absorption system is described for the simultaneous determination of low ambient levels of particulate mercury and volatile mercury compounds. Of the different filters checked for particle collection, quartz fibre filters have the best properties. Sampling characteristics were considered with respect to efficiency, reproducibility and duration of sampling. The homogeneity of the solid mercury deposit on the filter was tested. Possible enrichment during sampling by absorption of volatile mercury compounds and possible mercury losses by volatilization of solid compounds were examined. After sampling the mercury is released by pyrolysis and collected on a gold-coated sand absorber. In order to avoid deactivation of the absorber by condensation of pyrolysis products or interference during the subsequent desorption and atomic absorption measurement of the collected mercury, a heated catalytic convertor and two specific absorbers for organic substances are inserted in the analysis line.

Atmospheric particulate mercury consists essentially of inorganic compounds such as cinnabar and mercury oxides and of less volatile organic compounds as phenylmercury acetate. Besides these primary compounds, elemental mercury can also adhere to dust particles. Because of its affinity for a great variety of materials an estimated 50% of the elemental mercury present can be taken up by dust [1].

In the determination of atmospheric mercury, the principal distinction is between total particulate and total volatile mercury. After collection on filter pads, numerous techniques are available for analysis of the particulate matter, such as neutron activation analysis [2], x-ray fluorescence [3] and emission spectroscopy [4], but the most frequently used method is probably cold-vapour atomic absorption spectrometry. Two methods are usually preferred for sample destruction, i.e. wet digestion and pyrolysis [5, 6]. Acid digestion in a teflon pressure vessel is less practical because of the long decomposition time, large reagent blanks and the necessity for a reduction-aeration vessel [7]. Pyrolysis of the filter is more efficient and straightforward but serious interfering effects occur because of organic products which are also collected on the filter; a purifying trap can be inserted to eliminate those interferences. After this pyrolysis and purification, the

mercury is collected on a gold-coated sand absorber, thermally desorbed and finally measured at the 253.7-nm line in the optical cell of the MAS-50 spectrometer. Thus, essentially the same procedure is used as previously described for the determination of total volatile mercury [8].

EXPERIMENTAL

Air sampling

The air sampling set-up was similar to that described earlier [8], comprising a filter holder, and absorption tube, a membrane pump (KNF—N 05—ANE) and a calibrated dry gas meter. Samples were collected by drawing air through the system at flow rates of 2.5—3.5 l min^{-1}, the volume of air pumped depending on the expected mercury concentrations. For the collection of particulate mercury, a Gelman quartz-fibre filter (13 mm) was mounted in the polypropylene filter holder (Swinnex-13) modified by replacing the 4-mm i.d. entrance tube by a PVC tube (17 mm i.d., 50 mm long). The exposed filter area was approximately 80 mm^2. For the simultaneous collection of the total volatile mercury, an absorption tube filled with gold-coated sand was placed behind the prefilter [8]. All connections were made with Swagelok stainless steel fittings.

Purification procedure

To eliminate interfering pyrolysis products, an additional purifying step (Fig. 1) was added to the original procedure. During heating of the filter A at 800°C a clean nitrogen stream swept the volatilized mercury and interfering compounds through a silver wool plug B and the absorbers C, D and E. The remaining mercury was collected onto the gold absorber F. All tubes were of 6-mm i.d. quartz glass. The silica gel section C was 40-mm long and the alumina section D 10-mm long. Sections B, C and D were kept at 800°C. The magnesium perchlorate stage (20-mm long) was kept at room temperature. Nichrome wire (6 Ω m^{-1}) was used for the heating coils. The temperature of each coil was independently controlled by 14-A, 220-V a.c. input variable transformers. The nitrogen gas flow was adjusted to 0.020 l min^{-1}.

After sampling, the whole filter was placed in the first quartz tube. While the nitrogen stream passed through, the temperature of the heating coils T_1 and T_2 was adjusted to 800°C by means of the transformers. The filter was heated during 3 min. After pyrolysis, the gold absorber was disconnected, capped and stored for later analysis.

When fresh reagents were used, and before each series of analyses, the system was heated for several minutes to remove any water and mercury. After 20—25 pyrolyses, it is also desirable to clean the purification trap. This was done by heating the whole section while passing oxygen.

When this procedure is applied, one filter can be pyrolysed every 5 min.

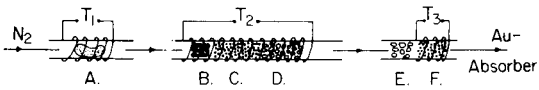

Fig. 1. Purification section. (A) Quartz fibre filter (Gelman); (B) silver wool plug (Merck p.a.); (C) silica gel (Merck, 35—70 mesh); (D) alumina (UCB p.a.); (E) $Mg(ClO_4)_2$ (UCB p.a.); (F) Au absorber. A—D are held at 800°C, and E, F at 25°C.

Spectrometric apparatus and procedure

All atomic absorption measurements were done with the equipment described previously for the determination of volatile mercury compounds [8]. After the purification, the mercury-loaded gold absorber was connected to a second permanent absorber. The two absorbers were consecutively desorbed and the mercury swept into the optical cell of the Coleman MAS-50 spectrometer. Output signals from this apparatus were fed to a recorder and an LDC 308 digital integrator for peak-area measurements.

Calibration was done by injecting known volumes of mercury-saturated air as described previously [8].

RESULTS AND DISCUSSION

Filter selection and collection efficiency

Various filters (membrane, organic fibre and inorganic fibre) can be used to collect particulate mercury. In the present case, membrane and organic fibre filters are unsuitable because the large amount of organic products during pyrolysis results in overload of the purification section. Quartz fibre filters (Gelman) have the advantages of low blank values, thermal stability at 800°C, and high collection efficiency. These filters have blank values corresponding to 2—15 ng Hg cm^{-2} but can easily be cleaned by heating at 200°C before sampling.

The efficiency of quartz fibre filters was compared to that of glass fibre filters by running three samplers in parallel. In the first experiment, two of them were equipped with glass fibre filters and the third with quartz fibre; in the second experiment, this set-up was reversed. In each case, 8 measurements of total particulate mercury were carried out. The two glass filters gave more variable results (93 ± 8% and 103 ± 15% efficiency normalized for 100% with the quartz filter) than the quartz filters (98 ± 6% and 105 ± 6% efficiency normalized for the glass filter), but the overall agreement was satisfactory.

During sampling, the filter or filter holder may collect a limited amount of mercury vapour by absorption; this would obviously result in excessive values for particulate mercury. However, the collected particulates may also lose mercury by volatilization in the air stream, thus causing low values. To check for possible absorption of mercury on the sampling system itself, 100-ng amounts of mercury vapour were injected first onto the filter holder alone, then onto a dry unloaded filter and finally onto a moistened filter

obtained by spotting a drop of water. The system was then purged with purified air at a flow rate of 3 l min^{-1}, nearly similar to the sampling rate. The unabsorbed mercury was collected on a gold absorber placed in line with the filter holder. After different purging times, the signal obtained from the mercury on the absorber was compared with the signal from a direct injection on the gold. The results, expressed as % recovery, are shown in Fig. 2. Almost 100% of the mercury is recovered after 2 min purging with the filter holder alone and with a dry filter. With a wet filter it takes about 5 min to reach this value. To study volatilization losses, a filter loaded with particulates containing about 35 ng of mercury was placed in a filter holder and purged with clean air for different periods of time (0—24 h), the volatilized mercury being collected on a gold absorber. After purging for 24 h, mercury was not detected on the gold.

Sampling reproducibility for quartz fibre filters was determined by running three samplers simultaneously. Table 1 shows the results of 5 runs for 24-h sampling times. The reproducibility of the particulate mercury determination is generally better than 10%.

In order to investigate the homogeneity of the particulate deposit on a large filter, total suspended particulates (TSP) were sampled on a Whatman GF/A glass fibre filter (110-mm diameter) up to a load of 130 mg with a high volume sampler [9]. From this filter, 43 circular spots (12.5-mm diameter) were punched as shown in Fig. 3(a) and subsequently analyzed; Fig. 3(b) shows the distribution of the mercury on the filter, as obtained with a computer program for plotting [10]. The lowest mercury value found was 7.4 ng, the highest 44.0 ng. Thus, an average value of 16.5 ng with a standard deviation of 60% was calculated. It therefore seems necessary to sample with small filters which can be analysed entirely. This also reduces the load on the purification section.

In order to evaluate the influence of sampling duration, 3 samplers were operated simultaneously in a 72-h experiment: the first for six consecutive 12-h periods, the second for three 24-h periods and the third for two 36-h periods. The results for particulate mercury are summarized in Table 2.

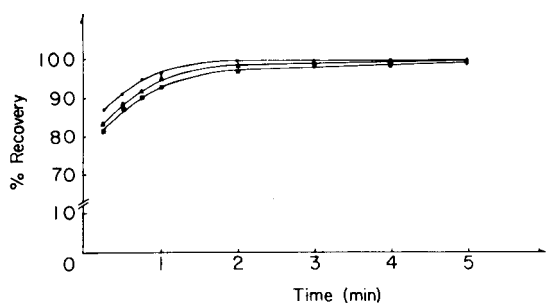

Fig. 2. Absorption of mercury vapour by the sampling system. (•) Filter holder alone; (▲) dry filter; (■) moist filter.

TABLE 1

Reproducibility of sampling with quartz fibre filters

Run	Particulate Hg (ng m^{-3})	R.s.d. (%)	Volatile Hg (ng m^{-3})	R.s.d. (%)
1	0.24 ± 0.02	9.1	3.65 ± 0.27	7.3
2	0.20 ± 0.01	6.5	2.87 ± 0.18	6.1
3	0.37 ± 0.03	8.1	3.89 ± 0.07	1.8
4	0.21 ± 0.02	7.6	3.46 ± 0.20	5.9
5	0.44 ± 0.04	9.9	4.01 ± 0.29	7.1

TABLE 2

Influence of sampling duration for particulate mercury expressed as ng Hg m^{-3}

Sampler 3 36-h periods	Sampler 1			Sampler 2 24-h periods
	Average for 36-h periods	12-h periods	Average for 24-h periods	
0.24	0.19	0.21 0.20	0.21	0.27
		0.15 0.24	0.20	0.19
0.22	0.23	0.27 0.17	0.22	0.20
0.23[a]		0.21[a]		0.22[a]

[a]Mean value.

The results obtained by taking the average of 2 or 3 sampling periods or by the 24- or 36-h sampling periods agree within about 20%. No significant losses as a function of sampling duration can be detected.

Purification efficiency

Filter pyrolysis has the important disadvantage that partly pyrolysed organic products can condense on the mercury collector. This results in deactivation of the absorber and non-specific light absorption during the subsequent desorption of mercury from the final absorber. Since the MAS-50 spectrometer has no possibilities for background correction, those interferences must be removed before the final desorption. The use of catalytic oxidizers, e.g. heated copper oxide, or of silver as reported by Trujillo and Campbell [5], seemed to be inefficient in the present system because de-

activation of the gold and the interfering light absorption were not prevented. The use of specific absorbers for organic substances, e.g. silica gel and alumina, can partially solve the problems. These absorbers have the disadvantage of becoming rapidly overloaded and have to be replaced after about 5 runs. A combination of a silver wool plug followed by specific absorbers as described by Nicholson [11] turned out to be most efficient. A silica gel section combined with an alumina section eliminates the remaining interferences. The whole system is heated to 800°C to ensure complete removal of the organics. The further magnesium perchlorate section retains water vapour at room temperature.

Applications

Table 3 shows some results for samples taken from areas with different degrees of contamination; both particulate mercury and total volatile mercury are measured. Location A is the building where the method was developed, and which is considered as nearly uncontaminated. Location B is a laboratory for polarography; as expected, the overall mercury levels are high. The large fraction associated with particulate matter seems to indicate an affinity of elemental mercury for dust [1]. Location C is situated outside location A. The results suggest the presence of a source of volatile mercury; depending on the wind direction during sampling, the ambient air concentrations varied widely.

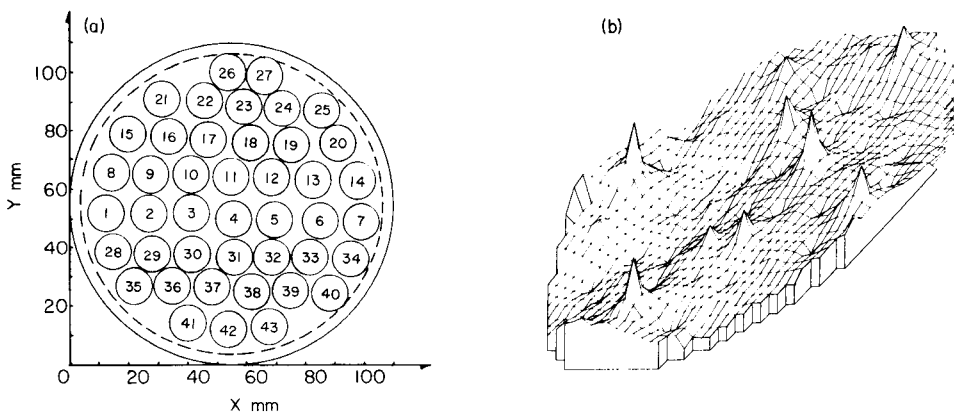

Fig. 3. (a) Punch pattern of the filter. (b) Perspective plot of the mercury distribution on a filter of 110-mm diameter.

TABLE 3

Results obtained for air samples at different locations

	Sample size (m^3)	Particulate Hg (ng m^{-3})	%	Volatile Hg (ng m^{-3})	%
Location A					
Lab.	0.200	41.1	22	145.5	78
Office	0.220	29.3	23	98.8	77
Balance room (dust-free)	0.340	4.1	3	115.0	97
Cyclotron hall	0.250	26.1	22	90.3	78
Location B					
Lab.	0.003	1430	43	1903	57
Balance room	0.005	821	42	1121	58
Office	0.020	177	46	205	54
Location C[a]					
Run 1	3400	0.3	7	3.9	93
2	3400	0.3	8	3.6	92
3	3200	0.2	6	3.7	94
4	3200	0.5	2	26.3	98
5	3200	0.3	1	34.2	99

[a]Runs 1—3 show the background level in the ambient air whereas runs 4 and 5 indicate a source of mercury vapour.

The authors are grateful to M. Nagels for technical assistance. One of them (R. D.) is indebted to the Interuniversitair Instituut voor Kernwetenschappen — IIKW for financial support.

REFERENCES

1 E. L. Kothny, The Three-Phase Equilibrium of Mercury in Nature, presented at the 162nd National American Chemical Society Meeting, Washington DC, September, 1971.
2 R. Dams, J. A. Robbins, K. A. Rahn and J. W. Winchester, Anal. Chem., 42 (1970) 861.
3 F. S. Goulding and J. M. Jaklevic, Report UCRL-20625 Lawrence Berkeley Laboratory, Berkeley, CA, May 1971.
4 N. L. Morrow and R. S. Brief, Environ. Sci. Technol., 5 (1971) 786.
5 P. E. Trujillo and E. E. Campbell, Anal. Chem., 47 (1975) 1629.
6 R. S. Braman and D. L. Johnson, Environ. Sci. Technol., 8 (1974) 996.
7 W. R. Hatch and W. L. Ott, Anal. Chem., 40 (1968) 2085.
8 R. Dumarey, R. Heindryckx, R. Dams and J. Hoste, Anal. Chim. Acta, 107 (1979) 159.
9 R. Dams and R. Heindryckx, Atmos. Environ., 7 (1973) 313.
10 J. Op de Beeck, INWG-CHEM-4. Graphics Software: The Contor-Tridim program package. Contour and perspective plotting for a function of two variables (November 1978).
11 R. A. Nicholson, Analyst, 102 (1977) 399.

Analytica Chimica Acta, 116 (1980) 119—125

SPECTROFLUORIMETRIC DETERMINATION OF PHARMACEUTICAL COMPOUNDS WITH THE CERIUM(IV)—CERIUM(III) SYSTEM

G. AMANN and G. GÜBITZ

Department of Pharmaceutical Chemistry, University of Graz, Graz (Austria)

R. W. FREI

Department of Analytical Chemistry, Free University, de Boelelaan 1083, 1081 NV Amsterdam (The Netherlands)

W. SANTI*

Analytical Research and Development, Pharmaceutical Division, Sandoz Ltd., 4002 Basle (Switzerland)

(Received 23rd October 1979)

SUMMARY

The compounds to be determined are oxidised by cerium(IV). The concentration of cerium(III) formed is measured spectrofluorimetrically. The method has been used both in solution and, by fluorodensitometry, on t.l.c. plates. Detection limits of some substances are 15 ng ml^{-1} for the solution method and 5 ng per spot for the t.l.c. method.

Armstrong et al. [1] observed that cerium(III) ions show a characteristic fluorescence in dilute sulphuric acid. Kirkbright et al. [2] determined arsenic(III), iron(II), iodide and oxalate by oxidation with cerium(IV) and spectrofluorimetric measurement of the cerium(III) formed. Katz et al. [3—7] employed this system in a new detection method for liquid chromatography. This principle was also used by Wolkoff and Larose for the determination of phenols [8] and polythionates [9] in aqueous h.p.l.c. effluents. The present study was undertaken to test the possible application of cerium(IV) oxidation to a wide range of pharmaceutical substances, such as analgesics of the morphine series, pyrazalone, salicylic acid derivatives, phenothiazines, local anaesthetics, sulphonamides, purines and various organic acids. The fluorescence measurements were carried out either in solution, or on t.l.c. plates which had been immersed in a solution of cerium(IV) sulphate.

EXPERIMENTAL

Apparatus

Fluorescence was measured with a Perkin-Elmer Model MPF 44 spectrofluorimeter with facilities for maintaining the cell holders at constant temperature, and with a t.l.c. accessory unit, in combination with a Perkin-Elmer Model 56 recorder and a Perkin-Elmer Minigrator M2 integrator.

Sample solutions were applied to the plates with microcaps (Drummond Scientific Co.).

Prepared silica gel plates MN Sil G without fluorescence indicator were obtained from Macherey-Nagel.

Reagents and solutions

Cerium(IV) sulphate, perchloric acid (70%) and sulphuric acid (conc.) were Merck analytical grade. Double-distilled water was used to prepare solutions of the test substances.

Cerium(IV) Sulphate solutions (2×10^{-4} M and 2×10^{-5} M). Dilute 0.2 ml or 0.02 ml of 0.1 M cerium sulphate solution to 100 ml with 0.35 M sulphuric acid. In order to avoid reduction of the cerium(IV) at the glass surface, pretreat the storage vessel with 0.1 M cerium(IV) solution. These solutions can be kept for one day in the refrigerator. (See 'Results and discussion'.)

Immersion reagent. Grind 20 g of cerium(IV) sulphate with 5 ml of concentrated sulphuric acid to a paste, and cautiously heat for 5 min while stirring constantly with a glass rod. Mix with 500 ml of water and 40 ml of 70% perchloric acid. Dilute 50 ml of this solution with 950 ml of 7% perchloric acid. This solution is stable for a week.

Developing systems. These were (in ratios by volume): (I) isopropanol—ethyl actate—water—ammonia liquor, 35:20:25:25; (II) benzene—isopropanol, 92:8; (III) acetone—ammonia liquor, 50:2; (IV) chloroform—methanol—formic acid, 90:10:5.

Compounds tested. These were acetylsalicylic acid, ascorbic acid, citric acid, isoniazid, morphine hydrochloride, codeine hydrochloride, aminophenazone, procaine hydrochloride and caffeine (from Herba, Graz); thioridazine, ergotamine methanesulphonate, propyphenazone,calcium gluconate and calcium lactobionate (from Sandoz, Basle); carbutamide (from Hoechst, Frankfurt). Two pharmaceutical preparations were also tested: calcium "Sandoz" ampoules with vitamin C (Preparation A) and Sandoz optalidon sugar-coated tablets (Preparation B).

Determination in solution

Mix 2 ml of the aqueous sample solution, 10^{-6}—10^{-5} M in the substance to be determined, with 2 ml of 2×10^{-4} M cerium(IV) solution (or 2×10^{-5} M for lower concentrations) and allow to react for 1 h at room temperature or 30 min at 60°C. Measure the fluorescence intensity at room temperature at an excitation wavelength of 260 nm and an emission wavelength of 350 nm. Treat three standard samples of suitable concentration and one blank in the same way.

Before first use, clean all reaction vessels with concentrated nitric acid and then treat them at least 3 times for 30-min periods with cerium(IV) solution under the reaction conditions to be used, until the blank value becomes constant.

Determination by the t.l.c. method

Spot 1 μl of sample solution onto the plate, and dry for 30 min at room temperature in a vacuum. After development of the plate, remove the solvent in a vacuum oven for 30 min at 50°C. Dip the plate into the cerium(IV) solution, allow it to drain, and leave it in a horizontal position for 1 h in the dark. Measure the fluorescence intensity at an excitation wavelength of 265 nm and an emission wavelength of 355 nm. To determine slowly reacting substances, follow the 1-h period at room temperature by 15 min in the drying oven at 50°C, and make the measurements immediately after cooling.

Procedure for pharmaceutical preparations

Preparation A. Dilute 2 ml of the solution contained in an ampoule to 10 ml, and place 1 μl of the diluted solution on a t.l.c. plate. For standardisation, place 1 μl of solutions containing calcium gluconate, calcium lactobionate and ascorbic acid, in concentrations corresponding to 80%, 100% and 120% of the expected analytical results, on the same plate according to the data-pair technique [10]. Dry the plate for 2 h in vacuum over calcium chloride at room temperature and then develop it with solvent system I. Dry for 2 h in a vacuum at room temperature. Dip into the cerium(IV) solution, allow to drain, keep for 1 h at room temperature and heat for 15 min at 50°C as described above.

Preparation B. Extract several times with methanol (total volume 25 ml) an exactly weighed quantity of powdered tablet corresponding to ca. 125 mg of propyphenazone and 25 mg of caffeine. Dilute 0.5 ml of the combined extract to 20 ml for determination of propyphenazone, and dilute 2.5 ml to 20 ml for determination of caffeine. Spot onto the plate 1 μl of each of these solutions and 1 μl of standard solutions containing propyphenazone at 100, 125 and 150 ng μl^{-1} and solutions of caffeine at the same concentrations. Develop in solvent-system II, and dry the plate for 1 h in a vacuum. Dip into the cerium(IV) solution and keep for 1 h at room temperature before making the measurements as described above.

RESULTS AND DISCUSSION

Figure 1 shows the excitation and emission spectra of cerium(III) ions recorded from measurements on a t.l.c. plate after reduction of cerium(IV). The spectra differ only very slightly from the solution spectra. A bathochromic shift of about 5 nm was observed in the excitation and emission spectra.

Determinations in solution

Cerium(IV) solutions in sulphuric acid of various concentrations and in perchloric acid were investigated. The stability of the reagent increases with increasing acid concentration, but at the same time the rate of oxidation

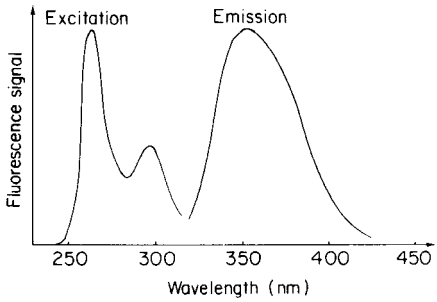

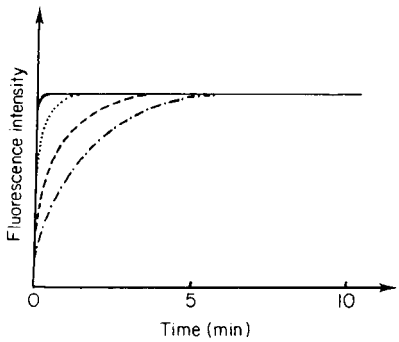

Fig. 1. Excitation and emission spectra of cerium (III) measured on the t.l.c. plate after reduction of cerium(IV).

Fig. 2. Rate of oxidation of isoniazid at 20°C with a four-fold molar excess of cerium(IV) sulphate in sulphuric acid concentrations of (—) 0.58 M, (...) 1.16 M, (- -) 1.75 M, (- . -) 2.34 M.

decreases sharply, as shown in Fig. 2 for the oxidation of isoniazid. This is rather surprising as the change in oxidation potential of cerium(IV) over the sulphuric acid range tested is very small [11]. Because of its higher oxidation potential, a perchloric acid solution of the reagent offers some advantages, but these are offset by the raised blank value and by significantly reduced stability of the reagent at higher temperatures. Addition of sodium bismuthate tends to stabilise the reagent, but a substantially lower fluorescence intensity is observed compared to that observed in reactions with untreated reagent. As indicated by the presence of bismuth ions in the solution, and contrary to statements in the literature [3—9], significant quantities of bismuthate dissolve, and re-oxidise the cerium(III) produced, thus diminishing the fluorescence. Therefore no stabiliser was used. If the reagent is freshly prepared, and the apparatus used is correctly pretreated, the blank can be kept small.

Various substances, including osmium tetroxide [2, 12, 13], ruthenium(III) [14], iodide [2], iodine monochloride [15], chromium(III) [16, 17], manganese(II) [10, 15, 18] and palladium(II) oxide were tested as possible catalysts for speeding up the reaction, with a view to its use in h.p.l.c. Significant catalytic action was observed only with palladium oxide and manganese(II) salts. However, with the increased reaction rate, there was the accompanying disadvantage of a raised blank value; consequently the use of catalysts did not result in an improved signal-to-noise ratio and was abandoned.

The oxidation rates of various groups of compounds in solution were investigated and were found to differ considerably depending on chemical structure. As shown in Fig. 3, however, a number of compounds reacted sufficiently rapidly at room temperature. Raising the reaction temperature

to 60°C shortened the reaction time considerably, making it possible to determine substances which react too slowly at room temperature (Fig. 4). The limits of detection (3 times the standard deviation of the blank value) were (in ng ml^{-1}): isoniazid, 14; ascorbic acid, 18; thioridazine, 20; ergotamine, 20; aminophenazone, 15 (all at 20°C); citric acid, 15; morphine, 25 (both at 60°C).

Determinations on t.l.c. plates

Only a limited selection of organic solvents could be used for developing the t.l.c. plate, because many organic solvents were too readily oxidised. Macherey-Nagel plates were suitable for use in the dipping process, whereas bubbles formed on the adsorbent layer of Merck plates. A 30—60-min reaction time with cerium(IV) at room temperature was sufficient for many pharmaceutical substances (Fig. 5). For slowly reacting compounds it was necessary to follow this by heating the plate at 50°C. The limits of detection (signal-to-noise = 3:1) for the various compounds are shown in Table 1, together with some of the chromatographic details. Figure 6 shows the separation of the components of a preparation containing calcium gluconate, calcium lactobionate and ascorbic acid.

Quantitative data and applications to pharmaceutical preparations

The rectilinear portion of the calibration graphs obtained by the solution method extends over more than one order of magnitude of concentration with a correlation coefficient of 0.996—0.999 for 5—7 points. With the t.l.c. method, the graph is rectilinear over one order of magnitude, with a correlation coefficient of 0.995 to 0.999. The relative standard deviation (10 measurements) is 0.5—2% for the solution method and 0.9—3% for the t.l.c. method.

Table 2 presents analytical data for two pharmaceutical combination preparations. Combination A was an injection solution, which after suitable

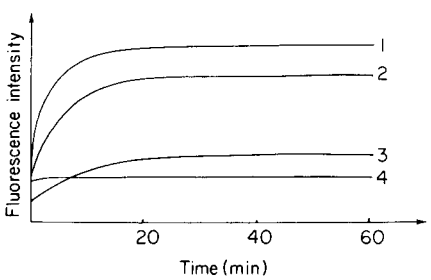

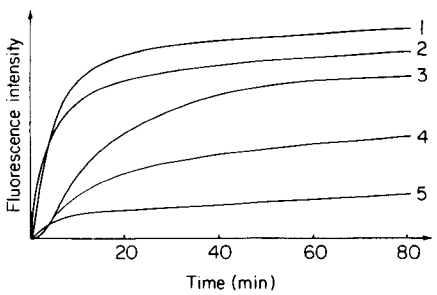

Fig. 3. Rate of oxidation of (1) thioridazine, (2) aminophenazone, (3) ascorbic acid, and (4) isoniazid in solution at 20°C.

Fig. 4. Rate of oxidation of (1) citric acid, (2) codeine, (3) tartaric acid, (4) calcium gluconate and (5) mandelic acid in solution at 60°C.

TABLE 1

Limits of detection and R_F values for reaction at 20°C except where specified

Compound	ng spot^{-1}	R_F	Developing system	Compound	ng spot^{-1}	R_F	Dev syst
Acetylsalicylic acid	20	0.06	III	Codeine HCl	40	0.24	III
Aminophenazone	5	0.12	II	Morphine HCl	10	0.14	III
Ca gluconate	200	0.38[a]	I	Procaine HCl	5	0.10	IV
Ca lactobionate	200	0.22[a]	I	Caffeine	30	0.08	II
Ascorbic acid	300	0.53	I	Propyphenazone	20	0.33	II
Carbutamide	5	0.08	III				

[a]Cerium(IV) reaction at 50°C.

dilution could be spotted onto the t.l.c. plate and assayed by using the procedure described. Preparation B contained three solid components, from which a methanol extract was prepared and diluted so as to give an optimum concentration of either propyphenazone or caffeine. The third component, butalbital, was the only compound tested which did not undergo oxidation.

Conclusions

The cerium(IV) oxidation procedure is applicable to the fluorimetric determination of a wide range of compounds of biological and pharmaceutical importance, both in solution and on t.l.c. plates. The rate data for reactions in solution again indicate the suitability of this technique to post-column reaction detection in h.p.l.c. [8]. Since 4—5 min reaction times are needed,

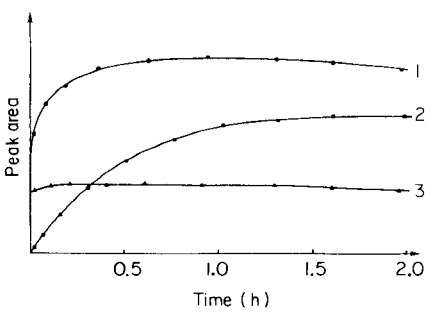

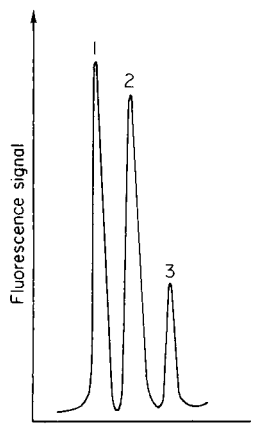

Fig. 5. Rate of oxidation of (1) propyphenazone, (2) codeine HCl and (3) isoniazid on t.l.c. plates at room temperature.

Fig. 6. Chromatogram of a pharmaceutical preparation containing (1) calcium lactobionate, (2) calcium gluconate, and (3) ascorbic acid.

TABLE 2

Analytical results for two pharmaceutical preparations

Preparation A	Theor. (mg)	Found[a] (mg)	%	R.s.d.	Preparation B	Theor. (mg)	Found[a] (mg)	%	R.s.d.
Ca gluconate	50.5	51.8	102.6	1.0	Propyphenazone	125	122.8	98.2	2.0
Ca lactobionate	87.0	89.0	102.3	1.1	Caffeine	25	24.4	97.6	2.7
Ascorbic acid	50.0	50.7	101.6	2.4	Butalbital	50	—	—	—

[a]Mean of 8 determinations.

both unsegmented [19] and segmented flow reactors [20] would be suitable. The method is sensitive and simple to carry out.

The work described is taken from the thesis of G. Amann, University of Graz, 1979.

REFERENCES

1 W. A. Armstrong, D. W. Grant and W. G. Humphers, Anal. Chem., 35 (1963) 1300.
2 G. F. Kirkbright, T. S. West and C. Woodward, Anal. Chim. Acta, 36 (1966) 298.
3 S. Katz and W. W. Pitt, Jr., Anal. Lett., 5(3) (1972) 117.
4 S. Katz, W. W. Pitt, Jr. and G. Jones, Jr., Clin. Chem., 19(8) (1973) 817.
5 S. Katz, W. W. Pitt, Jr. and J. E. Mrochek, J. Chromatogr., 104 (1975) 303.
6 S. Katz, S. R. Dinsmore and W. W. Pitt, Jr., Clin. Chem., 17 (1971) 731.
7 S. Katz, W. W. Pitt, Jr., J. E. Mrochek and S. R. Dinsmore, J. Chromatogr., 101 (1974) 193.
8 A. W. Wolkoff and R. H. Larose, J. Chromatogr., 99 (1974) 731.
9 A. W. Wolkoff and R. H. Larose, Anal. Chem., 47(7) (1975) 1003.
10 H. Bethke, W. Santi and R. W. Frei, J. Chromatogr. Sci., 12 (1974) 392.
11 G. F. Smith, Cerate Oxidimetry, 2nd edn., G. Frederick Smith Chemical Co., Columbus, Ohio, 1964.
12 K. Gleu, Fresenius Z. Anal. Chem., 95 (1933) 305.
13 R. D. S. Sauerbrunn and E. B. Sandell, Microchim. Acta, (1953) 22.
14 C. Surasiti and E. B. Sandell, Anal. Chim. Acta, 22 (1960) 261.
15 J. P. Watson, Analyst, 76 (1951) 177; cf. Fresenius Z. Anal. Chem., 135 (1952) 216.
16 N. N. Sharma and R. C. Mehrotra, Anal. Chim. Acta, 11 (1954) 417, 507; 13 (1955) 419.
17 N. N. Sharma, Fresenius Z. Anal. Chem., 157 (1957) 110.
18 W. H. McCurdy, Jr. and G. G. Guilbault, Anal. Chem., 33 (1961) 580.
19 R. W. Frei, L. Michel and W. Santi, J. Chromatogr., 126 (1976) 665.
20 J. C. Gfeller, G. Frey and R. W. Frei, J. Chromatogr., 142 (1977) 271.

Analytica Chimica Acta, 116 (1980) 127—135

PRECONCENTRATION OF SILVER(I), GOLD(III) AND PALLADIUM(II) IN SEA WATER WITH *p*-DIMETHYLAMINOBENZYLIDENERHODANINE SUPPORTED ON SILICA GEL

KIKUO TERADA*, KUMIKO MORIMOTO and TOSHIYASU KIBA

Department of Chemistry, Faculty of Science, Kanazawa University, Kanazawa, Ishikawa 920 (Japan)

(Received 12th November 1979)

SUMMARY

A water-insoluble chelating material, *p*-dimethylaminobenzylidenerhodanine on silica gel (DMABR—SG) is described for preconcentration of trace amounts of silver(I), gold(III) and palladium(II) from water samples. Radioactive tracers (^{110m}Ag and ^{198}Au) were used to study the behavior of silver and gold; palladium was monitored spectrophotometrically as its 1-(2-pyridylazo)naphthol complex in chloroform. In batch experiments, silver was quantitatively retained on the DMABR—SG at acidities ranging from 1.7 M to pH 5, and gold from 3 M to pH 5; equilibrium was achieved within 1 min for both elements. From sea water, silver ion was completely retained at pH 1.0—6.5 and gold ion at pH 1.0—3.5. In the case of palladium, shaking for about 20 min was required for quantitative retention at pH 1.0—5.0 for aqueous solution and at pH 1.0—7.0 for sea water. The chelating capacity of the DMABR—SG was 23 μmol Ag, 11 μmol Au and 11 μmol Pd per g. Quantitative recovery of silver and gold on DMABR—SG columns from sea water was achieved at higher flow rates (1—2 l h^{-1} and 2—3 l h^{-1}, respectively) than with other chelating resins, e.g., Chelex 100; palladium required slower flow rate (150 ml h^{-1}). Silver retained on the DMABR—SG column was completely eluted with 20 ml of 2.5% sodium thiosulfate solution but palladium remained on the column. Silver, gold and palladium were quantitatively eluted with 20 ml of 0.1% thiourea in 0.1 M hydrochloric acid.

The silver content of normal sea water [1] is 0.15—2.9 μg l^{-1} with an average of 0.29 μg l^{-1}, while the gold content appears to cover the range 4—27 ng l^{-1}. The palladium concentration in sea water does not appear to have been published. Numerous methods for the determination of silver and gold in natural waters have been described [2—6]. Preconcentration is always necessary. Losses of silver and gold by adsorption on container walls can be an important problem [7, 8]. West and West [9, 10] indicated that even in the presence of EDTA the adsorption of silver began to increase for storage times longer than 10 days. Therefore, complete recovery of these elements is likely to be achieved only when the separation of the metals from the water sample is done as quickly as possible after sample collection.

Ion-exchange resins with functional groups that react with silver, gold and palladium ions have been synthesized [11, 12] but none has been applied to ng l^{-1} concentrations in natural water samples. *p*-Dimethylamino-

benzylidenerhodanine has been used as a reagent for the spectrophotometric and spectrofluorimetric determinations of silver, gold and palladium [13, 14]. It is insoluble in water, but soluble in concentrated mineral acids and dioxane, moderately soluble in acetone and slightly soluble in chloroform and benzene. This paper describes the use of this reagent, impregnated on silica gel, for the selective preconcentration of silver, gold and palladium from natural waters.

EXPERIMENTAL

Reagents

p-Dimethylaminobenzylidenerhodanine (DMABR) and 1,4-dioxane were analytical-reagent grade. Standard solutions of the metals were prepared as follows: pure gold or palladium was dissolved in aqua regia and evaporated to dryness, a little hydrochloric acid was added and the solution was evaporated again; this step was repeated, and finally the residue was dissolved in 1 M nitric acid. Each stock solution contained 1000 mg l^{-1} of the metal.

Radioactive ^{198}Au was prepared by irradiation of the metal with thermal neutrons (4.67×10^{13} n cm^{-2} s^{-1}) for 60 min in the KUR nuclear reactor of Kyoto University. Radioactive ^{110m}Ag was purchased from the Radiochemical Centre (Amersham, England). The radioactive purities of the ^{110m}Ag and ^{198}Au were found to be 100% by γ-ray spectrometry. Silica gel (chromatographic grade; WAKOGEL C-100) was sieved through a stainless steel sieve, 60—80 mesh, soaked with twice its volume of (1 + 1) hydrochloric acid for 1 day, and then washed with deionized water until free from chloride. The silica gel was then soaked with twice its volume of (1 + 2) nitric acid for 1 day, washed with deionized water and dried at 110°C for 1 day.

Preparation of p-*dimethylaminobenzylidenerhodanine–silica gel (DMABR—SG).* About 90 g of silica gel (60—80 mesh) was stirred with 100 ml of dioxane containing DMABR (1 g). After standing for 1 day, the silica gel impregnated with the reagent and dioxane was dried at room temperature under reduced pressure for about 2 days to expel dioxane, and then heated at about 80°C to remove dioxane completely. The dry material was washed repeatedly with deionized water until the washings were colorless. Finally, the red-colored product was dried at about 80°C under reduced pressure for one day and stored in a darkened bottle.

Apparatus

Hitachi-Horiba pH-meters were used to check the pH of the aqueous solution. A well-type scintillation counter (Kobe Kogyo Co., Model STL-200; 44.5 × 50.8-mm NaI(Tl) crystal) was used for γ-counting. Aqueous solutions and DMABR—SG were shaken with an Iwaki VS electric shaker operating at 340 strokes min^{-1}. Other equipment included a Hirama spectrophotometer and a Hitachi 170-50 atomic absorption spectrometer. The

columns were glass tubes (10-mm i.d., 140-mm long) with a coarse sintered-glass disc and stopcock at the bottom.

Procedure for batch experiments

To a 50-ml polypropylene bottle were added 10 ml of buffer solution, 2 ml of each metal solution and 0.5 g of DMABR—SG; the contents were shaken vigorously by an electric shaker for 30 min at room temperature. The test solutions for silver and gold contained 16.8 μg ml^{-1} of each metal, spiked with ^{110m}Ag and ^{198}Au, while the palladium solution contained 4.2 μg Pd ml^{-1}. The pH of the aqueous solution was adjusted with sodium acetate plus hydrochloric acid for pH 1—5, or potassium dihydrogenphosphate plus sodium hydroxide for pH 6—8. (The pH of sea water was adjusted with hydrochloric acid and sodium hydroxide.) After the gel had settled, the supernatant solution was filtered through dry Toyo No. 5C filter paper. Aliquots of the filtrate (3 ml for Ag and Au, 2 ml for Pd) were pipetted into test tubes for γ-counting of ^{110m}Ag and ^{198}Au, and the recovery was calculated from the count rate. For palladium, 2 ml of the filtrate was used for the spectrophotometric determination with PAN [15]. The recovery of palladium was calculated as the ratio of the absorbance to that measured for the standard solution.

Procedure for column method

A glass column was filled with 5 g of DMABR—SG to give a bed height of 7 cm, and a disc of Toyo No. 5C filter paper was placed on top so as not to disturb the gel during sample passage. For experiments in which a 5-ml disposable syringe was tested as a column, a coarse sintered-glass disc was put at the bottom with a glass fiber filter (11-mm diameter) on top and then 2 g of DMABR—SG was added to give a bed height of 3.0 cm.

A given volume of an aqueous sample (1 l) containing the individual metal ions was adjusted to a suitable pH, and then percolated through the column at 0.15—3 l h^{-1} under mild suction. The upper level of the sample solution was maintained about 1 cm above the surface of the column bed. The column was washed with 20 ml of deionized water. The gel was transferred to a test tube and the γ-emission measured in order to calculate the percentage retention of silver and gold. Palladium retained on the gel was eluted with 0.015 M potassium cyanide at 1 ml min^{-1}. The effluent was diluted to the desired volume, treated with 3—4 ml of 10% sodium hypochlorite solution to decompose the cyanide and the excess of sodium hypochlorite was decomposed with formic acid. The pH was then adjusted to 3—4 with hydrochloric acid and sodium hydroxide, palladium was determined spectrophotometrically and the percentage retention of palladium was calculated.

Measurement of amount of DMABR absorbed on silica gel

Dry DMABR—SG (1 g) was placed into a glass column and 30 ml of concentrated hydrochloric acid was passed through to remove the reagent completely

from the column. The effluent was collected in a 50-ml measuring flask and diluted to the mark with concentrated hydrochloric acid. The absorbance of the solution was measured at 375 nm using concentrated hydrochloric acid as a reference.

RESULTS AND DISCUSSION

Characteristics of the chelating material

The amount of the reagent supported on the silica gel was found to be 7 ± 1 mg (26 ± 4 μmol) g^{-1}. The chelating capacities of this material for silver, gold and palladium were measured by the batch method using 20 ml of 100 ppm solutions. At pH 1, the capacity of the gel was calculated to be about 23 μmol g^{-1} for silver and 11 μmol g^{-1} for gold. The capacity for palladium at pH 2 was 11 μmol g^{-1}. Thus silver and gold appear to form a 1:1 complex with DMABR whereas palladium forms 1:2 complexes under these conditions. These results agree fairly well with those of Borissova et al. [16, 17] and Ayres and Narang [14] who used aqueous ethanol solutions. The chelating capacity of DMABR—SG is thus large enough to collect the metals from large volumes (e.g., 10 l) of sea water; for example, 10 l would contain about 100 ng of gold and 2 μg of silver. Even a 5-g portion of the gel has an exchange capacity of at least 10^5 times this amount of gold and about 10^3 times this amount of silver. The dry chelating material showed no change in its exchange capacity after storage for 6 months.

Effect of pH on recovery of silver, gold and palladium

The recovery of each metal ion from an aqueous solution and from sea water at various pH values was examined by the batch method, by using 12 ml of a solution which contained 16.8 μg Ag ml^{-1}, 16.8 μg Au ml^{-1} and 4.3 μg Pd ml^{-1}, equilibrated with 0.5 g of DMABR—SG. The results are shown in Fig. 1 and compared with those obtained with silica gel alone. Silver could be quantitatively retained from ≤1.7 M nitric acid in the case of aqueous solution and from sea water at a pH as low as 1.0. Retention of silver by silica gel alone was only 5% from aqueous solution at pH 6 and was zero from sea water. Gold was retained quantitatively from ≤2.5 M hydrochloric acid solution and at pH 1.0—3.5 from sea water, whereas untreated silica gel retained only 3.5% of the gold from aqueous solution at pH 6.5 and 5% from sea water at pH 5. Palladium was retained from both aqueous solution and sea water at pH 1—5, but in the case of silica gel alone, a maximum recovery of 32.2% was obtained from aqueous solution at pH 6.2 and about 3% from sea water at pH 2.5—5.9.

These results also indicate that there seems to be little possibility of separating these metal ions by elution at different pH values.

Effect of shaking time

The retention of silver and gold from aqueous solution at pH 1 and of

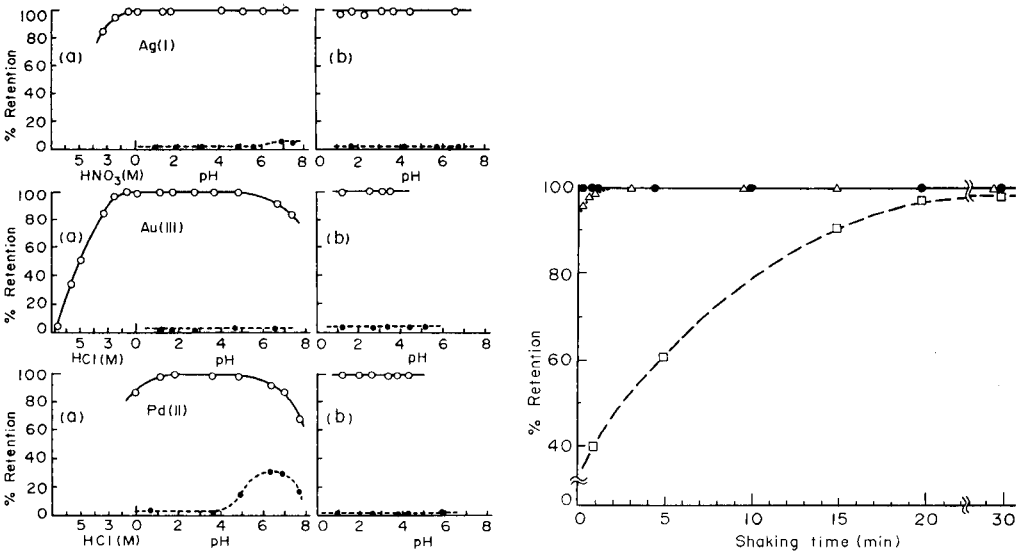

Fig. 1. Effect of pH on retention of silver(I), gold(III) and palladium(II) (for concentration, see text) from (a) aqueous solution and (b) sea water. (○) DMABR—SG; (●) untreated silica gel.

Fig. 2. Effect of shaking time on retention of (△) silver(I), (●) gold(III), and (□) palladium(II).

palladium at pH 2 were examined after various shaking times. The results in Fig. 2 show that silver and gold are retained very rapidly on the chelating material but palladium is absorbed slowly. Therefore, if a water sample is percolated rapidly through the column, palladium could pass through the column and be separated from silver and gold.

Retention of individual ions on the column

To examine the retention of each metal ion on the column, sea-water samples at pH 2 containing a metal at various concentrations were passed through the column at different flow rates. For silver and gold, the column length was 30 mm, and for palladium, 90 mm. Table 1 shows that silver at the 0.1—100 $\mu g\ l^{-1}$ level is quantitatively retained at flow rates of 0.8—1.0 $l\ h^{-1}$, gold retention is quantitative for the 0.026—100 $\mu g\ l^{-1}$ level at flow rates of 2.0—3.0 $l\ h^{-1}$, and palladium retention is quantitative at the 2.5—20 $\mu g\ l^{-1}$ level at flow rates of 0.15—0.2 $l\ h^{-1}$. Thus, preconcentration of silver from 5 l of water or of gold from 10 l of water can be achieved within 5 h and palladium from 2 l of water within 12 h. However, when the concentration of palladium is less than 2.5 $\mu g\ l^{-1}$ as is usual in natural waters, batch operation is preferred to the use of columns. These results also indicate that silver and gold could be separated from palladium at flow rates above 0.5 $l\ h^{-1}$.

TABLE 1

Recovery of silver, gold and palladium on a DMABR—SG column

Ag(I) ($\mu g\ l^{-1}$)	Flow rate ($l\ h^{-1}$)	Recovery (%)	Au(III) ($\mu g\ l^{-1}$)	Flow rate ($l\ h^{-1}$)	Recovery (%)	Pd(II) ($\mu g\ l^{-1}$)	Flow rate ($l\ h^{-1}$)	Recovery (%)
100	1.0	100	100	2.0	100[a]	20	0.15	100[c]
5	1.0	100		3.0	96.9[a]		0.5	6[c]
1	1.0	100	10	3.0	83.0[a]		1.0	4[c]
	1.2	77.3		2.4	99.0[b]	10	0.15	100[c]
0.1	0.8	100	1.3	2.0	97.8[b]	2.5	0.22	100[d]
			0.13	2.0	100[b]		0.25	71[d]
			0.026	2.4	100[b]		0.35	63[d]
				3.0	78.0[b]	0.2	0.15	38[d]

[a]1.5 g of DMABR—SG. [b]2 g of DMABR—SG. [c]0.1 M KCN as eluent. [d]0.1% thiourea in 0.1 M HCl as eluent.

Elution of metal ions

Several reagents known to mask silver were investigated for the elution. As shown in Table 2, when 25 ml of 0.1 M potassium cyanide, 0.1 M sodium thiosulfate or 0.1% thiourea in 0.1 M nitric acid were passed through the column, complete elution of up to 5 μg of silver was achieved. Moreover, 25 ml of 10^{-3} M thiosulfate solution was sufficient to release up to 3 μg of silver, this amount corresponding to about 15 l of sea water. The elution of gold was examined with acids at high concentration, as well as several other reagents (Table 2). When mineral acids were passed through the column, a large proportion of the reagent supported on the silica gel was released together with the gold—DMABR complex. Although 5% sodium hypochlorite quantitatively released gold from the column, a considerable amount of DMABR was also removed in the effluent. The 0.1 M sodium thiosulfate solution, which was an effective eluent for silver, eluted only 48% of the gold; 0.1 M potassium cyanide solution and 0.1% thiourea in 0.1 M hydrochloric acid were found to be most suitable for the elution of gold. These solvents could also be used for quantitative elution of up to 10 μg of palladium (Table 2). Thus the three metal ions can be eluted either with 25 ml of 0.1 M potassium cyanide solution or 0.1% thiourea in 0.1 M hydrochloric or nitric acid.

Effect of various substances on the retention of silver and gold

Various metal ions that might react with DMABR (platinum group metals, iron(III), copper(II), zinc(II), lead(II) and cadmium(II)) were examined for their effect on the absorption procedure. The results obtained by the batch method are shown in Fig. 3. Only cadmium(II) (2.5%) and iron(III) (5%) were absorbed at pH 2.5. Consequently, if the water sample is acidified to pH 2, silver, gold and palladium will be selectively separated from the common heavy metal ions.

TABLE 2

Elution of silver(I), gold(III), and palladium(II) retained on a DMABR—SG column with various eluents

Silver (5 μg)		Gold (1 μg)		Palladium (10 μg)	
Eluent	Recovery (%)	Eluent	Recovery (%)	Eluent	Recovery (%)
Acetone	32.0	6 M HCl	42.7	0.06 M KCN	98.0[b]
0.1 M KCN	98.4	8 M HCl	93.0	0.015 M KCN	100
0.2 M NH_3	11.5	9 M H_2SO_4	88.4	0.1% thiourea in 0.1 M HCl	100
5 M HNO_3	1.3	6 M H_2SO_4			
0.1 M $Na_2S_2O_3$	100	+ 5% NaCl	80.7	0.16 M $Na_2S_2O_3$	0
10^{-3} M $Na_2S_2O_3$	100[a]	0.1 M $Na_2S_2O_3$	47.7		
		1% NaClO	40.2		
0.1% thiourea in 0.1 M HNO_3	100	5% NaClO	96.4		
		0.015 M KCN	100		
		0.1% thiourea in 0.1 M HCl	100		

[a] 3 μg Ag. [b] 20 μg Pd.

The effect of these heavy metals on the retention of silver and gold on DMABR—SG was also examined. A 1-l sea-water sample at pH 2 containing 0.1 μg Ag l^{-1} or 10 μg Au l^{-1} as well as one of the other ions in the concentration range 1—1000 μg l^{-1} was passed through a column containing 2 g of DMABR—SG, at 1—2 l h^{-1}. The results are shown in Table 3. At these concentration levels no metal ions interfered with the retention of gold. In contrast, silver retention was significantly influenced by iron(III) and the platinum metals. Iron(III) appears to be retained as a hydrated oxide

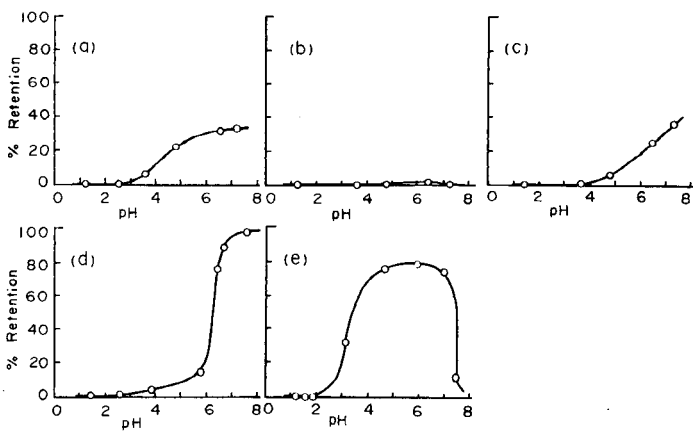

Fig. 3. Effect of pH on retention of (a) Cu(II), (b) Zn(II), (c) Pb(II), (d) Cd(II) and (e) Fe(III).

TABLE 3

Effect of metal ions and other compounds on the recovery of 0.1 μg of silver(I) and 10 μg of gold(III)

Metal ion	Conc. (ppb)	Recovery (%)		Substance	Conc. (M)	Recovery	
		Ag(I)	Au(III)			Ag(I)	Au(III)
Cu(II)	1	100		Citric acid	10^{-4}	52	100
	10	89			10^{-5}	54	
	100		97		10^{-6}	61	
Zn(II)	100	100		Tartaric acid	10^{-4}		100
	1000		97		10^{-6}	87	
Pb(II)	10	100	100	EDTA	10^{-4}		100
					10^{-5}	51	
Cd(II)	1	98			10^{-6}	88	
	10	82	100				
Fe(III)	1	70		Cysteine	10^{-4}		9
	10	64			10^{-5}		16
	100	55			10^{-6}	100	31
	1000	48	100		10^{-7}		63
Co(II)	10	100	100	NaSCN	10^{-4}		94
Ni(II)	100	71	97		10^{-6}	97	
Os(III)	10	34	97				
Re(VII)	10	22	98				
Ru(III)	10		100				
Rh(III)	10	41	100				
Ir(III)	10		96				
Pd(II)	10	68	96				
Ag(I)	10		95				
Pt(IV)	10	55					

or to pass through as colloidal particles containing silver ions. In general, 1 l of sea water contains about 0.3 μeq of total heavy metal ions, which is compatible with 0.05 g of DMABR—SG. Therefore, in practice, the interference of heavy metal ions, especially of platinum metals, may be neglected.

The effect of EDTA, citric acid, tartaric acid, cysteine and thiocyanate ions on the retention of silver and gold was also examined (Table 3). Only cysteine significantly influenced the retention of gold. Even at 10^{-7} M, it considerably decreased gold retention. Recovery of silver was decreased by citric acid, EDTA, tartaric acid and thiocyanate ions, but not by cysteine. However, since in natural waters, and especially in sea water, these substances are never found in concentrations as high as shown in Table 3, the effect of these substances may be neglected. In fact, the quantitative retention of silver, gold and palladium reported above was achieved from sea-water samples collected at Tsukumo Bay, Noto Peninsula, which are assumed to be more polluted by domestic activity than open sea water.

REFERENCES

1 R. W. Boyle, The Geochemistry of Silver and its Deposits, Geochem. Surv. Can. Bull., No. 160, 1968, p. 74.
2 D. P. Kharkar, K. K. Turekian and K. K. Bertine, Geochim. Cosmochim. Acta, 32 (1968) 285.
3 K. K. Turekian and D. F. Schutz, Geochim. Cosmochim. Acta, 29 (1965) 259.
4 T. T. Chao, M. J. Fishman and J. W. Ball, Anal. Chim. Acta, 47 (1969) 189.
5 H. V. Weiss and M. Lai, Anal. Chim. Acta, 28 (1963) 242.
6 K. H. Lieser, W. Calmano, E. Heuss and V. Neitzert, J. Radioanal. Chem., 37 (1977) 717.
7 T. T. Chao, E. A. Jenne and L. M. Heppting, U. S. Geol. Surv. Prof. Paper, 600-D, 1968, p. D13.
8 A. Chow, Talanta, 18 (1971) 453.
9 F. K. West and P. W. West, Anal. Chem., 38 (1966) 1566.
10 F. K. West and P. W. West, Anal. Chim. Acta, 37 (1967) 112.
11 N. L. Fishkova and V. A. Vilekin, Zh. Anal. Khim., 33 (1978) 897.
12 J. Marinenko and I. May, Anal. Chem., 40 (1968) 1137.
13 T. M. Cotton and A. A. Woolf, Anal. Chim. Acta, 22 (1960) 192.
14 G. H. Ayres and B. D. Narang, Anal. Chim. Acta, 24 (1961) 241.
15 Ōyōhishokubunseki No. 4, Kyōritsu Shuppan Co. Ltd., 1975, p. 298.
16 R. Borissova, M. Koeva and E. Topalova, Talanta, 22 (1975) 791.
17 R. Borissova, Talanta, 22 (1975) 797.

Analytica Chimica Acta, 116 (1980) 137—144

THE DETERMINATION OF DISSOLVED TOTAL NUCLEIC ACIDS IN NATURAL WATERS INCLUDING SEA WATER

EDGARDO HICKS and J. P. RILEY*

Department of Oceanography, University of Liverpool, P.O. Box 147, Liverpool L69 3BX (Gt. Britain)

(Received 21st December 1979)

SUMMARY

A procedure for the determination of natural levels of nucleic acids in lake and sea waters is described. The filtered samples are adjusted to pH 6.80 and passed through a column packed with spheroidal hydroxyapatite. Nucleic acids, which are quantitatively adsorbed, are eluted at 60°C with a 0.5 M phosphate buffer (pH 6.80) and hydrolysed. The resultant ribose is determined photometrically by the iron(III)—orcinol method. The procedure showed a coefficient of variation of 2.9% and 2.4% with lake and sea waters containing nucleic acids at the 47 and 79 $\mu g\ l^{-1}$ levels, respectively. No significant interference is caused by fulvic and humic acids, amino acids, carbohydrates and fatty acids at levels of 10 $mg\ l^{-1}$.

It has been known for a long time that, for much of the year, organic phosphorus compounds often constitute a considerable proportion of the dissolved phosphorus present in both lake and sea waters. Very little is known, however, about the nature of the individual compounds comprising this fraction. Azam and Hodson [1] have found concentrations of dissolved adenosine-5′-triphosphate (ATP) ranging from 0.1 to 0.6 $\mu g\ l^{-1}$ in ocean waters by a technique involving adsorption on charcoal followed by elution and determination of the ATP by the specific firefly luminescence method. Because of their biochemical significance, several attempts have been made to determine nucleic acids and their degradation products in natural waters; however, no unequivocal evidence for their existence has been found. Thus, Minear [2] has shown by the use of gel permeation chromatography that 20% of the organic phosphorus present in a lake water had a molecular weight of >200,000 daltons. Koenings and Hooper [3] have detected orcinol-reactive material in water from a bog lake, and this taken in conjunction with the fact that a concentrate prepared by lyophilization had an absorption maximum at 260 nm led them to conclude that RNA or its fragments were a major component of the dissolved organic phosphorus. Pillai and Ganguly [4] have claimed detection of DNA (20—80 $\mu g\ l^{-1}$) in sea water; however, the diphenylamine photometric method which they used to determine the preconcentrated DNA is far from specific for this compound.

Since most of this early work gave results of rather dubious validity, it was thought worthwhile as part of a current investigation in these laboratories into dissolved organic phosphorus in aquatic systems to develop a technique for the determination of total nucleic acids. The procedure described below involves preconcentration by adsorption onto hydroxyapatite, followed by elution of the nucleic acids and photometric determination of the ribose obtained from them by hydrolysis.

Preconcentration of nucleic acids

Since the concentrations of dissolved nucleic acids in natural waters are low, a preconcentration stage is necessary before they can be determined. A review of the literature suggested that a possible technique would be adsorption on hydroxyapatite. This material, which was originally used by Tiselius et al. [5] for chromatography of proteins, has been used for the separation [6] and chromatography [7] of nucleic acids. However, despite its desirable absorptive properties it has not been widely employed, probably because the spread of particle sizes of most commercial preparations made it difficult to achieve satisfactory flow rates. Although a number of attempts had been made to prepare a suitable product [8], it was not until a spheroidal form was developed at the Atomic Energy Research Establishment, Harwell, that a practically useful adsorbent became available. This material, which consists of mechanically strong porous spherical particles (diameter 75–185 μm), can be uniformly packed to give columns with acceptable and reproducible flow rates. The nucleic acids appear to be adsorbed by hydroxyapatite by electrostatic interaction between the negatively charged phosphate groups of the nucleic acids and the positively charged calcium atoms on the apatite lattice [9, 10]. In addition, adsorption is augmented by active phosphate groups in the lattice which tend to bind basic groups [11]. Elution of compounds from the adsorbent is usually brought about by the use of phosphate buffers which compete for the calcium sites on the lattice.

Experiments showed that both DNA and RNA could be adsorbed quantitatively (>98%) from spiked 1-l samples of both sea water and distilled water at pH 6.8 by means of 1 × 5-cm columns of spheroidal hydroxyapatite at a flow rate of ca. 3.0 ml min^{-1}. The capacity of such columns was found to be 100 μg of nucleic acid per gram of dry spheroids. Ions from the sample could be washed out of the columns without loss of nucleic acids by using 20 ml of 0.005 M phosphate buffer at pH 6.8. Quantitative elution of both DNA and RNA could be achieved by immersing the columns in a water bath at 60°C and passing 20 ml of 0.5 M phosphate buffer (pH 6.8) through them at a flow rate of 0.3 ml min^{-1}.

Photometric determination of nucleic acids

Mejbaum's method [12] was selected for the determination of the preconcentrated nucleic acids because of its sensitivity and selectivity. In this procedure the sample containing nucleic acid is heated at 100°C with a re-

agent containing iron(III) chloride and orcinol. This hydrolyses the nucleic acid yielding ribose which cyclizes to 2-furaldehyde which in turn reacts with the orcinol yielding a green compound, the absorbance of which is measured at 670 nm.

When a slightly modified version of Mejbaum's procedure (see Experimental section) was applied to 20-ml aliquots of 0.5 M phosphate buffer containing known amounts of RNA or DNA or 1:1 mixtures of DNA and RNA, both compounds were found to give a similar response, as noted by Dische [13]. Absorbances varied linearly with concentration up to at least 1250 μg of DNA or RNA per 20 ml of phosphate buffer. Triplicate calibration runs made in the range of amounts of nucleic acids likely to be recovered from 1—3-l samples of natural waters showed good reproducibility and a satisfactory adherence to linearity (Table 1).

Interferences

Tests were carried out to determine whether the more abundant types of organic compound present in natural waters would cause interference in the method. Preliminary experiments showed that 10-mg amounts of amino acids (alanine, glycine, arginine, valine-hydroxyproline, methionine and tryptophan) and a dibasic acid (pimelic acid) caused no interference in the photometric procedure itself. Considerable interference was, as anticipated [9, 14], experienced with a number of carbohydrates, such as glucose, fructose, mannose and xylose, which give green colours similar to those formed with ribose with the orcinol reagent. It was found, however, that carbohydrates were separated from nucleic acids during the preconcentration stage as they were not adsorbed by the hydroxyapatite. Under these circumstances, no interference was caused by 5 mg l^{-1} of the following: glucose, mannose, xylose, galactose, arabinose, ribose and fructose. There remained the possibility that some interference might be caused by the humic materials present in almost all natural waters. These substances were found to be moderately efficiently adsorbed by hydroxyapatite and could be eluted with 0.5 M phosphate buffer with an overall recovery of 25—31%. Significant amounts of them would thus be present at the colour-forming stage and might interfere. Several tests were therefore done with peat fulvic and humic acids as well as humic materials isolated from freshwater and sea water by

TABLE 1

Calibration of photometric procedure with RNA

μg RNA[a]	20	40	50	100	200
Absorbance[b]	0.042	0.090	0.113	0.221	0.443
Standard deviation	0.002	0.001	0.002	0.002	0.002
Absorbance/10μg RNA	0.0210	0.0225	0.0226	0.0221	0.0222

[a]per 50 ml final volume.
[b]Average of three measurements at 670 nm in 4-cm cuvette, less reagent blank of 0.018.

adsorption on Amberlite XAD-2 [16]. Unfortunately, the methods used for the preparation of these materials gave products which contained significant amounts of phosphorous (<0.4%P), much of which would probably have been present as nucleic acids. It was considered that allowance for these could be made by determining the total phosphorus content of the humic acid. This value could then be used to calculate the maximum percentage of nucleic acid which could be present in the sample (nucleic acids contain ca. 7% of phosphorus). The contribution which this would make to the absorbance in the orcinol method could thus be evaluated. Aliquots (1 l) of solutions of the humic samples at concentrations of 10 mg l^{-1} were processed as described in the Experimental section. For each of the samples, the measured absorbance was considerably less than (usually about half) that calculated from the phosphorus content, suggesting that the interference of humic materials in the method is negligible.

EXPERIMENTAL

Reagents and standards

Phosphate buffer (0.5 M). While stirring, gradually add 0.5 M potassium dihydrogenphosphate solution to 500 ml of 0.5 M dipotassium hydrogenphosphate solution until the pH of the mixture is 6.80 ± 0.02.

Phosphate buffer (0.005 M). Dilute 10 ml of 0.5 M phosphate buffer to about 900 ml and, if necessary, adjust the pH to 6.80 by cautious addition of 0.5 M potassium dihydrogenphosphate solution, before making up to volume.

Mixed reagent. Dissolve 2.5 g of chloroform-recrystallized orcinol (3,5-dihydroxytoluene) in 25 ml of ethanol; this solution is stable for only a few hours and should be prepared freshly when required. Dissolve 0.125 g of $FeCl_3 \cdot 6H_2O$ in 250 ml of concentrated hydrochloric acid. For the reagent, mix 25 ml of the orcinol solution with 25 ml of the iron(III) chloride solution. Prepared when required as the solution is stable for only a few hours.

Hydroxyapatite adsorbent. Wash spheroidal apatite (B.D.H. Chemicals) by gentle swirling followed by decantation, first with 2—3 times its own volume of 0.2 M sodium hydroxide, and then several times with 0.005 M phosphate buffer until the supernatant liquid has a pH of 6.8—6.9. Store the washed material under 0.005 M phosphate buffer. With a pipette, transfer a suspension of the hydroxyapatite to a 1-cm bore chromatographic column so as to pack a length of 5 cm. After packing, wash with 8—10 bed volumes of 0.005 M phosphate buffer. It is possible to use columns 3 or 4 times if, after removal of the top 1—2 mm, the packing is regenerated by back-washing with 15—20 ml of 0.1 M sodium hydroxide and then washing in the normal direction with 0.005 M phosphate buffer until the pH of the washings is <7.0. In handling the hydroxyapatite, it is essential to avoid strong agitation as the grains are very friable.

Standard RNA stock solution (200 μg RNA ml^{-1}). Dissolve 20.0 mg of RNA (sodium salt) in 5 ml of 0.5 M sodium hydroxide and dilute to 100 ml with distilled water. The solution is stable for at least four weeks at 4°C. Use this stock solution to prepare working standards containing 10, 25, 50 and 100 μg RNA ml^{-1} when required. The RNA used in the present investigation was a 'highly polymerized sodium salt derived from yeast' (B.D.H. Chemicals).

Treatment of apparatus

Conical and volumetric flasks were allowed to stand for several hours filled with 50% sulphuric acid. They were then thoroughly washed with distilled water.

Procedure

Immediately after collection, filter the sample through a Whatman GF/F glass-fibre filter (effective pore size 0.7 μm) using the minimum feasible vacuum (>0.5 atm) in order to prevent rupture of the more delicate phytoplankton cells. Add 2 ml of sodium azide solution (aqueous 3.2% w/v) per litre as a preservative. It is desirable to keep storage time to a minimum, but if it is not possible to commence the analysis immediately, the azide-treated samples can be stored for a few days in a refrigerator at 4°C.

To commence the analysis, adjust the pH of an appropriate aliquot (1—3 l) of the sample to 6.8 ± 0.1 by cautious addition of 0.5 M phosphate buffer. Allow the solution to pass through the 1 × 5 cm column of hydroxyapatite at a flow rate of about 3 ml min^{-1}. Wash the column with 20 ml of 0.005 M phosphate buffer. Reject the percolate and washings. Immerse the column in a waterbath at 60°C and after thermal equilibrium has been attained, elute the nucleic acids by passage of 20 ml of 0.5 M phosphate buffer at a flow rate of 0.3 ml min^{-1}. Collect the eluate in a 50-ml conical flask and add 20 ml of iron(III)—orcinol mixed reagent. After mixing, cover the flask with a bulb stopper and heat it in a boiling water bath for 45 min. Cool, and transfer the contents of the flask to a 50-ml calibrated flask using two 2.5-ml portions of ethanol. Dilute to volume with distilled water. Measure the absorbance of the resulting solution at 670 nm in a 4-cm cuvette against distilled water. Run a corresponding blank through the whole procedure, using distilled water. Standardize the procedure by placing 2-ml aliquots of the working standard RNA solution (equivalent to 20, 50, 100 and 200 μg of nucleic acid) in a series of 50 ml conical flasks. Add 18 ml of 0.5 M phosphate buffer and 20 ml of the iron(III)—orcinol mixed reagent. After mixing, cover the flask with a bulb stopper and heat for 45 min in a boiling water bath. Continue the procedure described for the samples. Carry out a corresponding reagent blank in the same manner, using 2 ml of distilled water in place of the working standards.

RESULTS

In order to test the precision of the method, replicate (6) analyses were done on both freshwater samples from Esthwaite Water and sea water from the English Channel. The average total nucleic acid concentrations and relative standard deviations found for these samples were 46.9 $\mu g\ l^{-1}$ (± 2.9%) and 78.7 $\mu g\ l^{-1}$ (± 2.4%), respectively. The accuracy of the procedure was checked by analysing, in triplicate, samples of English Channel sea water which had been stripped of nucleic acids by passage through Amberlite XAD-2 and then spiked with 100 μg of nucleic acid. Satisfactory recoveries (96—102%) of nucleic acids could be achieved (Table 2).

Following the development of the analytical method, a preliminary survey was made of the distribution of dissolved nucleic acids in the surface waters of the productive area of the English Channel in June 1978. The results (Table 3) showed that their concentration was fairly constant over the area studied (average 95 $\mu g\ l^{-1}$) and that these compounds comprised an important fraction (27—49%) of the total dissolved organic phosphorus.

During the analytical development work, it was observed that the patterns of the elution of DNA and RNA from the hydroxyapatite columns were quite reproducible (Fig. 1). It was therefore thought that an examination of the elution patterns obtained with sea-water samples might provide useful information about the nature of the dissolved polynucleotides. Accordingly, 3-l aliquots of filtered (0.7 μm) surface waters from the English Channel were passed through a series of 1 × 5 cm columns of hydroxyapatite as described in the Experimental section. After washing, the columns were eluted with 0.5 M phosphate buffer. Eluate fractions of 2 ml were collected and analysed for nucleic acids. The elution patterns obtained with the various samples are shown in Fig. 2. Although the peaks associated with RNA and DNA at a retention volume of ca. 4 ml occurred with all the samples, some also exhibited peaks with retention volumes of ca. 12 ml. The source of the latter peaks is uncertain, but they may reflect the presence of nucleotides having different sugar—base phosphate compositions as suggested by Kothari [15], or they may be related to the particular types of polynucleotides present.

TABLE 2

Percentage recovery of nucleic acids from spiked sea-water samples

Nucleic acid	Wt. (μg)	Recovery (%)	Mean ± s.d.
DNA	100	102, 99, 98	99 ± 2.1
RNA	100	99, 97, 101	99 ± 2.0
DNA + RNA	50 + 50	96, 101, 98	98 ± 2.5

TABLE 3

Dissolved nucleic acid concentrations in the surface waters of the English Channel in June 1978

Sample No.	Station	Lat.	Long.	Dissolved phosphorus (μg-at l^{-1})			Nucleic acids	
				Reactive	Total	Organic	(μg l^{-1})	as % of organic P
1	Start Point	50°13'N	03°36'W	0.45	1.35	0.90	108	27
2	Start Bay	50°15'N	03°38'W	0.67	1.41	0.74	110	34
3	V	50°03'N	03°53'W	0.41	1.22	0.81	99	28
4	L5-2	50°10'N	03°46'W	0.03	0.42	0.39	85	49
5	L5-3	50°09'N	03°45'W	0.06	0.48	0.42	71	38

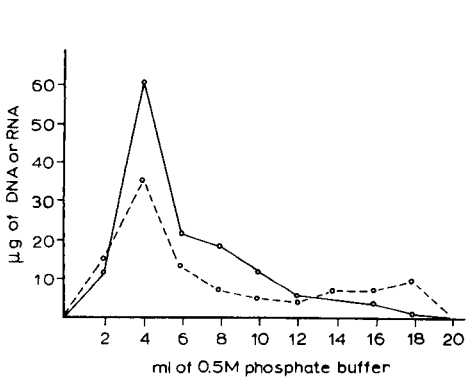

Fig. 1. Elution curves for DNA (continuous line) and RNA (broken line).

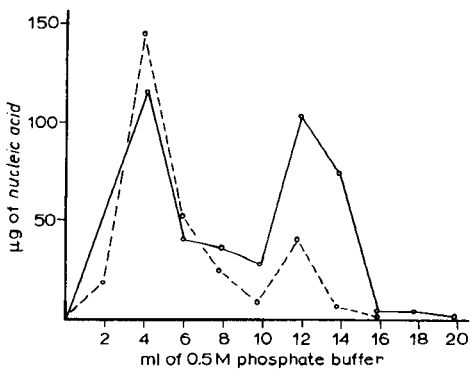

Fig. 2. Elution curves for nucleic acids recovered from water samples from the English Channel: (—) sample 1; (- - -) sample 4 (see Table 3).

The authors thank Mr. E. I. Butler and Mr. P. Toms, and the Master and crew of R.V. "Sarsia" for assistance in the collection of samples.

REFERENCES

1 F. Azam and R. E. Hodson, Nature, 267 (1977) 696.
2 R. A. Minear, Environ. Sci. Technol., 6 (1972) 431.
3 J. P. Koenings and F. H. Hooper, Mich. Acad., 5 (1973) 295.
4 T. N. Pillai and A. K. Ganguly, J. Mar. Biol. Ass. India, 14 (1972) 384.
5 A. Tiselius, S. Hjerten and Ö. Levin, Arch. Biochem. Biophys., 65 (1956) 132.
6 R. K. Main, M. J. Wilkins and L. J. Cole, J. Am. Chem. Soc., 81 (1959) 6490.
7 G. G. Markov and I. G. Ivanov, Anal. Biochem., 59 (1974) 555.
8 Y. Miyazama and C. A. Thomas, J. Mol. Biol., 11 (1965) 223.
9 G. Bernardi, in L. Grossman and K. Moldave (Eds.), Methods in Enzymology, Vol.21, Academic Press, New York, 1971.
10 G. Bernardi, Nature (London), 206 (1965) 779.

11 G. Bernardi, M. G. Giro, and C. Gaillard, Biochem. Biophys. Acta, 278 (1972) 409.
12 W. Mejbaum, Z. Physiol. Chem., 258 (1939) 117.
13 Z. Dische, in E. Chargaff and J. N. Davidson (Eds.) The Nucleic Acids: Chemistry and Biology, Vol. 1, Academic Press, New York, 1955.
14 B. O. Josefsson, L. Uppstrom and G. Ostling, Deep-Sea Res., 19 (1972) 385.
15 R. M. Kothari, J. Chromatogr., 53 (1970) 580.
16 R. F. C. Mantoura and J. P. Riley, Anal. Chim. Acta, 76 (1975) 97.

Analytica Chimica Acta, 116 (1980) 145—152

EXTRACTION ET DOSAGE PAR CHROMATOGRAPHIE EN PHASE GAZEUSE D'UN HERBICIDE (NEBURON) ET D'UN DE SES MÉTABOLITES (3,4-DICHLOROANILINE). APPLICATION À DES EAUX NATURELLES

A. COPIN*, J. DELMARCELLE, R. DELEU** et A. RENAUD**

Departement de Chimie Analytique, Faculté des Sciences Agronomiques de l'Etat, 5800 Gembloux (Belgique)

Ph. DREZE

Departement de Physique et Chimie-Physique et CAMIRA, Faculté des Sciences Agronomiques de l'Etat, 5800 Gembloux (Belgique)

(Reçu le 25 Octobre 1979)

SUMMARY

Extraction and gas chromatographic determination of a herbicide (Neburon) and a metabolite (3,4-dichloroaniline). Application to natural waters.

A method is reported for the simultaneous quantitative extraction of Neburon (a urea herbicide) and 3,4-dichloroaniline (one of its metabolites) at residue levels (10—100 $\mu g\ l^{-1}$) in natural waters of various origins. The acetylation conditions described for 3,4-dichloroaniline permit gas chromatographic determination of Neburon and of its metabolite.

RESUME

Les auteurs décrivent une méthode d'extraction quantitative qui est, en même temps, applicable au Neburon (herbicide de la famille des urées substituées) et à un de ses métabolites (3, 4-dichloroaniline) à l'état de résidus (10—100 $\mu g\ l^{-1}$) à partir d'eaux naturelles de diverses provenances. Ils présentent les conditions d'acétylation de la 3,4-dichloroaniline qui permettent un dosage par chromatographie en phase gazeuse du Neburon et de son métabolite.

La présence des herbicides appartenant à la famille des urées substituées dans les eaux de rivière, de ruissellement ou de percolation se révèle souvent fugace [1—3]. La disparition, même partielle, de la molécule initiale qui est attribuée à un processus physicochimique de dégradation aussi bien qu'à un processus biologique de métabolisation, induit l'apparition de molécules nouvelles.

Maier-Bode [4] ainsi que Geissbühler et al. [5] ont montré que le Neburon (1-n-butyl-3-(3,4-dichlorophényl)-1-méthylurée) après désalkylation et hydrolyse, donne naissance à de la 3,4-dichloroaniline. Le dosage de la 3,4-

**CRUPA, Section protection environnement (IRSIA).

dichloroaniline par spectrophotométrie dans le visible, après diazotation et copulation (réaction de Bratton—Marshall) a fait l'objet de divers traveaux [6—8]. Cette méthode a aussi été appliquée aux molécules initiales d'herbicide après séparation de celles-ci de leurs métabolites par chromatographie en couche mince et hydrolyse alcaline. La méthode spectrophotométrique, à moins qu'elle ne soit entièrement automatisée [9], ne se prête que difficilement à l'analyse en routine de ces deux molécules simultanément présentes.

Les possibilités de dosage du Neburon par chromatographie en phase gazeuse sont variées. Un certain nombre de méthodes s'appliquent à la molécule comme telle [10—12]. Fishbein et Zielinski [13] font précéder sa détermination instrumentale d'une silylation. Cette réaction qui porte sur le groupement NH de l'herbicide abaisse sa polarité et évite sa décomposition sur certaines colonnes de chromatographie. Tanaka et Wien [14] obtiennent le même résultat après méthylation. La 3,4-dichloroaniline peut être dosée directement par chromatographie en phase gazeuse [15], parfois aussi sous forme d'un dérivé halogéné [16, 17] ou dinitrophénylé [18]. Cependant, aucune des méthodes précitées n'assure la détermination simultanée de l'herbicide et de son métabolite. Dans ces conditions nous nous sommes attachés à la mise au point d'une technique d'extraction applicable à chacun d'eux à l'état de traces dans l'eau ($<100\ \mu g\ l^{-1}$). De plus, pour permettre leur dosage sur une seule colonne en chromatographie en phase gazeuse, nous avons recherché les conditions d'acétylation de la 3,4-dichloroaniline suffisament sélectives pour être sans effet sur le Neburon.

PARTIE EXPÉRIMENTALE

Réactifs

Le chloroforme de qualités PBV et le benzène technique sont distillés respectivement à 61°C et 80°C. La 3,4-dichloroaniline (m.p. 71°C) est commercialisée (Riedel de Haen; Pestanal 35827). De la 3,4-dichloroaniline tritiée en position-2 est utilisée comme traceur. Son activité spécifique est de 7500 mCi $mmol^{-1}$ et sa pureté radiochimique s'élève à 99%. Le Neburon et le β-hexachlorocyclohexane (β-BCH) sont recristallisés. L'anhydride chloracétique et le chlorure de chloroacétyle sont de qualité purum (Fluka). La solution scintillante est le Lumagel (1027; Lumac Systems).

Appareillage

L'appareil utilisé est un chromatographe Hewlett-Packard 5730 A. Il est équipé d'un détecteur à capture d'électrons au ^{63}Ni. Les températures du bloc d'injection et du détecteur sont maintenues respectivement à 250°C et 300°C.

Les mesures de radioactivité sont effectuées par scintillation liquide (Mark I, Nuclear-Chicago). Les échantillons sont préparés dans des fioles standard en polyéthylène de 20 ml. La liqueur scintillante est composée de 10 ml de Lumagel, 1 ml de mélange toluène—chloroforme (9:1 v/v) et

1 ml d'eau extraite d'un blanco. Une telle composition permet d'obtenir un même rendement de comptage (25,8% pour le tritium dans nos conditions) pour tous les échantillons quelle que soit la nature de la phase où est prélevée l'aliquote de 1 ml.

Le carbone organique et inorganique des eaux étudiées est dosé au moyen du TCM 420 de Carlo Erba (Milan) appartenant à la firme Van Ermengen (Louvain).

Mode opératoire

La mise au point analytique a porté sur trois types d'eau dont les caractéristiques sont reprises dans le Tableau 1.

Dans le cas de l'eau de rivière, l'échantillon est, dès sa réception, débarrassé des particules en suspension par filtration à travers un filtre MN713-1/4. Ensuite, dans une ampoule à décanter sont successivement versés 500 ml d'eau à analyser, 10 ml d'EDTA 0,1 M et du tampon NH_4OH—NH_4Cl 0,1 M pour porter le pH de l'ensemble à 8,5—9. L'extraction comprend une agitation manuelle d'une minute de l'échantillon avec 50 ml de chloroforme. Après décantation, le chloroforme, soutiré, traverse un filtre hydrofuge MN616-WA. Cette opération est répétée deux fois. Le volume du chloroforme est porté à 250 ml. Un premier prélèvement de 100 ml d'extrait est réservé au dosage du Neburon. Dans ce but, le chloroforme est évaporé à sec sous pression réduite, et le résidu d'évaporation est solubilisé dans un volume connu de benzène, dont 5 μl sont injectés en chromatographie.

Le deuxième prélèvement de 100 ml est consacré à l'analyse de la 3,4-dichloroaniline après acétylation. La phase organique est concentrée sous pression réduite à un volume d'environ 5 ml pour être quantitativement porté à 50 ml avec du benzène. L'acétylation est entreprise sur 20 ml de cette solution sur laquelle on fait agir 5 ml d'une solution benzénique à $2{,}8 \times 10^{-2}$ M d'anhydride chloracétique fraîchement préparée. Après 30 min de contact, l'excès d'acétylant est détruit par agitation avec une solution d'hydroxyde de sodium 0,5 M. La phase benzénique, après lavage jusqu'à neutralité avec de l'eau, est évaporée à sec. Le résidu est repris par un volume connu d'une solution benzénique de β-BCH à 0,214 μg ml^{-1} (étalon externe) pour être analysée par chromatographie.

TABLEAU 1

Caractéristiques des eaux

Origine	pH	Conductivité (μS à 20°C)	Dureté (F°)	C(mg l^{-1})	
				Organique	Inorganique
Eau boisson (Réseau distribution)	7,1	820	40—45	<0,5	60
Source (Naturelle F.S.A. Gx)	6,2—6,7	760	34	0,5—1	55
Rivière Mehaigne	7,3—7,7	700	30	8—10	52

RESULTATS ET DISCUSSION

Rendements d'extraction du Neburon et de la 3,4-dichloroaniline

L'extraction a été étudiée avec des concentrations de 20 et 75 $\mu g\ l^{-1}$ de 3,4-dichloroaniline contenant $3,2 \times 10^{-2}$ $\mu Ci\ ml^{-1}$ de produit tritié. Afin d'obtenir ces concentrations et cette radioactivité, la 3,4-dichloroaniline et son traceur sont ajoutés en solution méthanolique à l'eau de distribution et à l'eau de rivière dont les caractéristiques au niveau de l'adsorption sont totalement divergentes.

Les valeurs moyennes (pour 5 extractions) des pourcentages d'activité de chaque phase par rapport à l'activité initiale ainsi que les limites de confiance supérieures et inférieures de ces moyennes et du bilan sont reprises dans le Tableau 2. Il apparaît que l'activité retrouvée dans la phase aqueuse est de l'ordre de grandeur des impuretés contenues dans le produit de départ. En conséquence, l'extraction de la 3,4-dichloroaniline, dont le caractère basique est atténué par la présence de deux atomes de chlore, peut être considérée comme quantitative à partir des eaux aussi différentes que l'eau de distribution et l'eau de rivière.

Dans le tampon ammoniacal, la récupération du Neburon reste supérieure à 95% comme elle l'était pour les eaux dont le pH n'a pas été modifié [12] De plus, il n'y a pas lieu de craindre l'hydrolyse de cette molécule d'herbicide en 3,4-dichloroaniline; ce qui serait le cas si le pH était plus élevé [19]. Le recours aux techniques radiochimiques a en outre permis de montrer que l'évaporation à sec de solutions chloroformiques de 3,4-dichloroaniline conduit à des pertes importantes et non reproductibles de cette molécule (entre 50 et 80%).

Analyse par chromatographie en phase gazeuse du Neburon et de la 3,4-dichloroaniline

Les conditions de chromatographie du Neburon et les résultats obtenus avec des colonnes de Chromosorb W-HP ou Chromosorb W-AW-DMCS garnies de phase stationnaire du type DC550, OV1, SE30, QF1, OV17 et OV210 ont été décrites précédemment [12].

Les conditions d'acétylation de la 3,4-dichloroaniline. La comparaison a porté sur deux acétylants cités par Blau et King [20]: le chlorure de chloroacétyle et l'anhydride chloroacétique. Le chlorure de chloroacétyle (1 ml) à différentes concentrations (solutions de 10—100% v/v) est ajouté à 20 ml de solution benzénique contenant 10 μg de 3,4-dichloroaniline. Une solution benzénique à $2,8 \times 10^{-2}$ M de l'anhydride chloroacétique (5 ml) est mise en contact avec la même concentration de 3,4-dichloroaniline ($0,5\ \mu g\ ml^{-1}$). Aucune différence entre les hauteurs de pics obtenus en chromatographie en phase gazeuse n'a pu être mise en évidence. Par contre, les blancos en présence de chlorure de chloroacétyle, même aux plus faibles concentrations, présentent des pics dont l'intensité varie avec le lot du réactif. Les difficultés d'utilisation du chlorure ajoutées à sa moindre pureté nous ont amené à le rejeter au profit de l'anhydride chloroacétique.

TABLEAU 2

Rendement d'extraction en pourcentage de la 3,4-dichloroaniline[a]

	20 $\mu g\ l^{-1}$						75 $\mu g\ l^{-1}$					
	R_o		R_w		Bilan		R_o		R_w		Bilan	
	$\bar{X}$	IC	$\bar{X}$	IC	$\bar{X}$	IC	$\bar{X}$	IC	$\bar{X}$	IC	$\bar{X}$	IC
Eau de distribution	95,4	0,7	1,5	0,1	97,0	0,7	94,3	0,9	1,5	0,1	95,8	1,1
Eau de rivière	95,4	1,6	1,6	0,1	97,0	1,7	93,0	1,2	1,6	0,1	94,6	1,2

[a] X = moyenne. IC = intervalle de confiance, t 97,5 $\hat{\sigma}/n^{1/2}$. R_o = récupération dans la phase organique. R_w = récupération dans la phase aqueuse.

L'influence de concentrations croissantes en anhydride chloroacétique (1,4; 2,3; 2,8; 5,7 × 10^{-2} M et 2,3 × 10^{-1} M) a d'abord été étudiée sur 10 μg de 3,4-dichloroaniline dissoute dans 20 ml de benzène. La durée de réaction était 30 min. Les résultats (moyenne de 2 déterminations) exprimés par rapport à la hauteur du pic fourni par 1,07 ng de β-BCH sont repris dans le Fig. 1. Cette expérimentation, répétée deux fois, a conduit à des résultats semblabes. La hauteur du pic (et sa hauteur par rapport à celle du β-BCH) sont constantes entre 2,3 et 5,7 × 10^{-2} M d'acétylant. Par contre, la valeur de 1,4 × 10^{-2} M en anhydride chloroacétique conduit à des résultats plus faibles; en présence de 2,3 × 10^{-1} M d'acétylant, au contraire, les pics sont sensiblement plus importants. De plus, pour la concentration de 2,8 × 10^{-2} M en acétylant retenue, il existe une proportionnalité entre la hauteur du pic de chromatographie et les concentrations comprises entre 0,025 $\mu g\ ml^{-1}$ et 0,5 $\mu g\ ml^{-1}$ en 3,4-dichloroaniline.

Des durées de réaction de 15 min et 45 min conduisent à des résultats semblables. La réaction entreprise sur 10 μg de 3,4-dichloroaniline en présence des 5 ml de 2,8 × 10^{-2} M d'acétylant conduit après 15 min de réaction à une

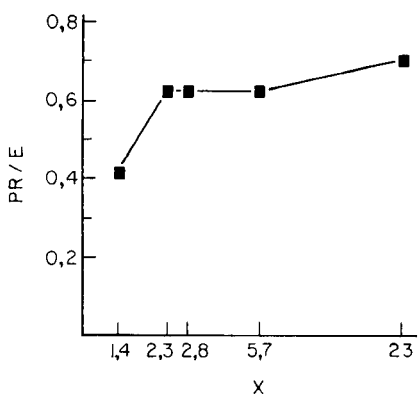

Fig. 1. L'influence de la concentration en anhydride chloroacétique. L'axe des X est gradué en 10^{-2} M d'anhydride chloroacétique. L'axe des Y reprend le rapport des hauteurs du produit de réaction (PR) sur celle de 1,07 ng de β-BCH (étalon externe) dans les mêmes conditions de chromatographie.

hauteur de 74% de celle de 1,07 ng de β-BCH avec un intervalle de confiance à un niveau de probabilité de 5% de ± 1,7%. Pour 45 min de réaction, la hauteur est de 77% de celle de la même quantité de β-BCH avec un intervalle de confiance à 95% de 8,6%.

Rendement de réaction et structure du produit. Tout en maintenant la même proportion d'acétylant par rapport à la 3,4-dichloroaniline, cette réaction a été répétée sur des quantités de l'ordre du mg de cette dernière. Après évaporation du benzène, le résidu repris dans l'acétone est recristallisé jusqu'à l'obtention d'un produit de point de fusion constant (103—103,5°C). L'analyse élémentaire de ce produit conduit à la formule brute $C_8H_6NOCl_3$. Elle concorde avec les résultats de la spectrométrie de masse. Celle-ci permet de confirmer le poids moléculaire de 238,6.

L'étude de spectre infrarouge laisse apparaître les bandes amide I et II respectivement à 5,95 μm (vibration de valence du -C=O) et à 6,50 μm (vibration de déformation NH). De plus, une bande située à 14,2 μm pourrait être attribuée à la vibration de valence de la liaison C—Cl du groupement $-CH_2Cl$ [21].

Par comparaison avec les résultats de la chromatographie en phase gazeuse de solutions titrées du produit de synthèse cristallisé, le rendement de l'acétylation suivant le mode opératoire décrit plus haut peut être estimé entre 92 et 95%.

Recherche des conditions de chromatographie en phase gazeuse. Le Tableau 3 reprend les temps de rétention et les limites inférieures de détection de la 3,4-dichloroaniline acétylée pour trois colonnes ainsi que les conditions opératoires choisies. Pour chacune des colonnes, la linéarité du détecteur, après saturation de la colonne, s'étend à au moins cent fois la limite inférieure de détection (LD). La présence, dans l'extrait, de Neburon, sur lequel l'acétylant, dans les conditions décrites est sans action, ne provoque aucun danger d'interférence. Pour la colonne 1, l'application d'une programmation de température débutant à 140°C pendant 6 min pour terminer par un palier à 220°C après une montée de 8°C min^{-1} permet de doser simultanément le Neburon et son métabolite.

Application de l'acétylation à des extraits d'eau

Pour juger de l'efficacité de la méthode d'analyse, les deux eaux naturelles (source; rivière) ont été enrichies par de la 3,4-dichloroaniline aux doses de 20 et 50 μg l^{-1}. Les valeurs moyennes, pour 5 analyses, des rendements de récupération ainsi que les intervalles de confiance de ces moyennes sont repris dans le Tableau 4 pour chacune des eaux et concentrations étudiées. Pour chacun des cas envisagés le dosage par acétylation conduit à des résultats exacts et précis et la limite de sensibilité de la méthode est comprise entre 5 et 10 μg l^{-1}. De plus, aucun des blancos n'a révélé aux niveaux du t_R de la 3,4-dichloroaniline comme au niveau de celui du Neburon une quelconque interférence analytique.

Les auteurs remercient le Professeur Jadot, Chimie organique, Université de Liège, pour l'analyse élémentaire (CHN), le Dr. Monseur, Institut de Recherches Chimiques de Tervueren, pour les spectres de masse, et l'Institut

TABLEAU 3

Temps de retention (t_R) de la 3,4-dichloroaniline acétylée en fonction de différents paramètres analytiques

Colonne No.	Type	Longueur (m)	Temp. (°C)	Débit gaz (ml min^{-1})	t_R (s)	t_R β-BCH	LD[a] (pg)
1	DC550 5% sur Chromosorb W-HP (100—120 mesh)	1,80	220	20	282	1,38	50
2	DC11 5% sur Chromosorb W-AW-DMCS (100—120 mesh)	1,80	190	27	150	1,79	150
3	GESE30 5% sur Chromosorb W-AW-DMCS (80—100 mesh)	1,20	170	20	216	2,05	250

[a] Limites inférieures de détection en produit pur.

TABLEAU 4

Rendement de récupération (en %) de la 3,4-dichloroaniline après acétylation[a]

	20 μg l^{-1}		50 μg l^{-1}	
	$\bar{X}$	*IC*	$\bar{X}$	*IC*
Eau de source	97,8	3,2	99,1	1,3
Eau de rivière	95,5	2,1	95,9	2,3

[a] *X* et *IC*, voir Tableau 2.

pour l'Encouragement de la Recherche Scientifique dans l'Industrie et l'Agriculture (IRSIA Bruxelles) qui a subventionné cette recherche.

BIBLIOGRAPHIE

1 A. Copin, R. Deleu et A. Bollinne, Semaine d'Etude, Agriculture et Hygiène des plantes, 8—12 Sept. 1975, 1975, p. 267.
2 R. Deleu, J. P. Barthelemy et A. Copin, J. Chromatogr., 134 (1977) 483.
3 A. Copin et R. Deleu, Pédologie, 28 (1978) 205.
4 H. Maier-Bode, Herbizide und ihre Rückstände, Ulmer, Stuttgart, 1971, pp. 175.
5 H. Geissbühler, H. Martin et G. Voss, dans P. C. Kearney et D. O. Kaufman (Eds.), Herbicides; chemistry, degradation and mode of action, Vol. 1, M. Dekker, New York, 1975, pp. 210.
6 M. A. El-Dib, J. Assoc. Off. Anal. Chem., 54 (1971) 1383.
7 M. A. El-Dib et A. Osama, J. Assoc. Off. Anal. Chem., 55 (1972) 1276.
8 G. Voss et H. Geissbühler, In A. S. Tahori (Ed.), Methods in Residue Analysis, Vol. 4, Gordon and Breach, New York, 1971, p. 225.
9 J. A. Guth et G. Voss, Weed Res., 11 (1971) 111.

10 C. E. McKone et R. J. Hance, J. Chromatogr., 36 (1968) 234.
11 C. E. McKone, J. Chromatogr., 44 (1969) 60.
12 R. Deleu et A. Copin, J. Chromatogr., 171 (1979) 263.
13 L. Fishbein et W. L. Zielinski, J. Chromatogr., 20 (1965) 9.
14 I. S. Tanaka et R. G. Wien, J. Chromatogr., 87 (1973) 85.
15 S. E. Katz et R. J. Strusz, J. Agric. Food Chem., 17 (1969) 1411.
16 J. Baunok et H. Geissbühler, Bull. Environ. Cont. Toxicol., 3 (1968) 7.
17 K. Kossman, in A. S. Tahori (Ed.), Methods in Residue Analysis, Vol. 4, Gordon and Breach, New York, 1971, p. 187.
18 I. C. Cohen et B. B. Wheals, J. Chromatogr., 43 (1969) 233.
19 W. K. Lowen, W. E. Bleidner, J. J. Kirkland et H. L. Pease, in S. Zweig (Ed.), Analytical Methods for Pesticides, Plant Growth Regulators and Food Additives, J. Wiley, New York, 1964, p. 157.
20 K. Blau et G. S. King, Handbook of Derivatives for Chromatography, Heyden, London, 1978, p. 107.
21 L. J. Bellamy, The Infrared Spectra of Complex Molecules, Vol. I, 3rd edn., Chapman and Hall, London, 1975.

Analytica Chimica Acta, 116 (1980) 153—160

EXTRAKTION VON BUNT- UND EISENMETALLEN MIT 1-PHENYL-3-METHYL-4-BENZOYLPYRAZOL-5-THION UND 1-PHENYL-3-METHYL-4-THIOBENZOYLPYRAZOL-5-ON†

E. UHLEMANN*, B. MAACK und M. RAAB**

Pädagogische Hochschule "Karl Liebknecht", 15-Potsdam-Sanssouci (Deutsche Demokratische Republik)

(Eingegangen den 23. Oktober 1979)

SUMMARY

Extraction of iron and heavy metal ions with 1-phenyl-3-methyl-4-benzoylpyrazol-5-thione and 1-phenyl-3-methyl-4-thiobenzoylpyrazol-5-one

The extraction of Mn, Fe(II), Co, Ni, Cu, Zn, Pb, Cd, and Fe(III) by the isomeric monothio derivatives of 1-phenyl-3-methyl-4-benzoylpyrazol-5-one has been measured by atomic absorption spectrometry. The influence of tartrate as a supporting ligand was calculated and the extraction parameters $pH_{1/2}$ and K_{ex} were determined. Extractions are possible from relatively acidic solutions; the behaviour of zinc is unusual. Iron(III) binds only two molecules of the extractant, whereas iron(II) forms the expected tris chelate by oxidation.

ZUSAMMENFASSUNG

Auf atomabsorptionsspektrometrischem Wege wurden die Extraktionskurven der isomeren Monothioderivate von 1-Phenyl-3-methyl-4-benzoylpyrazol-5-on für Mn, Fe(II), Co, Ni, Cu, Zn, Pb, Cd, und Fe(III) ermittelt. Es wurde der Einfluß von Tartrat als Hilfskomplexbildner berechnet und die Extraktionsparameter $pH_{1/2}$ und K_{ex} bestimmt. Die Extraktion der Metalle erfolgt bereits aus relativ saurer Lösung, wobei Zink eine Sonderstellung einnimmt. Bei der Extraktion von Eisen(III) werden überraschenderweise nur zwei Moleküle des Extraktionsmittels gebunden, während beim Eisen(II) durch Oxydation ein Tris-Chelat entsteht.

4-Acylpyrazol-5-one stellen ausgezeichnete Extraktionsmittel für Metalle dar [2, 3] und können in dieser Hinsicht sogar mit gewissen fluorierten β-Diketonen und Monothio-β-diketonen erfolgreich konkurrieren. Durch Einführung von Schwefel als Ligatoratom in das Ligandsystem der 4-Acylpyrazol-5-one ist eine Erhöhung der Selektivität und die Verschiebung der Extraktion in stärker saure Bereiche zu erwarten. Als Thioderivate des 1-Phenyl-3-methyl-4-benzoylpyrazol-5-ons wurden die beiden Isomeren 1-Phenyl-3-methyl-4-benzoylpyrazol-5-thion (I) und 1-Phenyl-3-methyl-4-thiobenzoylpyrazol-5-on (II) dargestellt und auf ihr Extraktionsvermögen

†Chelate von β-Dicarbonylverbindungen und ihren Derivaten Teil LII. Teil LI, siehe [1].

** Zentralinstitut für Ernährung der AdW der DDR, Potsdam-Rehbrücke.

für Mangan(II), Eisen(II), Cobalt(II), Nickel(II), Kupfer(II), Zink(II), Blei(II), Cadmium(II) und Eisen(II) untersucht. Weiterhin wurden die Extraktionsmittel selbst durch ihr Verteilungsverhältnis zwischen Chloroform und Wasser charakterisiert.

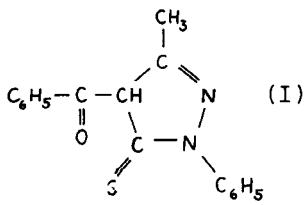

(I)

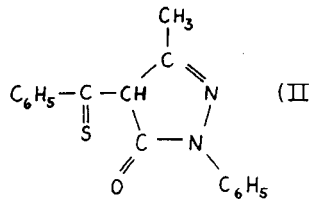

(II)

Um die Metallextraktion ohne Störung über einen weiten pH-Bereich verfolgen zu können, wurde vor der Extraktion Tartrat als Hilfskomplexbildner zugesetzt. Dadurch war auch die Bestimmung der Extraktionskurven im alkalischen Gebiet möglich, für das meist nur relativ wenige Angaben vorliegen. Als Analysenmethode diente die Atomabsorptionsspektrometrie. Jedoch war dabei die Metallionenkonzentration in der organischen Phase der direkten Messung nicht zugänglich, sie kann aber aus der Differenz der Ausgangskonzentration an Metall und der für die wäßrige Phase gemessenen Konzentration genügend genau ermittelt werden.

EXPERIMENTELLER TEIL

Extraktionsmittel

1-Phenyl-3-methyl-4-thiobenzoylpyrazol-5-on. 1-Phenyl-3-methylpyrazol-5-on (17,4 g; 0,1 mol) werden in 300 ml Dioxan gelöst und die Lösung am Rückfluß erhitzt. Unter ständigem Rühren gibt man dann 15 g (0,2 mol) Calciumhydroxid zu, wobei das Gemisch cremfarben wird. Nach 15 min erfolgt die Zugabe einer Lösung von 21,2 g (0,1 mol) Thiobenzoylthioglykolsäure [4] in 300 ml Dioxan. Die Lösung färbt sich rot. Man erhitzt unter ständigem Rühren noch weitere 30 min am Rückfluß. Am Ende der Umsetzung ist das Reaktionsgemisch leuchtend gelb geworden. Man löst in 1 l Eiswasser und gibt unter Rühren 250 ml 2 M Salzsäure (0,5 mol) zu. Aus der trüben orangen Lösung fällt allmählich ein gelber, feinkristalliner Niederschlag aus, der nach 24 Stunden abgesaugt wird. Zur Reinigung extrahiert man im Soxhlet mit Petrolether. [Ausbeute 23,5 g (80%); Schmp. 104—105°C (Alkohol).]

1-Phenyl-3-methyl-4-benzoylpyrazol-5-thion. Diese Substanz wurde nach den Angaben der Literatur [5] dargestellt.

Verteilungsverhältnis der Extraktionsmittel. Zur Bestimmung des Verteilungsverhältnisses in Abhängigkeit vom pH-Wert wurden jeweils 10 ml einer 4×10^{-3} M Lösung des Extraktionsmittels in Chloroform mit dem gleichen Volumen einer entsprechenden Pufferlösung der Ionenstärke 0,1 30 min geschüttelt. 10 min nach erfolgter Phasentrennung wurde die Extinktion der organischen Phase bei einer geeigneten Wellenlänge gemessen und in der

wäßrigen Phase nochmals eine pH-Kontrolle vorgenommen. Die Auftragung von log D gegen pH ergibt eine lineare Beziehung log D = log (K_v/K_s) —pH, aus der als Kenngröße des Extraktionsmittels der Quotient von Verteilungskoeffizient und Säurekonstante leicht ermittelt werden kann [6].

Durchführung der Extraktion

Als Metallstandardlösungen dienten 4×10^{-5} M Lösungen der Metallnitrate, die außerdem 2×10^{-4} M Kaliumnatriumtartrat als Hilfskomplexbildner und 10^{-1} M Natriumnitrat zur Gewährleistung einer konstanten Ionenstärke enthielten.

Zur Untersuchung der Zweiphasenverteilung wurden jeweils 10 ml 4×10^{-5} M wäßriger Metallsalzlösung mit 10 ml 4×10^{-3} M Lösung des Extraktionsmittels in Chloroform 30 min geschüttelt. Die Einstellung verschiedener pH-Werte erfolgte durch tropfenweise Zugabe von 1 M, 0,1 M und 0,01 M Salzsäure bzw. 1 M, 0,5 M, 0,2 M, 0,1 M und 0,01 M Natronlauge. Die Bestimmung des pH-Wertes der jeweiligen wäßrigen Phase wurde mit dem pH-Meßgerät MV84 (VEB Präzitronic, Dresden) das mit dem Elektrodensystem GA 50 N/SE 20 ausgerüstet ist, in einer Probe der Lösung vorgenommen. Ein weiterer Anteil der wäßrigen Phase diente der atomabsorptionsspektrometrischen Messung.

Für die Untersuchungen stand das Atomabsorptionsspektrometer AAS 1 (VEB Carl Zeiss, Jena) mit entsprechenden Hohlkatoden (VEB Narva, Berlin) zur Verfügung. Die Ermittlung der Metallionenkonzentration erfolgte nach dem Eichgeradenverfahren.

Berechnung der Verteilungskoeffizienten

Der Verteilungskoeffizient D ergibt sich aus dem Verhältnis der Metallkonzentrationen in organischer und wäßriger Phase. In Gegenwart eines Hilfskomplexbildners verringert sich aber die Konzentration freier Metallionen in der wäßrigen Phase. Die Messung liefert unter diesen Bedingungen den praktischen Verteilungskoeffizienten $D_{\text{prakt.}}$. Für das Verhältnis von D zu $D_{\text{prakt.}}$ ist im Falle des hier verwendeten Tartrats in logarithmischer Schreibweise zu formulieren:

$$\log D = \log D_{\text{prakt.}} + \log (1 + \beta_1 [\text{tart}^{2-}] + \beta_2 [\text{tart}^{2-}]^2),$$

wobei die Konzentration der Tartrationen nach

$$[\text{tart}^{2-}] = [\text{H}_2\ \text{tart}]_{\text{tot}}/(1 + [\text{H}^+]/K_2 + [\text{H}^+]^2/K_1.K_2)$$

ermittelt werden kann.

Die Berechnung zeigt, daß im untersuchten Bereich bei den Tartratkomplexen aller zweiwertigen Metalle nur die β_1-Werte von Bedeutung sind, während beim dreiwertigen Eisen mit ansteigendem pH auch die β_2-Werte an Gewicht gewinnen. Eine Zusammenstellung der Korrekturgrößen ist für ausgewählte Metalle in den Tabellen 1 und 2 gegeben. Die erforderliche Größenordnung erreichen diese Korrekturglieder wegen der relativ geringen

TABELLE 1

Korrekturglieder zur Berechnung von Verteilungskoeffizienten für Zink und Cobalt in Anwesenheit von Tartrat (K_{S1} = 9,6 × 10^{-5} mol l^{-1}; K_{S2} = 2,9 × 10^{-5} mol l^{-1} [7]; $\beta_{Zn\,tart}$ = 1,23 × 10^3 l mol^{-1}; $\beta_{Zn\,tart_2^{2-}}$ = 9,55 × 10^4 l mol^{-1}; $\beta_{Co\,tart}$ = 1,047 × 10^2 l mol^{-1} [8])

pH	$[tart^{2-}]$ (mol l^{-1})	$\frac{\beta_{Zntart}}{[tart^{2-}]}$	$\frac{\beta_{Zntart_2^{2-}}}{[tart^{2-}]^2}$	$\frac{\beta_{Cotart}}{[tart^{2-}]}$
3,0	2,70 × 10^{-6}	0,003	—	0,0001
4,0	4,16 × 10^{-5}	0,051	0,0002	0,001
5,0	1,48 × 10^{-4}	0,182	0,002	0,007
6,0	1,93 × 10^{-4}	0,238	0,003	0,008
7,0	1,99 × 10^{-4}	0,245	0,004	0,009

Tartratkonzentration nur, wenn die β_1-Werte der Tartratkomplexe größer als 10^3 l mol^{-1} sind. Dies trifft für Kupfer und Zink zu, trotzdem wird aber die Extraktion durch Tartratzusatz praktisch nicht beeinflußt, da sie in pH-Bereichen abläuft, wo Komplexbildung mit Tartrat noch nicht einsetzt.

Eine Korrektur der gemessenen Verteilungskoeffizienten $D_{prakt.}$ macht sich somit nur beim Eisen(III) erforderlich.

Aus der Darstellung von log D gegen pH können in üblicher Weise (vgl. z.B. [9]) die Extraktionsparameter n, $pH_{1/2}$ und K_{ex} ermittelt werden.

ERGEBNISSE UND DISKUSSION

Die Extraktionskurven der hier untersuchten isomeren Thiopyrazolonderivate für eine Anzahl von Bunt- und Eisenmetallionen sind in der Abb. 1 dargestellt. Danach bieten sich beide Extraktionsmittel vor allem für die Extraktion aus relativ stark sauren Lösungen an. Die Extraktion bleibt über einen weiten pH-Bereich bis in das stark alkalische Gebiet quantitativ. Lediglich beim Kupfer ist bereits in schwach saurer Lösung ein Abfall der Extraktion zu beobachten, der wahrscheinlich auf Redoxreaktionen mit dem Extraktionsmittel zurückzuführen ist.

Die Reihenfolge der Extrahierbarkeiten von Übergangsmetallionen entspricht nicht exakt der Irving—Williams-Reihe der Komplexstabilitäten. Offenbar besitzen beide Extraktionsmittel eine gewisse Selektivität für Zink, so daß dieses Metall direkt nach dem Kupfer und noch vor Cobalt und Nickel extrahiert wird.

Ein interessantes Verhalten zeigt auch Eisen. Eisen(III) wird bereits bei sehr tiefem pH extrahiert. Die Darstellung von log D gegen pH (Abb. 2) ergibt jeweils eine Gerade der Neigung 2; im Extrakt liegt also nicht das erwartete Tris-Chelat vor, sondern wahrscheinlich ein Komplex der Zusammensetzung FeL_2-NO_3. Ein ähnliches Verhalten wurde auch für die Extraktion von Eisen(III) aus Perchloratlösung mit 1-Phenyl-3-methyl-4-benzoylpyrazolon-5-on gefunden [10]. Bei Verwendung von Eisen(II)-sulfat erfolgt

TABELLE 2

Korrekturglieder zur Berechnung von Verteilungskoeffizienten für Eisen(III) in Anwesenheit von Tartrat ($K_{S1} = 9{,}6 \times 10^{-4}$ mol l^{-1}; $K_{S2} = 2{,}9 \times 10^{-5}$ mol l^{-1} [7]; $\beta_1 = 3{,}09 \times 10^{6}$ l mol^{-1}; $\beta_2 = 7{,}244 \times 10^{11}$ l mol^{-1} [8])

pH	$[tart^{2-}]$ (mol l^{-1})	$\beta_1[tart^{2-}]$	$\beta_2[tart^{2-}]^2$	$\log(1+\beta_1[tart^{2-}]+\beta_2[tart^{2-}]^2)$	pH	$[tart^{2-}]$ (mol l^{-1})	$\beta_1[tart^{2-}]$	$\beta_2[tart^{2-}]^2$	$\log(1+\beta_1[tart^{2-}]+\beta_2[tart^{2-}]^2)$
1,5	$5{,}39 \times 10^{-9}$	0,02		0,008	2,3	$1{,}86 \times 10^{-7}$	0,57	0,03	0,20
1,6	$8{,}51 \times 10^{-9}$	0,03		0,01	2,4	$2{,}83 \times 10^{-7}$	0,87	0,06	0,29
1,7	$1{,}33 \times 10^{-8}$	0,04		0,02	2,5	$4{,}26 \times 10^{-7}$	1,32	0,13	0,39
1,8	$2{,}09 \times 10^{-8}$	0,06		0,03	2,6	$8{,}04 \times 10^{-7}$	2,48	0,47	0,60
1,9	$3{,}23 \times 10^{-8}$	0,10		0,04	2,7	$9{,}44 \times 10^{-7}$	2,92	0,81	0,67
2,0	$5{,}07 \times 10^{-8}$	0,16		0,06	2,8	$1{,}31 \times 10^{-6}$	4,24	1,36	0,82
2,1	$7{,}87 \times 10^{-8}$	0,24		0,09	2,9	$1{,}97 \times 10^{-6}$	6,10	2,81	0,99
2,2	$1{,}21 \times 10^{-7}$	0,37	0,01	0,14	3,0	$2{,}70 \times 10^{-6}$	9,35	5,28	1,94

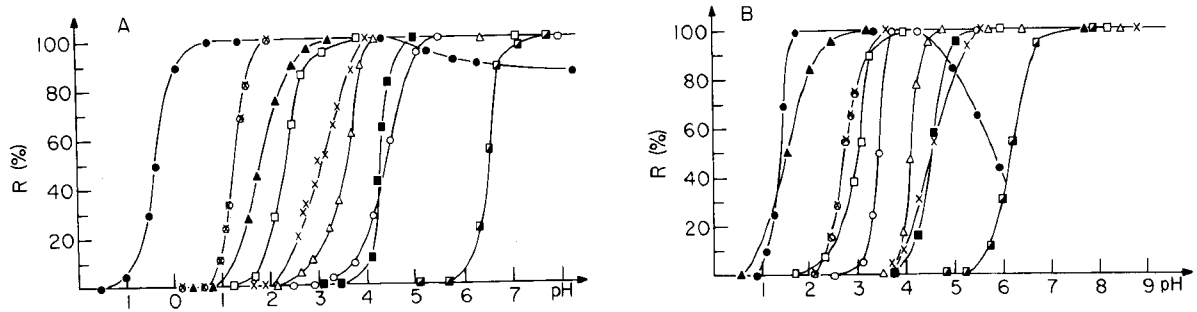

Abb. 1. Metallextraktion mit (A) 1-Phenyl-3-methyl-4-benzoylpyrazol-5-thion und (B) 1-Phenyl-3-methyl-4-thiobenzoylpyrazol-5-on: (●) Cu; (⊗) Pb; (▲) Fe(III); (□) Zn; (×) Cd; (△) Fe(II); (■) Ni; (○) Co; (▣) Mn.

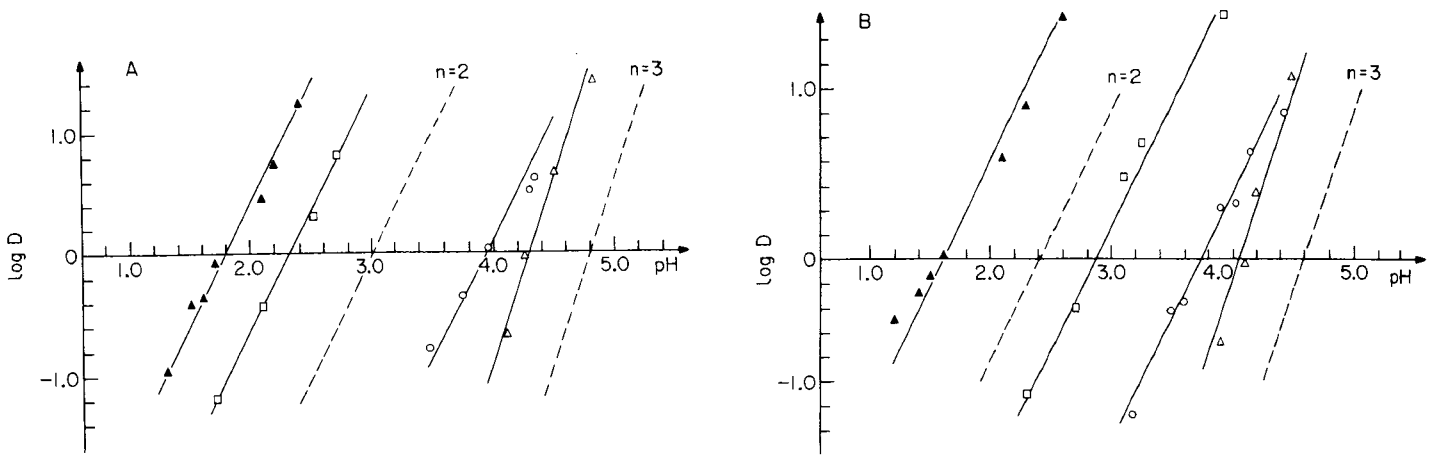

Abb. 2. Log D/pH-Diagramm für die Extraktion von (▲) Fe(III), (△) Fe(II), (○) Co(II) und (□) Zn(II) mit (A) 1-Phenyl-3-methyl-4-benzoylpyrazol-5-thion und (B) 1-Phenyl-3-methyl-4-thiobenzoylpyrazol-5-on.

TABELLE 3

Kenngrößen für die Metallextraktion mit Pyrazolonderivaten

	1-Phenyl-3-methyl-4-benzoylpyrazol-5-thion			1-Phenyl-3-methyl-4-thiobenzoylpyrazol-5-on			1-Phenyl-3-methyl-4-benzoylpyrazol-5-on
	$n_{exp.}$	$pH_{1/2}$	$\log K_{ex}$	$n_{exp.}$	$pH_{1/2}$	$\log K_{ex}$	$\log K_{ex}$
Cu	2,0	−0,3	+5,4	1,8	1,4	+2,0	+1,44 [9]
Pb	2,0	1,4	+2,0	2,0	3,0	+1,2	−3,7 [10]
			+1,2 [8]			+2,0 [8]	
Fe(III)	2,0	1,8	+1,2	3,0	1,6	+1,6	
Zn	2,0	2,35	+0,1	2,0	3,0	−1,2	−3,07 [11]
Cd	2,0	3,1	−1,3	1,9	4,5	−4,2	
Ni	2,1	3,5	−2,1	2,1	4,5	−4,2	−4,22 [12]
Co	2,0	4,4	−4,0	1,9	3,6	−2,4	
Fe(II)	3,0	4,30	−5,7	3,0	4,0	−4,8	−6,49 [13]
Mn	2,0	6,5	−8,2	2,0	6,2	−7,6	−7,25 [14]

die Extraktion erst oberhalb pH 3, es entsteht aber in diesem Falle — wie das log D/pH-Diagramm ausweist (Abb. 2) — ein Tris-Chelat FeL_3 unter gleichzeitiger Oxydation des Eisen-Zentralatoms. Dagegen wird Cobalt im untersuchten Bereich als Cobalt(II)-Chelat extrahiert. Die Kenngrößen der Extraktion sind in Tab. 3 zusammengestellt.

Im Vergleich mit dem zugrundeliegenden Acylpyrazolon weisen die beiden Monothio—pyrazolone deutlich größere Extraktionskonstanten (vgl. Tab. 3) auf, die wahrscheinlich auf eine höhere Komplexstabilität zurückzuführen sind. Weiterhin wird das Extraktionsvermögen wesentlich durch die Position des Schwefels im Molekül des Extraktionsmittels bestimmt. Dabei zeigt das 4-Benzoylpyrazol-5-thion (I) in allen Fällen die günstigeren $pH_{1/2}$- und K_{ex}-Werte. Die Ursache für das unterschiedliche Verhalten der beiden isomeren Extraktionsmittel ist in ihrem Verteilungsverhältnis selbst zu suchen. Die pH-Abhängigkeit der Verteilungskoeffizienten ist in Abb. 3 dargestellt. Daraus ergeben sich die Werte von $\log K_v/K_s$ für das 4-Benzoylpyrazol-5-thion (I) zu 8,56 ± 0,05 (Punkt A) und für das 4-Thiobenzoylpyrazol-5-on (II) zu 9,82 ± 0,06 (Punkt B). Da die Löslichkeiten beider Substanzen sehr ähnlich sind, üben letztlich die Säurestärken den entscheidenden Einfluß auf das Extraktionsvermögen aus.

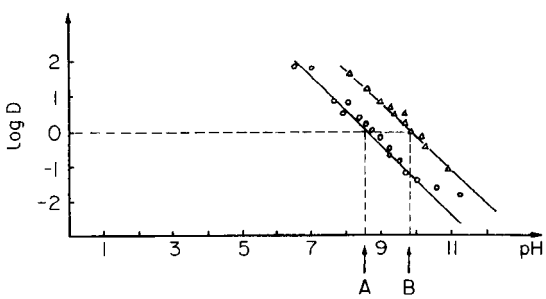

Abb. 3. pH-Abhängigkeit für die Verteilung der Extraktionsmittel. (○) 1-Phenyl-3-methyl-4-benzoylpyrazol-5-thion; (△) 1-Phenyl-3-methyl-4-thiobenzoylpyrazol-5-on.

LITERATUR

1 G. Klose, E. Ludwig und E. Uhlemann, Org. Magn. Reson., 10 (1977) 151.
2 Yu. A. Zolotov und N. M. Kusmin, Ekstrakzija Metallov Azilpirasolonami, Nauka, Moskva, 1977.
3 G. N. Rao und J. S. Thakur, J. Sci. Ind. Res., 34 (1975) 110.
4 F. Kurzer und A. Lawson, Org. Synth., 42 (1962) 100.
5 G. Wilke, W. Bechmann und E. Uhlemann, Z. Anorg. Allg. Chem., 428 (1977) 277.
6 E. B. Sandell, J. Am. Chem. Soc., 72 (1950) 4660.
7 K. Rauscher, J. Voigt, I. Wilke und K.-Th.Wilke, Chemische Tabellen und Rechentafeln für die analytische Praxis, VEB Deutscher Verlag für Grundstoffindustrie, Leipzig, 1968.
8 L. G. Sillén und G. Schwarzenbach, Stability constants of Metal-ion Complexes, The Chemical Society, London, 1970.
9 E. Uhlemann, W. Bechmann und E. Ludwig, Anal. Chim. Acta, 100 (1978) 635.
10 D. S. Narajan, E. K. Ivanova und V. K. Peshkova, Vestn. Univ. Moskau Ser. Khim., 1972, p. 707.
11 V. G. Lambrev und V. S. Vlasov, Zh. Anal. Khim., 25 (1970) 1638.
12 D. Dyrssen, Acta Chem. Scand., 10 (1956) 353.
13 B. S. Jensen, Acta Chem. Scand., 13 (1959) 1890.
14 A. N. Alybina, A. E. Dorfman, E. K. Ivanova und V. M. Peshkova, Zh. Neorg. Khim., 16 (1971) 446.
15 S. N. Joshi, E. K. Ivanova und V. M. Peshkova, Indian J. Chem., 11 (1973) 78.
16 Yu. A. Zolotov und L. G. Gavrilova, Zh. Anal. Khim., 25 (1970) 813; Radiokhimiya, 11 (1969) 389.

Analytica Chimica Acta, 116 (1980) 161—168

2,2'-DIPYRIDYL-2-QUINOLYLHYDRAZONE AS A REAGENT FOR THE SPECTROPHOTOMETRIC DETERMINATION OF METALS
The Extractive Spectrophotometric Determination of Palladium(II)

MAKOTO OTOMO

Department of Synthetic Chemistry, Nagoya Institute of Technology, Showa-ku, Nagoya 466 (Japan)

(Received 22nd October 1979)

SUMMARY

2,2'-Dipyridyl-2-quinolylhydrazone, DPQH, is proposed as a spectrophotometric reagent for certain metal ions. The composition, extractability and spectrophotometric characteristics of the complexes formed with 7 metal ions are reported. DPQH appears to be promising especially for palladium(II) and cobalt(II) in selectivity and for zinc(II) and cadmium(II) in sensitivity. A detailed study has been made for the extractive spectrophotometric determination of palladium(II) in the presence of chloride ions.

Numerous studies have been reported of the extraction into immiscible organic solvents of metals as their complexes with tridentate heterocyclic hydrazone ligands containing the functionality —N=C—C=N—NH—C=N—. The extraction behavior of their metal complexes has been interpreted in terms of the formation of an uncharged bis complex for divalent metal ions with coordination number 6, and the formation of a neutral ternary complex between a positively charged mono complex and a suitable anion, for divalent metal ions with coordination number 4 [1—5]. Considerable attention has also been directed in recent years to the preparation of new, nitrogen-containing heterocyclic hydrazones as suitable reagents in spectrophotometric or fluorimetric determinations of metals; the extent of the contribution of the particular heterocyclic systems attached to either the aldehyde (or ketone) or the hydrazine groups to the overall characteristics of the metal chelates formed has been discussed [5—10].

The purpose of this paper is to introduce a new ligand, 2,2'-dipyridyl-2-quinolylhydrazone (I, abbreviated as DPQH), as a useful and extremely sensitive colorimetric reagent for certain metal ions. The acidity constants of the ligand and the spectrophotometric characteristics of the palladium(II), iron(II), cobalt(III), zinc(II), mercury(II), copper(II) and cadmium(II) complexes are described. The palladium(II) complex is deprotonated in moderately acidic solutions. Thus, a very selective method for determining this cation with a simple extraction from hydrochloric acid solutions can be established.

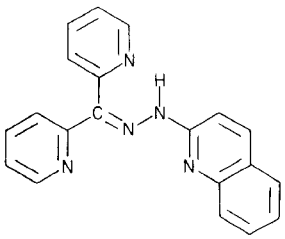

(I)

EXPERIMENTAL

Apparatus

A Nippon-Bunko UVIDEC-1 digital spectrophotometer and a Union Giken SM-401 high sensitivity recording spectrophotometer were used with matched 1.00-cm quartz cells. A Toa Dempa HM-6A pH meter was used with a combination electrode. In determinations of the acidity constants of the ligand in aqueous 20 (v/v%) ethanol solution (μ = 0.1), the pH readings were not corrected.

Reagents

DPQH. The ligand was prepared by interaction of di-2-pyridylketone (Aldrich Chemical Co.) and 2-hydrazinoquinoline (freshly synthesized from hydrazine and 2-chloroquinoline) in stoichiometric amounts and was recrystallized to constant melting point (155—156°C) from ligroin. (Analytical results: found 21.54% N; calculated for $C_{20}H_{15}N_5$ (m. w. 325.4), 21.52% N.) Solutions of 2.5×10^{-4} M (for palladium) and 1×10^{-3} M (for iron, zinc, mercury, copper and cadmium) DPQH in benzene and 1×10^{-3} M DPQH in ethanol (for cobalt) were prepared.

Solutions of metal ions, approximately 0.01 M, were prepared from their salts or pure metals (zinc, copper and cadmium) and standardized by conventional methods. Working solutions were prepared by dilution. Iron(II) solutions were freshly prepared, made acidic with sulfuric acid, and used on the same day.

Buffers. The following mixtures were used. Hydrochloric acid—sodium acetate (for iron), acetic acid—sodium acetate (for cobalt), phosphoric acid—disodium hydrogenphosphate (for mercury), disodium hydrogenphosphate—sodium carbonate (or sodium hydroxide) (for mercury and copper), and disodium hydrogenphosphate—ammonia—sodium hydroxide (for zinc and cadmium).

All other chemicals were of reagent-grade quality.

General procedure

With the exception of cobalt(II), the aqueous solution (10 or 20 ml)

containing a known quantity of metal buffered to the required pH was shaken for 15 min with 10 ml of DPQH in benzene in a 50-ml separatory funnel at 25°C. Under the experimental conditions, equilibrium was reached within 10 min but the rate appeared to be pH-dependent; for copper(II) and cadmium(II), pyridine and ammonia respectively were added to improve the rate. The absorbance of the benzene extract was measured at the wavelength for maximum absorbance.

For cobalt(II), the aqueous solution containing a known amount of the metal (3 ml) and 5 ml of acetate buffer was equilibrated with 5 ml of DPQH in ethanol in a 25-ml volumetric flask for 30 min. The solution was then acidified with sulfuric acid and diluted to the mark with water. The absorbance of the solution was measured at 528 nm against the reagent blank.

RESULTS AND DISCUSSION

The reagent, DPQH, which is believed to exist as the *anti* isomer, is a light yellow crystalline material soluble in most organic solvents. It is nearly insoluble in water but quite soluble in dilute acidic solution.

As is apparent from its structure(I), DPQH is tetrabasic, having also a dissociable imino-hydrogen in the molecule. Thus, the reagent exists in solution in any of the following forms depending upon the pH:

$$\overset{K_5}{\underset{}{}} \quad \overset{K_4}{\underset{}{}} \quad \overset{K_3}{\underset{}{}} \quad \overset{K_2}{\underset{}{}} \quad \overset{K_1}{\underset{}{}}$$

$$H_5L^{4+} \rightleftharpoons H_4L^{3+} \rightleftharpoons H_3L^{2+} \rightleftharpoons H_2L^{+} \rightleftharpoons HL \rightleftharpoons L^{-}$$

Spectrophotometrically, the acid—base equilibria can be followed only for K_3 and K_2 because they occur at reasonable pH; the first deprotonation (from C=N nitrogen) and the second deprotonation (from one of the two pyridine-nitrogens) of the cationic species (K_5 and K_4) take place competitively in fairly acidic solution below pH 1, while the final deprotonation of the uncharged reagent molecule (K_1) does not occur below pH 13 and is incomplete even in 2 M sodium hydroxide solution. The latter indicates that DPQH is a very weak acid (the pK_1 value of pyridine-2-aldehyde-2-quinolylhydrazone determined potentiometrically in 1:1 dioxane—water mixture was found to be 12.19 [11]), presumably because of the intramolecular hydrogen bonding between the imino-hydrogen and one of the two pyridine-nitrogens. Some of the results obtained are shown in Fig. 1; the measurements were performed in aqueous 20 (v/v%) ethanol to maintain a clear solution over the entire pH range. Absorbance measurements obtained at 400 and 390 nm lead to values of $pK_3 = 2.48$ (pyridine) and $pK_2 = 5.57$ (quinoline), respectively.

Metal complexes

The spectrophotometric characteristics of the metal complexes extracted into benzene are given in Table 1 along with those of the cobalt(III) complex

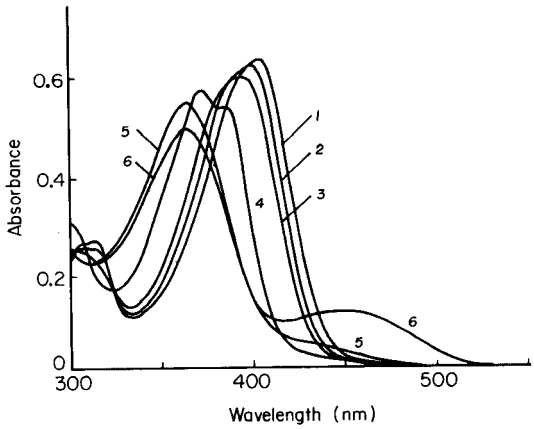

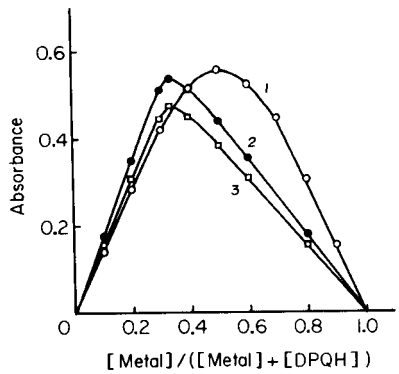

Fig. 1. Absorption spectra of 2.0 × 10^{-5} M DPQH in aqueous 20 (v/v%) ethanol at different pH values: (1) 2.9 M HCl; (2) 0.8 M HCl; (3) pH 1.10; (4) pH 4.22; (5) pH 7.19; (6) 0.64 M NaOH.

Fig. 2. Continuous variations plots for the palladium(II), cobalt(II) and cadmium(II) systems. (1) Pd(II)—DPQH: [Pd(II)] + [DPQH] = 3.0 × 10^{-5} M; 0.61 M HCl. (2) Cd(II)—DPQH: [Cd(II)] + [DPQH] = 1.95 × 10^{-5} M; pH, 13.0. (3) Co(II)—DPQH: [Co(II)] + [DPQH] = 3.6 × 10^{-5} M; initial pH, 5.0; final acidity, 2.5 M H_2SO_4.

TABLE 1

Spectrophotometric characteristics of metal—DPQH complexes

Metal ion	Optimal acidity of aqueous phase	λmax (nm)	ϵmax (× 10^4 l mol^{-1} cm^{-1})
Pd(II)	0.2—0.9 M (HCl)	604	2.21
		570	1.75
Fe(II)	pH 3.4—4.5[a]	645	1.30
		506	3.11
		475	3.01
Co(III)	2.5 M (H_2SO_4)[b]	528	4.18
Zn(II)	pH 7.6—9.1	510	8.21
Hg(II)	pH 7.6—11.6	505	6.37
Cu(II)	pH 8.0—12.7	505	5.04
Cd(II)	pH 12.5—13.5	511	8.78

[a]5 ml of 0.5% ascorbic acid was added. [b]Initial pH 4.0–6.0.

in sulfuric acid solution. The extractability of the metal ions would reflect the acidity of the imino-hydrogen in the ligand molecule complexed with these metal ions. The order of decreasing extractability iron(II) > zinc(II) > cadmium(II) is compatible with the observation of Green et al. [12] for the corresponding metal complexes of pyridine-2-aldehyde-2-pyridylhydrazone.

Continuous variations and mole ratio studies showed that the molar ratio of metal:ligand in these complexes was 1:2 except for the palladium(II)

complex, in which it was 1:1. Typical results for the palladium(II), cobalt(III) and cadmium(II) complexes are shown in Fig. 2.

The palladium(II) complex can be extracted from a highly acidic solution, provided that there is another ligand present which can occupy the fourth coordination position and produce an uncharged complex. The complex thus extracted has the characteristic absorption spectrum shown in Fig. 3. The above observations imply high selectivity of the reagent for the extractive analysis of palladium(II). In the presence of chloride ions, the plot of log D, the distribution ratio, against log $[Cl^-]$, the chloride ion concentration of the aqueous phase (0.3 M sulfuric acid solution), is initially linear with a slope of unity (Fig. 4); increase in the chloride ion concentration to more than 0.8 M leads to a constant value for D, showing that the complex extracted is PdLCl. Hydrochloric acid was therefore used in the palladium determination.

In aqueous solution, iron(II) forms complexes with maximum absorbance at 470 and 555 nm below pH 3 and at 470 and 595 nm above pH 4. But the complex extracted into benzene always exhibits three absorption maxima at 473, 506 and 645 nm, regardless of the acidity of the aqueous phase. Again, the absorption spectrum is characteristic for this ion, suggesting that iron(II) can be determined without interference from other metals by measuring the absorbance of the complex at 645 nm.

Cobalt(II) ion reacts with DPQH above pH 3 to form a bis cationic water-soluble complex. The metal ion in the complex has been shown to be in the trivalent state [3, 11, 12]. This complex is very stable and on addition of perchloric or sulfuric acid a bathochromic shift associated with a hyperchromic effect takes place from 507 to 528 nm. The value given in Table 1 for the molar absorptivity in 2.5 M sulfuric acid increases slightly with an

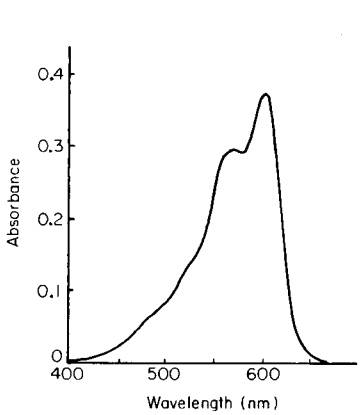

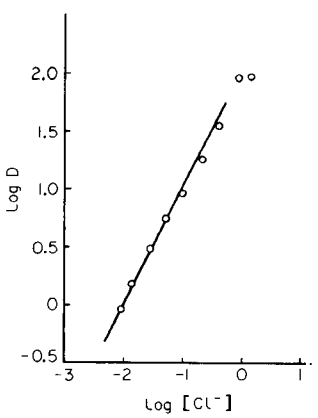

Fig. 3. Absorption spectrum of palladium(II)—DPQH complex in benzene. Pd(II), 1.7×10^{-5} M; HCl, 0.61 M; DPQH in benzene, 2.5×10^{-4} M.

Fig. 4. Relationship between log D and log $[Cl^-]$ for the palladium(II)—DPQH—chloride ion system. Pd(II), 2.0×10^{-5} M; H_2SO_4, 0.3 M; DPQH in benzene, 2.5×10^{-4} M.

increase in the acid concentration (about 2% in 6 M sulfuric acid). As the other metal complexes are destroyed by the addition of acid, there is no doubt that this will permit the establishment of a selective spectrophotometric determination of cobalt.

In the presence of small amounts of perchlorate or iodide or sufficient amounts of nitrate, the cobalt(III) complex can be extracted with chloroform. In these cases, the plot of log D against log [anion] is linear with a slope close to unity. The results indicate that doubly-deprotonated ion-pair complexes, $Co(III)L_2X$ (where X denotes a monovalent anion), are extracted; this is consistent with the observations of Chiswell et al. [13] for the cobalt(III) complex of pyridine-2-aldehyde-2-(4-methyl)quinolylhydrazone.

Zinc(II), mercury(II), copper(II) and cadmium(II) ions form complexes exhibiting wavelengths of maximum absorption at 505—511 nm and high molar absorptivities comparable with those of the dithizone complexes. The rate of extraction of these metal ions except for mercury(II) depends not only on the pH of the aqueous phase but also on the excess of the ligand and on the auxiliary complexing agents present. Under the experimental conditions of pH and the ligand concentration used, addition of 1.6×10^{-2} M pyridine for copper(II), 0.1 M ammonia for zinc(II) and 2 M ammonia for cadmium(II) is satisfactory for quantitative extraction within 10—15 min. All the four metal complexes are readily adaptable for the determination of the respective metal ions. It was found that, for cadmium(II), DPQH is much superior in sensitivity to 2,2'-dipyridyl-2-pyridylhydrazone reported by Alexaki-Tzivanidou et al. [14].

Determination of palladium(II)

The palladium(II) complex is readily extracted into various organic solvents such as aromatic hydrocarbons, halogenated hydrocarbons, acetate esters, aliphatic alcohols, methyl isobutyl ketone and nitrobenzene. Of these, benzene proved to give the highest absorbance. The complex is completely extracted from 0.2—0.9 M hydrochloric acid solution with one 10-ml portion of DPQH in benzene over the concentration range studied (see below). The color intensity of the complex was constant over the measured 20-h period. There is no interference from excess of ligand in the wavelength region above 450 nm.

Effects of experimental conditions. The absorbance of the organic phase, measured as a function of the hydrochloric acid concentration of the aqueous phase, was maximal and constant over the range 0.2—0.9 M. A mole ratio study demonstrated that only a three-fold molar excess of the ligand in the organic phase is necessary for maximal and reproducible absorbance. Addition of more reagent did not interfere with the formation and extraction of the complex.

Adherence to Beer's law. The analytical species of interest obeys Beer's law over the range 2×10^{-6}—4×10^{-5} M palladium(II) in the organic phase.

TABLE 2

Molar absorptivities of some palladium(II) complexes with nitrogen-containing heterocyclic hydrazones

Hydrazone (R_1—CH=N—NH—R_2)		Solvent	λmax (nm)	ϵmax ($\times 10^4$ l mol^{-1} cm^{-1})	Ref.
R_1	R_2				
2-Pyridyl	2-Pyridyl	*o*-Dichlorobenzene	562	1.65	[6]
2-Pyridyl	2-Quinolyl	Chloroform	594	1.15	[11]
2-Quinolyl	2-Pyridyl	Benzene	615	1.6	[6]
6-Phenanthridyl	2-Pyridyl	Benzene	635	2.0	[6]
6-Phenanthridyl	2-Quinolyl	Chloroform	640	1.2	[6]
2-Benzothiazolyl	2-Quinolyl	Benzene	647	2.14	[5]
DPQH		Benzene	604	2.21	—

TABLE 3

Effect of diverse ions on the determination of 22.3 μg of palladium(II)

Tolerance limit ([Iron]/[Pd(II)])	Ion
$\geqslant$10,000	Br^-, $C_2O_4^{2-}$, citrate, NO_3^-, PO_4^{3-}, tartrate
$\geqslant$100	Al, As(V), Cd, Co, Cr(III), Cu, Fe(II, III), Mn, Pb, Pt(IV), Rh, Sc, V(V), Zn, ClO_4†, NO_2^-
$\leqslant$100	Mo(VI)[a], Ru(III), Ti
$\leqslant$50	Cr(VI)[b], Hg(II), Os(VIII)
$\leqslant$15	Au(III)[c], Ir(III)[c], SCN^-
0—1	EDTA, I^-

[a]4 ml of tartrate was added. [b]4 ml of 0.01 M Fe(III) was added. [c]Chloroform was used as the solvent and the extract was washed with 10 ml of 0.1 M sodium acetate.

The spectrophotometric sensitivity for log (I_0/I) = 0.001 is 4.8×10^{-3} μg Pd cm^{-2}.

Comparison of sensitivity. Table 2 presents a comparison of the spectral properties of the palladium(II) complexes with several tridentate heterocyclic hydrazones described to date. The present ligand, DPQH, is the most sensitive reagent for palladium(II).

Effect of diverse ions. The possible interference of various ions was examined by introducing them into a solution containing 22.3 μg of palladium(II). The tolerance limit of an ion was fixed as the maximum amount causing an error no greater than 2% in the absorbance of the extract solution. The results are tabulated in Table 3. Of the platinum group metals tested, rhodium(III), ruthenium(III) and platinum(IV) up to about 100-fold molar ratio to palladium and osmium(VIII) up to a 50-fold molar amount

do not interfere with the determination. More than 2—3-fold amounts of gold(III) and iridium(III) interfere, forming yellow precipitates which are only slightly soluble in benzene. However, these metal ions can be tolerated up to about 15-fold molar amounts by using chloroform as the solvent instead of benzene, washing the chloroform extract with a solution of sodium acetate, and then measuring the absorbance of the organic phase at 603 nm. The molar absorptivity of the complex in chloroform is 2.01×10^4 l mol^{-1} cm^{-1} at 603 nm. Iodide and EDTA interfere severely by forming stable complexes with palladium(II) and must be absent.

This work was supported in part by a Grant-in-Aid for Scientific Research from the Ministry of Education, Science and Culture (Japan).

REFERENCES

1 F. Lions and K. V. Martin, J. Am. Chem. Soc., 80 (1958) 3858.
2 J. F. Geldard and F. Lions, J. Am. Chem. Soc., 84 (1962) 2262.
3 J. F. Geldard and F. Lions, Inorg. Chem., 2 (1963) 270.
4 M. A. Quddus and C. F. Bell, Anal. Chim. Acta, 42 (1968) 503.
5 M. Otomo and K. Kodama, Bunseki Kagaku, 26 (1977) 455.
6 V. Zátka, J. Abraham, J. Holzbecher and D. E. Ryan, Anal. Chim. Acta, 54 (1971) 65.
7 D. E. Ryan, F. Snape and M. Winpe, Anal. Chim. Acta, 58 (1972) 101.
8 G. S. Vasilikiotis, Th. Kouimtzis, C. Aposolopoulou and A. Voulgaropoulos, Anal. Chim. Acta, 70 (1974) 319.
9 M. Otomo and H. Noda, Microchem. J., 23 (1978) 297.
10 A. A. Schilt, P. C. Quinn and C. L. Johnson, Talanta, 26 (1979) 373.
11 M. L. Heit and D. E. Ryan, Anal. Chim. Acta, 32 (1965) 448.
12 R. W. Green, P. S. Hallman and F. Lions, Inorg. Chem., 3 (1964) 376.
13 B. Chiswell, J. F. Geldard, A. T. Phillip and F. Lions, Inorg. Chem., 3 (1964) 1272.
14 H. Alexaki-Tzivanidou, G. Kounenis and B. Elezoglou, Microchem. J., 23 (1978) 329.

Analytica Chimica Acta, 116 (1980) 169—173

Short Communication

TISSUE- AND BACTERIA-LOADED TUBULAR REACTORS FOR THE AUTOMATIC DETERMINATION OF GLUTAMINE

MARCO MASCINI** and G. A. RECHNITZ*

Department of Chemistry, University of Delaware, Newark, Delaware 19711 (U.S.A.)

(Received 19th November 1979)

Summary. Porcine kidney tissue or *Sarcina Flava* bacterial cells are used as biocatalysts for the conversion of glutamine to ammonia, which is monitored with a gas-sensing membrane electrode in an automated flow system. Conversion to ammonia is 100% for $\leqslant 10^{-4}$ M glutamine.

Immobilization of whole cells has recently been proposed [1] for analytical situations where immobilized purified enzymes would have disadvantages owing to inherent instability, intracellular attachment, or the need for cofactors and activators. At the same time, the use of immobilized enzymes in the form of packed-bed reactors, membrane reactors or open tubular reactors in automated analysis has been clearly established especially when the optimum pH of the enzyme reaction is not the same as that for the indicator system [2—5]. Such a situation pertains when immobilized enzymes are coupled to ammonia gas-sensing membrane electrodes but also if such electrodes are used in conjunction with tissue slices [6] or bacterial cells [7] because of the limited detection range of the ammonia electrode at neutral pH. Such limitations can be overcome in flow systems where the biocatalytic and indicator steps are carried out sequentially and at their respective pH optima. In this communication, some preliminary analytical features of the use of open tubular reactors containing porcine kidney slices or intact bacterial cells are demonstrated for the automatic flow analysis of glutamine with the ammonia gas-sensing electrode as detector. Such reactors are easy to assemble and are of negligible cost.

Experimental

Materials and equipment. A flow-through version of the Orion Model 95-10 ammonia electrode was used. Potential measurements were made with a Corning Model 12 Research pH meter and recorded with a Heath-Schlumberger Model SR-204 strip chart recorder. Bacterial cells were collected and washed with the aid of a high-speed centrifuge (Precision Scientific) while the sampler, dialyzer and peristaltic pump were from the Technicon Type II AutoAnalyzer.

**On leave from the University of Rome, Italy.

Pure strains of *Sarcina Flava* bacteria were obtained from the American Type Culture Collection and grown under their specified conditions. Tissue slices from fresh porcine kidney were prepared with a refrigerated microtome kept at dry ice temperatures. All potentiometric measurements were made at 30°C.

Preparation of the bio-catalytic reactors. Porcine kidney tissue slices (0.1 mm thick) were prepared with the aid of the microtome and were placed on nylon support nets (30 × 30 mm). To form the reactor, the tissue slices on the nylon support were rolled around a 3-mm diameter tygon rod and inserted into a glass tube (5 mm i.d., ca. 10 cm long). This arrangement reduced the dead volume to 0.5 ml while permitting solution flow. The tubular reactors were washed overnight with phosphate buffer (0.1 M, pH 7.8) containing 0.02% sodium azide preservative and were stored at room temperature. The flow rate was 0.6 ml min^{-1}.

Bacterial reactors were prepared by placing a slurry of freshly washed and centrifuged bacteria (0.5 ml) in the lower channel of a Technicon dialysis unit (No. A177-B010-78) with the aid of a syringe; the solutions for analysis pass along the upper channel. Channel length was ca. 25 cm with a volume of 0.3 ml. Bacterial reactors were kept at room temperature in contact with pH 7.5 Tris buffer. The flow system is shown in Fig. 1. A flow rate of 0.23 ml min^{-1} gave a reaction time of 1.5 min.

Results and discussion

The porcine kidney reactors were evaluated for several experimental variables. Figure 2A shows glutamine calibration curves obtained with three different tubular reactors (all 10 days old). Comparison of these curves with ammonia calibration curves obtained from the same system under the same conditions indicates nearly 100% conversion of glutamine in the 10^{-5} to 10^{-4} M range with a decline to 30% and 15% for 10^{-3} and 10^{-2} M glutamine, respectively. As a result, the glutamine calibration curve is near Nernstian at the lower concentrations ($\leqslant 10^{-4}$ M) but is approximately 35 mV per

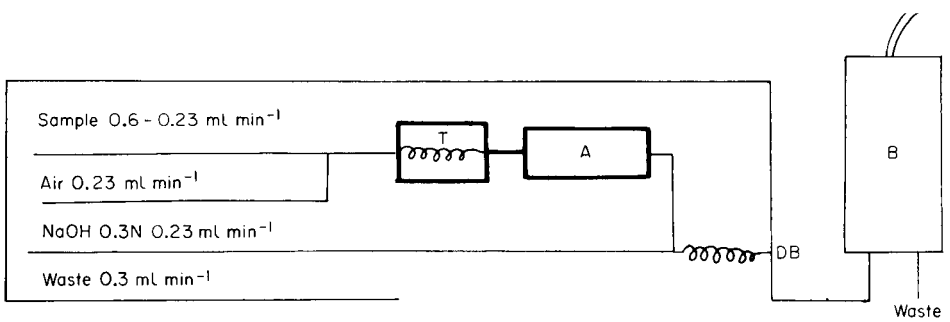

Fig. 1. The flow assembly. (A) Reactor; (B) NH_3 electrode with flow cap; (DB) debubbler; (T) thermostat (at 30°C).

decade at higher concentrations. Considering the small quantity of kidney tissue and the limited residence time of the sample in the tubular reactor, the extent of conversion is acceptable and indicates the high biocatalytic activity of the porcine kidney. It should also be noted that the similarity of the calibration curves from the three reactors is remarkably good, especially in view of the fact that no special care was taken in preparation of the tissue slices.

Figure 2B shows the effect of adding further reactors in series; a moderate increase in glutamine conversion efficiency is obtained. For example, 5×10^{-4} M glutamine is converted to the extent of 44% by a single reactor, 56% by 3 reactors and 72% by 5 reactors. Similarly, 10^{-3} M glutamine is 35%, 41%, and 60% converted by one, three and five reactors, respectively. In these experiments, sufficient time was allowed (10 min) for the final potentials to reach a stable value.

It can be concluded that the biocatalytic activity in the reactors is fairly constant but that there may be an equilibrium step limiting conversion at high glutamine concentrations; fortunately, the analytically important levels fall in the complete conversion range. To evaluate the biocatalytic activity of the reactors further, the integrated form of the Michaelis–Menten equation was employed for an open tube enzyme reactor: $FS - K\ln(1 - F) = K_T L Q^{-1}$, where F represents the fractional conversion of substrate to product, S is the initial substrate concentration (mM), K is the substrate concentration required to produce half the maximum reaction velocity ($\times$ mM), K_T is the tube specific activity (μmol min^{-1} cm^{-1}), L is the length of the tube (cm), and Q is the flow rate of substrate through the tube (cm^3 min^{-1}). The equation was tested for several tissue reactors. For activities in the 3–5 μmol min^{-1} cm^{-1} range, a good fit to the equation was found for

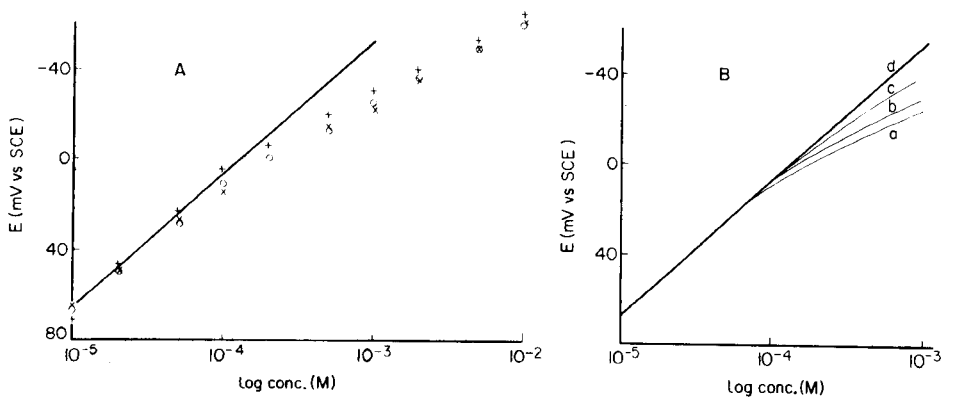

Fig. 2. Glutamine calibration curves. (A) For three different kidney tissue reactors, compared with an ammonia calibration (continuous line). (B) For an increasing number of reactors in sequence: (a) 1 reactor, (b) 3 reactors, (c) 5 reactors, (d) ammonia calibration.

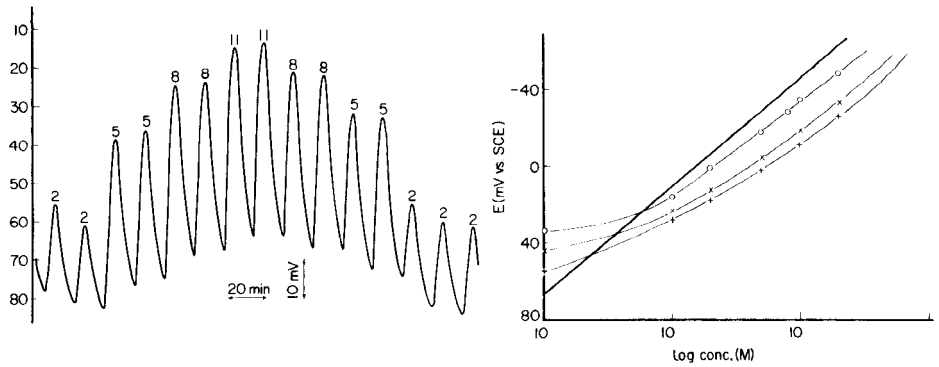

Fig. 3. Automated glutamine analyses with kidney tissue reactors, peak numbers relate to 2—11 X 10^{-5} M glutamine concentrations.

Fig. 4. Glutamine calibration curves for bacterial reactors (pH 7.5, Tris buffer). Age of reactor: (○) 3 days, (X) 10 days, (+) 15 days. Continuous heavy line is the ammonia calibration.

10^{-3}—10^{-4} M glutamine concentrations even though a pure enzyme system is not a very appropriate model for a reactor containing whole tissue slices.

The responses for a series of analyses are given in Fig. 3. Although the sampling time was reduced to 5 min (10-min wash), these data yielded a straight line calibration graph with a 59 mV/decade slope and 0.98 correlation coefficient. The sampling rate will be limited by retention effects in the column reactor; no attempts have yet been made to optimize this parameter.

It is especially noteworthy that the biocatalytic activity of the kidney tissue reactors did not change over the 20-day test period, even though the reactors were kept at room temperature throughout. This time stability represents one of the most important features of the tissue slice approach and suggests that attractive analytical savings in cost and time might be attainable.

The use of the *Sarcina Flava* bacterial cells in reactors for glutamine proved to be somewhat less attractive than that of kidney tissue slices. Some typical data obtained with the bacterial cells are shown in Fig. 4. The conversion efficiency of glutamine to ammonia was somewhat better for a new bacterial reactor, e.g. 80% at 10^{-4} M and 60% at 10^{-3} M, than for the tissue slice reactor, but these efficiencies declined to 50% and 25%, respectively, after 15 days at room temperature. It was also more difficult to reduce the background ammonia blank in the bacterial system, probably because of the high ammonia levels in the nutrient growth medium. Thus, for glutamine, the bacterial cell reactor offers some short-term advantages in terms of conversion efficiencies but the tissue-based reactors are superior for long-term operation.

This research was supported by NIH Grant GM-25312. One of us (M.M.) acknowledges the assistance of a NATO Senior Fellowship.

REFERENCES

1 I. Chibata, Pure Appl. Chem., 50(7) (1978) 667.
2 D. J. Inman and W. E. Hornby, Biochem. J., 129 (1973) 255.
3 J. Campbell, W. E. Hornby and D. L. Morris, Biochim. Biophys. Acta, 384 (1975) 307.
4 J. Campbell, A. S. Chawla and T. M. S. Chang, Anal. Biochem., 83 (1977) 330.
5 K. Matsumoto, H. Seijo, T. Watanabe, I. Karube, I. Satoh and S. Suzuki, Anal. Chim. Acta, 105 (1979) 429.
6 G. A. Rechnitz, M. A. Arnold and M. E. Meyerhoff, Nature, 278 (1979) 466.
7 G. A. Rechnitz, T. L. Riechel, R. K. Kobos and M. E. Meyerhoff, Science, 199 (1978) 440.

Analytica Chimica Acta, 116 (1980) 175—179

Short Communication

TITRATION OF MICROGRAM AMOUNTS OF SULPHIDE WITH A SULPHIDE-SELECTIVE ELECTRODE

T. M. FLORENCE* and YVONNE J. FARRAR

Analytical Chemistry Section, Australian Atomic Energy Commission Research Establishment, Lucas Heights, NSW, 2232 (Australia)

(Received 20th November 1979)

Summary. As little as 2 μg of sulphide can be titrated with lead nitrate solution and a sulphide-selective electrode for end-point detection. In the range 20—150 μg S the relative standard deviation is 2%. The titration is non-stoichiometric, some sulphide ion apparently being adsorbed on the lead sulphide precipitate. The deviation from stoichiometry depends on the titration medium, with 1 M NaOH—1.5 M hydrazine and NaOH—salicylate—ascorbate mixtures providing the most accurate results.

Titration of sulphide ion with a sulphide-selective electrode for end-point detection has been described for lead(II) [1—3], silver(I) [4, 5], and cadmium(II) [6] titrants. The titration is usually done in alkaline media to avoid loss of sulphur as H_2S and, with small amounts of sulphide, an anti-oxidant such as ascorbic acid or hydrazine must be added to prevent atmospheric oxidation. Hseu and Rechnitz [4] found that titration of 10^{-3}—10^{-2} M sulphide with 0.1 M silver nitrate gave results within 0.5% of the theoretical end-point for the formation of Ag_2S, and Barica [5] reported that 5—10 mg of sulphide could be titrated in distilled water with 0.06 M silver nitrate to an accuracy of 2—3%.

Little information has been published on the accuracy of the titration of microgram amounts of sulphide with metal ions, although Slanina et al. [3] claimed that no sulphide was lost by adsorption on lead sulphide, regardless of the quantity of PbS present, when the titrated solution was 4 M in potassium hydroxide and 1 M in hydroxylamine.

When the titration of 2—150 μg of sulphide was examined in various media, with lead(II) and other metal ions as titrant, none of the systems studied gave stoichiometric end-points; the most accurate results were obtained with lead(II) as titrant and 1 M NaOH—1.5 M hydrazine or the Orion SAOB I (NaOH—salicylate—ascorbate) mixture as titration medium. In 1 M NaOH—1.5 M hydrazine medium, the deviation from stoichiometry was constant for 2—150 μg of sulphide.

Experimental

Apparatus. For the potentiometric titrations, a Philips PW 9414 digital ion-activity meter was used with an Orion 94-16 sulphide/silver ion electrode

coupled to an Orion 90-02 double-junction reference electrode. Titrant was delivered from a 0.5-ml Agla syringe burette which was calibrated gravimetrically throughout its volume, the calibration was checked by an EDTA titration of a standard copper solution. The titration vessel was a 50-ml beaker, and the solution was stirred magnetically. When nitrogen deaeration was used, high-purity nitrogen was passed rapidly through the solution via a glass capillary.

Reagents. The 1×10^{-2} M lead nitrate titrant was acidified to pH 2 with nitric acid, and then standardised by titration with EDTA to a pyrogallol red end-point [7]. A purity of 97.5% was found for the lead nitrate used. Other metal ion titrant solutions were prepared and standardised appropriately.

A 0.1 M iodine solution was standardised against both standard sodium thiosulphate solution and arsenic trioxide; the two methods of standardisation agreed within 0.1%, and with the molarity calculated from the weight of iodine taken.

Standard 1×10^{-2} M sulphide in 1 M NaOH was prepared daily from large crystals of $Na_2S \cdot 9H_2O$ (theor. 13.35% S; Univar). This solution was standardised against iodine by pipetting 10.00 ml of standard 0.1 M iodine into a 500-ml conical flask, adding 190 ml of water, 20 ml of syrupy phosphoric acid, 25.00 ml of sulphide solution, and 3 ml of 1% starch solution; the excess of iodine was back-titrated with 0.1 M sodium thiosulphate. The Univar $Na_2S \cdot 9H_2O$ was found to contain 12.95% S. The same purity was found if the sulphide was dissolved in water rather than 1 M NaOH; the titration value was unchanged for at least 5 h. Thiosulphate and sulphite impurities, which also react with iodine, were determined in the Univar sodium sulphide after precipitation of sulphide with zinc [8]. The sodium sulphide was found to contain 0.64% thiosulphate and 1.18% sulphite. The molarity of the standard 1×10^{-2} M sulphide solution was corrected for these impurities.

Orion SAOB I sulphide anoxidant buffer was prepared from sodium hydroxide, salicylic acid, and ascorbic acid [9]. SAOB II buffer was prepared [10] by mixing 200 ml of 10 M NaOH, 35 g of ascorbic acid, 67 g of disodium-EDTA, and 600 ml of deaerated water in a 1-l volumetric flask until the solids had dissolved, and then diluting to volume with deaerated water.

General procedure. The titration solution (10.00 ml) was pipetted into a 50-ml beaker, the electrodes were placed in the solution, an aliquot of the standard sulphide solution was added from a calibrated micropipette, and the mixture was titrated potentiometrically from the Agla syringe burette. End-points were calculated from the second derivative.

Results and discussion

The standard 1×10^{-2} M sodium sulphide solution was stable for at least 5 h, and had the same titre whether it was prepared in water, 1 M NaOH, deaerated 1 M NaOH, or 1 M NaOH—1.5 M hydrazine. Dilution of the

standard sulphide solution, however, had to be done with 1 M NaOH—1.5 M hydrazine or significant losses of sulphide occurred. After standing for 40 min in a sealed flask, a 5×10^{-4} M sulphide solution in 1 M NaOH, prepared from the standard 1×10^{-2} M solution, lost 15% of its sulphide concentration, as determined by titration with lead(II) solution. The reaction between oxygen and sulphide in alkaline media is rapid and quantitative [11] and, because 1 M NaOH in equilibrium with air at 25°C contains about 2×10^{-4} M oxygen [12], sulphide solutions more dilute than 1×10^{-2} M must be prepared with an excess of antioxidant.

Table 1 summarises the results obtained for titration of sulphide in different media with lead nitrate. Orion SAOB I buffer gave the most accurate results, although the end-point was not as sharp as that obtained with 1 M NaOH—1.5 M hydrazine. Repetitive titrations of 20—150 μg of sulphide in 1 M NaOH—1.5 M hydrazine over a period of 3 months gave a mean recovery of 86.0%, with a relative standard deviation of 1.9% (n = 21). The mean recovery was independent of the amount of sulphide taken in the range 2—150 μg, and well defined end-points were obtained down to 2 μg of sulphur. No change in the end-point was observed when the titration was completed very rapidly by adding most of the required volume of lead(II) in one initial aliquot, or when nitrogen was passed through the 1 M NaOH—1.5 M hydrazine solution for 20 min before addition of sulphide and during the titration. In sodium hydroxide—ascorbic acid mixtures, maximum recoveries of sulphide were obtained when the ascorbate concentration was above 0.1 M [13] (Table 1). Sulphide recovery in a titration medium of 1 M NaOH—0.11 M ascorbate was independent of the amount of sulphide taken, and the potential steps were well defined.

The use of metal ions other than lead(II) for the titration of sulphide is shown in Table 2. No end-points were obtained when silver(I) or mercury(II) were used in solutions containing 1.5 M hydrazine, because these ions are reduced to the metal by strong reductants [6]. Cadmium gave large potential changes at the end-point for titrations in 1 M NaOH—1.5 M hydrazine and SAOB I solutions, but high results were obtained. The high titrations may be the result of some cadmium(II) being consumed by the formation of hydroxy species, and a similar effect may be the cause of the failure of zinc(II) as a titrant [14].

Microgram amounts of sulphide can be titrated with lead(II) with good precision in titration media consisting of 1 M NaOH plus ascorbic acid or hydrazine, or in the Orion SAOB buffers, but to avoid significant errors, the lead titrant must be standardised against a standard sulphide solution by the same procedure that will be used for the unknown. The low sulphide recoveries found in titration of solutions well protected against atmospheric oxidation by inclusion of an antioxidant are most likely caused by adsorption of sulphide ion on the lead sulphide precipitate; in 1 M NaOH—1.5 M hydrazine the stoichiometry of the precipitate would correspond to $PbS_{1.16}$. The independence of sulphide recovery and amount of sulphide taken shows that

heavy metal impurities or residual oxygen in the titration solution do not cause the low results.

TABLE 1

Titration of sulphide with lead(II) using a sulphide-selective electrode (20—150 μg of sulphide titrated in 10 ml of solution with 1×10^{-2} M $Pb(NO_3)_2$.)

Titration medium	Sulphide recovery (%)[a]	Potential jump (mV)	Titration medium	Sulphide recovery (%)[a]	Potential jump (mV)
Deaerated 0.01 M NaOH[b]	65.0	220	0.1 M NaOH—1.5 M hydrazine	70.1	180
Deaerated 0.1 M NaOH[b]	58.6	220	1 M NaOH—1.5 M hydrazine[c]	86.0[d]	150
Deaerated 1 M NaOH[b]	61.4	160	Orion SAOB I[e]	94.2	135
1 M NaOH, not deaerated	26.2	170	Orion SAOB II[f]	84.2	90
1 M NaOH—0.0057 M ascorbic acid	58.5	160	5 M NaOH—1 M hydroxylamine-HCl	66.0	100
1 M NaOH—0.028 M ascorbic acid	79.2	160			
1 M NaOH—0.11 M ascorbic acid[c]	83.9	160			
1 M NaOH—0.29 M ascorbic acid	83.7	160			

[a]Based on formation of stoichiometric PbS. [b]Deaerated with nitrogen for 20 min before adding sulphide, then nitrogen passed through solution during titration. [c]Deaeration with nitrogen did not change recovery. [d]Same result when lead acetate used as titrant. [e]Sodium hydroxide—salicylic acid—ascorbic acid. [f]Sodium hydroxide—ascorbic acid—EDTA.

TABLE 2

Titration of sulphide with some metal ions using a sulphide-selective electrode (40—110 μg of sulphide titrated in 10 ml of solution with 1×10^{-2} M metal ion.)

Titrant	Titration medium	Sulphide recovery (%)[a]	Potential change at end-point (mV)
Ag(I)	0.1 M NaOH + 0.15 M hydrazine	53.5	145
	1 M NaOH + 1.5 M hydrazine	no end-point	—
Hg(II)	1 M NaOH + 1.5 M hydrazine	no end-point	—
Cu(II)	1 M NaOH + 1.5 M hydrazine	73.4	220
Cd(II)	1 M NaOH + 1.5 M hydrazine	175[b]	260
Cd(II)	Orion SAOB I	108[b]	230
Zn(II)	1 M NaOH + 1.5 M hydrazine	no end-point	—

[a]Based on formation of stoichiometric CuS, CdS, and Ag_2S. [b]Recovery independent of amount of sulphide

REFERENCES

1 H. Clysters and F. Adams, Anal. Chim. Acta, 92 (1977) 251.
2 R. Naumann and Ch. Weber, Fresenius Z. Anal. Chem., 253 (1971) 111.
3 J. Slanina, J. Agterdenbos and B. Griepink, Mikrochim. Acta, 1970, 1225.
4 T. M. Hseu and G. A. Rechnitz, Anal. Chem., 40 (1968) 1054.
5 J. Barica, J. Fish. Res. Bd. Can., 30 (1973) 1589.
6 E. J. Green and D. Schnitker, Mar. Chem., 2 (1974) 111.
7 F. J. Welcher, The Analytical Uses of Ethylenediaminetetraacetic Acid, D. Van Nostrand, New York, 1958, p. 190.
8 Merck Standards, E. Merck, Darmstadt, 1971, pp. 848—9.
9 E. L. Donaldson and D. C. McMullan, Anal. Lett., A11 (1978) 39.
10 Orion Research Inc., Instruction Manual for Model 94-16 sulphide/silver ion electrode (1978).
11 T. M. Florence, J. Electroanal. Chem., 97 (1979) 219.
12 R. A. Horne, Marine Chemistry, Wiley-Interscience, New York, 1969, p. 198.
13 T. M. Florence and Y. J. Farrar, J. Electroanal. Chem., 41 (1973) 127.
14 A. Ringbom, Complexation in Analytical Chemistry, Interscience, New York, 1963.

Analytica Chimica Acta, 116 (1980) 181—184

Short Communication

SENSITIVE SOLID-PHASE CHEMILUMINESCENCE MICROASSAY OF THIOLS

RICHARD D. LIPPMAN

The Royal Institute of Technology, Division of Physical Chemistry, S-100 44 Stockholm 70 (Sweden)

(Received 5th October 1979)

Summary. A polysaccharide matrix binding a chemiluminescent thiol by a dithiol linkage is used to exchange with a thiol in the sample, and the chemiluminescence of the displaced thiol is measured. The detection limit is 5 picomole.

Isotopic analysis has shown than an effective exchange reaction takes place between thiols and disulfides [1, 2]. Fava et al. [1] found that the exchange was catalyzed by bases and the rate-determining nucleophilic displacement at the disulfide occurs with a strong mercaptide nucleophile in a S_N2 reaction:

$$R^1SH \longrightarrow R^1S^-$$
$$R^1S^- + R^2S - SR^3 \longrightarrow R^1S - SR^2 + R^3S^-$$

If R^1S^- is the thiol or other strong nucleophile to be determined, and the disulfide $R^2S - SR^3$ is a chemiluminescent thiol covalently bound to a solid thiol polysaccharide, e.g. Sepharose 6B, a thiol—disulfide interchange will occur in weakly alkaline solutions, as explained in Fig. 1, thus releasing into solution the chemiluminescent thiol in proportion to the amount of thiol bound. In this communication, the preparation of chemiluminescent thiol derived from luminol, and its application to the determination of some thiols based on the above exchange reaction are described.

Experimental

Reagents. Sepharose 6B (Pharmacia AB, Uppsala, Sweden), 3-aminophthalic acid hydrazide (EGA-Chemie AG, Heidenheim, West Germany) and other chemicals (Sigma Chemical Co., St. Louis, Missouri) were used as received, unless stated otherwise.

Preparation of mercaptoacetyl-3-aminophthalic acid hydrazide. Luminol (3-aminophthalic acid hydrazide, 2 g, 1.1×10^{-2} mol) was dissolved in 50 ml of freshly distilled dimethylformamide with the aid of ultrasonic mixing. Thiodiglycolic acid (1 g, 5.5×10^{-3} mol) was added and the mixture refluxed at 160°C for 2 h. After 1 h, 10 ml of water—dimethylformamide azeotrope was distilled off. The warm distillate was shaken with 100 ml of 0.5 M

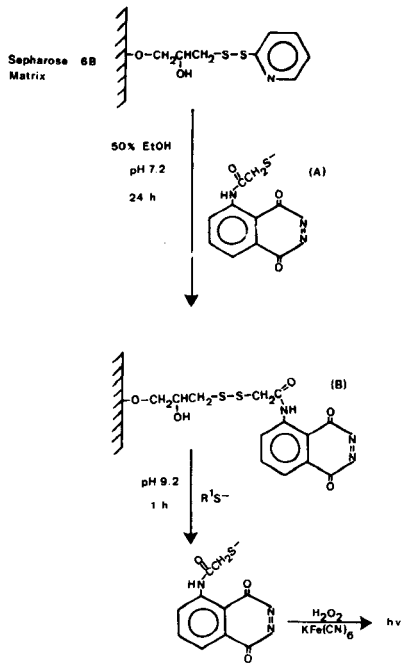

Fig. 1. The chemiluminescent thiol, mercaptoacetyl-3-aminophthalic acid hydrazide (A) replaces the 2-thiopyridyl group by solid-phase thio—disulfide interchange. The Sepharose 6B-(mercaptoacetyl)-3-aminophthalic acid hydrazide (B) reacts with the thiol sample after which the chemiluminescent assay is done with H_2O_2 and $K_3Fe(CN)_6$.

sodium hydrogen sulphite and poured over about 100 g of ice. The cream-brown powder obtained was filtered off and recrystallized 3 times from ethanol to give brown-yellow needles (m.p. 171—173°C; yield 1.4 g, 49%) which were stored under argon at 0°C.

Preparation of Sepharose 6B-(mercaptoacetyl)-3-amino phthalic acid hydrazide disulfide. Sepharose 6B (10 g) was soaked for 30 min at room temperature in 0.1 M Tris—HCl buffer, pH 7.0. The gel was washed with 3 portions of the buffer and filtered. An aqueous 50% ethanol solution (75 ml, apparent pH 7.2) containing the gel, 300 mg of the mercapto hydrazide, 0.2 mol of KCl, and 1 μmol of EDTA, was stirred magnetically for 24 h at room temperature. The pale yellow gel product was washed with the Tris—HCl buffer (ca. 1.5 l) until chemiluminescence could not be detected instrumentally on addition of 1 ml of 5 M sodium hydroxide, 5 ml of 1×10^{-4} M hydrogen peroxide, and 1 ml of 5 M potassium hexacyanoferrate(III) to 30 ml of washings. The gel product was filtered until dry and stored under argon at 0°C.

Assay procedure. In 0.1 M boric acid—sodium hydroxide buffer, pH 9.2, 50 mg of gel was mixed with a sample containing, e.g. L-cysteine, to give

a total volume of 30 ml, magnetically stirred for 1 h and filtered off. To the filtrate, 10 μl of 10 M hydrogen peroxide was added. Both this solution and 30 ml of 1 M potassium hexacyanoferrate(III) solution were degassed with argon and rapidly mixed in a 1-ml stopped-flow apparatus. Chemiluminescent emission was measured with a UDT-500 photodiode/operational amplifier unit (United Detector Technology, Santa Monica, California) and a strip-chart recorder.

Results and discussion

Figure 2 shows the intensity—concentration plot for luminol standards and that obtained by displacement reaction of 5 thiol standards. The luminol log—log graph has a slope of nearly unity, indicating a linear increase of intensity with concentration below 10^{-5} M. The slopes for the thiol standards all lie on the same line, which has a slope of nearly 60°. The limit of detection (3:1 signal-to-noise ratio) is 5×10^{-12} mol of thiol group which is somewhat higher than that for luminol. This is a result of the thiol nucleophile forming its own chemiluminescent intermediate. The mechanism of this intermediate formation may be explained as follows. According to results obtained from pulse radiology by Merenyi and Lind [3] in this laboratory, a

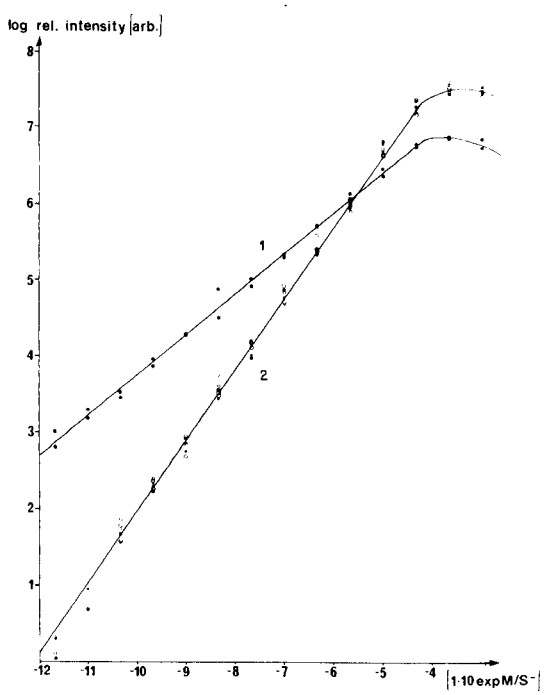

Fig. 2. Chemiluminescent assay of luminol (curve 1) and L-cysteine, reduced bovine insulin, reduced urease (jack beans), dihydrolipoic acid and dithiothreitol (Cleland's reagent) (curve 2).

first-order reaction occurs initially between hydroxide ion and luminol. Luminol then undergoes two second-order, kinetically-controlled radical reactions until one of its carbonyl carbons is nucleophilically attacked by a hydroperoxide radical in a slow, rate-determining, concerted reaction. It seems likely that this attack creates a peroxyhemiketal that is the precursor of the dioxetanone, the chemiluminescent-reactive intermediate. This suggestion is based on the facts [4] that hemiketals are stable only in alkaline solution, that thiols and hydroperoxide radicals are more nucleophilic in alkaline solution, and that luminol and other chemiluminescent and bioluminescent compounds are known to emit only in alkaline solutions. Therefore, the formation of the fairly stable luminol—peroxyhemiketal is competitively inhibited by the thiol nucleophilic attack which forms its own chemiluminescent thiolhemiketal intermediate. In bioluminescence, firefly luciferin was reported recently [5] to form a highly reactive chemiluminescent thiolketone. The quantum yield of this thiolketone is also strongly dependent on alkali concentration.

The sensitivity of the Sepharose-6B luminol disulfide method is comparable to the sensitivities obtained with radioimmunoassay, and the method is safer to use because exposure to radio-isotopes is avoided. It is also far more sensitive than current colorimetric methods, for example with Ellman's reagent [6]. Even greater sensitivities, similar to those obtained with luciferin —luciferase—ATP assay [7], which can detect 10^{-15} mol, may be possible, as indicated by current investigations into acridane-(9-carboxy-*m*-chlorophenolate)-10-acetyl-disulfoSepharose 6B. Greater sensitivities with Sepharose 6B luminol disulfide may be obtained at pH 11 and with the use of hematin, but this damages easily oxidized thiol and disulfide groups. It may also be possible that chemiluminescent thiol—disulfide reagents could be built upon a battery of chemiluminescent compounds covalently bonded to a polysaccharide with an amylosazonyl semicarbazide disulfide (m.p. 257—258.8°C) backbone. Also, other chemiluminescent-labelling reagents may be prepared from 3-(isocyanato)phthalic acid hydrazide (m.p. 291—294°C), recently synthesized by the author.

REFERENCES

1 A. Fava, G. Reichenbach and U. Peron, J. Am. Chem. Soc., 89 (1967) 6696.
2 R. G. Hiskey and M. A. Harpold, J. Org. Chem., 33 (1968) 559.
3 G. Merenyi and J. Lind, private communication.
4 E. G. Sander and W. P. Jencks, J. Am. Chem. Soc., 90 (1968) 4377; N. L. Allinger, M. P. Cava and D. C. De Jong (Eds.), Organic Chemistry, Worth Publishing, New York, 2nd edn., 1976, pp. 460—462.
5 E. H. White, N. Suzuki and J. D. Miano, J. Org. Chem., 12 (1978) 2366.
6 G. L. Ellman, Arch. Biochem. Biophys., 82 (1959) 70.
7 E. Schram, in Liquid Scintillation Counting, Vol. 2, Academic Press, New York, 1972, pp. 112—115.

Analytica Chimica Acta, 116 (1980) 185—190

Short Communication

EXTRACTION SPECTROPHOTOMETRIC DETERMINATION OF NIOBIUM IN ROCKS WITH SULFOCHLOROPHENOL S

A. E. CHILDRESS* and L. P. GREENLAND
U.S. Geological Survey, Reston, Va. 22092 (U.S.A.)
(Received 26th October 1979)

Summary. After acid decomposition and potassium pyrosulfate fusion, niobium (1—26 ppm) is separated from interfering elements by extraction into methyl isobutyl ketone from 6 M H_2SO_4—2 M HF and back-extracted into water. The niobium—sulfochlorophenol S complex is extracted into amyl alcohol.

An extraction spectrophotometric method utilizing 4-(2-pyridylazo)-resorcinol (PAR) has been in routine use by the U.S. Geological Survey for the past several years [1], but has not proven sufficiently sensitive to allow precise measurement of niobium in the 1—5 ppm range. This limitation and a recently noted systematic bias between spectrophotometric and neutron activation values [2, 3] led to investigation of alternative methods of niobium determination. The sulfochlorophenol S method described in this paper provides sensitivity down to 1 ppm, but fails to resolve the discrepancy between previous spectrophotometric and neutron activation values.

Experimental

Niobium standard solution. Weigh a portion (<0.2 g) of niobium metal. Dissolve in 20 ml of hot concentrated hydrofluoric acid in a platinum dish, add 25 ml of concentrated sulfuric acid, and evaporate to fumes of sulfur trioxide. Dilute to a final acid concentration of 5.6 M HF and 4.5 M H_2SO_4.

Procedure. Weigh 0.25 g of sample (1—40 ppm Nb) into a 50-ml platinum dish. Prepare standards by pipetting aliquots of a niobium standard solution to cover the 0.25—10 μg Nb range into 50-ml platinum dishes. Add 5 ml of concentrated nitric acid and 10 ml of concentrated hydrofluoric acid to each, and evaporate to dryness on a hot plate at 125°C. Fuse the residue with 2.0 g of potassium pyrosulfate and dissolve the fusion cake in 50 ml of 6 M H_2SO_4—2 M HF. Transfer the solution to a teflon separatory funnel and extract with 25 ml of methyl isobutyl ketone (MIBK). Remove the aqueous phase and wash the organic layer with a fresh 20-ml portion of 6 M H_2SO_4—2 M HF, discarding the wash. Back-extract the niobium with two 5-ml portions of water, collecting the extract in a teflon beaker. Add 1 ml of concentrated sulfuric acid plus 0.2 ml of 1% potassium chloride solution and

evaporate to dryness. Add 5 ml of 6 M HCl to the residue, cover and heat on a hot plate at 175°C for 30 min. Add 1.6 ml of 5% tartaric acid in 4 M HCl, 15 ml of water and 0.1 ml of thioglycollic acid. Prepare a blank by making these same additions to a beaker containing no niobium. Heat each solution for 15 min at 60°C. Add 0.3 ml of 0.3 M EDTA and 0.2 ml of an aqueous 0.1% sulfochlorophenol S solution, and heat for another 15 min. Transfer the solution to a separatory funnel, add 0.5 ml of 10% diphenylguanidine in concentrated HCl (freshly prepared), and extract with 5 ml of amyl alcohol. Discard the aqueous layer and add 1 ml of ethanol to the organic phase. Measure the absorbance of the organic phase in 1- or 5-cm cells at 656 nm against a blank taken through the whole procedure. Determine the concentration of niobium by comparison with the standards carried through the entire procedure.

Results and discussion

This method combines two extensively studied techniques, the separation of niobium from interfering elements by extraction from H_2SO_4—HF solutions with MIBK [4—7] and the extraction spectrophotometric determination of niobium with sulfochlorophenol S [8—13]. The MIBK extraction separates niobium from most elements found in rocks. Only elemental halogens, selenium and tellurium are coextracted to any appreciable extent [6]. After an evaporation step to remove hydrogen fluoride, the sulfochlorophenol S color is developed in an acidic medium, avoiding the heavy reliance on masking necessary with the less selective PAR. Although the selectivity of PAR increases dramatically in dilute mineral acid solutions, the corresponding loss of sensitivity makes this reaction of little practical value in rock analysis. Thus the current method provides higher sensitivity because of the 150% higher molar absorptivity than PAR and better selectivity because of the MIBK extraction and the ability of sulfochlorophenol S to form stable complexes with niobium in acidic media.

To provide an estimate of the precision of the method, three bottles each of nine U.S. Geological Survey standard rocks were randomized and sample portions analyzed over several weeks. The analyses, reported in Table 1, indicate that the standard deviation of a determination is generally better than 5% for concentrations of more than 9 ppm of niobium and ±19% for 1.6 ppm. These data also permit a one-way analysis of variance to test for homogeneity among bottles of the standard rocks. As shown by the *F*-ratios, the bottles of standards were found to be homogeneous at the 95% confidence level.

The results of this work are compared in Table 2 with those obtained in previous analyses. There is a systematic bias both between the two spectrophotometric techniques and between these and the neutron activation values; this is illustrated in Fig. 1.

Several possible sources of bias were investigated in some detail. The single niobium pentoxide sample used in previous work at the U.S. Geological

TABLE 1

Niobium determined in USGS Standard Rocks

Standard rock	Bottle (Split/position)	Nb conc. (ppm)	Mean ± s.d.	*F*-ratio
AGV-1	57/24	13.2, 13.1, 14.8	13.8 ± 0.6	1.11
	14/4	13.4, 13.6, 13.6		
	44/17	14.0, 14.7, 14.0		
GSP-1	4/25	26.5, 26.3, 25.4		
	80/2	24.5, 26.2, 26.6	26.0 ± 0.7	0.139
	43/23	26.3, 26.5, 25.4		
G-2	100/9	12.0, 11.9, 11.8		
	68/4	11.5, 11.8, 12.2	11.9 ± 0.2	0.696
	116/30	12.2, 12.2, 11.8		
BCR-1	2/6	11.6, 12.3, 12.2		
	41/30	12.1, 11.1, 11.4	11.7 ± 0.5	1.05
	47/1	10.9, 12.1, 11.5		
SDC-1	81/22	19.4, 18.4, 18.9		
	49/28	18.3, 17.9, 18.1	18.6 ± 0.5	2.86
	103/14	18.1, 18.9, 19.0		
RGM-1	51/28	8.4, 9.6, 9.7		
	63/19	9.6, 9.5, 9.4	9.2 ± 0.5	0.778
	19/18	9.3, 9.2, 8.5		
BHVO-1	9/6	17.6, 18.2, 18.2		
	53/7	18.1, 17.3, 18.2	18.0 ± 0.3	0.393
	14/30	18.3, 18.2, 17.9		
QLO-1	33/16	10.1, 10.5, 9.8		
	51/7	11.9, 10.6, 9.9	10.3 ± 0.7	1.20
	49/6	9.4, 10.0, 10.5		
DNC-1	0788	1.7, 1.3, 2.0		
		1.6, 1.4, 1.8		
	1464	1.0, 1.4, 1.2	1.6 ± 0.3	0.239
		1.8, 2.3, 1.5		
	1304	1.2, 1.4, 1.3		
		1.6, 2.0, 1.5		

Survey was compared with standards prepared from spectrographically pure niobium pentoxide and from niobium metal. The results of this comparison were in excellent agreement. In addition, the niobium metal standard was checked by gravimetric analysis and found to be within 2% of the expected value.

Because the neutron activation procedure relied on acid decomposition alone, whereas both spectrophotometric techniques used a fusion as well as an acid decomposition, the lower activation values could possibly have reflected incomplete dissolution of the sample. The spectrophotometric

TABLE 2

Comparison of niobium concentrations (ppm) obtained by various techniques for standard rocks

Standard rock	AGV-1	GSP-1	G-2	BCR-1	SDC-1	RGM-1	BHVO-1	QI
Spectrophotometry, this work	13.8	26.0	11.9	11.7	18.6	9.2	18.0	1(
Spectrophotometry, PAR [1]	15.7	28.7	13.4	15.6	21.1	9.4	21.0	1]
Spectrophotometry, isotope dilution-PAR [4]	15.0	29.4	13.3	13.5				
Spectrophotometry, thiocyanate [14]	16.0	27.5	12.6	23.6				
Neutron activation [2]	12.3	20.1	9.8	10.6	16.0	8.1	16.3	
X.r.f. [15]	13	24	12	14				
X.r.f. [16]		25.4		11.3				
X.r.f.[a]	15.0 (10—21.7)	23.1 (19—28.3	10.6 (8—16.1)	19.6 (9—40)				

[a]Ref [2], Table 1; mean and range are given.

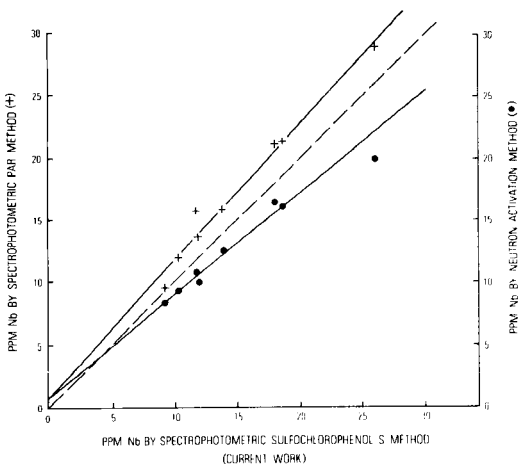

Fig. 1. Plot illustrating positive systematic bias of spectrophotometric results (+) and negative systematic bias of neutron activation results (•) in relation to the current method. Perfect agreement between methods is represented by the dashed line.

results shown in Table 3 compare this acid decomposition—MIBK extraction procedure [2, 3] with the acid decomposition plus fusion and MIBK extraction used in this method, both followed by sulphochlorophenol S determination. These data demonstrate the adequacy of acid decomposition for the standard rocks analyzed in this work. Because of the widespread occurrence of niobium in acid-resistant minerals, however, the procedure involving fusion must still be regarded as more generally satisfactory for samples of unknown composition.

TABLE 3

Comparison of spectrophotometric determinations of niobium[a]

Standard rock	Acid decomposition [2, 3]	Present procedure
AGV-1	14.4 (3)	13.8
GSP-1	26.1 (2)	26.0
G-2	11.7 (3)	11.9
BCR-1	11.6 (4)	11.7
RGM-1	8.8 (3)	9.2
BHVO-1	18.3 (6)	18.0
QLO-1	10.0 (5)	10.3

[a]Numbers in parentheses indicate number of replicates. For the present procedure, the values given are the means of nine replicate determinations.

Table 2 shows that the three previous spectrophotometric techniques used at the U.S. Geological Survey are in good agreement with one another. They are also independent of one another in the sense that different separations and color reagents were used. Thus an elemental interference is unlikely to be common to all three methods and to be of similar magnitude in each case. Also, the fact that the bias between methods is systematic, regardless of rock type, further decreases the likelihood that an elemental interference is the source of the discrepancy. Although a comparison of mean x-ray fluorescence values [2] (Table 2) demonstrates as good an agreement with the spectrophotometric as with the neutron activation values, the range is such that no meaningful comparison can be made. However, although the bias cannot be accounted for, it is small enough to assert that the absolute accuracy of the present method is ±15% of the true value.

We are grateful to E. Y. Campbell for her many helpful comments and for comparing the niobium standards.

REFERENCES

1 L. P. Greenland and E. Y. Campbell, J. Res. U.S. Geol. Surv., 2 (1974) 353.
2 R. O. Allen and E. Steinnes, Geostandards Newsl., 3 (1979) 57.
3 R. O. Allen and E. Steinnes, Anal. Chem., 50 (1978) 903.
4 L. P. Greenland and E. Y. Campbell, Anal. Chim. Acta, 49 (1970) 109.
5 F. Nelson, R. M. Rush and K. A. Kraus, J. Am. Chem. Soc., 82 (1960) 339.
6 P. C. Stevenson and H. G. Hicks, Anal. Chem., 25 (1953) 1517.
7 H. G. Hicks and R. S. Gilbert, Anal. Chem., 26 (1954) 1205.
8 S. V. Elinson, Russ. Chem. Rev., 44 (1975) 707.
9 T. Sakaki, J. Jpn. Inst. Metals, 33 (1969) 1092.
10 S. B. Savin, I. D. Pisarenko, E. I. Yurchenko and Yu. M. Dedkov, Zh. Anal. Khim., 21 (1966) 669.
11 E. N. Paschenko, L. A. Vasil'eva, V. F. Mal'tsev and N. P. Volkova, Zavod. Lab., 39 (1973) 1297.

12 S. B. Savin, P. N. Romanov and Yu. G. Eremin, Zh. Anal. Khim., 12 (1966) 1423.
13 S. B. Savin, V. A. Bortsova and E. N. Malkina, Zh. Anal. Khim., 20 (1965) 947.
14 F. S. Grimaldi, Anal. Chem., 32 (1960) 119.
15 E. Jagoutz and C. Palme, Anal. Chem., 50 (1978) 1555.
16 J. P. Willis, L. H. Ahrens, R. V. Danchin, A. J. Erlank, J. J. Gurney, P. K. Hofmeyr, T. S. McCarthy and M. J. Orren, Proc. 2nd Lunar Science Conf., Geochim. Cosmochim. Acta, Suppl. 2, (1971) 1123.

Analytica Chimica Acta, 116 (1980) 191—193

Short Communication

A SPECTROPHOTOMETRIC METHOD FOR THE DETERMINATION OF ANIONIC SURFACTANTS AT $\mu g\ l^{-1}$ LEVELS

S. RAMA BHAT, P. T. CRISP**, J. M. ECKERT* and N. A. GIBSON

Department of Inorganic Chemistry, University of Sydney, Sydney, N.S.W. 2006 (Australia)

(Received 2nd November 1979)

Summary. The anionic surfactant is extracted into chloroform as a neutral complex with the bis(ethylenediamine)copper(II) cation, and copper(II) is determined spectrophotometrically after addition of 1-(2-pyridylazo)-2-naphthol and diethylamine. With a 200-ml water sample, the limit of detection is 5 $\mu g\ l^{-1}$ (as linear alkyl sulphonic acids). The method is simple and is directly applicable to fresh, estuarine and marine waters.

Earlier papers [1, 2] described a method for the determination of anionic surfactants based on the extraction of surfactant anions into chloroform as an inner-sphere complex with the bis(ethylenediamine)copper(II) cation [3]; the determination is completed, for surfactant concentrations above 100 $\mu g\ l^{-1}$, by either spectrophotometry of the extract or flame a.a.s. of an acid back-extract [1] and, at levels below 100 $\mu g\ l^{-1}$, by graphite furnace a.a.s. [2].

The work reported in this communication was prompted by requests for a more sensitive spectrophotometric version of the method. The extraction system remains the same. The new procedure, in common with the earlier one, requires a single extraction and is insensitive to ionic interferences. It is applicable, without modification, to fresh, estuarine and sea-water samples. By the use of a smaller volume of chloroform and of 1-(2-pyridylazo)-2-naphthol (PAN), with diethylamine, as the spectrophotometric reagent for copper in the extract, a detection limit of 5 $\mu g\ l^{-1}$, as linear alkyl sulphonic acids (LAS), is obtained.

Experimental

Standard reference anionic surfactant solution. A solution containing 5.68% (w/w) active LAS, of mean molecular weight 316, was obtained from the U.S. Environmental Protection Agency. This solution was used to prepare a stock standard solution containing 1000 mg LAS l^{-1} which was diluted further as required.

**Present address: Department of Chemistry, The University of Wollongong, Wollongong, N.S.W. 2500, Australia.

Copper—ethylenediamine reagent. Dissolve 62.3 g of copper sulphate pentahydrate and 49.6 g of ammonium sulphate in water. Add 45.1 g (50 ml) of 1,2-diaminoethane (ethylenediamine) and dilute to 1 l with water. The reagent is stable for at least a month.

PAN reagent. Dissolve 0.375 g of PAN (Merck) in absolute ethanol. Add 22.0 g (31.4 ml) of diethylamine (Merck) and dilute to 1 l with absolute ethanol. If care is taken to prevent evaporation, this reagent is stable for at least two months.

A Varian-Techtron model 635 spectrophotometer was used.

Recommended procedure. Place a suitable volume of the water for analysis in a 250-ml separating funnel and, if necessary, adjust the pH to 5—9. Any volume of water up to 200 ml may be sampled but it should contain not more than 250 μg of LAS. Adjust the volume to about 200 ml with water and add 10.0 ml of copper—ethylenediamine reagent and 10.0 ml of chloroform. Shake the funnel for 1 min and allow to stand until the phases separate.

Run about 7 ml of the organic phase into a dry 15-ml graduated centrifuge tube, taking care that no droplets of the aqueous phase pass into the tube. Cover the top of the tube with a 5-cm square of aluminium foil and centrifuge at 2500 r.p.m. for 5 min. Pipette a 5.0-ml aliquot of the clarified extract into a small glass-stoppered flask. Add 1.0 ml of PAN reagent and shake the flask to mix well. Measure the absorbance of this solution at 560 nm with a 5:1 chloroform—ethanol solution in the reference cell. The colour developed by the PAN reagent is stable for at least 24 h.

Carry out a blank determination with 200 ml of distilled water. The blank absorbance should not be more than 0.025. Calculate the surfactant concentration in the sample by comparison with standards.

Results and discussion

PAN is a sensitive reagent for copper(II) in water, the determination involving extraction of a copper—PAN complex into an organic solvent and spectrophotometry of the extract [4]. In the present work, however, the copper(II) is already in an organic solvent, as the bis(ethylenediamine)-copper(II)—surfactant complex, and PAN by itself was found to generate little colour in the extract. Full sensitivity was restored by the inclusion of an organic base in the PAN reagent; of the bases tested, diethylamine was the most efficient.

In the presence of diethylamine, copper(II) in the extract was shown, by construction of a Job's plot, to form a bis complex with PAN. A value of 4.1×10^4 l mol^{-1} cm^{-1} was obtained for ϵ_{max} of this complex at 560 nm (in chloroform—ethanol solution). The base promotes formation of the complex by deprotonating PAN. Its use in an organic solvent substitutes for the control of pH in extraction of the complex from an aqueous phase.

Calibration. In the range 0—250 μg, the amount of anionic surfactant present (y μg, as LAS) could be calculated from the measured absorbance (x),

TABLE 1

Precision of proposed method

LAS taken[a] (μg)	s (μg)	s_r (%)	LAS taken[a] (μg)	s (μg)	s_r (%)
2.5	0.3	12	50.0	1.2	2
10.0	0.3	3	250.0	2.0	1
25.0	0.5	2			

[a]12 determinations were carried out at each level.

TABLE 2

Recovery of LAS from sea water

LAS added[a] (μg)	Mean LAS found[b] (μg)	s (μg)	Recovery (%)
0	<1	0.3	—
2.5	2.1	0.4	84
10.0	9.3	0.4	93
25.0	23.3	0.9	93
50.0	47.4	2.0	95
250.0	243.0	2.6	97

[a]To 200 ml of sea water. [b]Mean of 8 determinations.

obtained with 1-cm cells and corrected for the blank, by means of the equation $y = 186.4x$.

Precision and limit of detection. The precision of the proposed method was assessed by carrying out repeated determinations of standard LAS solutions. The results are shown in Table 1.

The limit of detection, taken as the amount of surfactant which gave an absorbance equal to twice the standard deviation of a set of at least 10 absorbance readings at or near blank level, was found to be 1 μg, as LAS (corresponding to a concentration of 5 μg LAS l^{-1} for a sample volume of 200 ml).

Interferences. The pattern of interferences was similar to that reported in the earlier papers [1, 2]. In particular, no positive interferences were observed. The applicability of the method to marine waters is confirmed by the recovery data in Table 2.

REFERENCES

1 P. T. Crisp, J. M. Eckert and N. A. Gibson, Anal. Chim. Acta, 78 (1975) 391.
2 P. T. Crisp, J. M. Eckert, N. A. Gibson, G. F. Kirkbright and T. S. West, Anal. Chim. Acta, 87 (1976) 97.
3 P. J. M. W. L. Birker, P. T. Crisp and C. J. Moore, Acta Crystallogr., Sect. B., 33 (1977) 3194.
4 See, e.g., Z. Marczenko, Spectrophotometric Determination of Elements, Ellis Horwood, Chichester, 1976.

Analytica Chimica Acta, 116 (1980) 195—198

Short Communication

MEANS OF DISTINGUISHING SELENIUM PEAKS FROM SULFUR PEAKS IN GAS CHROMATOGRAPHY WITH A FLAME PHOTOMETRIC DETECTOR

JAMES R. HANCOCK, CHRISTOPHER G. FLINN and WALTER A. AUE*

Department of Chemistry, Dalhousie University, Halifax, Nova Scotia (Canada)

(Received 9th October 1979)

Summary. Flow optimization, optical discrimination, and doping with carbon disulfide or methane were tested as means of distinguishing selenium peaks from sulfur peaks in a flame photometric detector. Optical discrimination is the best choice if a dual-channel detector is available. For single-channel detectors, methane doping quenches the sulfur peak more severely than the selenium peak, thus allowing the peaks to be identified.

Many complex samples of current interest contain compounds of sulfur; some also contain compounds of selenium. Volatile organic derivatives of these two elements are sometimes separated by gas chromatography and determined by a flame photometric detector (FPD).

When a complex mixture is analyzed by such means, peaks can be due to any element that produces luminescence, e.g. Sn, Ge, N, P, As, Fe, Cr, S, Se, Te and B. A variety of methods can be used to define the element responsible for a particular peak, most of which make use of dispersive optics. In this paper, the question of how to distinguish peaks of selenium from those of sulfur is examined.

The problem arises because the band systems of S_2 and Se_2 overlap extensively; hence it is not possible to select a wavelength at which only selenium would respond. Yet, selenium compounds in natural samples would often be accompanied by even larger amounts of comparable sulfur compounds. To cope with this problem, a search for analytically exploitable differences between sulfur and selenium response was carried out on the Shimadzu FPD used for earlier studies [1, 2], and four options are described below.

Flow optimization

In general, changes in flow conditions — of air, hydrogen and nitrogen — bring about parallel changes in sulfur and selenium response [1]. But with an energy-starved flame (very low air flow), selenium response is depressed less than sulfur response. This effect is demonstrated in Fig. 1. Exploiting it appears unprofitable, however, since the flame is easily extinguished by the solvent peak under these conditions.

Optical discrimination

This method requires a dual-channel FPD: one channel for quantitative selenium detection, and the other for a simultaneous, qualitative check that the peak is not due to sulfur.

To select a reasonable combination of dispersive elements for this purpose, both the sensitivity and selectivity of selenium analysis must be considered. The FPD is less sensitive for selenium than for sulfur, and using a broad optical range helps to improve the sensitivity. The range should be selected at long wavelengths for selectivity purposes, since the S_2 bands diminish slowly in that direction. For the sulfur channel with its qualitative task, a narrow-width interference filter, centered on an S_2 band at as short a wavelength as possible, would appear the best choice. A large number of filters available were tested according to these guidelines. The best combination of these proved to be a 500-nm cut-off filter for selenium determination opposite a 365-nm narrow-band interference filter for sulfur detection. Figure 2 shows chromatograms from the same injections as seen by the two channels, with and without filter. This optical method appears to be the best choice when a dual-channel FPD is available.

With only a single-channel FPD at hand, two injections per sample must be used. Because changing optics is cumbersome, two short-term doping methods were investigated.

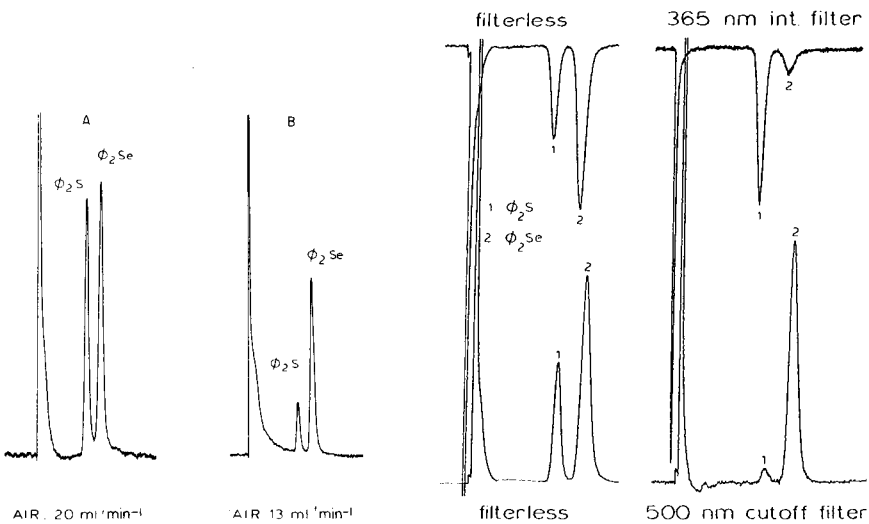

Fig. 1. Flow optimization, no optical filters. (A) Regular conditions: column, 3% OV-101 on Carbowax 20M-modified Chromosorb W, isothermal at 180°C; flow rates in ml min^{-1}, 40 H_2, 30 N_2, 20 air; detector and injection port at 250°C; injected: 2 ng of diphenylsulfide and 20 ng of diphenylselenide. (B) Similar, but 13 ml air min^{-1}.

Fig. 2. Optical discrimination, demonstrated in a dual-channel recording. Filters are indicated on the graph. Otherwise conditions were regular, as noted in Fig. 1.

Carbon disulfide doping

Previous research [2] has shown that selenium response (as well as sulfur response) can be enhanced by a sulfur-doped background. Tentatively, this effect has been attributed to generation of electronically excited SeS. Now, if the wavelength of a typical S_2 band is selected and one of the detector gases is doped with a suitable sulfur compound, sulfur peaks will be positive as usual, but selenium peaks will turn negative (sulfur is taken from the background, i.e. the baseline, to form SeS). Figure 3 shows the same sample run with and without sulfur doping. This approach does work; however, it must be judged inferior — in terms of overall chromatographic performance as well as ease of application — to the following, preferred doping method.

Methane doping

A hydrocarbon co-eluting with sulfur or selenium depresses their responses; however, compounds of selenium are less susceptible to carbon quenching than are those of sulfur [1]. Very important in the present context, the fraction quenched is independent of analyte concentration, i.e. a certain level of the quenching agent decreases the response by a constant percentage. Hence a small stream of methane, which can be easily switched on and off, is all that is needed to distinguish a selenium peak from a sulfur peak. Switching methane on and off is not detrimental to detector stability, as is demon-

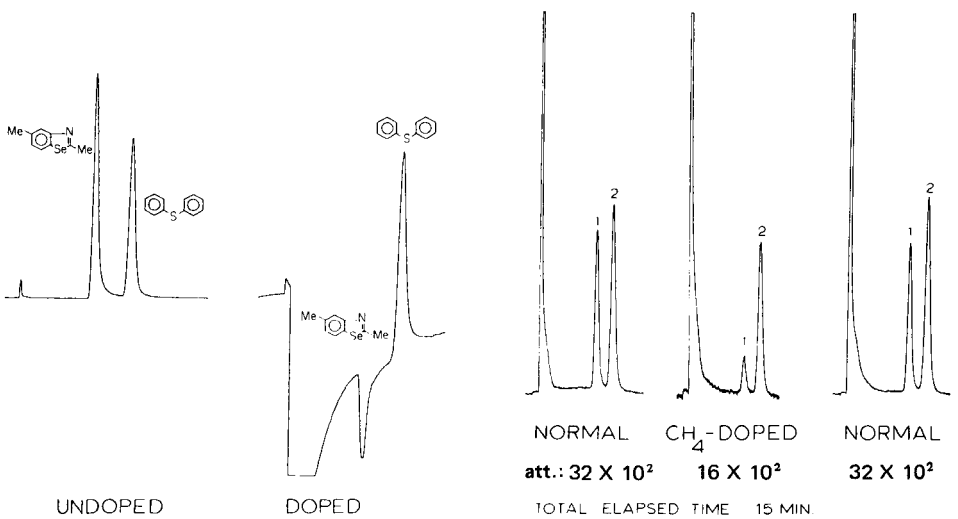

Fig. 3. Carbon disulfide doping, with a 365-nm interference filter (10.7-nm bandwidth) and column at 160°C. Injected: 200 ng of 2,5-dimethyldibenzoselenazole and 20 ng of diphenylsulfide. Other conditions were regular, as given in Fig. 1.

Fig. 4. Methane doping, no optical filters. Regular conditions as in Fig. 1, with the same compounds.

strated in Fig. 4 with three consecutive chromatograms of the same mixture run within 15 min. The respective drops in response under methane doping clearly establish that one peak contains sulfur and the other selenium.

This study was supported by a grant from Environment Canada, Water Resources, and NRC grant A-9604.

REFERENCES

1 C. G. Flinn and W. A. Aue, J. Chromatogr., 153 (1978) 49.
2 W. A. Aue and C. G. Flinn, J. Chromatogr., 158 (1978) 161.

Analytica Chimica Acta, 116 (1980) 199—203

Short Communication

SEPARATION OF URANIUM(VI) BY LIQUID—SOLID EXTRACTION WITH TRI-n-OCTYLPHOSPHINE OXIDE DILUTED WITH NAPHTHALENE

YASUMASA SHIGETOMI, TAKEHIRO KOJIMA and HIDEAKI KAMBA

Department of Chemistry, Okayama College of Science, 1-1, Ridai-chō, Okayama-shi 700 (Japan)

YUROKU YAMAMOTO*

Department of Chemistry, Faculty of Science, Hiroshima University, Hiroshima 730 (Japan)

(Received 5th November 1979)

Summary. Liquid—liquid distribution with tri-n-octylphosphine oxide (TOPO) and molten naphthalene has been investigated for the extraction of 20 metals from nitric acid and hydrochloric acid solutions. Uranium is quantitatively extracted from 1 M nitric acid or hydrochloric acid by using 100 mg of TOPO and 200 mg of naphthalene and shaking for 5 min at 80°C, and separated from transition metals, alkaline earth metals and rare earth metals (except scandium). Addition of naphthalene increases the extraction efficiency.

Solvent extraction with tri-n-butylphosphate (TBP) or tri-n-octylphosphine oxide (TOPO) diluted with cyclohexane, etc., has been widely studied [1—5]. Separation of trace metals by homogeneous extraction has been described [6—8]. The separation of various metals by solid—liquid extraction with molten naphthalene has been reported [9]. Recent studies [10] on the separation of uranium from sea water by adsorption on gels containing various metal hydroxides required alternative methods for the separation and determination of trace amounts of uranium. The present communication is focused on the separation of uranium by extraction with TOPO and molten naphthalene.

Experimental

Reagents. All reagents were of analytical grade. Standard uranium(VI) solution(1000 mg l^{-1}) was prepared by dissolving 0.422 g of uranyl nitrate in demineralized water and diluting to 100 ml. Stock solutions of alkaline earth, rare earth and transition metals (10^{-2} M) were prepared in 0.1 M nitric acid or hydrochloric acid.

Procedure. A solution containing 100—400 μg of each metal was transferred to a 100-ml Erlenmeyer flask with a tightly fitting stopper. The acidity was adjusted to 0.1—4 M with nitric acid or hydrochloric acid and the

solution was diluted to 25 ml with water. Then 100 mg of TOPO and 200 mg of naphthalene were added and the flask was heated on a water bath at about 80°C until the naphthalene melted completely. After vigorous shaking for 5 min, the flask was removed from the bath and cooled to room temperature. After the crystalline phase had separated completely, the mixture was filtered through quantitative-grade paper (5A) and the solid was washed with a little water. The filtrate and washings were transferred to a 50-ml volumetric flask and diluted to the mark with water. Uranium was determined colorimetrically with TOPO and 1-(2-pyridylazo)-2-naphthol(PAN) [11]. Zirconium(IV), magnesium(II), calcium(II), strontium(II), barium(II), yttrium(III), scandium(III), lanthanum(III), cerium(III), neodymium(III), vanadium(V), chromium(III), manganese(II), iron(III), cobalt(II), nickel(II), copper(II), zinc(II) and aluminium(III) were determined spectrophotometrically with appropriate chromogenic agents.

Uranium was back-extracted by shaking the naphthalene phase with 1 M sodium carbonate solution (25 ml) at 80°C.

Results and discussion

Effects of extraction parameters. Uranium(VI) (100 μg) was quantitatively extracted from 1 M nitric acid solution into 1 g of naphthalene provided that at least 100 mg of TOPO was present; up to 400 mg of TOPO could be used. Uranium(VI) was not extracted in the absence of TOPO. The percentage extraction was estimated by determining uranium in the aqueous phase after the extraction. When naphthalene was not used, uranium (100 μg) could still be extracted into molten TOPO (100 mg) at 55°C, but it was difficult to separate the phases. When more than 200 mg of naphthalene (up to 2 g) was added, the TOPO phase was easily separated as a solid on cooling. A shaking time of 5 min sufficed to extract 100 μg of uranium in 25 ml of sample solution as in the recommended procedure.

Extraction of diverse metals from nitric acid solutions. Twenty metal ions were examined at various concentrations of nitric acid (0.1—4 M) with 100 mg of TOPO and 200 mg of naphthalene. The results are shown in Fig. 1. Negligible extraction was obtained for magnesium and the alkaline earth metals, and for the transition metals tested. Decreases in extraction were generally observed as the acid concentration increased. Scandium was moderately extracted. Uranium and zirconium were exceptionally well extracted.

Extraction of diverse metals from hydrochloric solutions. The extraction of the 20 metals from hydrochloric acid solution was examined. Magnesium and the alkaline earth metals were not extracted. The extraction patterns for Er(III), Mn(II), Ni(II) and Al(III) were very similar to those shown in Fig. 1. The extraction patterns for the other ions studied are shown in Fig. 2. Increases in the extractability of vanadium, iron, copper, zinc and scandium were observed with increased acidity. Uranium and zirconium were well extracted from hydrochloric acid solution. As is clear from Fig. 2,

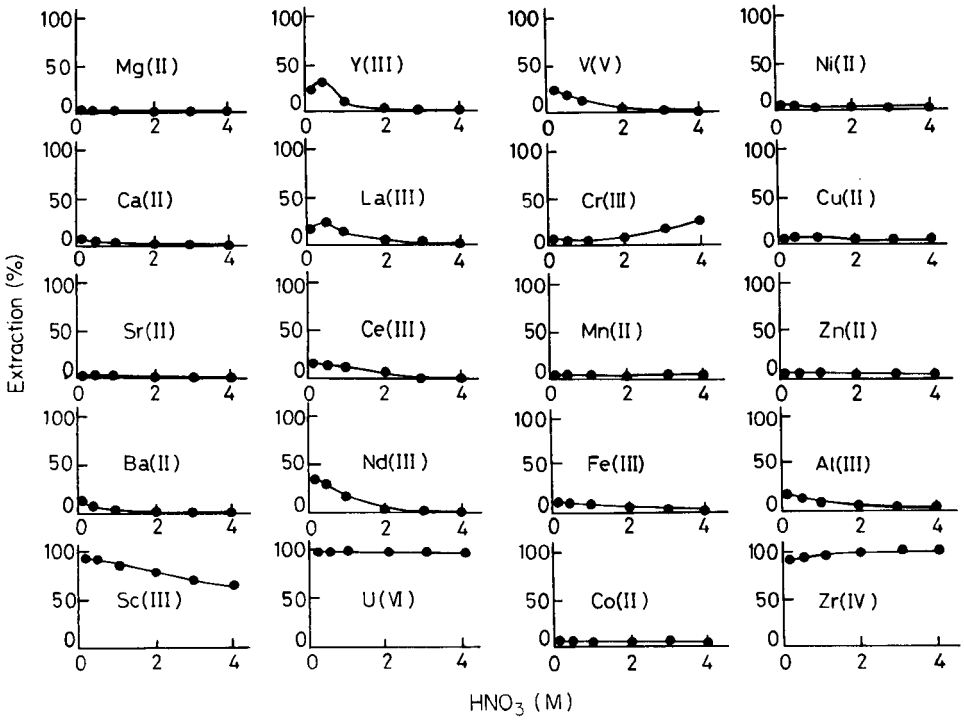

Fig. 1. Effect of the molarity of nitric acid on the extraction of metals into the TOPO—naphthalene phase at 80°C. Conditions: TOPO, 100 mg; naphthalene, 200 mg; metal ions, 10^{-4}—10^{-5} M; contact time, 5 min.

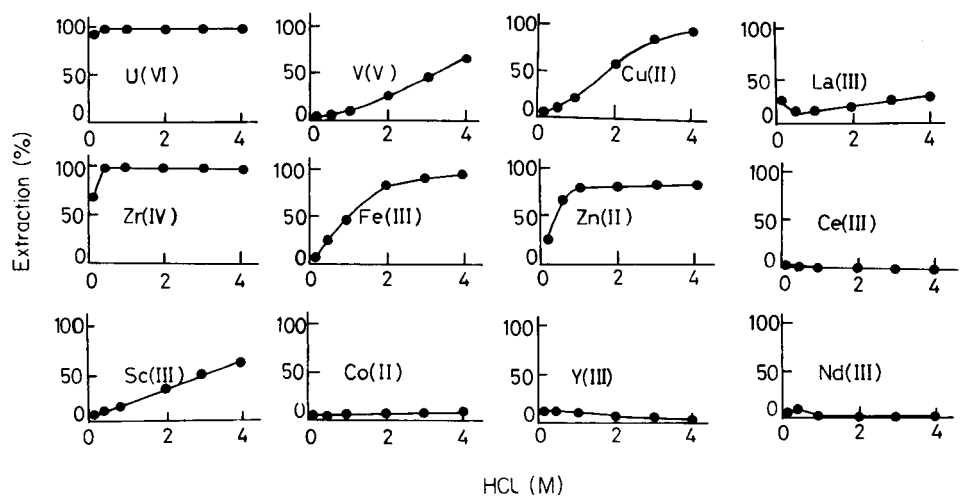

Fig. 2. Effect of the molarity of hydrochloric acid on the extraction of metals into the TOPO—naphthalene phase at 80°C. Other conditions as in Fig. 1.

uranium can be separated from alkaline earth metals and some transition metals, but not from iron, copper, vanadium, zinc or scandium.

Back-extraction of uranium. It is common knowledge that uranium forms stable complexes with carbonate ions. The back-extraction of uranium from the TOPO phase diluted with naphthalene was studied with sodium carbonate and ammonium carbonate (Table 1); 84.3% of the uranium was stripped with 1 M sodium carbonate solution but the recovery reached 97.5% when two back-extractions were done. When 1 M ammonium carbonate solution was used, back-extraction was essentially quantitative after two treatments, but the degree of stripping was poorer than that with sodium carbonate as the concentration of carbonate decreased. This can be attributed to the decomposition of ammonium carbonate even at 80°C.

Separation of uranium from other metals. From the extraction curves shown, it is clear that uranium can be separated from rare earth, alkaline earth and various transition metals. As an example. the separation of uranium from iron, strontium and lanthanum was examined by using 3 M nitric acid solution (Table 2). It was found that 100 μg of uranium could be quantitatively separated from iron (140—700 μg), strontium (45—898 μg) and

TABLE 1

Back-extraction of uranium (100 μg) from the TOPO—naphthalene phase with sodium carbonate or ammonium carbonate at 80°C

Na_2CO_3(M)	0.10	0.50	1.00	$(NH_4)_2CO_3$(M)	0.10	0.50	1
U(VI) Stripped (%)	69.66	82.00	84.27	U(VI) Stripped (%)	7.81	63.40	87
	90.80[a]	96.75[a]	97.51[a]		14.85[a]	86.45[a]	98

[a]Total percentage of uranium stripped in two back-extractions.

TABLE 2

Separation of uranium (100 μg) from iron, strontium and lanthanum in 3 M nitric acid solution

Ion added	Amount added (μg)	U(VI) extracted (μg)	Unextracted metal[a] (μg)	Ion added	Amount added (μg)	U(VI) extracted (μg)	Unextr metal[a] (μg)
Fe(III)	140	98.9	137	La(III)	69.8	98.5	58.2
	350	98.3	347		140	98.5	129
	700	97.7	685		349	97.8	353
					698	95.7	698
Sr(II)	44.9	98.6	43.9		1400	98.7	1450
	89.9	98.0	89.6				
	225	97.9	218				
	449	98.9	438				
	898	97.7	863				

[a]Amount of metal remaining in the aqueous phase.

lanthanum (69.8—1400 μg). It is also clear that the extraction efficiency is improved by using naphthalene instead of cyclohexane, etc.

REFERENCES

1 Y. Marcus and A. S. Kertes, Ion Exchange and Solvent Extraction of Metal Complexes, J. Wiley, New York, 1969, 650 pp.
2 J. C. White and W. J. Ross, NAS-NA 3102, 1961.
3 T. Ishimori, K. Kimura, T. Fujino and H. Murata, J. At. Energy Soc. Jpn., 4 (1962) 41.
4 T. Ishimori, K. Watanabe and E. Nakamura, Bull. Chem. Soc. Jpn., 33 (1960) 636.
5 T. Ishimori, K. Watanabe and T. Fujino, J. At. Energy Soc. Jpn., 3 (1961) 19.
6 H. L. Finston, E. T. Williams and A. S. Kertes, J. Inorg. Nucl. Chem., 41 (1979) 420.
7 K. Murata, Y. Yokoyama and S. Ikeda, Anal. Chem., 44 (1972) 805.
8 B. G. Stephens and H. A. Suddeth, Anal. Chem., 39 (1967) 1478.
9 See, e.g., M. Satake, Y. Matsumura and T. Fujinaga, Talanta, 25 (1978) 718; T. Fujinaga, M. Satake and T. Yonekubo, Bull. Chem. Soc. Jpn., 46 (1973) 2090; Bunseki Kagaku, 18 (1969) 1113; N. Ichinose, S. Yamada, N. Sakurai, T. Fujiyama and N. Masuda, Fresenius Z. Anal. Chem., 293 (1978) 23.
10 Y. Shigetomi, T. Kojima and M. Shinagawa, J. Nucl. Sci. Technol., 14 (1977) 811; J. At. Energy Soc., 18 (1976) 796.
11 R. J. Baltisberger, Anal. Chem., 36 (1964) 2369.

Analytica Chimica Acta, 116 (1980) 205—210

Short Communication

DETERMINATION OF METALS IN SMALL SAMPLES BY ATOMIC ABSORPTION AND EMISSION SPECTROMETRY WITH DISCRETE NEBULIZATION

TETSUO UCHIDA, ISAO KOJIMA and CHUZO IIDA*

Laboratory of Analytical Chemistry, Department of Engineering Sciences, Nagoya Institute of Technology, Gokiso-cho, Showa-ku, Nagoya 466 (Japan)

(Received 13th August 1979)

Summary. Eight elements in NBS-SRM 1577 bovine liver and other biological standards are determined by flame atomic absorption (Ca, Cu, Fe, Mg, Mn and Zn) and emission (K and Na) spectrometry. Samples (2 mg) weighed into a 3.8-ml teflon vessel are decomposed with 40 μl of (5 + 1) nitric—perchloric acids in a sealed teflon vessel. A 75-μl or 100-μl aliquot of the diluted sample solution is injected into a small teflon funnel coupled directly to the nebulizer needle of the spectrometer. The results obtained agree well with certified values: the standard deviation is about 2%.

In flame atomic absorption spectrometry (a.a.s.), 1—4 ml of sample solution is generally used for the determination of a single element. For multi-element determinations, the volume of sample solution or the amounts of original sample must be large. Thus for small amounts of sample, the concentration of elements to be determined may be less than their detection limit as a result of the high dilution after sample decomposition, necessary to allow the determination of a series of elements. To overcome this difficulty, it is possible to determine an element by flame a.a.s. in a microliter sample volume ($\lesssim$100 μl). Various workers [1—4] have studied this technique, proving that nebulization of a 100-μl sample gives the same sensitivity as that obtained by conventional nebulization. Two nebulization techniques have been proposed for small volumes, i.e. nebulization from a small teflon funnel coupled directly to the nebulizer needle [1—3, 5—7] or from a small hole cut in the surface of a teflon rod [4]. These methods have been applied to the determination of elements in NBS-SRM 1571 orchard leaves [2], serum [2], fish [8], NBS-SRM 1577 bovine liver [4], steel [9] and blood [9].

Many workers [10—12] have reported that the decomposition of organic materials, silicates, etc. with an acid mixture is easily done in a sealed teflon vessel at room or elevated temperatures. However, it was not known whether the decomposition of milligram amounts of organic materials was possible with small volumes of acid in such vessels.

The present communication deals with the decomposition of milligram amounts of biological materials with small volumes of nitric and perchloric

acids in a teflon vessel, followed by atomic absorption (a.a.s.) or emission (a.e.s.) determination of the elements with a discrete nebulization technique. The proposed method has been successfully applied to the determination of eight elements in standard biological samples.

Experimental

Reagents. The acids used were of SSG quality (Wako Pure Chemicals Co.). Twice-distilled water was used for all dilutions.

Metal stock solutions (2000 ppm, 0.5 M HCl or HNO_3) were prepared by dissolving metals (Cu and Zn, 99.999%; Mitsuwa Pure Chemicals Co.) or metal compounds (MgO ignited at ca. 1000°C, $CaCO_3$, Fe_2O_3, MnO_2, all Johnson Matthey Specpure; KCl and NaCl, Merck p.a.) in HCl or HNO_3 and diluting to 200 g.

Lanthanum stock solution (1% w/v in 0.1 M HNO_3) was prepared from La_2O_3 (99.99%; Nakarai Pure Chemicals Co.).

Working mixed standard solutions were prepared gravimetrically by diluting the stock solutions to the appropriate concentration in 10-ml polypropylene bottles. These solutions contained the eight elements and the same concentrations of nitric and perchloric acids as in the sample solutions.

Apparatus. A Hitachi Model 518 atomic absorption spectrometer equipped with a 100-mm burner head (acetylene—air flame) was used in conjunction with a fast-response strip-chart recorder (Rikadenki B-281, Mark II). The flow rate of auxiliary air could be freely varied at a constant sample aspiration rate. The optimum operating conditions were: acetylene, 3.3 l min^{-1} (0.5 kg cm^{-2}); air, 4.8 l min^{-1} (1.5 kg cm^{-2}) for the nebulizer and 11.0 l min^{-1} (1.5 kg cm^{-2}) auxiliary; burner height, position 2.5; sample flow rate, 3.2 ml min^{-1}. The wavelengths used were: Cu, 324.8 nm; Zn, 213.9 nm; Fe, 248.3 nm; Mn, 279.5 nm; Ca, 422.7 nm; Mg, 285.2 nm; Na, 589.0 nm; and K, 766.5 nm. Solutions ($\lesssim$100 μl) were nebulized by injection into a small teflon funnel coupled directly to the nebulizer needle (Fig. 1).

Powdered samples (1—2 mg) were weighed on a Chyo Jupitor M_1-20A microbalance. An agate mortar and pestle are used to repulverize standards. Gilson (P5000, P1000, P200) and Nichiryo (Juster V50) micropipettes were used for dilution.

Samples were decomposed in the sealed digestion bomb shown in Fig. 2. This bomb contains two teflon vessels, an inner 3.8-ml (ca. 5.8 g) mini-vessel with a cap and an outer 23-ml vessel.

Recommended procedure. The sample (2 mg) was weighed into the mini-vessel and 40 μl of (5 + 1) nitric acid—perchloric acid was added. The small vessel was placed in the large vessel which was then sealed. After decomposition for 3 h at 130°C, and cooling to room temperature, the contents of the mini-vessel were diluted to 1.5 g (analytical balance) with twice-distilled water. Aliquots of this solution (100 or 75 μl for a.a.s. and 100 μl for a.e.s.) were injected for measurement. Calibration curves were prepared with the same volumes of solution. For calcium, 2000 ppm lanthanum was tolerated.

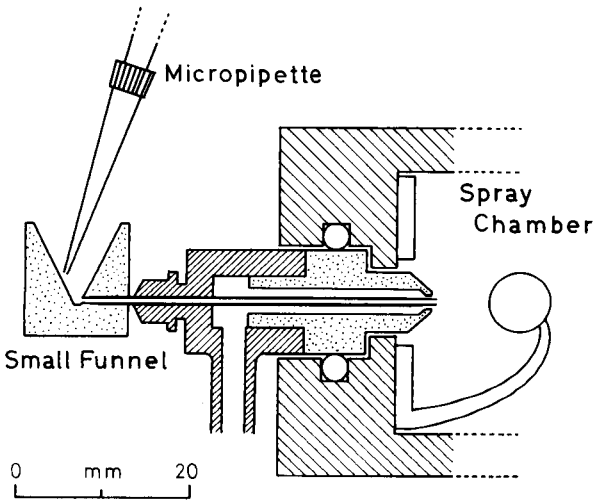

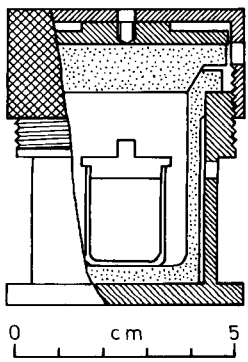

Fig. 1. Schematic diagram of discrete nebulization assembly.

Fig. 2. Sealed acid digestion vessel, showing inner (3.8 ml) and outer (23 ml) teflon vessels.

Washing of equipment. Teflon vessels and polyethylene and polypropylene bottles were cleaned by soaking first in 4 M HNO_3 for a day at room temperature, 6 M HCl for two days at 90°C, and 0.1 M HCl for three days at 90°C, in a teflon tank, and finally by washing with distilled water. Clean bottles and vessels were dried under reduced pressure at ambient temperature.

Results and discussion

Nebulization technique. Up to 100 μl of sample solution is injected as shown in Fig. 1. Figure 3 shows the spike-like signals obtained with various volumes (10—1000 μl) of 0.5 ppm copper solutions at the sample flow rate of 3.2 ml min^{-1}. The signal increases with injected volume up to about 60 μl; thereafter, the signal intensity remains the same as that obtained by continuous nebulization. However, the injected volume necessary to obtain the same signal as that of continuous nebulization is about 100 μl for the flame emission of 10 ppm sodium, because the electrical circuitry for emission measurements is more highly damped. In the present study, 75 μl (Cu, Fe, Ca, Mg, Mn) and 100 μl (Zn) were used for a.a.s. and 100 μl (Na, K) for a.e.s.

The reproducibilities of the signals obtained for various volumes of 0.5 ppm copper solution and 10 ppm sodium solution are given in Table 1. The relative standard deviation for 75-μl samples in atomic absorption and 100-μl samples in emission is similar to that obtained by continuous nebulization.

Sample decomposition. The effects of time and temperature on the decomposition of 5 mg of bovine liver were studied at 100—150°C and for 1—5 h, in a similar way to previous studies [12]. With decomposition at 130°C,

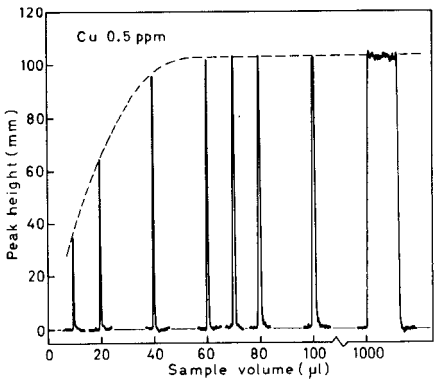

Fig. 3. Effect of injected sample volume on absorption signal for copper.

TABLE 1

Reproducibility of peak height (n = 10)

Method	Volume (μl)	Peak height (mm)	S.d. (mm)	R.s.d. (%)
A.a.s.	20	66.8	2.2	3.3
(0.5 ppm Cu)	40	95.8	1.4	1.4
	75	104.0	0.9	0.9
A.e.s.	20	56.9	1.0	1.8
(10 ppm Na)	50	89.3	1.2	1.3
	100	121.8	0.7	0.6

no significant differences were observed in the results for Cu, Fe, Zn, Na, K, Ca or Mg with digestion times of 1—5 h. However, sample solutions obtained by digestion below 110°C for less than 2 h were a little viscous, and could be ejected from the micropipette tip only with difficulty, making it difficult to obtain reproducible results. Solutions from samples decomposed above 120°C for longer than 3 h did not adhere to the tip wall and reproducible results were easily obtained. Therefore, it is recommended that samples are decomposed at 130°C for 3 h.

It was shown previously [12] that 500 mg of sample was completely decomposed by a mixture of concentrated nitric (5 ml) and perchloric (1 ml) acids in a sealed teflon vessel for 2 h at 120°C. For the decomposition of 5-mg amounts of sample, the volume of acid mixture used was decreased proportionately, i.e. a mixture of nitric (50 μl) and perchloric (10 μl) acids was used. Satisfactory results were obtained, but for the decomposition of 2-mg (or 1-mg) samples, about twice the proportional volume of acid mixture was used (40 μl or 20 μl), to ensure adequate

TABLE 2

Results for different weights of NBS-SRM 1577 bovine liver

Sample weight (mg)	Final amount	Element (ppm)						
		Cu	Zn	Fe	Na	K	Ca	Mg
250	25 ml	189	134	276	—	—	119	600
25	25 ml	181	128	237	—	—	124	572
5	2.5 g	189	132	266	2390	9840	127	593
2	1.5 g	195	127	274	2420	9690	127	602
1	0.5 g	193	—	—	2500	—	—	602
Certified values		193 ±10	130 ±13	268 ±8	2430 ±130	9700 ±600	124 ±6	604 ±9

TABLE 3

Results for NBS-SRM 1577 bovine liver in 2-mg and 1-mg samples

	Element (ppm)						
	Cu	Zn	Fe	Na	K	Ca	Mg
Bovine liver 2 mg → final weight 1.5 g; 40 μl (5 + 1) HNO_3—$HClO_4$							
Mean[a]	195 ± 4	127 ± 4	274 ± 5	2420 ± 50	9690 ± 220	127 ± 7	602 ± 11
Certified value	193 ± 10	130 ± 13	268 ± 8	2430 ± 130	9700 ± 600	124 ± 6	604 ± 9
Bovine liver 1 mg → final weight 0.5 g; 20 μl (5 + 1) HNO_3—$HClO_4$							
Mean[a]	193 ± 4	—	—	2500 ± 120	—	—	602 ± 9

[a]Mean of 5 complete analyses.

moistening of the sample. The results obtained (Tables 2—4) show that the sample was completely decomposed by such small amounts of the acid mixture. The solutions obtained after dilution as described in the Procedure were clear and not viscous.

Spectrometric measurements. The absorbance of calcium and the emission intensity of potassium decrease with increasing perchloric acid concentration, whereas the absorbance of Cu, Zn, Mg, Fe and Mn and the emission intensity of Na are not affected by varying amounts of perchloric acid less than 0.5 M. For all eight elements studied, the presence of nitric acid below 0.5 M does not alter the signals. Thus the same concentration of perchloric acid was added to the standard solution of elements used for preparing calibration graphs.

As NBS-SRM 1577 bovine liver contains 1.1% phosphorus, the final solution contains less than 25 ppm of phosphorus. It was found that the addition of lanthanum to give a concentration of 2000 ppm in the final solution allowed calcium to be determined without interference from

TABLE 4

Results for 8 elements in biological samples (ppm) (n = 5)

Element	Shark powder			SRM 50, Albacore tuna			SRM 1566 Oyste	
	This work	Na.a. [13]	A.a.s./a.e.s. (14)	This work	Na.a. [13]	A.a.s./a.e.s. [15]	This work	Va [16
Cu	(0.8)	—	—	(3.5)	3.32	—	63	63
Zn	(12)	10	15	(16)	13.5	—	860	859
Fe	(12)	27	12	53	57	—	209	195
Mn	(0.6)	—	—	(0.9)	0.7	—	19	—
Ca	242	—	200	140—310	—	287	880—3370	1500
Mg	984	—	1080	1150	—	1180	1280	1270
Na	2990	3510	4060	1020	1030	1150	4920	—
K	15500	15700	17200	12700	12800	12800	9770	9810

(Sample 5 mg → final weight 1.5 g (10 mg → 0.5 g).)

⩽100 ppm of phosphorus. This was achieved by adding 50 μl of the lanthanum solution (1% w/v) to 200 μl of sample solution and then injecting 75 μl of the mixture. Lanthanum was also added to the standard calcium solutions.

Analysis of bovine liver. Results for seven elements in NBS-SRM 1577 bovine liver obtained with various sample sizes are summarized in Table 2. The 250-mg and 25-mg samples were decomposed in two steps, at 90°C for 3 h and then at 120°C for 3 h; the small samples were decomposed as recommended above. Reproducibility and accuracy are satisfactory. The results obtained for 2-mg samples and for 1-mg samples (Table 3) also show reasonable precision and accuracy.

Analysis of other biological standards. The recommended method was applied to the analysis of shark powder (Tokyo University) and NBS albacore tuna and oyster tissue (Table 4).

REFERENCES

1 E. Sebastiani, K. Ohls and G. Riemer, Fresenius Z. Anal. Chem., 264 (1973) 105.
2 D. C. Manning, At. Abs. Newsl., 14 (1975) 99.
3 H. Berndt and E. Jackwerth, Spectrochim. Acta, Part B, 30 (1975) 169.
4 T. Uchida, I. Kojima and C. Iida, Bunseki Kagaku, 27 (1978) T44.
5 E. Jackwerth and H. Berndt, Anal. Chim. Acta, 74 (1975) 299.
6 H. Berndt and E. Jackwerth, At. Absorpt. Newsl., 15 (1976) 109.
7 P. D. Goulden, At. Absorpt. Newsl., 16 (1977) 121.
8 G. J. Ramelow and T. I. Balkas, Anal. Lett., 10 (1977) 733.
9 K. C. Thompson and R. G. Godden, Analyst, 101 (1976) 96, 174.
10 B. Bernas, At. Absorpt. Newsl., 9 (1970) 52.
11 T. Uchida, M. Nagase, I. Kojima and C. Iida, Anal. Chim. Acta, 94 (1977) 275.
12 C. Iida, T. Uchida and I. Kojima, Anal. Chim. Acta, 113 (1980) 361, and references therein.
13 K. Kudo, private communication.
14 Y. Dokiya, S. Kurosawa, S. Toda and K. Fuwa, Bull Chem. Soc. Jpn., 51 (1978) 3649.
15 Y. Dokiya, private communication.
16 T. L. Barnes, private communication.

Analytica Chimica Acta, 116 (1980) 211—216

Book Reviews

T. Torok, J. Mika and E. Gegus, *Emission Spectrochemical Analysis*, Akademiai Kiado, Budapest, and Adam Hilger, Bristol, 1978, 692 pp, price £31.50.

This must be one of the most comprehensive treatments of any analytical technique to be produced, and as such, a copy should be available in every laboratory in which emission spectrochemical analysis is carried out. The approach is uncompromisingly practical and even the experienced emission spectroscopist will get much value from the book. The emphasis is also on the analytical chemistry of this technique rather than the optical and electronic design of instrumentation, so that readers looking for information on recent developments in photodiode arrays, echelle spectrometers, etc. will be disappointed.

The first three main chapters deal with sampling, radiation sources and the conditions affecting line intensities. Both the sampling and radiation sources chapters are divided according to the different types of sample, metals and alloys, non-conducting solid substances, solutions and liquid substances and gases. The comprehensive nature of the text can be illustrated by taking an example from this list. For metals and alloys, the authors discuss the sampling of analysis of solid factory products, of metal chips, powders and cast samples and then cover reference and standard samples. Under radiation sources, they cover the type of electrodes used for excitation, the effect of rotation of electrodes and of the gas atmosphere during discharge, and also the methods of obtaining local micro-spectral analysis. In the third of these chapters, the authors include the effects of electrical excitation conditions, the effects of the physical and chemical properties of the sample and interferences, the resolution of the emission signal with respect to space and time and optical problems such as background, line overlap, self-absorption and selection of analytical line pairs for comparison.

Following these basic chapters are three chapters dealing, respectively, with spectrographic analysis, spectrometric analysis and visual spectroscopic analysis. All aspects of these techniques appear to be covered thoroughly, from the processing of photographic emulsions to the methods of interpretation, reference samples, background and spectral corrections and typical analytical procedures. The authors also give useful hints on methods of evaluating instruments and the choice of technique and intrument for particular analytical problems and finally discuss the installation and organisation of the instrumental technique in a laboratory. In addition, they include a useful comparison of spectrometric and spectrographic methods. The final chapter deals with methods of evaluating the results and the book is completed with extensive (over 130 pages) tables of useful

data on the metals and their compounds, wavelengths, homologous line pairs for the semiquantitative spectrographic analysis of many different materials, and the compositions and analytical conditions suitable for spectrochemical analysis of many types of material using different types of instruments.

The above details have been mentioned to give a realistic impression of the contents of this text but represent only some of the salient features. The reviewer has no doubt of the immense practical value of this book.

J. M. Ottaway

J. B. Dawson (Ed.), *Annual Reports on Analytical Atomic Spectroscopy Reviewing 1977*, Chemical Society, London, 1978, ix + 291 pp., price £17.50.

This extremely useful review publication continues in its original format, the first section devoted to fundamentals and instrumentation, the second to methodology. Developments in all aspects of analytical atomic spectroscopy are covered, as well as related topics such as molecular emissions in flames. The great current interest in areas such as plasmas and carbon furnace atomizers is reflected in the extent of coverage by the reviewers. In addition, there are useful tabulations of available instrumentation, and of suppliers of spectrographic graphite electrodes, standard solutions and reagents for atomic absorption spectrometry, and organometallic and spectrographic standards. The continuing but perhaps slowing growth of the subject is reflected in an increase of nine pages and twenty five references (1707 papers and lectures are reviewed) over the 1976 Review. For the first time, the book is in hardback.

For anyone involved in analytical flame spectroscopy or related fields, this book should be indispensable. As with other Chemical Society publications, the book will not be found on bookshop shelves, and has to be ordered from the Chemical Society. The little extra effort required to do this, however, will be greatly rewarded by the value of the review material.

A. Townshend

M. Slavin, *Atomic Absorption Spectroscopy*, 2nd edn., Wiley-Interscience, New York, 1978, 193 pp., price £14.

This second edition is a revision, by the father, of the son's (Walter Slavin) first edition of 1968 (Volume 25 in the Chemical Analysis series of monographs), and is addressed according to the preface "to the practical worker at the bench, whom I think of as a person interested primarily in analytical chemistry" (presumably he means chemical analysis) "and only marginally in atomic and optical theory". This orientation is, in fact, borne

out as, although 18% of the text is devoted to atomic and optical theory, the treatments are oversimplified and contain many errors. Unfortunately, the sections on interference effects and calibration procedures are similar in content, rendering the book virtually useless as a student text. The 21 pages of physical and chemical data provide a compact source of useful practical information. However, the 38 pages of extended summaries (with comments) serve only to illustrate the wide variety of sample types that can be analysed, and are no substitute for the original literature. Although several reviews are cited, some major and continuously updated reviews are omitted. The historical introduction makes interesting reading through the author's personal, almost enthusiastic, style of writing; unfortunately this interest quickly gives way to irritation as the theoretical sections are tackled. Perkin-Elmer get a good plug and the index is poor.

J. F. Tyson

O. Budevsky, *Foundations of Chemical Analysis*, Ellis Horwood, Chichester, 1979, 372 pp., price £18.50.

Research and developments in instrumental analytical chemistry over the last two decades have induced in many universities and colleges neglect of the study and teaching of basic reaction chemistry, classical separations and the associated thermodynamics. This text is therefore welcome in drawing attention to the foundations of chemical analysis.

The simplest description of the text is that it is an East-European equivalent to Laitinen and Harris's *Chemical Analysis*. The early chapters deal with revision of basic thermodynamics, the significance and use of equilibrium constants, graphical methods in analytical chemistry, the structure and properties of water and non-aqueous solvents, acid—base equilibria and indicators. The bulk of the text is concerned with volumetric methods. The expositions of titrations in non-aqueous media, use of side-reaction coefficients and conditional stability constants are particularly clear and helpful. Gravimetric methods are dismissed in 15 pages. The only instrumental method discussed is potentiometry; detailed treatments are given for indicator electrodes, reference electrodes, determination of pH, and graphical methods (including that of Gran) for the determination of equivalence points, but there is no account of the specification for, or the design of, any measurement devices.

It is regrettable that the author did not include solvent extraction or references to the sources used in preparation of the text. This latter defect seriously detracts from the value of an otherwise good approach to selected aspects of chemical analysis. The non-expert or the beginner will have great difficulty in following up points of interest. The text contains much of value to those who teach basic chemistry or chemical analysis courses.

D. Thorburn Burns

John Burgess, *Metal Ions in Solution*, ISBN-0-85312-027-7, Ellis Horwood, Chichester, 1978, 481 pp., price £25.00 (hardback), £8.50 (paperback).

The behaviour of metal ions in solution is an important aspect of much of analytical chemistry. The formation of complexes and precipitates, and redox and acid—base reactions can all involve metal ions, so that a thorough grasp of the nature of metal ions in solution, and of the kinetics and mechanisms of their reactions, is an essential basis for the development of a wide variety of reliable analytical procedures. The present book provides such a background in a very clear, pleasant and comprehensive manner. It deals with solvation (aqueous and non-aqueous) in some detail, including methods of investigation of solvation. Redox potentials, hydrolysis and polymerization, and the kinetics and mechanism of complex formation are also described. There is a vast amount of factual information, and each chapter is extensively referenced. The book is written at the senior undergraduate level, and should be of great value to all chemists who are involved with metal ions in solution, not least, of course, analytical chemists.

A. Townshend

J. W. Bridges and L. F. Chasseaud (Eds.), *Progress in Drug Metabolism, Vol. 3*, J. Wiley, Chichester, 1979, ix + 372 pp., price £19.25.

Few branches of analytical chemistry are of more importance than its application to drug metabolism studies. It is therefore appropriate that this volume, which certainly maintains the high quality of its predecessors, includes two reviews of direct interest to analysts. The first, by D. A. Schooley and G. B. Quistad, deals with "High-pressure, High-resolution Liquid Chromatography and its Application to Pesticide Analysis and Biochemistry." It incorporates a brief, but lucid, introduction to the theory and experimental practice of h.p.l.c., but is mainly devoted to an extensive survey of the applications of this technique to many types of pesticide. Much of the information is tabulated in a particularly clear and useful format. The second review, "Rational Analysis of Drugs in Biological Fluids with Particular Reference to the Tricyclic Antidepressants", is by W. Riess, S. Brechbühler and J. P. Dubois. Their stimulating article summarises critically the principal methods used in the analysis of the tricyclics (and, of course, of many other drugs) and emphasises in a salutary manner the methodological and interpretative difficulties of such analyses. Analysts working in the life sciences may well find that this book (excellently produced, and — by modern standards — moderately priced) is worth buying for these two articles alone.

J. N. Miller

G. W. Cullen and C. C. Wang (Eds.), *Heteroepitaxial Semiconductors for Electronic Devices*, Springer-Verlag, Berlin, 1978, xi + 299 pp., price DM 158; $79.00.

The editors, who belong to R.C.A. Laboratories, dedicate this book to their management, "who feel that communication with our scientific colleagues is part of our job". They go on to explain that their purpose is to describe in some detail the preparation and characterisation of hetero-epitaxial thin films of silicon, III—V compounds and alloys, and II—VI compounds deposited on sapphire and spinel substrates. Applications are indicated. The book therefore concerns a "coalescence of technologies"; the authors of individual chapters have worked closely together at R.C.A. Laboratories but their intent has been to describe the development of the field including pertinent work by other research groups. The result is a text of considerable interest and value to scientists and technologists working on the research and development of electronic devices. Parts of it would make good background reading for analytical chemists contributing to the manufacture of devices, but there is little of direct use to the analytical chemist, or of interest to him, outside the field of device production.

Specifically, there is some account of the application of secondary-ion mass spectrometry in determining impurity profiles, of low-energy electron diffraction and Auger analysis in the vacuum heteroepitaxial growth of silicon. Mention is made of a variety of other techniques, including Rutherford ion-scattering, electron spectroscopy, etc., and of physical measurements that permit the derivation of dopant densities, albeit non-specifically. There are references to good reviews but nowhere in the book is sufficient detail given for it to be useful to the analytical chemist faced with a specific problem.

The book is excellently produced and it may be welcomed by a particular kind of technologist; for the general reader it is ferociously expensive and there are many better surveys of modern instrumental techniques for the analysis of semi-conductor surfaces.

J. P. G. Farr

G. Brooks King, W. E. Caldwell and M. B. Williams, *Laboratory Experiments in College Chemistry*, D. Van Nostrand, New York, 4th edn., 1979, x + 334 pp., £5.95 (paperback).

The experiments are designed to accompany the authors' College Chemistry (7th edn.) and to provide a full year's course in general chemistry. The contents cover simple analytical, physical and inorganic chemistry with only a few experiments in organic chemistry, and every effort has been made to reduce potential hazards and the use of dangerous chemicals. The standard of the material is a blend of O- and A-level chemistry in the United Kingdom. Those concerned with trends in chemical education might like to note that,

in response to requests, a section on qualitative analysis of some common anions and cations has been restored to this edition. A less desirable feature is the insistence on totally standardised laboratory reports. To expedite correcting and marking, separate report sheets are included for each experiment, with graph paper if needed. The whole book is perforated so that reports may be detached and handed in. The text which remains might also be regarded as disposable. U.K. sales are unlikely to be great in that the book does not meet the syllabus requirements for any A-level board nor is it likely they would accept standardised reports for the whole of a practical course.

D. Thorburn Burns

ACA announcements

GABOR SZASZ PRIZE FOR CLINICAL ENZYMOLOGY 1981

The Deutsche Gesellschaft für Klinische Chemie will award the first Gabor Szasz prize in 1981. This prize, worth DM 10,000, is donated by the Deutsche Gesellschaft für Klinische Chemie e.V., in honour of the late Gabor Szasz, for outstanding advances in the field of clinical enzymology with special bearing on methodological or theoretical progresses. Applications for the prize in 1981 must be accompanied by scientific papers published or accepted for publication during the period January 1, 1979 and December 31, 1980. Applications (three copies) must be submitted before November 15, 1980 to the Secretary of the Prize Committee, Prof. Dr. G. Gundlach, Zentrum für Biochemie der Justus Liebig-Universität, Friedrichstr. 24, 63-Giessen, F.R.G.

ANNOUNCEMENTS OF MEETINGS

INTERNATIONAL SYMPOSIUM ON ELECTROANALYSIS IN CLINICAL ENVIRONMENTAL AND PHARMACEUTICAL CHEMISTRY, April 13–16, 1981, UWIST, Cardiff, Wales, United Kingdom

This Symposium is organised by The Electroanalytical Group of The Analytical Division of The Chemical Society. The programme of the Symposium will emphasise methodology and applications of electroanalytical methods, especially regarding ion-selective electrodes, gas sensors and polarography. Aspects of development, operation and mechanisms as well as new areas, such as piezoelectric crystals will be included where these are likely to have relevance to the progress of electroanalysis in the biomedical and environmental fields.

Contact: Short Courses Section (Electroanalysis Symposium), UWIST, Cardiff CF1 3NU, Wales, United Kingdom.

EXPOCHEM '80, an international exposition of analytical instrumentation in the industrial and biomedical fields, will be held at the Astrohall in Houston, Texas on October 6–9, 1980.

The technical programme will consist of presentations by the leading authorities in most areas of analytical chemistry from throughout the world. Topics to be included are: emission spectroscopy, automation, environmental analysis, new instrumentation, surface analysis, pharmaceutical analysis and data treatment. The chromatography section will be represented by the 15th International Symposium on Advances in Chromatography which will be included as part of EXPOCHEM '80. Current developments in gas chromatography, high performance liquid chromatography, high performance thin-layer chromatography and gas chromatography–mass spectrometry will be presented. Intensive short courses on a variety of subjects will be given on the weekend prior to the exposition.

Inquiries regarding exhibition space, technical programme or short courses should be directed to: Dr. Albert Zlatkis, Chemistry Department, University of Houston, Texas 77004, U.S.A. or phone (713) 749-2623.

CALENDAR OF FORTHCOMING MEETINGS

April 17–19, 1980 Athens, Greece	**Balkan Chemistry Days – All aspects of research chemistry** Contact: B.C.D.'s Secretariat, The Association of Greek Chemists, 27, Kaningos Street, Athens (147), Greece.
April 21–25, 1980 Boston, U.S.A.	**2nd International Congress on Phosphorous Compounds** Contact: IMPHOS, 8, rue de Pentievre, 75008, Paris, France.
April 22–24, 1980 London, Great Britain	**Labware 80** Contact: Labware Promotions, 28 Worple Road, London SW19 4EE, Great Britain.

April 23, 1980 Birmingham, Great Britain	**Chemical Society/Analytical Division – Newer Techniques of Analysis** Contact: Miss P.E. Hutchinson, Analytical Division, The Chemical Society, Burlington House, London W1V 0BN, Great Britain. Tel. 01–734 9971.
April 23–25, 1980 King of Prissia, Pa., U.S.A.	**ACS – 14th Middle Atlantic Regional Meeting** Contact: Henry C. Beck, P.O. Box 133, Swarthmore, Pa. 19081, U.S.A. Tel. (215) 387-2255.
April 27–29, 1980 Neuherberg/Munich, F.R.G.	**First International Workshop on Trace Element Analytical Chemistry in Medicine and Biology** Contact: Dr. P. Schramel, Gesellschaft für Strahlen- und Umweltforschung, Physikalisch-Technische Abteilung, Ingolstädter Landstrasse 1, D-8042 Neuherberg, F.R.G.
April 29–May 2, 1980 Munich, F.R.G.	**Biochemische Analytik 80 (7th European Conference on Biochemical and Instrumental Analysis)** Contact: Dr. Rosmarie Vogel, Nussbaumstr. 20, P.O. Box 200324, D-8000 Munich 2, F.R.G. Tel. (089) 15 14 19.
May 25–30, 1980 New York, N.Y., U.S.A.	**28th Annual Conference of the Amer. Soc. for Mass Spectrometry** Contact: Dr. H.M. Fales, c/o NIH, Building 10, Room 7N 322, Bethesda, Md. 20014, U.S.A.
May 27–30, 1980 Balaton Lake, Hungary	**4th Symposium on Ion Exchange** Contact: Professor J. Inczédy, Organizing Committee, 4th Int. Symposium on Ion Exch., P.O. Box 28, Veszprém, H-8201 Hungary.
May 28–30, 1980 Dortmund, F.R.G.	**10th Annual Symposium on the Analytical Chemistry of Pollutants** Contact: J. Wendenburg, Gesellschaft Deutscher Chemiker, P.O. Box 900440, D-6000 Frankfurt/Main, F.R.G. Tel. (0611) 791 73 66. (Further details published in Vol. 113, No. 2)
May 30, 1980 Glasgow, Scotland, Great Britain	**High Speed Automatic Analysis** Contact: D.G. Porter, Laboratory of the Government Chemist, Cornwall House, Stamford Street, London SE1 9NQ, Great Britain.
June 2–3, 1980 Petten, The Netherlands	**Workshop on Ion-Chromatography – Development of Ion-Chromatography Techniques and Application of Ion-Chromatography** Contact: Dr. J. Slanina, Workshop on Ion-Chromatography, ECN, 1755 ZG Petten, The Netherlands.
June 4–5, 1980 Scarborough, Great Britain	**33rd Chemists' Conference – British Independent Steel Producers Association** Contact: Mr. L.L. Green, The British Independent Steel Producers Assoc., 4 Melbourne Ave., Sheffield S10 2QL, Great Britain. (Further details published in Vol. 122, No. 1)
June 8–11, 1980 Ottawa, Ontario, Canada	**63rd Canadian Chemical Conference and Exhibition** Contact: Don Emmerson, 151 Slater St., Suite 906, Ottawa, Ontario, Canada K1P 5H3, Tel. 613-233-5623.
June 10–13, 1980 Ghent, Belgium	**3rd International Symposium on Quantitative Mass Spectrometry in Life Sciences** Contact: Professor A.P. De Leenheer, Laboratoria voor Medische Biochemie en Klinische Analyse, de Pintelaan 135, B-9000 Ghent, Belgium.
June 16–18, 1980 Milan, Italy	**7th International Symposium on Mass Spectrometry in Biochemistry, Medicine and Environmental Research** Contact: Dr. A. Frigerio, Istituto di Ricerche Farmacologiche "Mario Negri", Via Eritrea 62, 20157 Milan, Italy.
June 18–19, 1980 London, Great Britain	**Nuclear Magnetic Resonance Spectroscopy in Solids** Contact: The Executive Secretary, The Royal Society, 6 Carlton House Terrace, London SW1Y 5AG, Great Britain.

June 18–20, 1980 Brigham Young U, Provo, Utah, U.S.A.	**2nd Symposium on Environmental Analytical Chemistry** Contact: Delbert J. Eatough, 271 FB, Thermochemical Institute, Brigham Young U, Provo, Utah 84602, U.S.A.
June 23–27, 1980 Birmingham, Great Britain	**Eurochem 80** Contact: Andrew Dedman, Clapp & Polick Europe Ltd., 232 Acton Lane, London W4 5DL, Great Britain.
June 26–29, 1980 Strasbourg, France	**International Symposium: Affinity Chromatography and Molecular Interaction** Contact: Dr. J.M. Egly, Faculté de Médicine, Institut de Chimie Biologique, 11 rue Humann, 67085 Strasbourg Cédex, France.
June 30–July 4, 1980 Cannes, France	**13th International Symposium on Chromatography** Contact: GAMS, 88 Boulevard Malesherbes, 75008 Paris, France.
July 7–11, 1980 Brussels, Belgium	**2nd International Congress on Toxicology** Contact: Secretariat, SdR Assosiated, 16 Avenue des Abeilles, B–1050 Brussels, Belgium.
July 20–26, 1980 Lancaster, Great Britain	**SAC 80** Contact: The Secretary, Analytical Division, The Chemical Society, Burlington House, London W1V 0BN, Great Britain. (Further details published in Vol. 106, No. 2 and Vol. 113, No. 2)
Aug. 3–9, 1980 London, Great Britain	**Clinical Pharmacology and Therapeutics** Contact: Conference Associates, 34 Stanford Road, London W8 5PZ, Great Britain.
Aug. 4–8, 1980 Denver, Colo., U.S.A.	**Conference on Applications of X-Ray Analysis** Contact: Mrs. Mildred Cain, Denver Research Institute, University of Denver, Denver, Colo.,80208, U.S.A. Tel. 303/753-2141.
Aug. 4–9, 1980 Ottawa, Canada	**7th International Conference on Raman Spectroscopy** Contact: Mr. Ken Charbonneau, Conference Services, National Research Council of Canada, Ottawa, Ontario, Canada K1A OR6.
Aug. 17–23, 1980 Wolfeboro, N.H., U.S.A.	**Gordon Research Conference on Vibrational Spectroscopy** Contact: Dr. Erich Ipsen, Bell Laboratories, Holmdel, N.J. 07733, U.S.A.
Aug. 18–22, 1980 Brighton, Great Britain	**Micro 80** Contact: The Royal Microscopical Society, 37/38 St. Clements, Oxford OX4 1AJ, Great Britain.
Aug. 24–29, 1980 San Francisco, Calif., U.S.A.	**ACS 180th National Conference – 2nd Chemical Congress of the North Amer. Continent** Contact: A.T. Winstead, 1155 16th Street, N.W. Washington, D.C. 20036, U.S.A.
Aug. 24–31, 1980 Rzeszów, Poland	**2nd International Summer School on Data Processing in Chemistry DPC '80** Contact: Prof. Dr. Z. Hippe, Dept. of Physical Chemistry, Technical University, 35-959 Rzeszów, Poland. (Further details published in Vol. 122, No. 1)
Aug. 25–29, 1980 Prague, Czechoslovakia	**J. Heyrovský Memorial Congress on Polarography** Contact: Czechoslovak Academy of Sciences, J. Heyrovský Institute of Physical Chemistry and Electrochemistry, Vlasská 9, CS-118 40 Praha 1, Czechoslovakia. (Further details published in Vol. 113, No. 2)
Aug. 25–30, 1980 Graz, Austria	**8th International Microchemical Symposium** Contact: Prof. Dr. A. Holasek, Institut für Medizinische Biochemie, Universität Graz, Harrachgasse 21, A-8010 Graz, Austria. Tel. (0 316) 32 5 32 or 76 5 91. (Further details published in Vol. 109, No. 1 and Vol. 110, No. 2).

Aug. 25–30, 1980 Delft, The Netherlands	**Joint ISMAR–Ampère International Conference on Magnetic Resonance** Contact: ISMAR-Ampère 1980, Postbus 30424, NL.2500 GK Den Haag, The Netherlands.
Aug. 31–Sept. 5, 1980 Kuparovice Castle, Czechoslovakia	**IIIrd Brno Symposium on MolecularBiophysics: Electroanalysis of Biopolymers** Contact: Dr. E. Palecak, Institute of Biophysics, Czechoslovak Academy of Sciences, Královopolská 135, 612 65 Brno, Czechoslovakia.
Sep. 2–5, 1980 Prague, Czechoslovakia	**VII European Symposium on Connective Tissue Research** Contact: Dr. Z. Deyl, Physiological Institute Czechoslovak Academy of Sciences, 142 20 Budejovická 1083, Prague 4, Czechoslovakia.
Sep. 6–12, 1980 Liège, Belgium	**International Solvent Extraction Conference 1980 (ISEC '80)** Contact: Conference Secretariat ISEC '80, Department of Chemistry, University of Liège, Sart Tilman, B–4000 Liège, Belgium. (Further details published in Vol. 107)
Sep. 6–12, 1980 Bath, Great Britain	**IMLS Triennial Conference** Contact: K. Case, Area Central Laboratory, Royal United Hospital, Bath BA1 3NG, Great Britain.
Sep. 7–12, 1980 Florence, Italy	**IUPAC International Symposium on Macromolecules (Structural Order in Polymers)** Contact: Macro IUPAC 80, Fondazione Giovanni Lorenzini, Via Monte Napoleone 23, 20121 Milan, Italy.
Sep. 8–10, 1980 Oxford, Great Britain	**Photoelectrochemistry Discussion** Contact: Dr. M.D. Archer, Dept. of Physical Chemistry, Univ. of Cambridge, Lensfield Road, Cambridge, Great Britain.
Sep. 9–12, 1980 Eindhoven, The Netherlands	**2nd International Symposium on Isotachophoresis** Contact: ITP 80, Afd. Instrumentele Analyse, Technische Hogeschool Eindhoven, Postbus 513, 5600 MB Eindhoven, The Netherlands.
Sep. 15–19, 1980 York, Great Britain	**10th European Solid State Device Research Conference** Contact: The Institute of Physics, 47 Belgrave Square, London SW7, Great Britain.
Sep. 16–19, 1980 Bratislava, Czechoslovakia	**6th International Symposium on Advances and Application of Chromatography in Industry** Contact: Dr. Ján Remeň, Analytical Section ČS VTS,pri n.p. Slovnaft, 82300 Bratislava, Czechoslovakia.
Sep. 22–26, 1980 Cannes, France	**8th International Vacuum Congress – 4th International Conference on Solid Surfaces – 3rd European Conference on Surface Science** Contact: Société Francaise du Vide, 19 Rue Renard, F–75004 Paris, France.
Sep. 22–26, 1980 Paris, France	**European Conference on Chemical Pathways in the Environment** Contact: Dr. C. Troyanowsky, Société de Chimie physique, 10, rue Vauquelin, F-75005 Paris, France. Tel. 707-54-48.
Sep. 23–25, 1980 Cardiff, Great Britain	**Chemical Society/Analytical Division – CS Autumn meeting: Trace and Ultratrace Analysis** Contact: The Secretary, Analytical Division, The Chemical Society, Burlington House, London W1V 0BN, Great Britain.
Sep. 24–28, 1980 Hamburg, F.R.G.	**EMBO-EMBL** **Workshop on X-ray and Neutron Scattering of Biological Structure** Contact: Prof. H. Stuhrmann, EMBL c/o DESY, Notkestrasse 85, D-2000 Hamburg 52, F.R.G.

Sep. 28–Oct. 3, 1980 Philadelphia, Pa., U.S.A.	**7th Annual Meeting of Federation of Analytical Chemistry and Spectroscopy Societies (FACSS)** Contact: Mrs. J.G. Graselli, c/o Standard Oil Co., 4440 Warrensville Road, Cleveland, Ohio 44128, U.S.A.
Sep. 29–Oct. 3, 1980 York, Great Britain	**Modern Radiochemical Practice** Contact: The Secretary, Analytical Division, Chemical Society, Burlington House, London W1V 0BN, Great Britain.
Oct. 6–9, 1980 Houston, Texas, U.S.A.	**EXPOCHEM '80** Contact: Professor A. Zlatkis, Chemistry Department, University of Houston, Houston, Texas 77004, U.S.A. Tel. (713) 749-2623.
Oct. 6–9, 1980 Houston, Texas, U.S.A.	**Chromatography '80 – 15th International Symposium on Advances in Chromatography** Contact: Professor A. Zlatkis, Chemistry Department, University of Houston, Houston, Texas 77004, U.S.A. Tel. (713) 749 2623. (Further details published in Vol. 115)
Oct. 9–15, 1980 Dusseldorf, West Germany	**INTERKAMA '80 – International Congress and Trade Fair for Instrumentation and Automation** Contact: German/American Chamber of Commerce, 666 Fifth Avenue, New York, NY 10019, U.S.A.
Oct. 16–17, 1980 Teddington, Middx., Great Britain	**Quantitative Surface Analysis** Contact: The Meetings Officer, The Institute of Physics, 47 Belgrave Square, London SW1X 8QZ, Great Britain.
Oct. 19–23, 1980 Washington, D.C., U.S.A.	**Annual Meeting of Assoc. of Official Analytical Chemists** Contact: K.M. Fominaya, Box 540, Benjamin Franklin Station, Washington, D.C. 20044, U.S.A.
Oct. 22–24, 1980 Rome. Italy	**Workshop on TCDD and Related Compounds** Contact: Prof. Dr. O. Hutzinger, University of Amsterdam, Nieuwe Achtergracht 166, Amsterdam, The Netherlands. (Further details published in Vol. 122, No. 1)
Oct. 27–31, 1980 Endorf bei Rosenheim/ Bayern, F.R.G.	**EUCHEM – CONFERENCE: Die Darstellung logischer Strukturen in der Chemie durch Modelle und die Lösung chemischer Probleme mittels Computern** Contact: GDCh–Geschäftsstelle, P.O. Box 90 04 40, D–6000 Frankfurt/M 90, F.R.G.
Nov. 19–21, 1980 New York, N.Y., U.S.A.	**19th Eastern Analytical Symposium** Contact: Norman Gardner, Exposition Manager, 73 Ethel Street, Metuchen, N.J. 08840, U.S.A. Tel. (201) 548 7377.
Dec. 16–17, 1980 Brighton, Great Britain	**Chromatography, Equilibria and Kinetics** Contact: Mrs. Y.A. Fish, The Chemical Society, Burlington House, London W1V 0BN, Great Britain. Tel. 01-7349971.
Apr. 13–16, 1981 Cardiff, Wales, United Kingdom	**International Symposium on Electroanalysis in Clinical Environmental and Pharmaceutical Chemistry** Contact: Short Courses Section (Electroanalysis Symposium), UWIST, Cardiff CF1 3NU, Wales, United Kingdom.
July 6–9, 1981 Strasbourg, France	**27th IUPAC Symposium on Macromolecules** Contact: Secretariat, Macro 1981, Société de Chimie Industrielle, 28, rue Saint-Dominique, 75007 Paris, France.
Aug. 16–22, 1981 Vancouver, Canada	**28th Congress International Union of Pure and Applied Chemistry** Contact: Congress Secretariat, 28th IUPAC Congress, c/o The Chemical Institute of Canada, 151, Slater Street, Suite 906, Ottawa, Ontario, Canada K1P 5H3.

Aug. 23–28, 1981 University of Auckland, New Zealand	**Golden Jubilee Conference "Chemistry in the Service of Man"** Contact: Dr. D.J. McLennan, Chemistry Dept., Univ. of Auckland, Auckland, New Zealand.
Aug. 23–28, 1981 Espoo, Finland	**Euroanalysis IV – Triennal Conference of the Federation of European Chemical Societies** Contact: Professor L. Niinistoe, Department of Chemistry, Helsinki University of Technology, SF–02150 Espoo 15, Finland. (Further details published in Vol. 109, No. 1)
Aug. 30–Sep. 5, 1981 Vienna, Austria	**XI International Congress of Clinical Chemistry. – IV European Congress of Clinical Chemistry** Contact: Congress Secretariat, Interconvention, P.O. Box 35, A–1095 Vienna, Austria. Tel. (0222) 42 13 52.
Sep. 1–4, 1981 Siofok, Hungary	**3rd Danube Symposium on Chromatography** Contact: Hungarian Chemical Society, H–1368 Budapest, P.O.B. 240, Hungary. Tel: Budapest 427–343. (Further details published in Vol. 115)

Vapor-Liquid Equilibrium Data Bibliography and Supplements

compiled by I. WICHTERLE, J. LINEK and E. HÁLA, Institute of Chemical Process Fundamentals, Czechoslovak Academy of Science, Prague.

Vapor-Liquid Equilibrium Data Bibliography

The book comprises a bibliographic index by compounds, of all vapor-liquid equilibrium data measured between 1900 and December 1972. The Substances in the tables are listed according to the well-known Hill system used in the Chemical Abstracts formula index and the whole procedure has been fully computerized. This is largely due to the amount of input data processed and to update the information more readily. Containing over 4800 references, the value of the book is in locating the source of original data.

"...The enormity of the accomplishment may be gauged from the fact that it requires over 4800 references to cover the subject... ...It should be of great help to the 'workers in the chemical industry who have to deal with problems of distillation and rectification' for whom it is intended."

Journal of the American Chemical Society

"...Trial searches made by this reviewer were carried out quickly and efficiently... it should be of real utility, especially to process design engineers, who need data on particular systems."

A.I.C.H.E. Journal

1973 viii + 1053 pages
Price: US $85.25/Dfl. 175.00
ISBN: 0-444-41161-5

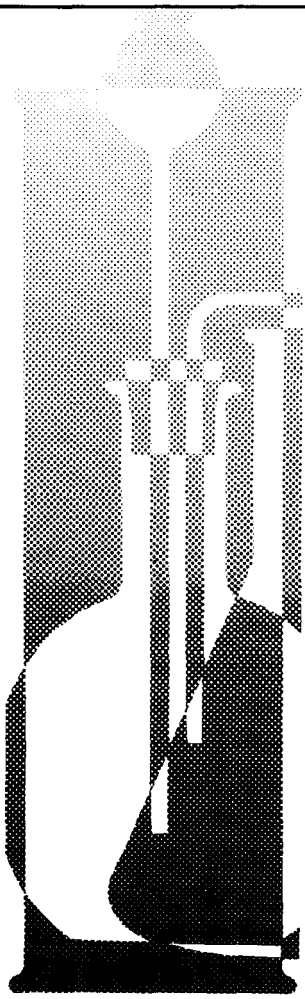

Supplement I

This first supplement reviews the literature measured and reported from January 1973 through December 1975. Comprising over 1000 references, the objective of the work is to list additional information.

'... the book by Wichterle and its supplement are of real help to all engineers, physical chemists and metallurgists dealing with vapor-liquid equilibria."

Fluid Phase Equilibria

1976 viii + 333 pages
Price: US $48.75/Dfl. 100.00
ISBN: 0-444-41464-9

NEW

Supplement II

This second supplement covers the literature of systems whose vapor-liquid equilibria have been measured and reported from January 1976 until December 1978.

1979 viii + 286 pages
Price: US $61.00/Dfl. 125.00
ISBN: 0-444-41822-9

This work together with its two supplements, will prove invaluable to those involved in the chemical problems of distillation and rectification in the chemical industry. By indicating where to find the necessary data, it will be of help in the development, design and rational operation of distillation equipment.

ELSEVIER

P.O. Box 211,
1000 AE Amsterdam
The Netherlands
52 Vanderbilt Avenue,
New York, NY 10017,
USA.

7160

CHEMORHEOLOGY OF POLYMERS

by K. MURAKAMI *and* K. ONO,
Chemical Research Institute of Non-Aqueous Solutions, Tohoku University, Sendai, Japan

POLYMER SCIENCE LIBRARY 1

Polymer Science is one of the new disciplines to emerge in its own right in the second half of the twentieth century. *The Polymer Science Library* has been launched to fulfil the need for a series of books on polymer materials which presents and collates accounts of the contemporary state-of-the-art in already established fields and provides a comprehensive guide to newer developments and research.

This first volume presents a condensed selection of the basic and fundamental knowledge of polymer degradation and stabilization mechanisms which other texts in the field have failed to explore fully. At sufficiently high temperatures, polymeric materials are subject to chemical reactions which affect their structural properties. These changes are reflected in the visco-elastic behaviour of the material. Chemorheology is therefore, by definition, the changes in visco-elastic behaviour induced by chemical reactions. It is a relatively new discipline and encompasses the physical and chemical aspects involved in the elucidation of the mechanisms, at a molecular level, of structural changes of polymers during their degradation.

The studies presented here should stimulate further research and applications in areas where the lifetime of polymers may be controlled by means of additives, chemical modifications and synthesis, and where this knowledge is applied to thermal-, light-, oxidation-, ozon-, and chemical resistant polymers, flame retardant polymeric materials and disposable plastics.

CONTENTS: **Introduction. Single Degradation of Crosslinked Polymers.** (I) Scission along Main Chains. (II) Scission at Crosslinkages. (III) Interchange Reaction. (IV) The Location of Scissions along Main Chains or at Crosslinkages. **Multi-degradation of Crosslinked Polymers.** (I) Cleavage at Crosslinks and along Main Chains. (II) Exchange Reaction with Cleavage at Crosslinkages and/or along Main Chains. **Crosslinking Reaction.** (I) Mechanism of Crosslinking Reaction. (II) Crosslinking Reactions at Low Temperatures. (III) Abnormal Behaviour in Crosslinking Reactions. **Application of Dynamic Mechanical Methods to Chemorheology.** (I) Dynamic Mechanical Properties of Crosslinked Polymers Undergoing Oxidation. (II) Dynamic Chemorheology in Large Deformations. **Applications of Chemorheology.** (I) Plastics. (II) Textiles. (III) Paints and Adhesives. Subject Index.

1979 x + 216 pages US $ 48.75/Dfl. 100.00
ISBN: 0-444-41831-8

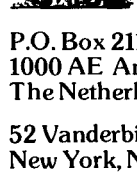

ELSEVIER

P.O. Box 211,
1000 AE Amsterdam
The Netherlands

52 Vanderbilt Ave
New York, N.Y. 10017

7159

The Dutch guilder price is definitive. US $ price is subject to exchange rate fluctuations.

(continued from outside of cover)

Molecular emission cavity analysis. Part 16. Determination of boron, selenium and other elements by using a flame generated within the cavity
S. L. Bogdanski, E. Henden and A. Townshend (Birmingham, Gt. Britain) 93
Atomic absorption spectrometric determination of the total content and distribution of chromium in blood serum
E. Graf-Harsányi and F. J. Langmyhr (Oslo, Norway) 105
Determination of total particulate mercury in air with the Coleman mercury analyzer system
R. Dumarey, R. Heindryckx and R. Dams (Gent, Belgium) 111
Spectrofluorimetric determination of pharmaceutical compounds with the cerium(IV)—cerium(III) system
G. Amann, G, Gübitz (Graz, Austria), R. W. Frei (Amsterdam, The Netherlands) and W. Santi (Basle, Switzerland) 119
Preconcentration of silver(I), gold(III) and palladium(II) in sea water with *p*-dimethylamino-benzylidenerhodanine supported on silica gel
K. Terada, K. Morimoto and T. Kiba (Ishikawa, Japan) 127
The determination of dissolved total nucleic acids in natural waters including sea water
E. Hicks and J. P. Riley (Liverpool, Gt. Britain) 137
Extraction et dosage par chromatographie en phase gazeuse d'un herbicide (Neburon) et d'un de ses métabolites (1 3,4-dichloroaniline). Application à des eaux naturelles
A. Copin, J. Delmarcelle, R. Deleu, A. Renaud et Ph. Dreze (Gembloux, Belgium) 145
Extraktion von Bunt- und Eisenmetallen mit 1-Phenyl-3-methyl-4-benzoylpyrazol-5-thion und 1-Phenyl-3-methyl-4-thiobenzoylpyrazol-5-on
E. Uhlemann, B. Maack und M. Raab (Potsdam, D.D.R.) 153
2,2'-Dipyridyl-2-quinolyhydrazone as a reagent for the spectrophometric determination of metals. The extractive spectrophotometric determination of palladium(II)
M. Otomo (Nagoya, Japan) 161

Short Communications

Tissue- and bacteria-loaded tubular reactors for the automatic determination of glutamine
M. Mascini and G. A. Rechnitz (Newark, DE, U.S.A.) 169
Titration of microgram amounts of sulphide with a sulphide-selective electrode
T. M. Florence and Y. J. Farrar (Lucas Heights, NSW, Australia) 175
Sensitive solid-phase chemiluminescence microassay of thiols
R. D. Lippman (Stockholm, Sweden) 181
Extraction spectrophotometric determination of niobium in rocks with sulfochlorophenols
A. E. Childress and L. P. Greenland (Reston, VA, U.S.A.) 185
A spectrophotometric method for the determination of anionic surfactants at $\mu g\ l^{-1}$ levels
S. Rama Bhat, P. T. Crisp, J. M. Eckert and N. A. Gibson (Sydney, N.S.W., Australia) . . 191
Means of distinguishing selenium peaks from sulphur peaks in gas chromatography with a flame photometric detector
J. R. Hancock, C. G. Flinn and W. A. Aue (Halifax, Nova Scotia, Canada) 195
Separation of uranium(VI) by liquid—solid extraction with tri-n-octylphosphine oxide diluted with naphthalene
Y. Shigetomi, T. Kojima, H. Kamba (Okayama-shi, Japan) and Y. Yamamoto (Hiroshima, Japan) 199
Determination of metals in small samples by atomic absorption and emission spectrometry with discrete nebulization
T. Uchida, I. Kojima and C. Iida (Nagoya, Japan) 205

Book Reviews 211

CONTENTS

Determination of trace amounts of some phenylamide pesticides by resonance Raman spectrometry
S. Higuchi, O. Aiko and S. Tanaka (Tokyo, Japan) 1
A versatile spectrometer for secondary x-ray fluorescence excitation
L. Højslet Christensen, S. E. Rasmussen, N. Pind and K. Henriksen (Aarhus, Denmark) . . 7
Qualitative examination of chemically-modified silica surfaces by near-infrared photoacoustic spectroscopy
C. H. Lochmüller and D. R. Wilder (Durham, NC, U.S.A.) 19
Measurement of etching after irradiation with charged particles by using the matrix activation
M. Valladon, G. Blondiaux, A. Giovagnoli, C. Koemmerer and J. L. Debrun (Orleans, France) 25
Amperometric flow-through wire detector: a practical design with high sensitivity
J. A. Lown, R. Koile and D. C. Johnson (Ames, IA, U.S.A.) 33
Anodic detection of arsenic(III) in a flow-through platinum electrode for flow-injection analysis
J. A. Lown and D. C. Johnson (Ames, IA, U.S.A.) 41
Model experiments for determinations of zinc—amino acid complexes in biological fluids by polarography
E. O. Martins and G. Johansson (Lund, Sweden) 53
A potentiometric microbial sensor based on immobilized *Escherichia coli* for glutamic acid
M. Hikuma, H. Obana, T. Yasuda (Kawasaki, Japan), I. Karube and S. Suzuki (Yokohama, Japan). 61
Polarographic analysis for corticosteroids. Part 4. Determination of corticosteroids in multi-component and complex pharmaceutical preparations
H. S. de Boer, P. H. Lansaat and W. J. van Oort (Utrecht, The Netherlands) 69
The conditional constant as error variable in the evaluation of stability constants from combined pH and pM measurements
E. R. Still (Åbo, Finland) 77
Comparative study on the precision of potentiometric techniques applied with ion-selective electrodes. Part 3. Potentiometric titrations
G. Horvai and E. Pungor (Budapest, Hungary) 87

(continued on inside page of cover)

Printed in The Netherlands.